THE UNIVERSITY
of EDINBURGH

Mechanisms to reverse impaired macrophage function in COPD

Eilíse M Ryan

THE UNIVERSITY
of EDINBURGH

A Thesis Presented for the Degree of Doctor of Philosophy

University of Edinburgh

2019

Declaration

I declare that the content of this thesis is my own work and that all contributions and collaborations have been explicitly acknowledged in the text. No material presented in thesis has been submitted to any other university or for any other degree.

Eilíse M Ryan

30.07.2019

Abstract

COPD is major health problem and is set to become the third leading cause of death globally by 2030. To date we have no therapies which significantly alter the course of this debilitating disease. The lungs of COPD patients are characterised by chronic inflammation which results in airway narrowing and tissue destruction and persists even after smoking cessation.

Patients with COPD experience defective innate immunity, characterized in part by macrophage dysfunction. In established disease, COPD macrophages have impaired phagocytosis of bacteria and apoptotic cells (efferocytosis). There is evidence that COPD macrophages have altered expression of a transcription factor, Nrf2, the master regulator of antioxidant defences. I hypothesised that impaired macrophage functions in COPD share common mechanistic defects. These defects may relate to cellular energetics and or antioxidant responses.

To address if macrophage dysfunction in COPD was regulated by the lung microenvironment alone, I isolated macrophages from the airways [Alveolar macrophages (AM)], and from the peripherally circulating blood [Monocyte-derived macrophages (MDM)], of COPD and Healthy donors . I found that in COPD both AM and MDM had impaired bacterial phagocytosis and efferocytosis. I also found that efferocytosis and phagocytosis rates were closely correlated , suggesting a shared underlying mechanistic defect.

Efferocytosis and phagocytosis rates also correlated with markers of disease severity in COPD.

Dynamic metabolic profiling of macrophages, using Seahorse technology, revealed that AM and MDM from COPD patients have impaired energy reserves in both glycolysis and oxidative phosphorylation. Whilst experiencing reduced reserves in both of these central metabolic pathways , Seahorse evaluation also revealed an apparent over reliance on glycolysis in COPD macrophages . This was mirrored in LC-MS (liquid chromatography mass spectrometry) analysis of resting state macrophages. LC-MS revealed a global up regulation of the glycolytic intermediaries in resting state AM and MDM from COPD Donors.

In parallel with this work , I established that COPD AM display an impaired transcriptional response to infection with *Streptococcus pneumoniae*, which primarily related to failure to mount an adequate anti-oxidant response. Manipulation of the anti-oxidant pathway with highly specific activators of Nrf2, enhanced bacterial phagocytosis and efferocytosis in COPD AM and MDM. Moreover ,treatment with Nrf2 agonists increased TCA cycle intermediaries, and restored redox balance to the cell, as assessed by LC-MS. Using transcriptomics analysis we identified a number of key metabolic targets which differed at baseline between COPD AM and Healthy Donor AM, with key shifts in metabolism induced by Nrf2 activation in COPD AM.

In summary I have established that there is a global defect in macrophage function in COPD, which is not singularly driven by tissue specific factors. I

have determined that both AM and MDM from COPD patients have an impaired bioenergetic profile and I suggest that this may be the common underlying mechanism driving the phenotype. I have demonstrated a failure in COPD AM to mount an anti-oxidant response. I have subsequently shown a reversal of impaired macrophage function in COPD using a highly specific Nrf2 activator .Lastly, I have evidence that the Nrf2 mediated restoration of macrophage function in COPD is due, in part, to metabolic reprogramming, with a skewing towards oxidative phosphorylation. This highlights both the therapeutic potential for metabolic reprogramming in COPD and the role of Nrf2 activation in modulating disease behaviour in COPD.

Lay Summary

Chronic obstructive pulmonary disease (COPD) is a chronic lung condition which is estimated to become the third leading cause of death globally, by 2030. None of the currently available treatments prevent the condition from deteriorating. Typically, hospital admissions are caused by infections and patients who get frequent infections deteriorate more rapidly.

Specialised cells in the body called macrophages should protect patients from infections. They also play a major role in “mopping up” dead cells and debris left over after an infection has been controlled. If these dying cells are not removed properly, they can leak the toxic substances they had to fight infection, into the surrounding tissues, causing damage. We have found that macrophages, both from the lung and from the circulating blood of COPD patients, are unable to effectively clear bacteria or to mop up dying cells, as they should. We think this is because their metabolism is different to “Healthy cells” and this renders them exhausted and unable to carry out their normal function. Activating antioxidant pathways helps the body to deal with stresses, such as infection. We activated these pathways in macrophages from COPD patients, using a new drug therapy. This partially restored normal function to the macrophages of COPD patients. We think this is because increasing antioxidant signals in these cells switches their metabolism back to normal. Importantly, we think this could be used as a new drug therapy in patients with COPD to help reduce recurrent infections and the damage that they cause.

Acknowledgements

First and foremost, I would first like to thank my two supervisors, Professor Moira Whyte and Professor Sarah Walmsley for their tremendous encouragement, support, guidance and all round excellent company throughout my PhD. It has been a real privilege to work with two such inspirational people and I am very grateful for the opportunity.

I have thoroughly enjoyed being a member of the fantastic Walmsley/Whyte group and I would like to thank all members, past and present, for their help and friendship during my research. I would particularly like to thank Dr Emily Watts for her support when I was preparing my Wellcome Fellowship application.

I am very grateful to our collaborator, Professor David Dockrell, for his input into this project and for generously gifting me a transcriptomics data set to reanalyse for this research. I would also like to thank Dr Bart Ghesquière and Wesley Vermaelen at the VIB Center for Cancer Biology in Leuven for running the HPLC-MS metabolic samples. Both Angie Fawkes and John Thompson, of the University of Edinburgh, have been a font of knowledge for preparing samples for and later analysing our transcriptomics data. I am very grateful to my Respiratory colleagues, in particular to Dr John Mc Cafferty, for facilitating patient recruitment. I would also like to thank Professor David Singh, from the University of Manchester, for his assistance in recruiting additional patients.

The University of Edinburgh Centre for Inflammation Research is an incredible place to work, with a particular ethos of collaboration and compassion towards those just starting their research career. I am very grateful to all those who made my time there so enjoyable. I am particularly grateful to Professors Ian Dransfield and Adriano Rossi for the guidance they provided as my Thesis Committee Supervisors.

This project was funded by a Wellcome Trust Clinical training fellowship and I am very grateful to The Wellcome Trust for this wonderful opportunity.

I am forever indebted to the many patients who enthusiastically donated both their time and their cells to this research, in full knowledge that progression of the field would likely benefit those coming behind them, rather than themselves.

I would like to thank my family for their unwavering love and support throughout the years. In particular, I would like to thank my husband, Andy, for endless cups of tea and for being a perpetual calm in a storm.

Lastly, this thesis is dedicated in loving memory to my father, the only person in the world who would have enjoyed proofreading it!

Abbreviations

ADP - Adenosine diphosphate

AM - Alveolar Macrophages

AMP - Adenosine monophosphate

AMPK - 5'AMP-activated protein kinase

AN - Apoptotic Neutrophils

ATP - Adenosine triphosphate

BAL - Bronchoalveolar Lavage

Cas9 - CRISPR associated protein 9

CAT - COPD Assessment Test

COPD - Chronic Obstructive Pulmonary Disease

COPD MAP Consortium - The COPD MRC/ABPI Partnership

CPT1 - Carnitine palmitoyltransferase 1

CRISPR - Clustered Regularly Interspaced Short Palindromic Repeats

CSE - Cigarette Smoke Exposure

ECAR - Extracellular Acidification Rate

FAO - Fatty Acid Synthesis

FEV_1 - Forced Expiratory Volume in 1 Second

FMLP - *N*- formylmethionine-leucyl-phenylalanine

FVC - Forced Vital Capacity

GM-CSF - Granulocyte-macrophage colony-stimulating factor

GR - Glycolytic Reserve

GTP - Guanosine Triphosphate

GWAS - Genome-Wide Association Studies

HC - Healthy Control

HIF - Hypoxia Inducible Factor

HPLC-MS - High Performance Liquid Chromatography Mass Spectrometry

KEAP1 - Kelch-like ECH associated protein 1

LPS - Lipopolysaccharide

MARCO - Macrophage Receptor with Collagenous Structure

MDM - Monocyte-derived Macrophage

ME1 - Malic Enzyme 1

MERTK - Mer proto-oncogene Tyrosine Kinase

MMP - Matrix Metalloproteinase

MOI – Multiplicity of Infection

mRNA - messenger Ribonucleic Acid

mROS - mitochondrial Reactive Oxygen Species

mTOR - Mammalian Target of Rapamycin

NADPH - Nicotinamide Adenine Dinucleotide Phosphate

NFLS – Normal Lung Function Smokers

NrF2 - Nuclear Factor erythroid 2-realted factor 2

NTHi - Non Typable *Haemophilus influenzae*

OCR - Oxygen Consumption Rate

PBMC – Peripheral Blood Mononuclear Cell

PGC-1β - Peroxisome proliferator-activated receptor-gamma coactivator-1 β

PINK 1- PTEN-induced kinase 1

PPP - Pentose Phosphate Pathway

RHO - Ras homolog gene family

RNA - Ribonucleic Acid

ROS - Reactive Oxygen Species

RPMI - Roswell Park Memorial Institute Media

SPN - *Streptococcus pneumoniae*

SRC - Spare Respiratory Capacity

STAT6 - Signal Transducer and activator of transcription 6

TBST – Tris Buffered Saline with Tween

TNF-α - Tumour Necrosis Factor alpha

Contents

Declaration ..... **ii**
Abstract ..... **iii**
Lay Summary ..... **vi**
Acknowledgements ..... **vii**
Abbreviations ..... **ix**
1 Introduction **1**
1.1 Macrophages in Innate Immunity 1
1.1.1 Macrophage Ontogeny 1
1.1.2 Macrophage phenotype and function 4
1.2 COPD- a disease of Innate Immunity? 6
1.2.1 Defective innate immunity in COPD 6
1.2.2 The role of macrophages in the pathogenesis of COPD 9
1.2.3 Advances in the treatment of macrophage dysfunction in COPD 11
1.3 Summary 13
2 Methods and Materials **15**
2.1 Patient Recruitment 15
2.2 Peripheral Blood Mononuclear Cell, Neutrophil Isolation and generation of Autologous serum 16
2.3 Cytocentrifuge slide preparation 17
2.4 Monocyte Derived Macrophage Culture 18
2.5 Alveolar Macrophage Isolation and Culture 19
2.6 Macrophage Protein Lysis Protocol 21
2.7 Western Blotting 22
2.8 Maintaining Bacterial Stock 23
2.9 Miles-Misra Dilution 24
2.10 Opsonising Streptococcus pneumoniae 25
2.11 Assessment of Bacterial Internalisation at 4 hours post-infection 25
2.12 Neutrophil Staining with PKH26 and Flow Efferocytosis assay 28
2.13 Nrf2 activation via pharmalogical compounds 31
2.14 Seahorse Assays 31
2.15 Measuring Glucose uptake via a 2NBDG Assay 34
2.16 Measuring Intracellular Glycogen Stores 34
2.17 Measuring BAL nutrient levels 35
2.18 HPLC-MS analysis of metabolite abundance 35
2.19 RNA Sample generation and extraction 37

2.20 Transcriptomics Data and Analysis 38
2.21 Taqman analysis of Gene expression 40
3 Macrophages from COPD donors have defective function 42
3.1 Introduction 42
3.2 Demographic data of recruited patients 49
3.3 Alveolar and Monocyte-derived macrophages from COPD donors have impaired bacterial phagocytosis and efferocytosis 51
3.4 COPD macrophages have preserved early bacterial killing 54
3.5 Decreased opsonic bacterial phagocytosis in COPD correlates with markers of disease severity, but not with age 56
3.6 Efferocytosis by COPD macrophages correlates with markers of disease severity, but not with age 58
3.7 Phagocytosis rates correlate with efferocytosis rates suggesting a common underlying mechansim 60
3.8 COPD macrophages display a globally reduced transcriptional response to infection with S. pneumoniae 62
3.9 Discussion 70
4 COPD macrophages display an altered metabolic profile 77
4.1 Introduction 77
4.2 AM from COPD and Healthy Donors differ in their baseline transcriptional profile 88
4.3 AM from COPD have an altered metabolic response to Streptococcus pneumoniae 92
4.4 Metabolically profiling COPD macrophages in real time 94
4.5 COPD AM display impaired bioenergetics compared to Healthy Donors 97
4.6 COPD AM primarily upregulate glycolysis to meet increased energy demand 100
4.7 COPD MDM exhibit reduced energetic reserves when compared to Healthy donors 104
4.8 Energy phenotyping reveals a divergent response in COPD MDM compared to COPD AM 107
4.9 Resting state COPD Macrophages upregulate the glycolytic pathway, as detected by LC-MS 110
4.10 Energy Charge is reduced in COPD AM compared to Healthy donors 113
4.11 Differential substrate availability for glycolysis does not account for altered metabolism in COPD macrophages 115
4.12 Profiling of Bronchoalveolar lavage fluid suggests that availability of substrate in the alveolar space does not differ between COPD and Healthy donors 118
4.13 COPD AM display a refractory metabolic profile. 120

4.14 Discussion 124
5 COPD macrophage dysfunction is rescued by activation of the Nrf2 module 130
5.1 Introduction 130
5.2 COPD Alveolar Macrophages fail to appropriately upregulate the Nrf2 module following infection with serotype D39 Streptococcus Pneumoniae 138
5.3 Treatment with the Nrf2 activator, Sulforaphane, upregulates the Anti-Oxidant Response element in Alveolar and Monocyte-derived macrophages 141
5.4 Activation of Nrf2 by Sulforaphane partially recues impaired bacterial macrophage phagocytosis in COPD , with preserved anti-microbial killing 143
5.5 Treatment with Sulforaphane rescues defective efferocytosis in both Alveolar and Monocyte-Derived Macrophages in COPD patients 145
5.6 Treatment with a novel, highly specific Nrf2 activator also upregulates HO-1 in COPD macrophages 147
5.7 Treatment with the specific Nrf2 activator, Compound A significantly enhances both bacterial phagocytosis and efferocytosis in AM and MDM from COPD donors, but not Healthy donors 150
5.8 Compound A enhances COPD macrophage bacterial internalisation and efferocytosis in a dose dependent manner without impairing bacterial killing 153
5.9 Utilizing a published specific Nrf2 activator, Compound 7 , to target macrophage dysfunction in COPD 155
5.10 The Nrf2 agonist Compound 7, significantly enhances efferocytosis and bacterial phagocytosis in COPD MDM and AM, but not in Healthy donor macrophages 157
5.11 Treatment with Compound 7 induces transcriptional change in COPD and Healthy Alveolar Macrophages 159
5.12 COPD AM transcriptional profile more closely resembles Healthy AM , after treatment with Compound 7 161
5.13 Transcriptional changes induced by Compound 7-mediated Nrf2 activation, are disease specific 164
5.14 Nrf2 activation via Compound 7 reprogrammes COPD AM metabolism leading to improved cellular energetics 167
5.15 Nrf2 improves cellular redox balance in COPD AM. 171
5.16 Activation of the Nrf2 Module does not increase macrophage phagocytosis or efferocytosis in Healthy Volunteers, including under hostile culture conditions: 173
5.17 ME1 expression is reduced in COPD AM at baseline and augmented following treatment with Nrf2 177

5.18 Discussion 180
6 Discussion and Future Directions 186
6.1 Discussion 186
6.2 Future directions 190
6.3 Conclusions 195
7 References: 196
8 Appendices: 210
8.1 Appendix 1: Percoll Preparations 210
8.2 Appendix 2: Western Blot 210
8.3 Appendix 3 Seahorse Compounds 212
8.4 Appendix 4: Report from Edinburgh Clinical Research Facility Genetics Core for Total RNA sequencing data E161715 RNA-Seq : 213
8.5 Appendix 5: cDNA generation and TaqMan analysis 215
8.6 Appendix 6: GOLD Criteria for COPD severity 216
8.7 Appendix 7: COPD Assessment Test 217

List of Figures:

Figure 2.1: Optimisation of Efferocytosis assay. 30
Figure 3.2: Demographic data. 50
Figure 3.3: COPD donors have impaired phagocytosis and efferocytosis compared to Healthy Volunteers. 53
Figure 3.4: COPD Macrophages show no defect in early phase bacterial killing and COPD donors maintain their ability to produce opsonins… 55
Figure 3.5: Opsonised macrophage bacterial phagocytosis correlates with markers of disease severity but not with age. 57
Figure 3.6: Efferocytosis by COPD AM only, correlates with markers of disease severity age. Macrophage efferocytosis does not correlate with age. 59
Figure 3.7: Correlation of phagocytosis rates with efferocytosis rates in AM and MDM from both COPD and Healthy Donors. 61
Figure 3.8.1: Affymetrix array reveals a reduced transcriptional response to *S. pneumoniae* in COPD Alveolar Macrophages. 65
Figure 3.8.2: Transcription of phagocytic receptors is minimally changed in COPD Alveolar Macrophages following infection with *S.pneumoniae*. 66
Figure 3.8.3: Transcription of the efferocytosis pathway is largely unaltered in Alveolar Macrophages at 4hours post initial incubation with *S.pneumoniae*. 67
Figure 3.8.4: Co-incubation with *S. pneumoniae* induces differential transcriptional programmes in actin cytoskeletal organisation, in Healthy and COPD AM. 68
Figure 3.8.5: Schematic of key elements of cytoskeleton re arrangement required for phagocytosis. 69
Figure 4.1: Macrophages can engage different metabolic pathways to drive energy production. 79
Figure 4.2.1: RNA-seq profiling reveals differences in baseline transcription between COPD and Healthy AM. 90
Figure 4.2.2: Transcriptional regulation of metabolism differs between COPD and Healthy AM at baseline. 91
Figure 4.3: Affymetrix array reveals abnormal metabolic responses to infection in COPD AM. 93
Figure 4.4: Seahorse profiling of cellular energetics. 96
Figure 4.5.1: COPD Alveolar Macrophages display altered metabolic profiles with reduced energy reserves. 98
Figure 4.5.2: Basal OCR rates are reduced in COPD AM. 99

Figure 4.6.1: Mitochondrial stress testing suggests a redundancy in mitochondrial units in Healthy AM , which is not present in COPD AM. 102
Figure 4.6.2: COPD AM have an over reliance on glycolysis to meet increased energy demand. 103
Figure 4.7.1: COPD Monocyte-Derived Macrophages display altered metabolic profiles with reduced energy reserves. 105
Figure 4.7.2: Basal metabolic rates are comparable in COPD and Healthy MDM. 106
Figure 4.8.1: COPD MDM display similar rates of ATP linked OCR to Healthy MDM. 108
Figure 4.8.2: Energy Phenotyping of COPD MDM revealed a suppressed maximal energetic response, but comparable utilization of oxidative metabolism and glycolysis. 109
Figure 4.9.1: Resting state COPD AM and MDM exhibit a global increase in Glycolytic intermediaries. 111
Figure 4.9.2. COPD and Healthy Donor AM display comparable levels of TCA cycle intermediaries. 112
Figure 4.10: Resting state COPD AM have reduced Energy availability compared to Healthy Donor AM 114
Figure 4.11: Differences in glycolytic rates are not determined by differential glucose uptake/glycogen breakdown in COPD Macrophages. 117
Figure 4.12: Profiling of Bronchoalveolar lavage fluid suggests substrate availability fluid does not account for metabolic differences in COPD macrophages. 119
Figure 4.13: Healthy donor macrophages display efferocytosis mediated enhancement of oxidative metabolism. 122
Figure 4.14: Proposed mechanism for altered metabolic status in COPD. 129
Figure 5.1: Nrf2 mediated modulation of cellular metabolism and anti-oxidant responses. Known Nrf2 targets are listed in *black italics*. 134
Figure 5.2: Affymetrix array reveals aberrant stress response to infection in COPD donors. 140
Figure 5.3: Sulforaphane disrupts the KEAP1/NrF2 complex to activate the Anti-oxidant Response Element (ARE). 142
Figure 5.4: Treatment with Sulforaphane increases phagocytosis of serotype 14 *S. pneumoniae* in COPD without compromising intracellular bacterial killing. 144
Figure 5.5: Treatment with Sulforaphane partially recues efferocytosis in COPD macrophages. 146

Figure 5.6: Highly specific activation of Nrf2 upregulates HO-1 in Healthy and COPD Donor MDM. 149
Figure 5.7: The Nrf2 activator, Compound A ,enhances efferocytosis and bacterial phagocytosis in COPD AM and MDM. 152
Figure 5.8: Dose response of Compound A in COPD MDM and AM , with no change detected in early bacterial killing following treatment. 154
Figure 5.9: Compound 7 prevents Nrf2/KEAP1 binding , leading to activation of the Anti-oxidant Response Element (ARE). 156
Figure 5.10: The Nrf2 agonist Compound 7, enhances efferocytosis and bacterial phagocytosis in COPD MDM and AM..... 158
Figure 5.11: Nrf2 activation induces a significant transcriptional response in COPD and Healthy Donor AM..... 160
Figure 5.12.1: Nrf2 activation induces a transcriptional shift in COPD AM towards Healthy AM. 162
Figure 5.12.2: COPD AM correlate more closely with Healthy AM after treatment with Compound 7. 163
Figure 5.13: Nrf2 activation induces a divergent transcriptional responses in COPD vs Healthy donor AM. 165
Figure 5.14.1: Nrf2 activation leads to a significant increase in TCA cycle metabolite abundance. 169
Figure 5.14.2 Nrf2 activation improves cellular energetics. 170
Figure 5.15: Nrf2 activation improves cellular redox state. 172
Figure 5.16.1: Nrf2 activation does not enhance MDM phagocytosis or efferocytosis in Healthy Volunteers. 175
Figure 5.16.2: Nrf2 activation augments neither efferocytosis nor phagocytosis in cells cultured in hypoxic and glucose deprived environments. 176
Figure 5.17: Nrf2 activation restores ME1 expression in COPD AM. ... 179

1 Introduction

1.1 *Macrophages in Innate Immunity*

The innate immune system is the first line of defence against invading pathogens. It has a dual role; to provide initial control of infection and to initiate an adaptive immune response. The innate immune system comprises physical barriers such as epithelial layers and mucus in the airways, soluble factors including antimicrobial peptides, and cells such as neutrophils, macrophages and dendritic cells. The lack of specificity of the mediators of the innate response means that a balance must be struck between effective immunity without excessive 'self' injury. As central orchestrators of innate immunity, successful fine tuning of macrophage function is critical for striking this balance. Disruption of homeostasis, for example in disease, subverts this equilibrium and can lead, not only to failure of first line defences, but also to progressive and irreversible destruction of surrounding tissue.

1.1.1 Macrophage Ontogeny

Monocytes and macrophages are key effectors of the innate immune response and by virtue of their ability to process and present antigen, they also form a link between adaptive and innate immunity. They represent a diverse population of cells which possess a high degree of plasticity and heterogeneity. There have been numerous attempts to classify macrophages into groups based on function etc., but no system to date has captured the

intricacy of a cell population whose phenotype and even origins, are constantly evolving based on microenvironmental cues. Broadly, macrophages can be divided into Monocyte-derived Macrophages (MDM) and Tissue (or Resident) Macrophages. Monocytes are released into circulation from reservoirs in the bone marrow, blood and spleen. They are recruited to sites of infection and inflammation and subject to the microenvironment encountered, can differentiate into activated macrophages with variable phenotypes. Tissue macrophages are a distinct and tissue specific population of cells with roles suited to their anatomical and physiological niche. They include Kupffer cells in the liver, microglial cells in the brain and Alveolar Macrophages (AM) in the lung[1]. It was originally believed that tissue macrophages were replenished by circulating blood-monocytes originating from a bone marrow progenitor, which differentiated into macrophages on tissue infiltration[2]. In recent years, seminal murine fate mapping studies and advances in transcriptional profiling including single cell RNA-seq, have refuted this hypothesis and highlighted that macrophages have several origins during ontology, which persist into adult life[3]. The new paradigm is that tissue macrophages are seeded in waves during embryonic development, with studies suggesting that Alveolar Macrophages are predominantly seeded from Fetal liver monocytes, within the first week of life[4,5]. Moreover, this embryonically seeded macrophage population, is able to self-renew in the steady state. However, if homeostasis is disrupted, for example during infection, tissues recruit circulating monocytes which infiltrate and differentiate into macrophages [6]. Interestingly, as inflammation resolves

following Acute Lung Injury, resident macrophages once again become the predominant population. Thus, it appears that MDM are rapidly recruited to tackle injury, then having served their purpose, they are swiftly removed via efferocytosis, restoring the lung to pre-injury homeostasis[7]. Importantly, infiltrating MDM take on some, but not all of the characteristics, of resident tissue macrophages, and remain transcriptionally and in some cases functionally distinct. This varies depending on the organ, but studies have suggested that local cues and tissue imprinting in the lung play a more significant role in developing and shaping the phenotype of macrophages than in other organs. Embryonic host-derived and postnatal donor-derived murine AM were found to be highly transcriptionally concordant, with less than 5% of total genes seemingly governed solely by origin. An example of one such gene was MARCO, a scavenger receptor which plays a major role in macrophage mediated host defence and was only expressed by host derived AM[8]. Impaired tissue imprinting, for example in the diseased state, could possibly render these populations more dissimilar. This has been proposed as one explanation for the finding that bone marrow derived Kupffer cells take on only 50% of the characteristics of resident cells, following damage to the organ during requisite irradiation[9]. It is important to note that fate mapping studies to date have been conducted singularly in animal models and that our understanding of the origin and lineage of human macrophages lags behind, for obvious technical reasons. Evidence is accumulating however, that macrophages in humans, and more specifically

lung macrophages, share a similar divide of “original tissue” macrophages and infiltrating MDM which are distinct cell populations [10,11].

1.1.2 Macrophage phenotype and function

Macrophages, and in particular MDM, are often classified on a binary polarisation division of pro-inflammatory, antimicrobial “M1” macrophages or anti-inflammatory, “M2” macrophages, which participate in tissue remodelling. This is based on phenotypic changes induced by cytokine signalling, ligation of pattern recognition receptors, response to circulating mediators and the nature of the microenvironment, encompassing, for example substrate availability[12]. In reality, it is unlikely these exclusive roles are a realistic representation of the complex interplay which exists in vivo. Macrophages possess the highest degree of plasticity of any cell within the haemopoietic system. At any given time a macrophage may shift from a “pro inflammatory” polarisation state after exposure to a pathogen to a “pro-resolution” state following cues from surrounding apoptosing cells. The polarisation phenotype seen in each tissue/and or disease state is likely a spectrum created by both the cell itself and the microenvironment in which it exists.

This high degree of plasticity enables macrophages to carry out a diverse range of functions. In health, macrophages act as immune sentinels surveying for tissue injury and infection. They are essential for host defense through their capacity to phagocytose and subsequently kill bacteria. Alveolar macrophages can clear pathogens and debris from the alveoli, typically with

minimal inflammatory consequences, thus preventing excessive tissue damage[13]. However, if macrophage defenses become overwhelmed by invading pathogens, they trigger an inflammatory response by releasing an array of pro inflammatory cytokines and mediators, which guide infiltrating immune cells to the site of injury/infection. Release of this inflammatory milieu is necessary for amplifying the inflammatory response, but if the inflammatory cascade proceeds unchecked, it can have also have deleterious effects on the surrounding tissues. Thus, once the danger has passed, careful and rapid dismantling of the inflammatory response is required to prevent further host cell damage[14]. Once again, macrophages have a central role in co-ordinating this process. Inflammation resolution requires apoptosis of the large population of infiltrating neutrophils and macrophage efferocytosis of these cells safely removes them and their toxic granule contents from the site of injury. Furthermore, macrophage efferocytosis triggers release of anti-inflammatory IL-10 and TGFβ which further polarise macrophages towards an anti-inflammatory state [15,16]. IL-10 release has also been shown to abrogate LPS mediated neutrophil survival[17]. Thus macrophages ensure that the inflammatory response is well controlled and disassembled once the “threat” has been removed.

As mentioned, both internal and external stimuli induce phenotypic shifts in macrophages. What is now abundantly evident is that metabolic reprogramming is intrinsically linked to macrophage function and activation states. Quiescent macrophages have a large capacity for mitochondrial

metabolism and oxidative phosphorylation. However, pro-inflammatory stimuli such as LPS cause macrophages to undergo a phenotypic shift towards glycolysis as their main source of ATP[18]. This facilitates the rapid generation of ATP which is required for pro inflammatory function but renders the cells vulnerable to metabolic exhaustion. By products of glycolytic metabolism can in turn augment “M1” polarisation of macrophages. Similarly M2/anti-inflammatory macrophages possess a distinct and divergent metabolic signature. They are heavily reliant on mitochondrial metabolism - both oxidative phosphorylation and fatty acid oxidation. Disruption of these metabolic pathways, and subsequent loss of their signalling metabolic intermediaries results in impairment of M2 phenotype[19].

As key effectors of the innate immune response, macrophages are well equipped with the machinery to combat pathogens, generate an inflammatory response and carefully orchestrate inflammation resolution. Their high degree of phenotypic plasticity is essential for their wide ranging function and is reliant on successful rewiring of cellular metabolism. The role of intracellular redox balance and effective metabolic reprogramming in governing macrophage function will be discussed in more depth throughout this thesis.

1.2 *COPD- a disease of Innate Immunity?*

1.2.1 Defective innate immunity in COPD

Chronic obstructive pulmonary disease (COPD) is a major cause of morbidity and mortality worldwide and is predicted to become the third leading cause of

death globally by 2030[20]. In the U.K 1.2 million people have a diagnosis of COPD but it is estimated that a further 2 million people are currently undiagnosed. Existing therapies do not have a major disease-modifying impact and many patients have progressive airflow obstruction despite long-term inhaled and oral treatments.

Cigarette smoke is the major cause, with an ever increasing recognition of additional contribution from environmental pollutants[21]. However, while the triggers for COPD have been identified, the primary mechanisms driving disease pathogenesis are yet to discovered. As some smokers appear to be protected from COPD, there has always been much interest in elucidating a genetic predisposition. Unfortunately, while identifying several genetic loci associated with COPD, the GWAS COPD cohort, failed to unearth a unifying molecular mechanism or to attribute hereditability to the disease[22]. It is likely that a genomic approach to COPD is hindered by the prominent heterogeneity of the disease and a failure to identify markers by which to accurately group patients. Alpha-1 anti trypsin deficiency is evidently the exception to this, whereby a known inherited mutation in the protease inhibitor leads to development of pulmonary emphysema, and in some patients, liver cirrhosis.

The histological hallmark of COPD is persistent inflammation of the airways, resulting in airflow limitation (measured by a decline in forced expiratory volume in 1 second (FEV1), chronic bronchitis and emphysema. This

inflammation persists in people with COPD, even following smoking cessation[23]. In established disease, severe chronic oxidant stress and defective innate immunity may down-regulate host-pathogen responses, resulting in inflammation that is damaging but also ineffective[24]. Inhaled toxins such as cigarette smoke, contain high levels of Reactive Oxygen species (ROS), which is likely the initial trigger for large quantities of inflammatory cells to gather in the lungs of these patients. It also triggers endogenous ROS production in these cells and additional ROS release, coupled with other inflammatory mediators, puts in place a cycle of chronic oxidant stress. While there is increased cellularity in the lungs of smokers, it is not currently known why the initial inflammatory reaction evoked by exposure to cigarette smoke, does not progress to disease pathology in all smokers[25]. By contrast, in COPD, there is evidence of widespread impairment of innate immunity with defective epithelial, dendritic cell, neutrophil and macrophage function all described in the context of the disease. In COPD, mucus secreting goblet cells in the epithelial lining undergo hyperplasia, further exacerbating airways obstruction and causing significant symptomatology in patients[26]. Increased permeability of the epithelial barrier has also been described[27]. Dendritic cells are reduced in numbers and activation states in COPD and there is evidence that they have impaired presentation of viral antigen[28,29]. In contrast, neutrophils, rather than exhibiting suppressed immunity, predominantly contribute to disease

pathology by persistent recruitment to and infiltration of lung tissue with release of highly destructive neutrophils derived proteases such as neutrophil elastase[30]. It has also been shown that while neutrophils in COPD display faster speed of chemotaxis, they have impaired directional accuracy to the potent chemokine fMLP [31]. However, as the first line of defense in the innate immune system, macrophage dysfunction in COPD is perhaps the greatest contributor to disease pathology.

1.2.2 The role of macrophages in the pathogenesis of COPD

It has long been established that macrophages play a major role in the pathogenesis of COPD. Alveolar macrophages are present in high numbers in the airways and airway secretions of patients with COPD, In fact, their abundance correlates directly with disease severity[32]. Conversely, macrophage depletion in murine models, protects form Cigarette Smoke Exposure mediated pulmonary inflammation[33].

Clinical exacerbations of COPD, frequently associated with acute bacterial infection, accelerate decline in lung function and increase hospitalisation and mortality[24]. The presence of pathogenic bacteria in the lower airways, a feature of COPD, is strongly associated with exacerbation frequency and increased inflammation[34]. The increased numbers of airway macrophages in COPD, coupled with these high rates of infection and colonisation, indicate a major disconnect whereby excessive cellular inflammation results in ineffective immunity. This disconnect is now understood to be largely driven

by macrophage dysfunction. COPD macrophages have defective bacterial phagocytosis, leading to further recruitment of innate immune cells and ongoing release of damaging inflammatory mediators[35]. Macrophage phagocytosis of bacteria that colonise the lungs in COPD, such as non-typeable *Haemophilus influenzae* and *Streptococcus pneumoniae* is greatly reduced in disease [36,37,38]. In vitro analysis of AM function has confirmed reductions as high as 50% [37]. Macrophage dysfunction also extends to impaired inflammation resolution. Failure to efferocytose apoptotic cells has been confirmed in COPD macrophages, with reductions between 20-40% demonstrated[39]. Failure to clear apoptotic cells enables them to undergo secondary necrosis, releasing large quantities of potentially toxic granules and further contributing to an already inflammatory environment. Interestingly, a number of studies have demonstrated normal uptake of polystyrene beads by COPD AM[40]. Initial studies suggested this was due a specific impairment of efferocytosis in COPD macrophages, but normal uptake of beads compared to uptake of bacteria, has been documented also [36]. It is possible that either the energy requirement for uptake, or the processes engaged in uptake of inert particles are distinct and unaffected in COPD. It also stresses the importance of using physiologically relevant targets. Reports of efferocytosis and phagocytosis rates in smokers with preserved lung function (NLFS) vary between studies. Normal AM phagocytosis and efferocytosis in NLFS compared to never smokers have been described [36,38]. In contrast a study by Hodge et al reported reduced rates in current smokers, but importantly efferocytosis was reduced further

still in COPD patients and smoking cessation failed to restore macrophage function in COPD patients[40,23].

In conjunction with impaired macrophage internalisation rates, macrophages in COPD also upregulate several molecules known to induce pulmonary tissue damage. The release of MMP (matrix metalloproteinases) 9 and 12 is increased in AM from COPD patients [41,42]. MMPs are known to degrade the alveolar wall matrix and have long been implicated in COPD pathogenesis. In fact, cigarette smoke exposed MME $^{-/-}$ mice (also known as MMP-12) are protected from developing emphysema. Production of NADPH oxidase, leading to increased levels of ROS and subsequent elevated oxidant stress, is also increased in COPD AM[43]. Thus, defective AM and MDM function in COPD leads to inflammation that is both ineffective and skews the balance towards “self-injury” in the lung.

1.2.3 Advances in the treatment of macrophage dysfunction in COPD

Once established as a key cause for disease pathogenesis and progression, there have been numerous attempts to understand and reverse the impaired phagocytic phenotype of COPD. Studies have predominantly focused on pharmalogical augmentation of COPD macrophage function, with several studies attempting to work backwards to the mechanistic level. The macrolide antibiotic, Azithromycin, possess both anti-bacterial and anti–inflammatory properties and has been shown to improve phagocytosis and efferocytosis

rates, though a mechanism was not investigated[44]. Moreover, utilization of this as a therapy is limited by the very justified concerns of antibiotic resistance. The use of glucocorticoids, a drug commonly employed to treat COPD, have been shown to improve efferocytosis rates but impair phagocytosis of bacteria. Treatment with fluticasone was found to reduce release of inflammatory cytokines such as TNFα and IL-12 , but also prevented acidification of the phagolysosome, leading to reduced bacterial killing[45]. This may explain the increased rate of Community Acquired pneumonia seen in patients on inhaled-corticosteroids. The cholesterol lowering drug Lovastatin, was found to augment efferocytosis specifically in COPD macrophages, in a HMG-CoA reductase dependent manner. Inhibition of HMG-CoA reductase- the mechanism of action of statins- decreases levels of the metabolic intermediary Mevalonate[46]. Mevalonate is known to regulate the process of geranylgeranylation- a form of post translational modification which provides a membrane anchor for proteins. This is particularly relevant as the Rho GTPases, central regulators of efferocytosis, undergo geranylgeranylated-mediated lipid anchoring for optimal functioning[47]. More recently, the increasingly recognised role of specialised proresolving mediators (SPM's) in inflammation resolution has led to the exploration of their potential role in enhancing efferocytosis in cigarette - smoke-exposure exposed MDM[48]. Lastly, as chronic oxidant stress is a defining feature of COPD, efforts have focused on restoring redox balance in these patients. A cardinal study by Harvey et al found that by targeting redox balance in the cell they could augment COPD macrophage phagocytosis.

They treated cells with Sulforaphane, a phytochemical compound which increases the cytosolic pool of the master regulator of the antioxidant response element, Nrf2. Sulforaphane enhanced COPD macrophage phagocytosis in an apparently MARCO dependent fashion[49]. Altered redox balance in COPD is the focus of Chapter 5 of this thesis and is discussed in more detail there.

1.3 *Summary*

In summary, macrophages are the central mediators of innate immunity. Through key phenotypic shifts, they orchestrate both the inflammatory response to injury, and, critically, also regulate the highly co-ordinated process of inflammation resolution. Much of these shifts in phenotype are directed by the microenvironment but also require intact cell signalling and metabolic rewiring to take place. The role of macrophage dysfunction in COPD has been recognised for decades and individual studies have identified specific pathways which are altered in disease. However we still lack an overarching mechanism for COPD macrophage dysfunction, particularly outwith the direct noxious effect of cigarette smoke and environmental pollutants. The existence of impaired phagocytosis and efferocytosis rates in COPD suggests a potential shared mechanistic defect. As both phagocytosis and efferocytosis have high energy requirements [50], defective cellular energetics and or metabolism would have a major effect on these processes. A failure to undergo appropriate metabolic reprogramming

in response to various stimuli could also lead to impaired macrophage function and may account for the altered polarisation state seen in COPD macrophages[51]. Emerging evidence points towards a role for antioxidant responses - which are known to be defective in COPD - in supporting metabolic reprogramming and macrophage activation. To date, no study has investigated metabolism in COPD macrophages nor evaluated the link between it and the antioxidant response.

Thus, for this body of work our overall hypothesis was that impaired macrophage functions in COPD share common mechanistic defects and that these defects may relate to cellular energetics and antioxidant responses.

Our aims were to define these functional defects in parallel with profiling the bioenergetics and antioxidant status of both COPD and healthy donor macrophages. Ultimately we wished to explore the possibility of restoring function in COPD macrophages by manipulating these pathways.

2 Methods and Materials

2.1 *Patient Recruitment*

This study was approved by the South East Scotland Research Ethics Committee (REC Ref 15/SS/0095, CPMS ID 30704 , IRAS ID 181196). Patients were recruited through the Clinical Research Facility at the Royal Infirmary of Edinburgh, the Western General Hospital, and through existing NHS bronchoscopy lists in NHS Lothian. COPD donors had an FEV_1/FVC ratio of <0.70 and GOLD Stage 1,2 and 3 patients were included, as were current smokers and ex-smokers. Healthy Bronchoscopy Donors had normal spirometry and were never, ex or current smokers. Patients with diabetes, renal failure, liver failure, cardiac failure, active malignancy or other major respiratory diagnosis eg asthma/bronchiectasis were excluded . Healthy Volunteers for blood donation were age matched +/- 5 years and were recruited through the Centre for Inflammation Research Blood Resource, Queens Medical Research Institute, Edinburgh. Peripheral venous blood was taken from healthy volunteers with written informed consent as approved by the Centre for Inflammation Research Blood Resource Management Committee. Study Title : The Role Of Inflammation in Human Immunity (AMREC 15-HV-013).

2.2 *Peripheral Blood Mononuclear Cell, Neutrophil Isolation and generation of Autologous serum*

Peripheral blood mononuclear cells (PBMC) and neutrophils were isolated from blood using dextran sedimentation with discontinuous Percoll gradients. A 21 gauge needle was used to draw blood. 36ml of blood was decanted into tubes containing 4ml sterile 3.8% Sodium Citrate and mixed gently by inverting the tube. Cells were then centrifuged at 350g, acceleration (acc.) 5, deceleration (dec.) 5, for 20 minutes to separate the cell layer from the Platelet Rich Plasma (PRP) layer. The upper PRP layer was carefully aspirated and the cell layer beneath was mixed with 6ml of 37°C 6% Dextran stocks and topped up to 50ml with 37°C 0.9% Sodium Chloride (NaCl). The tubes were carefully inverted and bubbles were aspirated from the surface with a sterile Pasteur pipette to reduce potential activation. The tubes were then left for 25-30 minutes at 37°C to sediment. At this point, to generate autologous serum, 220μl of Calcium Chloride was added to 10ml of the PRP layer and placed in the water bath for approximately 30 mins to generate a platelet plug with surrounding platelet depleted plasma. After dextran sedimentation and separation, the cell-rich upper layer was aspirated and transferred to a Falcon tube, made up to 50ml with 37°C 0.9% NaCl and spun at 300g for 6 minutes, acc. 5 , dec. 5, to generate a leucocyte pellet. A Percoll gradient was then used to separate granulocytes from the whole leucocyte population. A stock solution of 90% Percoll (GE Healthcare) was made using 10% vol. of 10X PBS. 73%, 61% and 49% Percoll were made by

dilution of the 90% stock with 1X PBS as outlined in Appendix 1. Gradients were made up in 15ml polystyrene Falcon tubes. Using a sterile Pasteur pipette throughout, 3ml of 73% Percoll was pipetted into the bottom of the tube and 3ml of 61% Percoll was gently layered on top. The leucocyte pellet was then resuspended in 3ml of the 49% Percoll and carefully layered onto the 61% layer. The Percoll gradient was centrifuged at 720g for 20 minutes (acc. 1, dec. 0). Following cell layer separation on the gradient, the upper layer of Peripheral Blood Mononuclear Cells (PBMC) was aspirated carefully using a sterile Pasteur pipette and transferred to a clean 50ml Falcon tube. The lower layer of Polymorphonuclear Leukocytes (primarily neutrophils), was similarly removed and transferred to a clean Falcon tube. 20ml 1x PBS was added to the neutrophils and PBMCs and cell number was calculated using an Improved Neubauer haemocytometer. Cells were then divided based on requirement, centrifuged at 300g, acc. 5 , dec. 5, for a further 6 minutes at 20°C and resuspended in media. Purity was determined via morphology on Cytospins.

2.3 *Cytocentrifuge slide preparation*

Cytocentrifuge slides (Cytospins) were utilised to assess cellular morphology throughout experiments. To generate Cytospins a glass slide, filter paper and cytospin chamber with a funnel for cells, were held together with a slide holder. 100μl-200μl of cell suspension ($1x10^5$-$5x10^5$ cells), was pipetted into the funnel and the cytospin was centrifuged at 300 revolutions per minute (rpm) for 3 minutes in a CytoSpin3 cytocentrifuge (Thermo Scientific). Slides

were fixed with 100% methanol and stained using the Shandon Kwik-Diff staining system (Thermo Scientific). Slides were first stained with Eosin (90seconds) and then with Methylene Blue (30seconds) to delineate nuclear structures. Slides were mounted using DPX mountant (Sigma-Aldrich) and a glass cover slide was added.

2.4 *Monocyte Derived Macrophage Culture*

Based on intended experiments, cells were cultured via Method A or Method B. Method A was used for functional assays (bacterial internalisation, bacterial killing and efferocytosis assays). For assays that required removal of cultured macrophages for transplantation into an assay specific plate (i.e. Seahorse assays), cells were cultured via Method B.

Method A: PBMC were re suspended in RPMI 1640 (Sigma-Aldrich R8758) without serum at a dilution of 4 x 10^6 /ml. 500μl of this solution was pipetted into 24-well cell culture plates (Costar). Plates were then incubated for one hour at 37C, 5% CO_2. Following this the media was aspirated and replaced with complete media (RPMI containing 10% Heat Inactivated Fetal Calf Serum (FCS, Gibco, 10500-064), 1ml per well, for the duration of their culture period. The media was changed again the following day and there after every 3-4 days. Cells were cultured for a total of 12-14 days prior to use. No antibiotics were used in the media throughout culture.

Method B: After isolation of the PBMC layer , monocytes were isolated via the Miltenyi Biotec Pan Monocyte Isolation kit (130-096-537) and Miltenyi

Monocyte Isolation Columns (130042401), following manufacturer's instructions. Isolated monocytes were counted via an Improved Neubauer haemocytometer. 4 x 10^6 monocytes were then plated into Corning Low Adherence Flasks (CLS3815-24EA) in 5 ml of complete media as above. An additional 5ml of complete media was added on Day 4 of culture. Cells were cultured for 8-9 days prior to removal. To remove, flasks were left on ice for 30mins, then flasks were tapped vigorously on both sides and cells were removed by washing with a 5ml stripette. Flasks were then given a final wash with cold PBS and examined under the microscope to ensure sufficient removal. Cells were counted following staining with 0.4% Trypan Blue, to exclude non-viable cells, and plated as required into assay specific plates. Recovered yield of viable cells ranges from 40%-60% [38].

2.5 *Alveolar Macrophage Isolation and Culture*

Bronchoalveolar Fluid (BAL) was collected from COPD and Healthy donors as per ethics protocol. After inspection of the airways during bronchoscopy, the scope was wedged into the Right Middle Lobe (RML). 2-4 ml of lidocaine was then instilled via the scope into the RML, prior to injecting a total of 240ml of saline in 40ml aliquots. The first 40ml of return was discarded/sent for routine culture and sensitivity, due to the high content of epithelial cells. If the RML was deemed inappropriate to wash, the Right Upper lobe was used. Following bronchoscopy, samples were kept on ice in 50ml Falcon tubes and transported to the lab immediately. Whole BAL fluid was sieved into a 50ml Falcon tube through a sterile 100μm cell strainer and spun at 400g,

acceleration 5, deceleration 5, for 10 min, at 4°C. Supernatant was removed, flash frozen on dry ice and stored at -80°C. The cell pellet was vortexed as soon as possible to avoid clumping of cells and re-suspended in up to 10ml of Antibiotic Media (RPMI 1640 [Sigma] with 10% heat inactivated FCS [Gibco], 1% Penicillin [Lonza DE17-603E] and Amphotericin [fungizone GIBCO 15290-026 0.5µg/mL]). Viable cells were counted using a haemocytometer and 0.4% Trypan Blue. An aliquot was prepared for Cytospin to assess purity. Rarely, if there were significant quantities of Red Blood cells macroscopically or on the counting chamber, 10ml of cell suspension was spun on a 12.5mL Ficoll (Sigma-Aldrich) gradient, washed x1 in 20ml of PBS and re-suspended in media for recount. Alternatively RBCs were lysed by adding 400µl of deionized sterile H_20 to the cell pellet for 30 seconds before adding 30 ml of PBS, then spun as above and recounted. Following counting, cells were washed at 400g, for 10 mins at 4°C and resuspended at 400,000 trypan negative cells per 1ml of media. 500µl of cell suspension was then pipetted per well of a 24-well TC plate (Costar) and incubated in a humidified chamber at 37^0C and 5% CO_2. After 60 mins, this was removed and 1ml of fresh Antibiotic Media was added to each well. **D+1-** Media was changed the following day for complete media that did <u>not</u> contain antibiotics (RPMI 1640 with 10% HI FCS) if cells were to be used for a bacterial internalisation assay, otherwise, old media was replaced with fresh antibiotic media (as detailed above). **D+2 -**Wells were washed gently with media and fresh basic media was added in preparation for assays. Cytospins

were prepared on D0 and D3 . Cells were 93% -97% Alveolar macrophages as assessed by Cytospin morphology [38].

2.6 *Macrophage Protein Lysis Protocol*

Monocyte derived macrophages (MDM) were cultured as above or Alveolar Macrophages (AM) for a period of 3 days, prior to lysis for protein in 24 well plates (Costar). Tissue culture plates were put on ice with 200ul of "Scraping Buffer" for 10-30 mins. Scraping buffer = 5ml PBS, 200μl EDTA (2.5mM), 500ul of BSA (1%). Proteinase Inhibitors were included in the scraping buffer (Protease inhibitor cocktail 4:100 [Roche], EDTA-Free Protease inhibitor cocktail 3 1:100 [Merck Millipore] and phenylmethanesulfonylfluoride (PMSF) 1:100 [Sigma-Aldrich]). Cells were then removed in scraping buffer with a cell scraper (Sarstedt), 3 wells were combined per lysate. The suspension was first pelleted (5mins at 300G at 4 degrees) in a 1.5ml eppendorf. Supernatant was discarded and the pellet was resuspended in 25μl of RIPA buffer (Thermoscientific, 889900). Again, the above ratios of proteinase inhibitors were added to the RIPA buffer. The eppendorf was placed on ice for 20-30min and vortexed every 5-10 min. It was then frozen on dry ice and stored in -80^{0}C overnight or for longer. For use, it was defrosted on ice, vortexed & spun at 400g 4°C for 10min – the supernatant was then removed and pipetted into a newly labelled eppendorf. Supernatants were heated on a hot plate at 100°C for 10 minutes to denature proteins. A Pierce BCA assay (Thermo Scientific) was used to calculate protein concentration in the supernatant (RIPA buffer alone was used as the blank for the samples). To

generate samples,20μg of protein was mixed thoroughly with 20μl of 2xSDS lysis buffer and the sample was topped up, if required to 45μl using dH_2O. Samples were stored at -80°C and boiled for 5 minutes at 99°C, prior to use. 40μl of sample was loaded into each well for western blotting.

2.7 *Western Blotting*

Macrophage protein lysates were analysed for protein expression by western blot. Details of the gels and buffers used are in Appendix 2. Proteins were separated by SDS-PAGE using the BioRad mini-protean system prior to wet transfer onto PVDF membrane (Merck Millipore). Membranes were blocked using 5% skimmed milk powder for a minimum of 2 hours. Primary antibodies were made up in 5% skimmed milk in 1X TBS-Tween (TBST, 0.05% Tween) and membranes were incubated at 4°C overnight on a rolling platform. Antibodies used were against Heme-oxygenase-1 (HO- 1) (Santa Cruz, sc-10789, rabbit polyclonal ,1:1000) or Tubulin (Sigma, T5168, mouse monoclonal ,1:1000). The following morning, membranes underwent three 10-minute washes in 1X TBST prior to incubation with Donkey Anti-Rabbit secondary antibody (Life Technologies, SA1-200 ,1:400) for 1 hour at room temperature. The membrane then again underwent three 10-minute washes in 1X TBST prior to developing in enhanced chemiluminescent (ECL) detection reagent (GE Healthcare). Protein detection was then carried out using a Konica SRX-101A table top processor, 1 minute exposure was optimal for HO-1. Protein quantification was normalised to a loading control as follows: The membrane was stripped using Restore Western Blot stripping

buffer (Thermo Scientific), washed with dH_2O and then re-probed for the loading control protein β-Actin (Sigma, T5168, mouse monoclonal 1:1000) on a rolling platform, with primary and secondary antibodies as above. The membrane was then developed, and protein content was normalised using ImageJ densitometry detection.

2.8 *Maintaining Bacterial Stock*

As *Streptococcus pneumoniae (S. pneumoniae)* is a Class II pathogen, all experiments were carried out in a Cat 2 laboratory, in a laminar flow hood, following all Cat 2 lab standard operating procedures. On day 1 *Streptococcus pneumoniae* Serotype 14 master stock (NCTC11902- kindly gifted by Professor David Dockrell) was thawed on the bench. After mixing the sample, one drop was streaked out onto a blood agar plate (Colombia Blood Agar Oxoid, VWR Int) via a sterilized loop and then incubated overnight at 37°C 5%CO_2. On day 2, 50ml broth of brain/heart infusion + 20% FCS (Gibco) was made up. Approximately 10 colonies of *S. pneumoniae* from the blood agar plate was removed via a sterilized loop and mixed into 25ml of broth. Three aliquots were prepared as such. A further aliquot of broth, without *S. pneumoniae*, was kept as a blank. The aliquots and the "broth only" blank, were incubated on a continuous mixer plate for approximately 4.5 hours. The OD of 1ml from each Falcon was measured in a spectrophotometer at 600nm. The blank broth was used to zero the spectrophotometer. This was repeated every 30mins until the OD approached 0.6 – the cuvette was then kept in the reader until the OD

reached 0.6 exactly. The broth was then immediately removed from the incubator, aliquoted into 1ml eppendorfs and frozen at -80°C. The following day two aliquots were thawed, spun at 9000g for 3 minutes and washed x3 in PBS. Three 10μl drops from each of the 8 dilutions (of Miles Misra , see below) were then plated onto blood agar plates and cultured overnight in 37 °C. Stock concentration was calculated as total colonies per 3 x 10μl, divided by 30, multiplied by 1000 and the average of both thawed aliquots was used to determine final stock concentration.

2.9 *Miles-Misra Dilution*

To determine bacterial concentration eight 1.5 ml eppendorfs with 900μL of sterile PBS each, were placed in a rack and labelled '1' to '8'. 100μL of bacterial suspension was added to vial '1', generating a 1 in 10 dilution. Eppendorf "1" was then vortexed and using a new tip, 100μL from this vial was added to vial '2' –to generate a 1:100 dilution. This was repeated for each subsequent vial until a $1:10^8$ dilution was achieved . Finally, three x 10μL drops of each vial were placed into a quadrant of a blood agar plates (VWR Int.), in order of eppendorf "8" down to "1". Plates were then incubated overnight at 37°C, 5%CO_2 . Cfu/ml was calculated by (Number of colonies in quadrant / 30) = CFU per μL. This was multiplied by 1000 to give CFU per mL and then by $10^{\text{quadrant number}}$ to factor in dilution e.g. 14 colonies in Quadrant 6. Bacterial count = (14/30) x 1000 x 10^6 = 4.7 x 10^8 CFU per mL.

2.10 *Opsonising Streptococcus pneumoniae*

S. pneumoniae immune serum was generated by pooling serum from a group of inoculated healthy volunteers who had received the polysaccharide pneumococcal vaccine. Blood was drawn using a 21 gauge needle. 36ml of blood was decanted into tubes containing 4ml sterile 3.8% Sodium Citrate and mixed gently by inverting the tube. Cells were then centrifuged at 350g, acceleration 5, deceleration 5, for 20 minutes to separate the cell layer from Platelet Rich Plasma (PRP) layer. The upper PRP layer was carefully aspirated and 220μl of Calcium Chloride was added to each 10ml of the PRP layer and placed in the water bath for approximately 30 mins to generate a platelet plug with surrounding platelet depleted plasma. Plasma was then aliquoted and stored at -80°C. A vial of bacteria was thawed and washed as above x 3 in PBS. After the third spin, the pellet was resuspended in 500ul RPMI (Sigma) containing 10% of *S. pneumoniae* immune serum. The vial was then incubated on a shaking platform at 37 °C for 30 minutes before being spun down and washed as before x 2 in PBS. The pellet was finally resuspended 1ml RPMI (Sigma) [38].

2.11 *Assessment of Bacterial Internalisation at 4 hours post-infection*

Cells (MDM or AM) were cultured in in 24-well plates, with approximately 200,000 cells per well for Monocyte-Derived Macrophages (MDM) and Alveolar Macrophages (AM). All conditions were carried out in a minimum of duplicates and with a 2 x MOI of zero (ie no bacteria added) as a control for

cross contamination of *S. pneumoniae.* Wells were washed with PBS x2 before adding 1ml of fresh, antibiotic free, complete media per well. Opsonised *Streptococcus pneumoniae* was added directly to the well at a multiplicity of infection of 10:1 (MOI 10:1). The tissue culture (TC) plate was then placed on ice for 1 hour, to optimise bacterial binding, before being moved to a 37°C, 5% CO_2, incubator for 3 hours. After 4 hours total co-incubation with *S. pneumoniae*, cells were washed x3 in PBS. For each wash the well was filled completely with PBS to remove any potential adherent bacteria. 1ml of RPMI containing 40 units of benzylpenicillin (Sigma, P3032) and 20 µg/ml of gentamycin (Sigma G4918) was then added to each well to kill extracellular bacteria and the TC plate was returned to the incubator for 30 min. After 30min, cells were washed x3 with PBS. Again, each well was filled to the top to remove any residual antibiotics which could alter the viability readout. A Miles-Misra dilution was carried out on the last supernatant/PBS wash removed to provide a pre-lysis bacterial count. Cells were then lysed in 250µl 2% Saponin (Sigma-Aldrich) for 12 minutes exactly at 37°C, 5% CO_2. At twelve minutes exactly, using a pipette tip, wells were scraped thoroughly followed by rapid, vigorous pipetting to ensure all cells were broken open. 750µl of PBS was then added to the well immediately and a second Miles-Misra was conducted to determine lysed viable count. The quantity of bacteria internalised was calculated by deducting the first Miles Misra count from the second (i.e. [viable bacteria following lysis] minus [viable bacteria in the pre lysis wash]). The pre-lysis count, if the assay is

performed correctly, should only contain 1-2 colonies.

For bacterial killing at later time points: After cells were incubated with 40u benzylpenicillin and 20 µg/ml gentamycin for 30 min at 37°C, they were washed 3X PBS, and incubated with 0.75µg/ml vancomycin (Sigma). At the designated time, eg 4-8 hours, vancomycin was washed off x3 with PBS and the pre-lysis wash was plated as above. Cells were then lysed in 250µl 2% Saponin for 12 minutes, as before and the supernatant plated out.

To measure **bacterial internalisation in hypoxia,** cell were cultured for 12 days prior to the assay in a hypoxic chamber at 1% O_2 (Ruskin INVIO$_{2)}$. On the day of the assay, complete media and PBS were equilibrated for four hours in the hypoxic chamber. All steps outlined above were conducted in the hypoxic chamber (ie no transfer to incubator). Blood agar plates were then grown overnight in a standard 37^{o}C, 5% CO_2 incubator.

To measure **bacterial internalisation in a glucose deprived environment**, standard complete media was replaced with a Glucose deplete media (Gibco, 11879-020) and supplemented with dialysed FCS 10% (Dialysed by tangential flow filtration using 10,000 MW cut off filters), Life Technologies, 26400044) for 16 hours prior to conducting the experiment. Both an MOI of 0, and wells with standard glucose replete media, were used as a control [52].

2.12 *Neutrophil Staining with PKH26 and Flow Efferocytosis assay*

Neutrophils were stained with a PKH26 labelling kit (PKH26GL, Sigma-Aldrich). PKH26 is a yellow-orange fluorescent dye with long aliphatic tails that insert into the lipid regions of the cell membrane. Neutrophils were freshly isolated from a Percoll prep as described in 2.2. Prior to staining , approximately 1 million cells were removed for an “unstained sample” for flow settings and resuspended in **serum free** media at 5 x10^6 cells/ml. 20 million cells were then washed in **serum free** media at 400g for 5mins. 1ml of Diluent B was added to the pellet followed by 1ml dye (4μl dye + 996μl of Diluent B). After 2-5 mins staining was stopped by addition of 2ml of FCS/Autologous serum. Staining was noticeable better with autologous serum. Cells were then washed x 3 in complete media (400g, 5min) and re - suspended at 5 x10^6 cells/ml and plated in a 96 well plate (Costar 2595) at 150ul per well. Cells were cultured for 20h resulting in 70-80% apoptotic cells, and less than 5% necrotic cells by trypan blue exclusion - verified by Annexin V-Topro3 staining*(BD Biosciences).The apoptotic neutrophils were added to the macrophages at an MOI 5:1, including an MOI of 0 for macrophage gating. On a separate TC plate, apoptotic neutrophils were added to macrophages but kept on ice from the beginning of incubation to act as an internalisation control. After 90 minutes, cells were vigorously washed x 2, with warm PBS via a Pasteur, and a final wash with ice cold PBS to aid removal of macrophages. Cells were then scraped in 250μl of PBS ,or

alternatively 250 μl of Trypsin (Gibco) was added to each well and incubated at 37°C, for 8 minutes prior to removal with cell scraper (Sarstedt). Efferocytosis was then assessed on a BD FACS Calibur flow cytometer (Becton Dickinson) through excitation with a 488nm laser filtered through a 585nm dichroic bandpass filter (FL2).

For Annexin-Topro staining approx. 750,000 neutrophils were pelleted at 2000rpm for 3 minutes in an Eppendorf Minispin (Z606235) then resuspended in 95μl of Annexin binding buffer (BD Biosciences). 5μl of Annexin was then added to the suspension and incubated for 20 minutes on ice. In the mean time 1ml of Annexin binding buffer was added to 9mls of distilled H_2O. 5mls of this mix was then added to 1μl of Topro= 1:5000. Topro was added to the above Annexin stained neutrophils immediately prior to analysis on flow cytometry [71].

To assess **efferocytosis in a hypoxic environment**, cells were cultured for 12 days prior to the assay in a hypoxic chamber (as above-1% O_2). Apoptotic neutrophils (not cultured in hypoxia) were then co incubated with hypoxic macrophages and the assay was performed as outlined above.

To assess efferocytosis in a **glucose deprived environment**, cells were cultured as normal but complete media was replaced with Glucose deplete media (Gibco, 11879-020) and supplemented with dialysed FCS 10% (Life Technologies, 26400044), for 16 hours prior to conducting the experiment.

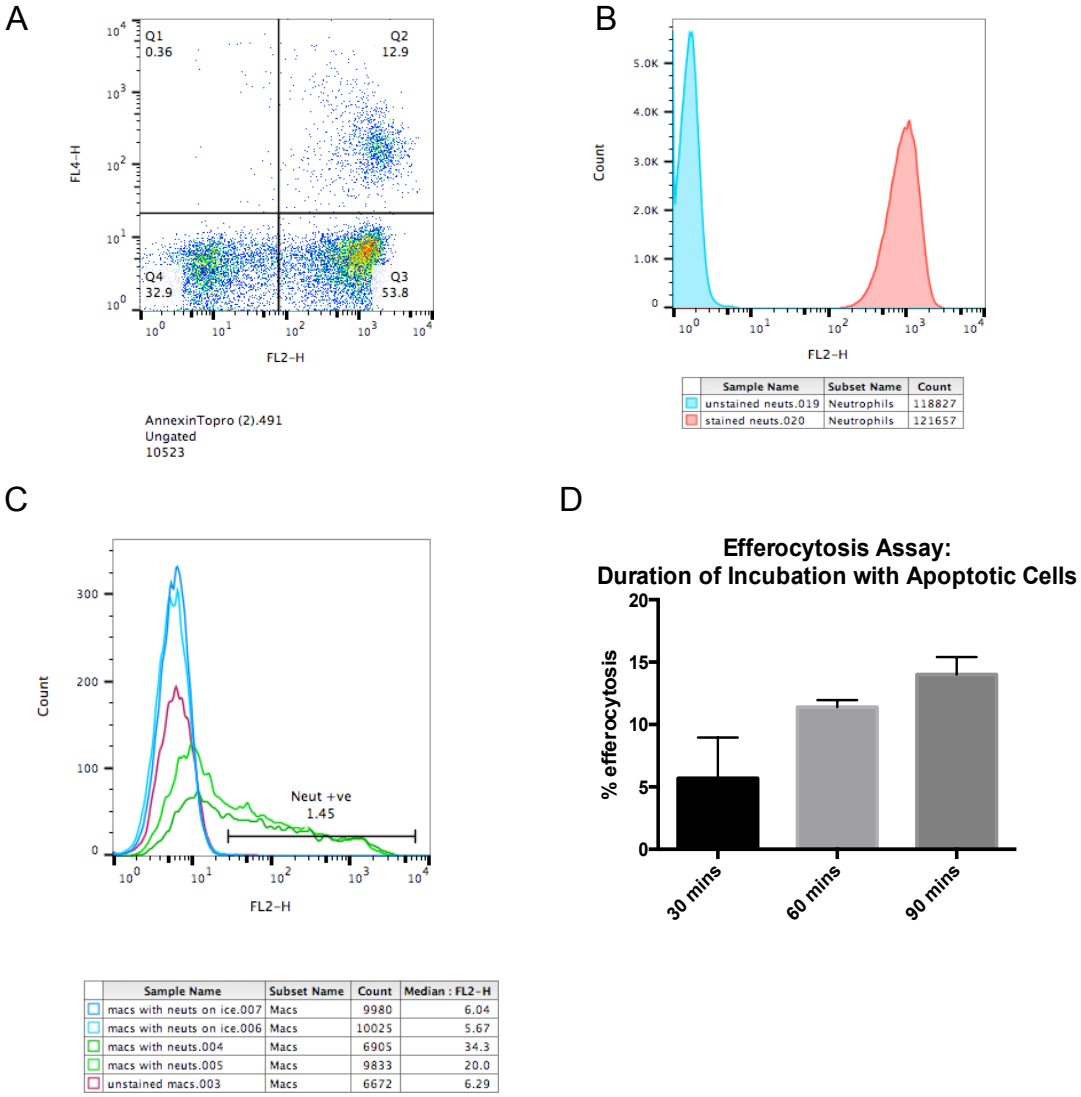

Figure 2.1: Optimisation of Efferocytosis assay.
(A)Annexin/Topro staining of 20hr apoptotic neutrophils showing 69% apoptotic, <1% necrotic neutrophils. (B) Freshly isolated neutrophils were stained with PKH26 membrane dye, integrity of dye maintained at 20hrs. (C) Adherent non internalised neutrophils were successfully washed off after 90 mins incubation, as evidenced by the Ice Control (blue) compared to the Macrophage only (pink) condition on the histogram. (D) 90 mins incubation is optimal for maximal detection of efferocytosis.

2.13 *Nrf2 activation via pharmacological compounds*

Where used, cells were pre-treated with Nrf2 activating compounds for 16 hours prior to performing assays. Compounds A,B,C and 7 were supplied by GSK under an existing MTA via COPD MAP and Sulforaphane was purchased from Sigma (S6317). Compounds were resuspended in DMSO , which was used as a vehicle control in non Nrf2 treated wells. Doses for sulforaphane were based on previous work by our group and published literature. Dose ranging for the GSK compounds were supplied by GSK based on the EC50 for previous assays. I then generated dose response curves for specific assays . Final doses used were Sulforaphane=10μM, Compound A, B and C = 10nM, Compound 7 =0.065μM.

2.14 *Seahorse Assays*

For MDM Seahorse Assays, cells were cultured using Method B, outlined above. AM were seeded into Seahorse Assay Plates immediately following isolation. 24 hours prior to performing the assay, both MDM and AM were seeded into Xe24 seahorse assay plate (MDM=V8,100882-004, AM= V7-PS,1000777-004 Agilent), at a density of 250,000 in 300μl and 210,000 in 300μl per well, respectively, for 45 mins at room temperature, before an additional 200μl of complete media was added to each well. This ensured an even distribution of cells throughout the well. 4 wells per plate, minimum, were kept cell free to calculate background during the assay. A Seahorse Xe24 Cartridge plate was hydrated using Seahorse calibration media

(Agilent) for at least 8 hours prior to the assay at 37°C, in a sealed bag. All cells were subjected to either/both a glycolytic and mitochondrial stress test.

For the ***Glycolytic Stress Test*** , 30ml of media was made using 29.7ml of Seahorse Media (Agilent 103575) with 300μl of L-Glutamine (Gibco, 25030081) giving a final concentration of 2mM. Media was warmed to 37°C before the pH was adjusted to pH 7.4 by addition of NaOH. Media was then filter sterilised through a 0.2μM filter. All wells were then washed x 2 with warm PBS and 500μl of Seahorse Glycolytic Stress Test media was added to each well before incubating the plate at 37°C, with **NO CO_2** for 45 min. Glucose, Oligomycin and 2DG compounds were prepared and added to the Seahorse Cartridge plate as per Appendix 3. Following the injection of each compound, three readings were taken 8 minutes apart totalling 3 cycles x 24 mins each. Glycolysis, Maximal Glycolytic Rate and Glycolytic Reserve were calculated during the assay and exported to Excel for analysis via the Glycolytic Stress Report Generator on Wave software.

For the ***Mitochondrial Stress Test***, 30ml of media was made using 29.7ml of Seahorse Media with 300μl(2mM)of L-Glutamine, 300μl(1mM) of sodium pyruvate (Sigma 5836) and 0.054g(10mM) dextrose (Sigma, G7021). Again media was warmed, pH adjusted, filter sterilized and incubated with cells for 45 mins, as above, at 37°C,**NO CO_2** . Oligomycin, FCCP and Antimycin& Rotenone A compounds were prepared and added to the Seahorse Cartridge plate as per Appendix 3 and the assay was run as above (3 x 24 min cycles).

Basal Oxygen Consumption, Maximal Respiratory Capacity, Spare Respiratory Capacity and Proton Leak were calculated during the assay and exported to Excel for analysis via the Mitochondrial Stress Report Generator on Wave software. A Cell Energy Phenotyping report was also exported for analysis [53].

Following either assays, lysates for protein quantification were made by adding 80ul of RIPA to each well and scraping thoroughly for a count of 60 seconds. Samples were then boiled at 100 ^{o}C for five minutes and a Pierce BCA assay (Thermo Scientific) was used to calculate protein concentration in the supernatant. ECAR/OCR readings were then normalised to μg protein/ml.

Seahorse and Co-incubation with Apoptotic neutrophils: When used macrophages were co incubated with 20hr apoptotic neutrophils (generated as outlined above in 2.12) for 90min prior to vigorous washing for removal of any non-internalised neutrophils. Standard complete media was then replaced with the relevant Seahorse Media as above for 45 minutes prior to performing the assay. For Healthy Donor macrophages a standard MOI 10:2 was used, for COPD macrophages the MOI was increased to 15:2 to adjust for differential internalisation rates.

Seahorse and Polarisation of Alveolar Macrophages: To determine if polarisation influenced macrophage metabolism as detected by Seahorse, AM were pre-treated with 20ng/ml IL-4 (68-8780-63, eBioscience) and 20ng/ml IL-13 (571102, BioLegend) or 20ng/ml IL-10 (217-IL, R&D) for 16hrs

prior to performing the assay. Wells were then washed and assay performed as before.

2.15 *Measuring Glucose uptake via a 2NBDG Assay*

Uptake of 2NBDG was measured as a surrogate for glucose uptake using a 2NBDG kit (Cayman Chemical 600470). Cells were incubated in glucose free media (Gibco, 11879-020) for 90min. 250μl of 240μM proprietary glucose was added to each well for 60 mins before adding the Cell Based assay buffer and incubation on ice for 10 min. Supernatant was aspirated and 100μl of 1:100 Infra-Red Fixed viability (Biolegend, 423195) stain was added, incubated for 10mins, light protected on a shaking platform. 200μl of cell Based Assay buffer was then added and the TC plate was incubated on ice for 10min prior to scraping and analysis on a Attune NXT flow cytometer. Wells were pre-treated for 24hours with Apigenin (included in the kit) to inhibit 2NBDG, as a control.

2.16 *Measuring Intracellular Glycogen Stores*

Glycogen stores were measured in both Monocyte-Derived Macrophages (MDM) and Alveolar Macrophages (AM), cultured as outlined above. Three wells of approximately 200,000 cells per well ,were combined per condition . Wells were rapidly washed with cold PBS on ice x 3 to remove any media. Cells were then scraped in 200μl H_20 per well and lysates were transferred to cooled eppendorfs (3 wells per eppendorf) and boiled at 100°C for 10 min. Samples were spun at 13,000g for 5 mins at 4°C, the supernatant was

transferred to fresh eppendorfs and the cells pellet was stored for protein quantification via a Pierce BCA assay (Thermo Scientific). Glycogen levels were determined via a fluorometric plate based assay (Sigma Aldrich MAK016-1KT), the supernatant was used at a 1:2 dilution and the assay run as per the manufacturer's protocol [54] .

2.17 *Measuring BAL nutrient levels*

Aliquots of Bronchoalveolar Lavage Fluid (BALF), generated as described in 2.5, were thawed on ice. All nutrient concentrations were determined using fluorometric/colorimetric plate based assays, as per the manufacturer's protocol and the optimal dilution of samples was ascertained for each different analyte. The optimised dilutions and incubations were as follows:

Glucose (Biovision K606-100)	1 in 2 dilution	10 min incubation
Glutamine (Abcam 197011)	1 in 2 dilution	60 min incubation
Lactate (Abcam 65330)	1 in 2 dilution	30 min incubation

2.18 *HPLC-MS analysis of metabolite abundance*

Samples were generated from MDM (method A) and AM cultured as outlined in 2.5. 3 wells were combined for each condition (approximately 600,000

cells total). All samples were kept on ice during the experiment. NaCl, eppendorfs and Methanol (80% Methanol, 20% dH_2O) were kept on dry ice. Cells were washed x 3 with cold NaCl. 300μl of Methanol was added to the first well, thoroughly scraped then rapidly transferred to the next well and scraped, for all 3 wells before the 300μl was transferred to the cooled eppendorfs. Samples were stored for at least 24 hours in -80°C before being thawed on ice and spun at 10,000g for 10 mins at 4°C. Supernatant was carefully removed and cell pellet was stored for protein count. The total volume of sample was recorded at this stage to adjust for any discrepancies due to evaporation, if required.

For normalisation to protein content, 200μl of 200 mM NaOH solution was added to each pellet. Samples were then boiled at 95°C for 20min, cooled on ice and spun down for 10min at 400g. Protein content was measured using a Pierce BCA assay (Thermo Scientific).

Samples were analysed using Dionex UltiMate 3000 LC System (Thermo Scientific) coupled to a Q Exactive Orbitrap mass spectrometer (Thermo Scientific) operated in negative mode, by our collaborators ,Dr Bart Ghesquière and Wesley Vermaelen at the VIB Center for Cancer Biology in Leuven. Data collection was performed using Xcalibur software (Thermo Scientific). As there have been issues with the computer generated interpretation of metabolite peaks in the past, each peak for each metabolite

was manually measured by me, to ensure quality control. All data values were subsequently corrected for protein content based on the BCA assay.

2.19 *RNA Sample generation and extraction*

For MDM and AM , 3 wells were pooled per condition (approximately 600,000) cells). Cells were centrifuged at 300G for 5 minutes at 4°C, supernatant was discarded and cells were washed in PBS. This was repeated x 2. Following the final spin, supernatant was removed and cells were lysed in 600µl mirVANA lysis/binding buffer (Invitrogen) pipetting up and down 5 times to aid lysis before being stored in the -80°C. Before RNA extraction, samples were thawed on ice and 40µl of miRNA Homogenate Additive was added before vortexing for 30 seconds. Samples were incubated on ice for 10 minutes. 600µl of Acid-Phenol:Chloroform was added to the sample before vortexing for 30 seconds to mix, and the mixture centrifuged for 5 minutes at 10,000g at room temperature.
The aqueous phase was removed from the sample and put in a sterile RNAse-free tube. A volume of 100% ethanol 1.25 times that of the extracted aqueous phase was then added. Lysates was added to a filter cartridge over a clean collection tube and centrifuged for 15 seconds at 10,000g. Flow-through was discarded and 700µl miRNA Wash Solution 1 was added to the filter and centrifuged for 30 seconds at 10,000g. Flow-through was then discarded and 500µl Wash Solution 2/3 was added to the filter and centrifuged for 15 seconds at 10,000g. Flow through was discarded and a second wash was repeated using 500µl Wash Solution 2/3. Following the

second wash, the filter and collection tube were centrifuged for 1 minute at 10,000g to remove residual fluid from the filter. The filter cartridge was transferred to a fresh collection tube and 40µl of pre-heated (95 C) RNAse-free H20 added to the filter, and the assembly centrifuged for 30 seconds at 13,000G to recover RNA. Flow-through was run through the filter again for 30 seconds at 13,000G to ensure maximum recovery. RNA purity and abundance was measured using a NanoDrop Spectrophotometer (ThermoFisher Scientific). DNA and protein contamination was ascertained through ratio of absorbance at 260nm/280nm and 260nm/230nm, respectively. Samples were treated with 1µl TURBO DNAse (Invitrogen) and incubated at 37 C in the heat block for 30 minutes. 2µl of DNAse inactivation reagent (Invitrogen) was added and sample centrifuged at 10,000g for 90 seconds at 4C to pellet inactivation beads. Samples were then reanalysed with the NanoDrop for final RNA concentration [54].

2.20 *Transcriptomics Data and Analysis*

Transcriptomics Data Set A: Total RNA sequencing data set with COPD +/- Compound 7 vs Healthy AM +/- Compound 7. RNA samples were generated as above. RNA was quantified again via Qubit at the Western CRF, and Total RNA sequencing was run by the Edinburgh Clinical Research Facility Genetics Core as detailed in the report in Appendix 4.

Bioinformatic analysis was carried out by Dr John Thompson of Thomson Bioinformatics, Edinburgh UK. In brief raw sequencing FastQ files were mapped to the reference genome (UCSC hg19) using the STAR

alignment tool (STAR 2.6.1a) with filters applied to allow no more than 5 mismatches per read, read QC scores above a defined normalised threshold score of 0.66 and multimapping alignment scores no greater than 1. Following mapping overall metrics were analysed to assess the quality of each run (i.e. % reads passing QC thresholds following removal of abundant RNA reads, median coverage uniformity statistics and comparative genomic alignment distribution analyses). Transcripts Per Million (TPM) scores were then calculated for each gene across all samples. Differentially expressed genes were defined as genes displaying greater than Log2 1.5 fold change and with P-values <0.05 between two sample cohorts.

Transcriptomics Data Set B*:* COPD AM +/- D39 *Streptococcus Pneumoniae* vs Healthy AM +/- D39 *Streptococcus Pneumoniae* Affymetrix Array. . *** I did not generate this affymetrix data myself. I acquired it through a collaboration with Professor David Dockrell. I then analysed it myself , focusing on the cellular stress response and metabolism. Therefore the below information was supplied to me by Drs Joby Cole/ Martin Bewley who originally processed the samples.

RNA was extracted and hybridized onto the Affymetrix HG-U133 plus 2.0 Array. Data were analysed in R using affyPML and Limma. Enrichment analysis of Gene Ontology (GO) terms using a hypergeometric model (BiNGO App) in Cytoscape 3.0 was performed for differentially expressed genes. False discovery rates (FDR) were corrected with the Benjamini-Hochberg procedure.

2.21 *Taqman analysis of Gene expression*

The quantity of RNA used to generate cDNA was dependent on the nature of the samples and was usually in the region of 250ng. *For samples which were used to complete a data set with Transcriptomics Data set A , RNA QC and quantification was carried out by the Edinburgh Clinical Research Facility Genomics Core, to ensure consistency.

Samples for direct comparison were always normalised to generate the same quantity of cDNA and were made up to 12.4µl in RNase-free water. cDNA was made using AMV reverse transcriptase and random primers (Promega), details of the master mix used are in Appendix 5. Samples were run on a Techne Thermal cycler as follows:

- 23°C for 5 minutes
- 42°C for 2 hours
- 99°C for 2 minutes (to heat inactivate AMV RT)

Samples were stored at -20°C until use.

Gene expression was analysed using predesigned qPCR primer/probe assays (detailed in Appendix 5) and Prime Time Gene Expression Mastermix (IDT, Leuven). For all assays, samples were run in duplicate and the gene of interest expressed relative to expression of a housekeeping gene (beta-actin). Assays were run on a 7900HT Fast real-time PCR system (Applied

Biosystems) with the following negative controls: no RNA, no RT and no cDNA. Data was analysed using SDS 2.0 software (Thermo Scientific)

3 Macrophages from COPD donors have defective function

3.1 *Introduction*

In health alveolar macrophages (AM) play a critical role in maintaining homeostasis in the lung, an organ which directly interfaces with the external environment. Macrophage phagocytosis of pathogens, particulate matter and apoptotic cellular debris, results in key alterations in gene transcription, metabolic programming, antigen presentation and cytokine release and as such macrophage phagocytosis plays a critical role in triggering the innate and adaptive immune response[55,56,57].

Macrophages are highly responsive to the extracellular environment and are characterised by high degree of phenotypic plasticity. Traditional dogma dictated a strict M1 (pro inflammatory) M2 (anti-inflammatory) divide in macrophage phenotype, driven mostly by cytokine stimulation. In reality, in vivo macrophage activation is likely an ever evolving continuum of this polarisation spectrum, constantly changing and reacting to external stimuli. Macrophage exposure to, and subsequent phagocytosis of bacteria induces a proinflammatory programme, with release of inflammatory cytokines such as TNFα and IL-1 and a switch from oxidative phosphorylation to glycolysis. Knock down of HIF1α abrogates this inflammatory programme in macrophages [58,59]. Efferocytosis by macrophages protects local tissue from

the deleterious effects of necrotic cellular debris but it also initiates inflammation resolution by secreting IL-10 and TGFβ. “M2” stimuli such as apoptotic cells have been shown to reprogramme macrophages towards fatty acid oxidation and oxidative phosphorylation[60].

Fate-mapping studies in murine models indicate that alveolar macrophages can self-renew in the homeostatic state. However, during infection for example, peripherally circulating monocytes are recruited to the injured lung where they undergo differentiation into macrophages, taking on some, but not all, of the characteristics of the tissue resident macrophage[3]. A recent study was the first to tackle this concept in human lungs by utilizing a multi parameter approach to classify mononuclear phagocyte subsets in the non-diseased lung. This revealed the presence of diverse myeloid populations, even in the health. In addition to Alveolar Macrophages, there were four distinct populations, including a seemingly monocyte derived population of airway macrophages[10]. It is likely that the relative contributions of each subset may change during a chronic inflammatory state, such as COPD.

This is one possible explanation for the major dichotomy which exists in COPD lungs. Whilst the numbers of almost all immune cells are increased in the lungs of patients with COPD, macrophage numbers are upwards of five times the amount found in the non-diseased lung. In fact, macrophage abundance, unlike other innate immune cells, directly correlates with disease severity[61]. This represents a major disconnect in innate immunity as despite increased numbers of macrophages in the airways of these patients, there is

pathogen persistence coupled with chronic inflammation. One hypothesis is that due to the chronic distribution of homeostasis in COPD, a higher proportion of macrophages in COPD airways are recruited from peripherally circulating monocytes, with differing functional capacity to the resident cells. However a study by Ravi et al showed that COPD monocytes have decreased migratory ability and suggested that increased macrophage numbers in COPD lungs may be due to delayed apoptosis[62]. This would mirror recent findings that alveolar macrophage apoptosis is required for late stage killing of streptococcus, but does not occur in COPD lungs[38]. Thus, the origin of airway macrophages in COPD still remains unclear. However, it is extremely likely that a combination of differential macrophage origins, coupled with the combative inflammatory microenvironment of the COPD lung, is likely driving the profound macrophage dysfunction seen in COPD.

To date changes across a catalogue of macrophage functions have been described in COPD. Exposure of macrophages to cigarette smoke leads to upregulation of several molecules known to induce tissue damage in COPD, such as MMP-9,MMP-12 – long implicated in lung parenchymal destruction - and NADPH oxidase, leading to increased levels of ROS and subsequent elevated oxidant stress[43]. Increased chemokine release further exacerbates a highly cellular and inflammatory environment, with amplified release of IL-8 and TNFα (potent neutrophil chemokines) and CCL2 (monocyte chemoattractant protein 1)[63]. However, arguably the most crucial defect in

COPD macrophages is their impaired bacterial phagocytosis and efferocytosis (phagocytosis of apoptotic cells).

A number of in vitro studies have shown that in COPD, AM phagocytosis of bacteria which colonise the lungs of these patients, such as non-typeable *Haemophilus influenzae* (ntHi) and *Streptococcus pneumoniae* (Spn), is greatly reduced. A similar defect has been described for efferocytosis of apoptotic cells [36,37,40]. Whilst reduced phagocytosis and efferocytosis has been described in the macrophages of smokers with preserved spirometry, this defect is significantly more pronounced in COPD patients, regardless of their smoking status, with reductions as high as 20-50% described across both processes [37,60]. This phenotype is not confined to the lung and has been demonstrated in circulating COPD Monocyte-Derived Macrophages, though study findings have conflicted between groups. A study by Taylor et al and more recently work published in conjunction with our collaborator Professor David Dockrell, confirmed a bacterial phagocytic defect in monocyte-derived macrophages from COPD patients[38,36]. This finding challenges the long held concept that macrophage dysfunction in COPD is caused by the direct insult of cigarette smoke and the inflammation perpetuated by it. If COPD monocyte-derived macrophages display impaired function prior to migrating to the lung, it is unlikely that this phenotype could be rescued via tissue imprinting by a diseased organ. Once again, this speaks to the concept that an increased presence of monocyte-derived macrophages in the COPD lung,

leads to an increased overall macrophage presence with poor macrophage mediated immunity.

The discovery of impaired bacterial phagocytosis in a group of patients where colonisation, a major risk factor for exacerbation, morbidity and mortality, can be as high as 50%, has resulted in many studies aimed at determining the specific cause for impaired internalisation rates in COPD[34]. Bacterial phagocytosis involves recognition of the invading pathogen by pathogen-recognition receptors and a subsequent complex co-ordination of pathways relating to transcription, metabolism, protein modification etc, eventually culminating in pathogen internalisation and its destruction within the phagolysosome. Thus, many groups have interrogated macrophage surface marker expression as a possible source for impaired pathogen uptake. A number of these markers such as HLADR, CD80, CD163, and TLR3 have been identified as differentially expressed between COPD and Healthy macrophages[64,65]. However, there is a lack of consensus across studies and this, coupled with phagocytic defects found across a wide range of pathogens and apoptotic bodies, suggests that discrepancies in cell surface marker expression is unlikely to be the main driver of the phenotype. Interestingly, one study did find that COPD AM displayed a higher number of both M1 and M2 markers, with dual polarisation progressing with disease severity, suggesting that COPD AM do have a unique disease-specific phenotype[66]. Detailed transcriptional analysis of airways macrophages by Shaykhiev et al also found a distinct phenotypic pattern. Though now

recognised to be an overly rigid view of macrophage function, they compared COPD airway macrophages to known polarised macrophage modules and found that COPD AM possess a distinct transcriptional phenotype at baseline, with partial M1 downregulation and partial M2 upregulation[51]. Similarly, a study in which the transcriptional profile of COPD AM was compared to a generated library of 299 macrophage activation transcriptomes, revealed an unexpected loss of inflammatory signatures in the COPD cohort[67] . Whilst very informative studies, they do emphasise the need to couple transcriptional profiling with functional assays as to date these have revealed a highly inflammatory response in COPD AM, with impaired “M2” functions ie efferocytosis.

Thus, defective macrophage function is a major driver of persistent inflammation, the histological hallmark of COPD. There exists a major disconnect in immune responses as despite increased numbers of macrophages in the airways of these patients, there is pathogen persistence coupled with chronic inflammation. It is currently non known if this is due to a different cohort of macrophages populating the lung in COPD or primarily due by local environmental factors. Whilst many immune responses are altered in COPD, in vitro studies suggest that impaired macrophage bacterial phagocytosis and efferocytosis may be a major driver of disease. There is evidence for an impaired transcriptional programme at baseline in COPD AM [50], and certain surface marker expression has been found to be altered, albeit with some variability, but the specific driver of impaired macrophage

function has yet to be elucidated. It is currently unknown if cigarette smoke exposure triggers an inherent macrophage defect in susceptible individuals, or whether a defect already exists which is propagated by cigarette smoke exposure and the causal relationship leading to altered function in MDM merits particular attention.

Regardless of the cause , impaired macrophage phagocytosis and efferocytosis further perpetuates inflammation by leading to ongoing recruitment of immune cells with excess levels of pro inflammatory cytokines, chemokines and ROS generation, leading to severe tissue damage. Thus, defective AM and MDM function in COPD leads to persistent inflammation that is both highly damaging and ineffective.

We hypothesized that both bacterial phagocytosis and efferocytosis would be reduced in COPD macrophages. Crucially, we wished to separate macrophage dysfunction driven by local tissue specific factors from a systemic defect arising in the bone marrow, by profiling both AM and MDM from COPD patients and Healthy Controls. We sought to gain insight into the mechanisms driving macrophage dysfunction and to understand the physiological relevance it had for patient outcomes.

Results:

3.2 *Demographic data of recruited patients*

To characterise macrophage dysfunction in COPD, donors were recruited for either bronchoscopy, venepuncture or both procedures (Chapter 2.1).

Donors with COPD, free from exacerbation, were age matched to Healthy Control donors ± 7 years (mean age). COPD and Healthy Non-smokers had a female:male distribution of 52%:48% and 60%:40% respectively. Healthy smokers were all male. Forced expiratory Volume in one second (FEV_1) was significantly lower in COPD donors as expected, p=<0.0001, unpaired t-test.

Our COPD cohort included mild (25%) moderate (52%), severe (21%) and very severe disease (2%), as per the GOLD classification system (Appendix 6). 25 of 42 patients with COPD (52%) had a history of frequent exacerbations (>2/yr). There was no significant difference in pack-years of cigarette exposure between COPD donors and Healthy Smokers (p=0.11, unpaired t-test). 45% of our COPD donors continued to smoke. The COPD Assessment test (CAT) is a validated health-related quality-of-life questionnaire (Appendix 7) and was used to measure symptoms, with a higher score indicating worse symptomology. 82 % or 39/48 COPD donors had CAT scores >10, standardly used as a cut off to stratify patients with more severe symptoms (GOLD guidelines 2019). Approximately 50% of our cohort were not prescribed an inhaled steroid at the time of recruitment.

	Healthy Non smokers	Healthy Smokers	Subjects with COPD
No of Subjects	20	5	48
Age (yr)	53 (31-70)	50 (36-68)	60 (39-77)
Sex female/male	12/8	0/5	25/23
FEV1 (L)	3.1 ± 0.7	3.5 ± 0.3	1.7 ± 0.5
FEV1 (% predicted)	105 ± 12.9	98 ± 4.1	64 ± 17.30
Gold Stage	N/A	N/A	12 Stage 1 25 Stage 2 10 Stage 3 1 Stage 4
Exacerbation per year 0/ >1/>2 / ≥3	N/A	N/A	14/9/18/7
Smoking status Current/Ex/Never	0/0/20	5/0/0	22/26/0
Pack years	n/a	30 ± 10	36 ± 14
CAT score (Max 40)	N/A	N/A	16 ± 8
Inhaled Medication: ICS+LABA / LAMA / SABA	N/A	N/A	25/32/31

Figure 3.2: Demographic data.
Patients were recruited via the RIE Clinical Research Facility and existing NHS bronchoscopy lists. Not all patients underwent both bronchoscopy and venepuncture. Values are presented as mean ± SD or range. FEV_1= Forced Expiratory Volume in 1 second, Gold Stage classification of COPD severity, (Appendix 6). CAT score = COPD symptom Assessment Test (Appendix 7). Pack year = 20 cigarettes per day for 1 year. ICS= Inhaled corticosteroid, LABA= Long acting Beta Agonist, LAMA= Long Acting Anti Muscarinic, SABA= Short Acting Beta Agonist.

3.3 *Alveolar and Monocyte-derived macrophages from COPD donors have impaired bacterial phagocytosis and efferocytosis*

To establish if COPD macrophage dysfunction was a result of tissue specific factors, airway macrophages and peripherally circulating monocyte-derived macrophages from COPD donors were compared to Healthy controls. Alveolar Macrophages (AM) were isolated from bronchoalveolar lavage fluid . As discussed BAL fluid macrophages likely represent a heterogenous macrophage population consisting of tissue resident macrophages and infiltrating peripherally derived Monocyte-derived macrophages (MDM) . The relative contribution of macrophages from each source likely differs between Healthy and COPD donors. Blood MDM were isolated from peripheral blood and both AM and MDM were purified via the adherence method, as outlined in Chapter 2.3.

Macrophages were co-incubated with live opsonised S14 *S.pneumoniae* (Figure 3.3 A+B) and PKH26 labelled apoptotic neutrophils (Figure 3.3 C+D) to establish internalisation rates. COPD AM bacterial phagocytosis was significantly reduced compared to Healthy Controls (n= 8 and 6, mean bacterial count recovered 2.36 vs 3.2 cfu/ml). Efferocytosis rates were also significantly reduced in COPD AM compared to Healthy Donors (n=11 and 8, mean 34**%** vs 13**%**).

We then performed these assays in monocyte-derived macrophages (MDM) to delineate the effect of the inflammatory niche on macrophage function, from the systemic effects of COPD. Strikingly, MDM exhibited the same defect in phagocytosis and efferocytosis as COPD AM (Figure 3 B+D). COPD mean MDM bacterial phagocytosis was significantly reduced compared to Healthy MDM (n= 8, mean bacterial count recovered 2.99 vs 3.51 cfu/ml). Similarly, efferocytosis was significantly lower in COPD donors (n=10, 14% vs 33%). While internalisation rates were reduced in both MDM and AM, COPD AM displayed a greater percentage reduction in function compared to Healthy donor , in both phagocytosis and efferocytosis (= 27% vs 15% and 62%vs 58% respectively).

Rates were lowest in current smokers across both processes, as previously described[68], but macrophage dysfunction did not recover in COPD patients who were no longer active smokers.

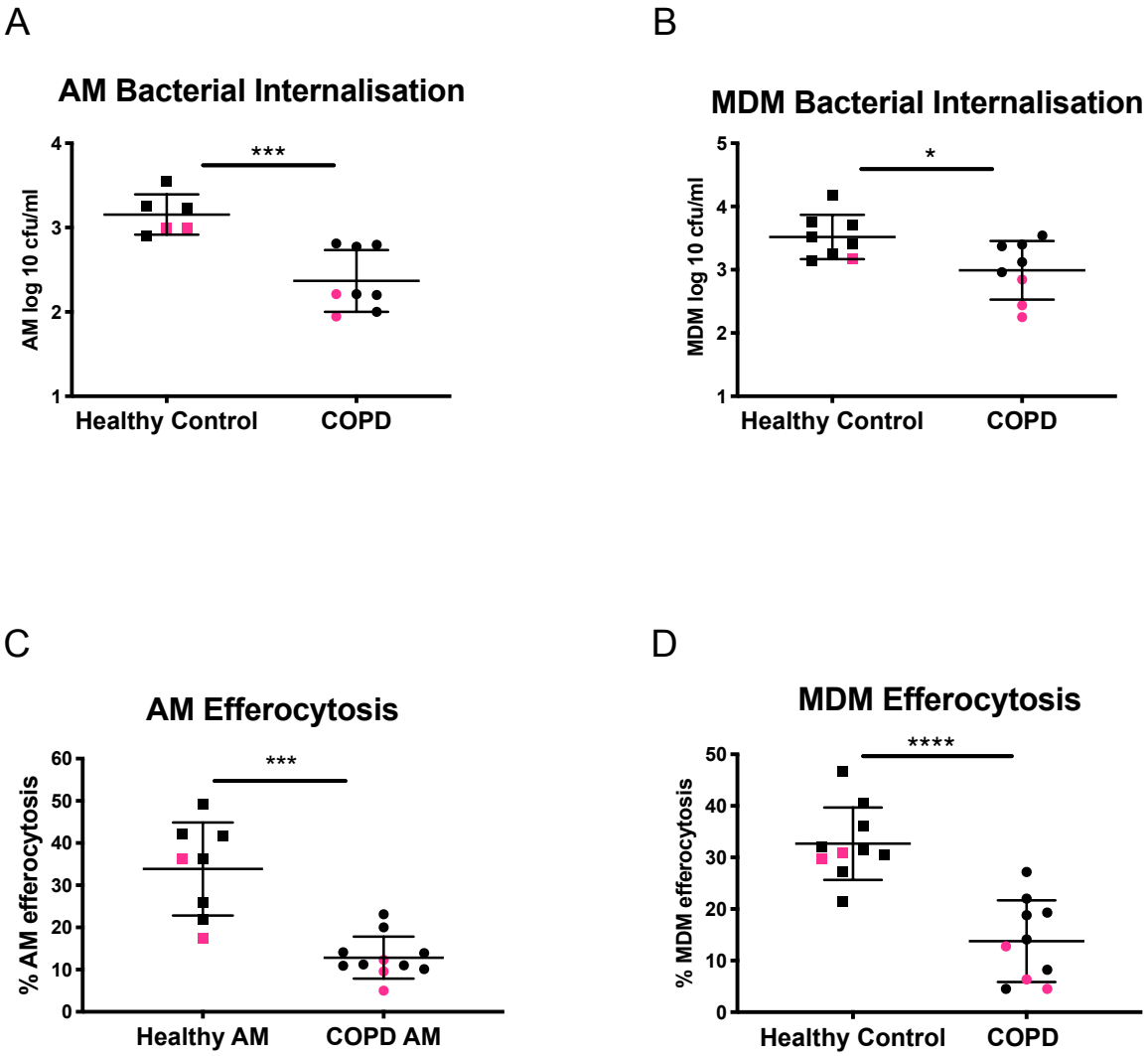

Figure 3.3: COPD donors have impaired phagocytosis and efferocytosis compared to Healthy Volunteers.
(A-D) Alveolar and Monocyte-Derived Macrophages from Healthy Controls and COPD Donors were challenged with (A,B) opsonised serotype 14 *S. pneumoniae*, 4h post challenge, numbers of viable bacteria were measured or (C,D), co-incubated with PKH26 labelled 20h apoptotic neutrophils and efferocytosis rates were measured by flow cytometry. ● = current smokers. P values calculated by unpaired t-test, *P ≤0.05, *** P≤0.001 ****P≤0.0001.

3.4 *COPD macrophages have preserved early bacterial killing*

To establish if the high rates of colonisation which characterize COPD airways were due to a combination of both impaired phagocytosis and impaired bacterial killing, we compared early (up to 10 hrs) bacterial killing in COPD donors. Late stage killing is mediated via macrophage apoptosis and has previously been shown to be defective in COPD[69].

S. pneumoniae was opsonised with serum from vaccinated donors (as per 2.10). Cells were then co-incubated with opsonised and non opsonised S14 *S. pneumoniae* and after the addition of antibiotics at four hours, were lysed at sequential time points. While internalisation rates were lower in COPD, as described, the slope of recovered cfu/ml was comparable between COPD and Healthy donors, confirming that they do not have a defect in early *Streptococcus pneumoniae* killing (Figure 3.4 A-D). These assays were performed by Dr Martin Bewley , a post-doctoral researcher in the lab of our collaborator on this project, Professor David Dockrell and have been published [38].

It is important to note the prominent defect in opsonic bacteria phagocytosis in the COPD donors. Reduced availability of opsonin could potentially lead to downregulation of opsonin mediated phagocytosis and a greater defect in this pathway. Consequently, we interrogated bronchoalveolar lavage (BAL) fluid from donors and confirmed that unconcentrated BAL samples from COPD donors had comparable levels of pneumococcal antibodies to Healthy donors (Figure 3.4 E).

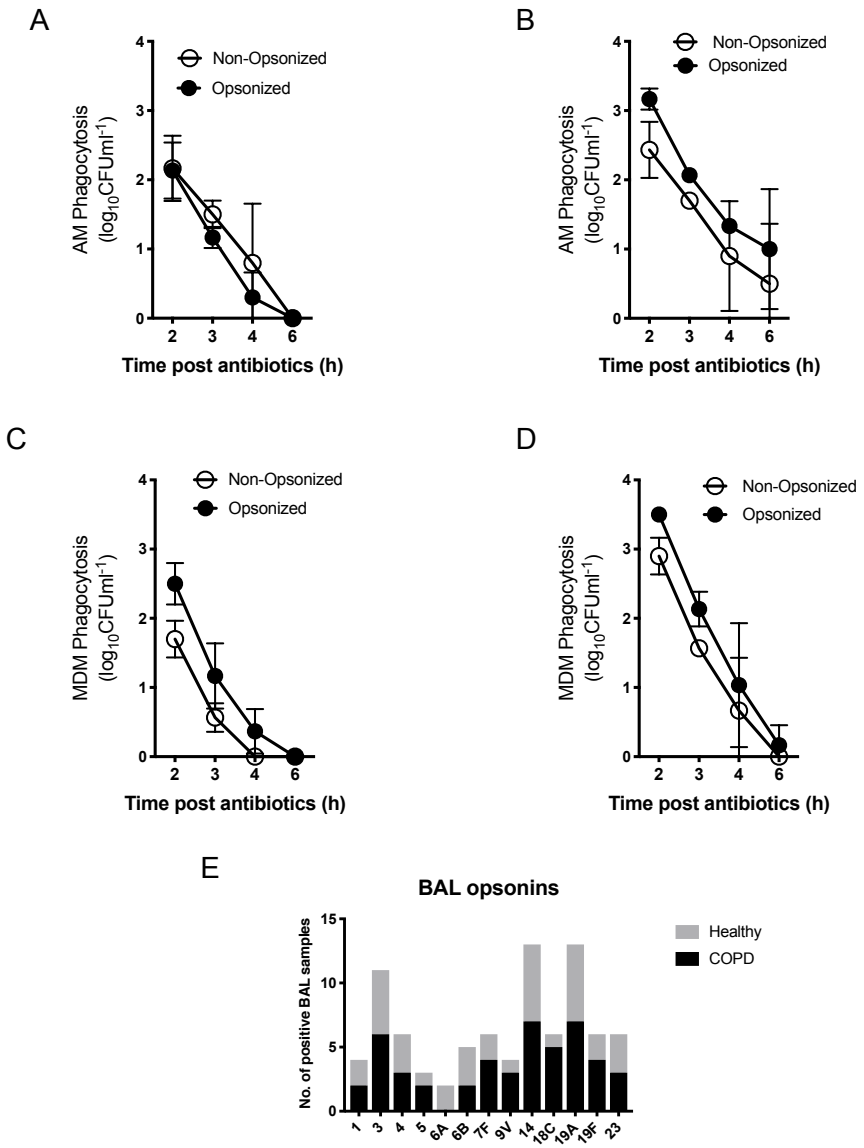

Figure 3.4: COPD Macrophages show no defect in early phase bacterial killing and COPD donors maintain their ability to produce opsonins. AM or MDM were collected from patients with COPD (A and C) or Healthy Donors (B and D) and were challenged with non-opsonised or opsonised serotype 14 S. pneumoniae for 4h, before extracellular bacteria were killed by the addition of antibiotics. At the designated time post antibiotics, viable bacteria in duplicate wells were measured, n=3. No significant differences were seen in any groups.(E) Pneumococcal antibodies were detectable by multiplex immunoassay in bronchoalveolar fluid from COPD (n=16) and Healthy (n=13) donors.

♦Experiments in Figures A-D were performed by Dr Martin Bewley

3.5 *Decreased opsonic bacterial phagocytosis in COPD correlates with markers of disease severity, but not with age*

To establish if there was a direct clinical read out of impaired bacterial phagocytosis in COPD, correlation analysis of opsonized phagocytosis of *S. pneumoniae* against FEV_1 was performed. FEV_1 is an objective marker of airway inflammation and narrowing and is the central component of COPD severity stratification. We found a significant relationship between FEV_1 % predicted (Actual Donor FEV1 as a % of their predicted FEV1 based on height and age) and macrophage bacterial phagocytosis (Figure 3.5 A). Similarly we found a negative correlation between impaired opsonic bacterial phagocytosis and scores representative of increased symptom severity (high CAT scores- Appendix 7) (Figure 3.5 B). Unlike age related findings in other innate immune cells[30], macrophage opsonic bacterial phagocytosis did not correlate with donor age (Figure 3.5 C).

Figures 3.5 A + B were compiled in conjunction with data produced by Dr Martin Bewley, a post-doctoral researcher in the lab of our collaborator on this project Professor David Dockrell.

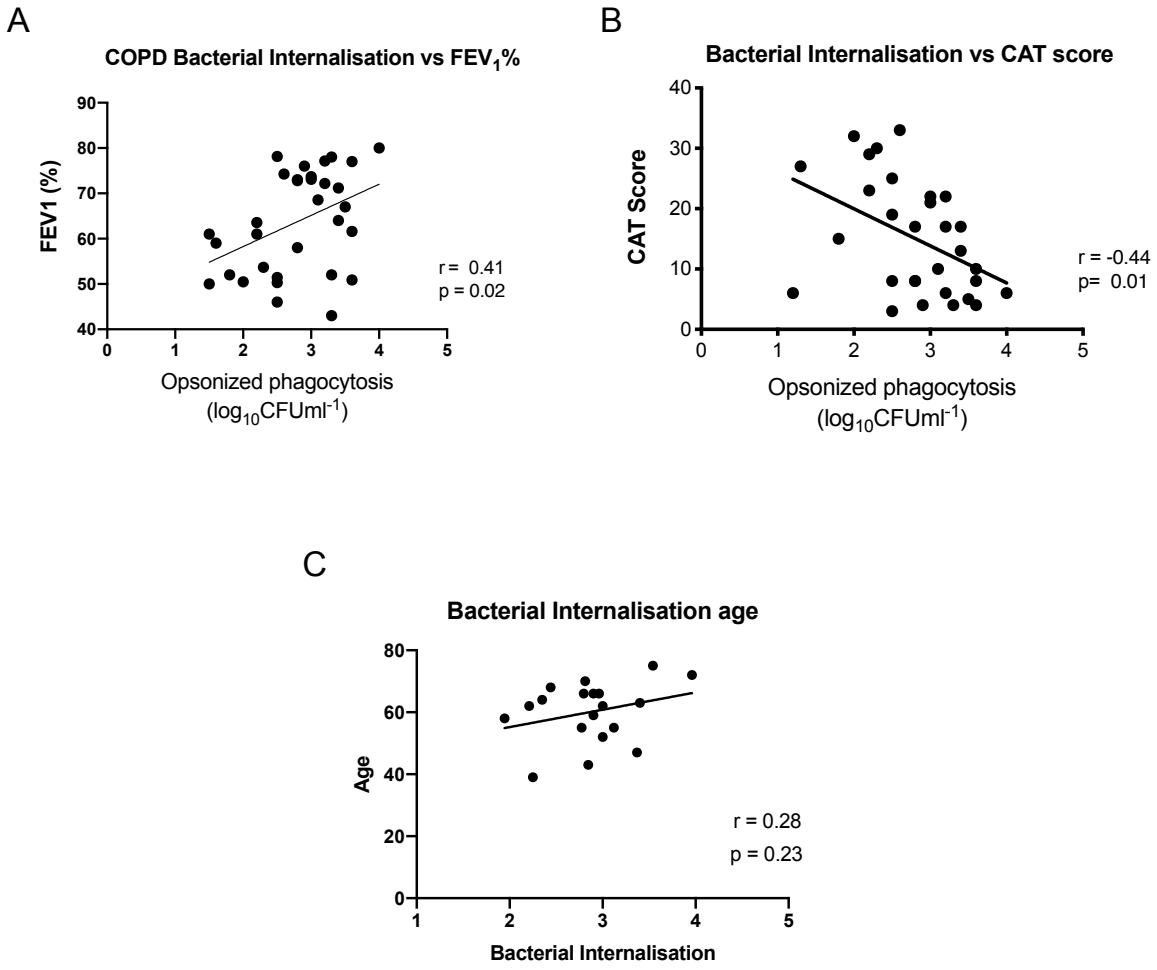

Figure 3.5: Opsonised macrophage bacterial phagocytosis correlates with markers of disease severity but not with age.
Opsonised bacterial phagocytosis correlates with FEV_1% predicted (A) and symptom severity as measured by the CAT score (B). There was no significant correlation between opsonised bacterial phagocytosis and age (C). Pearson's correlation coefficient (r) and p values shown.

3.6 *Efferocytosis by COPD macrophages correlates with markers of disease severity, but not with age*

To determine the clinical impact of impaired efferocytosis, macrophage efferocytosis was correlated with makers of disease severity. AM Efferocytosis from COPD donors was highly correlated with objective measures of airflow limitation (FEV_1% predicted) (Figure 3.6 A). In contrast, no significant correlation was seen between peripherally circulating MDM and FEV_1% (Figure 3.6 B). COPD macrophage efferocytosis rates were negatively correlated with self-reported markers of disease severity, as measured by the CAT questionnaire(Appendix 7) (Figure 3.6 C). Corresponding to our findings in bacterial phagocytosis, neither COPD nor Healthy donor macrophage efferocytosis rates correlated with age- shown as a cumulative plot (Figure 3.6 D).

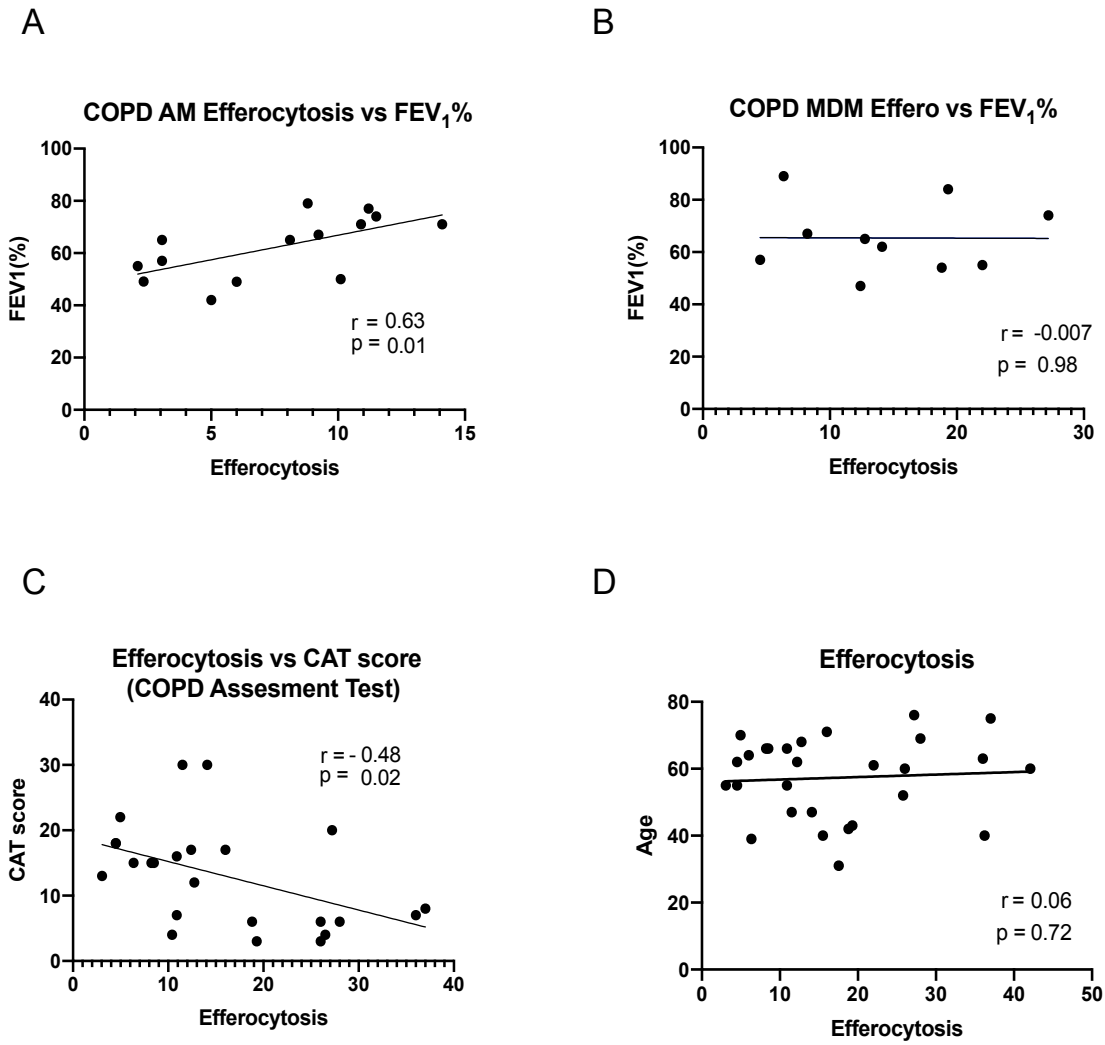

Figure 3.6: Efferocytosis by COPD AM only, correlates with markers of disease severity age. Macrophage efferocytosis does not correlate with age.

(A) COPD AM display a high correlation with FEV_1% ,whilst (B) MDM efferocytosis does not. Overall COPD macrophage efferocytosis negatively correlates with symptoms of disease severity as measured by the CAT score. All donor macrophage efferocytosis does not correlate with age. Pearson's correlation coefficient (r) and P values shown.

3.7 *Phagocytosis rates correlate with efferocytosis rates suggesting a common underlying mechansim*

We questioned if a shared mechanistic defect was driving macrophage dysfunction in COPD. To investigate this we correlated bacterial phagocytosis with efferocytosis in each donor and found a high degree of correlation in both AM and MDM, providing compelling evidence for a shared underlying defect causing impaired phagocytosis and efferocytosis in COPD macrophages (Figure 3.7 A+B).

A

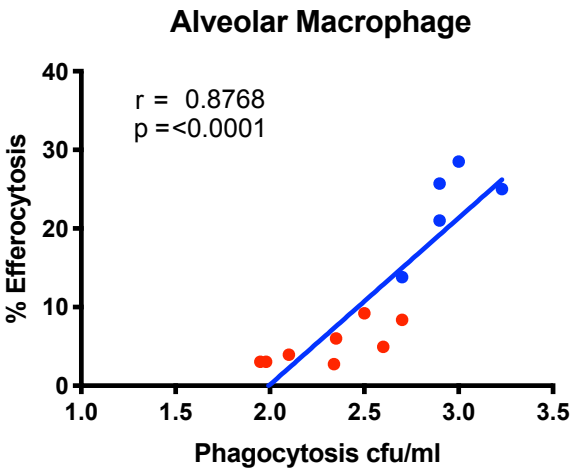

B

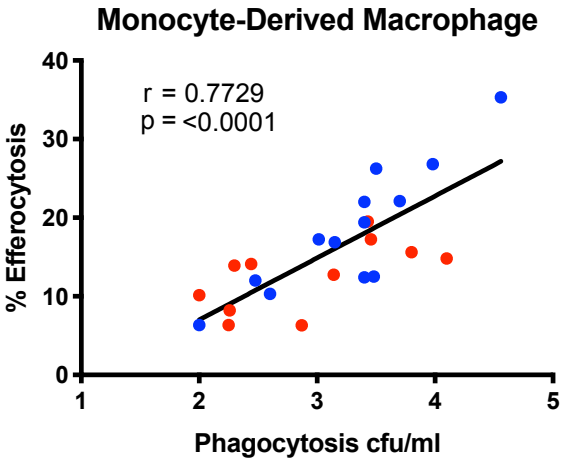

Figure 3.7: Correlation of phagocytosis rates with efferocytosis rates in AM and MDM from both COPD and Healthy Donors.
Efferocytosis of PKH26 labelled apoptotic neutrophils was correlated with phagocytosis of *S. pneumoniae* S14 in both Alveolar (A) and Monocyte-Derived Macrophages (B) from COPD and Healthy donors. ● = COPD donors. ● = Healthy donors. Pearson's correlation coefficient (r) and P values shown.

3.8 *COPD macrophages display a globally reduced transcriptional response to infection with S. pneumoniae*

To gain mechanistic insight into the defects driving macrophage dysfunction in COPD, we compared the transcriptional response of COPD and Healthy AM to opsonized *S. pneumoniae*. This specific experimental scenario was chosen over ingestion of apoptotic neutrophils, as we would be unable to entirely delineate the macrophage transcriptional signal from that of the apoptotic neutrophils, following ingestion. In addition, as phagocytosis closely correlated with efferocytosis, we hypothesised that findings related to broader cellular function would be applicable to both processes.

AM from non-smoking COPD and Healthy donors were co-incubated with opsonised D39 *S. pneumoniae* for 4h at a multiplicity of infection (MOI) of 10:1, and the transcriptional response was assessed via an Affymetrix array (Figure 3.8.1 A). There were significantly fewer differentially expressed genes, both up and down-regulated, in COPD AM in response to infection than in Healthy AM (Figure 3.8.1 B).

Interrogation of phagocytic pathways, such as surface marker expression and actin rearrangement, revealed a divergent transcriptional response to infection between COPD and Healthy AM (Figure 3.8.2). Remarkably, at four hours, only complement receptors were upregulated in Healthy AM, with no change in transcription seen in COPD AM. However, MARCO, a key

scavenger receptor for bacterial phagocytosis, was upregulated in COPD AM but not in Healthy AM. This is in contrast to previous findings that MARCO expression is lower in COPD cells and is particularly interesting in light of the potential role of MARCO in delineating AM from infiltrating MDM [8,49].

Pathogen exposure triggers a pro inflammatory response from AM, but as AM also play a critical role in orchestrating inflammation resolution, we queried if efferocytosis pathways may be upregulated in anticipation of this, following co-incubation with *S. pneumoniae*. At a four hour time point transcription of these pathways remained largely unaltered in both COPD and Healthy control AM (Figure 3.8.3). Interestingly, at this time point, only the efferocytosis receptor, MERTK, ligation of which supresses inflammatory cytokine release, was altered. It was downregulated in Healthy AM, but remained transcriptionally unaltered in COPD AM. Transcription of Protein S, a bridging molecule involved in ligation of efferocytosis receptors, including MERTK, was also downregulated in Healthy AM only[70].

The engulfment of foreign particles involves the careful and complex rearrangement of the actin cytoskeleton. We examined the transcriptional response to infection across core elements of actin organisation. Small Rho GTP-ases (eg RhoA, Rac1 Rac2, Cdc-42) bind to varied effectors such as protein kinases and actin binding proteins to affect local assembly of actin filaments.

The Arp2/3 complex nucleates branched actin and ,in conjunction with members of the Wiskott-Aldrich syndrome family protein (WAVE 2, WIP/WASP), orchestrates critical actin remodelling during phagocytosis[71]. Failure to downregulate the Rho-GTPase activating protein, ARGHAP25, has been shown to prevent closure of the phagocytotic cup[72]. We found that these co-ordinators of actin organisation were appropriately upregulated in Healthy AM, but with the exception of RhoA, no transcriptional change was induced in COPD AM following infection.

Differential transcription responses between Healthy and COPD AM, were not limited to phagocytotic mechanisms. Pathways relating to fundamental cellular processes such as metabolism and anti-oxidant responses were also differentially regulated (data not shown here, discussed in Chapters 4+5).

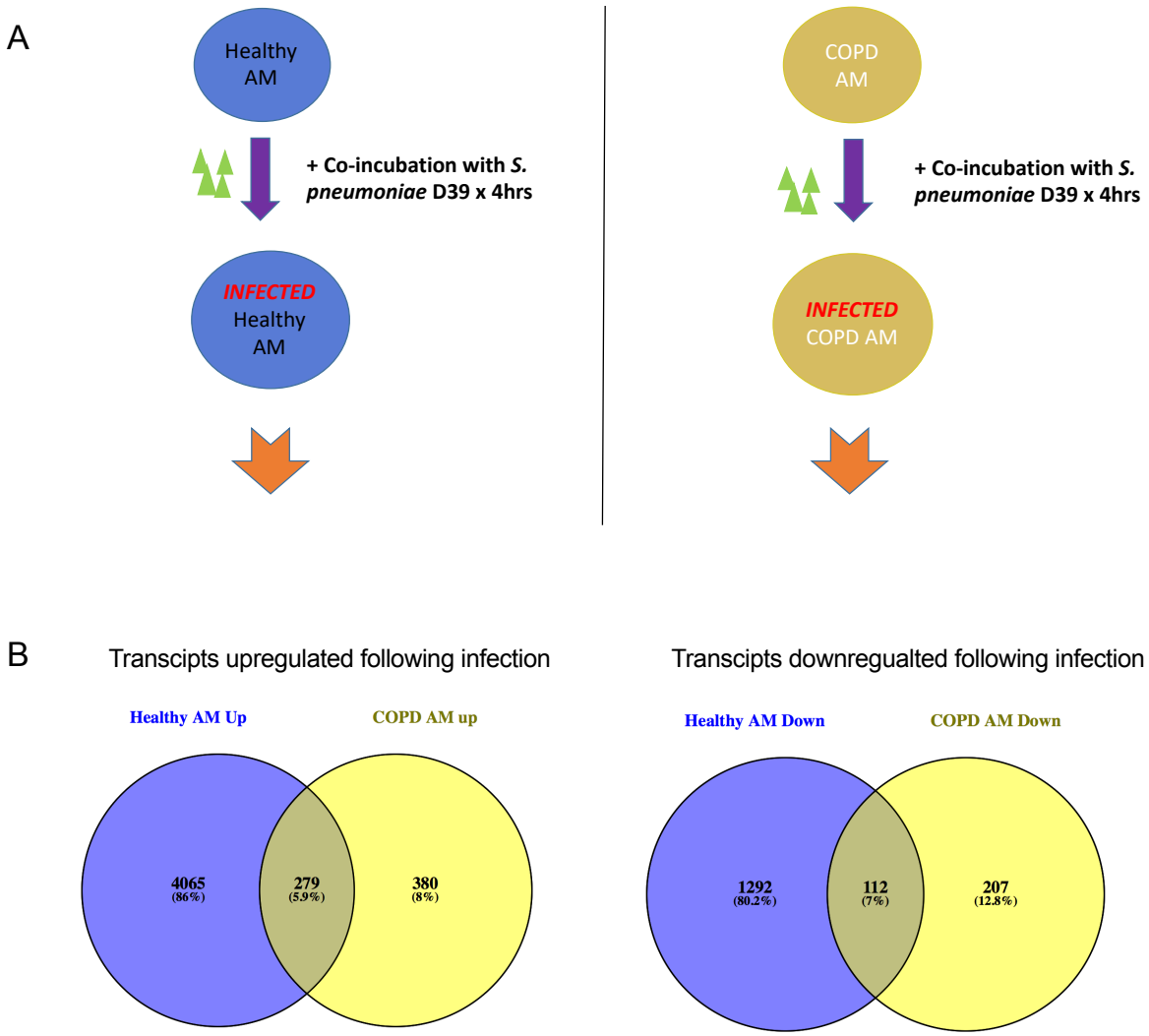

Figure 3.8.1: Affymetrix array reveals a reduced transcriptional response to *S. pneumoniae* in COPD Alveolar Macrophages.
AM from COPD and Healthy Control donors were exposed to D39 S. pneumoniae, MOI 10:1, for 4 hours, before total cellular RNA was collected for transcriptional analysis. (A) Schematic representation of experimental conditions. (B) Venn diagram illustrating the number of genes upregulated or downregulated in Alveolar Macrophages in response to infection with S. pneumoniae D39

Phagocytosis Receptors:	Ensemble ID:	COPD AM:	Healthy AM:
CD36	ENSG00000135218	⟷	↓
MARCO	ENSG00000019169	↑	↓
SCAR1	ENSG00000038945	⟷	↓
Cd32b	ENSG00000072694	⟷	↓
CD32c	ENSG00000244682	⟷	↓
Complement Receptor 1/CD35	ENSG00000203710	⟷	↑
Complement Receptor 3/ CD18	ENSG00000160255	⟷	↑
Complement Receptor 3A/CD11B	ENSG00000169896	⟷	⟷
TLR 1-6		⟷	⟷

Figure 3.8.2: Transcription of phagocytic receptors is minimally changed in COPD Alveolar Macrophages following infection with *S.pneumoniae*.

In response to infection with *S. pneumoniae*, Healthy Controls alter transcription of phagocytic receptors, in particular upregulating transcription of complement receptors. Transcription of the scavenger receptor, MARCO, was upregulated in COPD AM in response to infection.

Efferocytosis Specific Receptors:		COPD AM:	Healthy AM:
TIM1	ENSG00000113249	⟷	⟷
TIM3	ENSG00000135077	⟷	⟷
TIM4	ENSG00000145850	⟷	⟷
Stabilin-1	ENSG00000010327	⟷	⟷
Stabilin-4	ENSG00000136011	⟷	⟷
RAGE	ENSG00000204305	⟷	⟷
MERTK	ENSG00000153208	↓ (-1.23)	↓ (-1.64)
Axl	ENSG00000167601	⟷	⟷
LRP	ENSG00000123384	⟷	⟷
Rab11a	ENSG00000103769	⟷	⟷
Tyro3	ENSG00000092445	⟷	⟷
$\alpha_v\beta_{3/5}$	ENSG00000138448	⟷	⟷
SCARA3	ENSG00000168077	⟷	⟷
CD14	ENSG00000170458	⟷	⟷
Bridging Molecules for Efferocytosis			
Thrombospondin	ENSG00000137801	⟷	⟷
Gas6	ENSG00000183087	⟷	⟷
Protein S	ENSG00000184500	⟷	↓
MFGE8	ENSG00000140545	⟷	⟷

Figure 3.8.3: Transcription of the efferocytosis pathway is largely unaltered in Alveolar Macrophages at 4hours post initial incubation with *S.pneumoniae*.

With the exception of MERTK, receptors which specifically mediate efferocytosis were transcriptionally unaltered in both COPD and Healthy Control AM after 4 hours of co-incubation with *S.pneumoniae*. Transcription of the bridging molecule protein S was downregulated in Healthy AM but was unchanged in COPD AM. Log_2 fold change in gene expression listed in brackets where genes are altered in the same direction in both COPD and Healthy AM.

ACTIN/CYTO-SKELETON	ENSEMBLE ID	COPD AM:	Healthy AM:
RhoA	ENSG00000067560	↑	↔
Rac1	ENSG00000136238	↔	↑
Rac2	ENSG00000128340	↑ (0.74)	↑ (0.88)
FNBP1	ENSG00000187239	↔	↑
PAK1	ENSG00000149269	↔	↑
PIPK51B	ENSG00000107242	↔	↑
Arf6	ENSG00000165527	↔	↑
ARPC2	ENSG00000163466	↔	↑
ARPC5	ENSG00000162704	↔	↑
ARPC5L	ENSG00000136950	↔	↑
WAVE2	ENSG00000158195	↑ (0.35)	↑ (0.815)
WIP/WAS2	ENSG00000115935	↔	↑
HS1	ENSG00000143575	↔	↑
ARHGAP25	ENSG00000163219	↔	↓
PKC α	ENSG00000154229	↑ (0.7)	↑ (1.76)
MARCKS	ENSG00000277443	↔	↑
MacMarcks	ENSG00000175130	↔	↑
Profilin 1	ENSG00000108518	↔	↑

Figure 3.8.4: Co-incubation with *S. pneumoniae* induces differential transcriptional programmes in actin cytoskeletal organisation, in Healthy and COPD AM.

Healthy AM alter transcription of key components of the actin cytoskeleton required for successful phagocytosis, following co-incubation with *S. pneumoniae*. COPD AM alter some but not all of these components and uniquely upregulate RhoA, in response to infection. Log_2 fold change in gene expression listed in brackets where genes are altered in the same direction in both COPD and Healthy AM

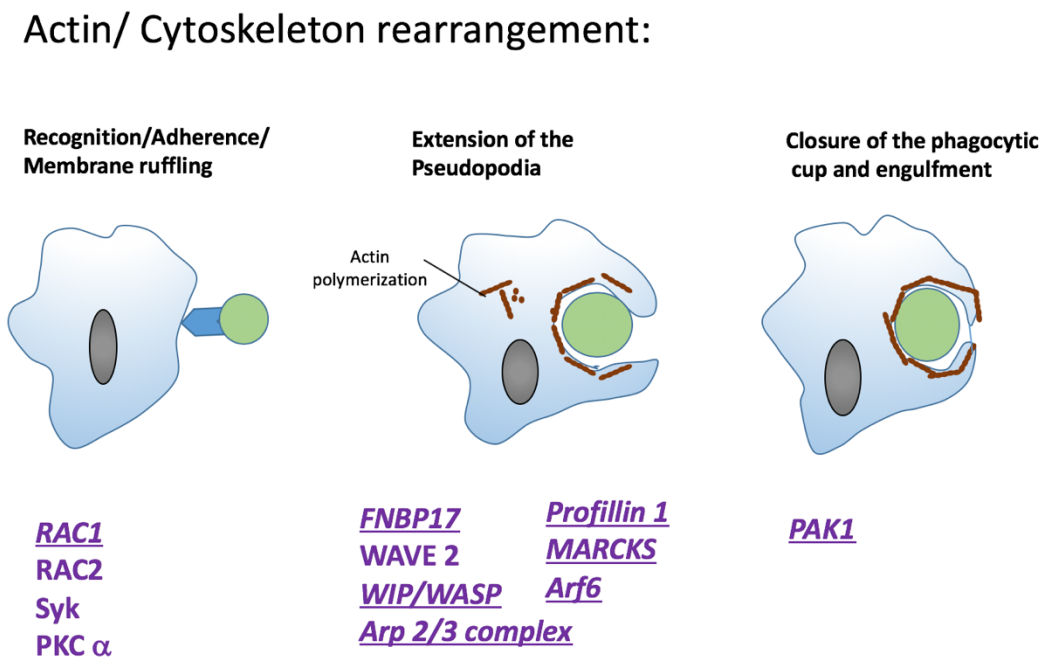

Figure 3.8.5: Schematic of key elements of cytoskeleton re arrangement required for phagocytosis.
Key alterations in the actin cytoskeleton during phagocytosis are transcriptionally altered in Healthy but not COPD AM in response to co-incubation with *S. pneumoniae*.

3.9 *Discussion*

The data in this chapter outlines the main phenotype of macrophage dysfunction in COPD. Crucially by recruiting patients for both bronchoscopy and venepuncture, we have been able to define this phenotype both in alveolar macrophages, directly influenced by the lung microenvironment, and in peripherally derived monocyte-derived macrophages, existing in an oxygen and nutrient rich environment.

In keeping with previous findings, AM from COPD donors had reduced bacterial phagocytosis of *S pneumoniae* and efferocytosis of apoptotic neutrophils.[37,40]. Interestingly , in our hands, COPD MDM also displayed dysregulated phagocytic capacity suggesting macrophage dysfunction in COPD is not solely governed by lung specific factors. There has been much debate over conflicting findings in functional assays of COPD MDM, with some studies finding a similar defect to that found in AM and others finding the defect in AM alone[37]. It has been hypothesised that this discrepancy was due to the use of certain cytokines eg GM-CSF, driving the cell towards a more " tissue like " phenotype during culture[36]. Differentiation using cytokines introduces a major element of variability as there is potentially an altered response to cytokine stimulation in a diseased state. Instead our MDM were differentiated using the well-established adherence method, without use of cytokines to "drive a polarisation state", thus removing this variable[38]. It is consequently all the more striking to observe the phenotype in MDM, which have been cultured for ≥12 days in a substrate

replete environment. This suggests that the mechanism for macrophage dysfunction is hard wired in this population and not corrected by excess substrate availability. There is now a major focus on the potential epigenetic nature of COPD as a disease entity and this data provides evidence that a global defect rather than tissue specific modulation is altering macrophage function in COPD. This in turn invites discussion as to why this defect is so predominantly manifest in the lung? This may be due, in part, to the direct interface between the external environment/pathogens and immune cells of the lung. There may be aberrant tissue imprinting on infiltrating cells due to existing damage from cigarette smoke. Alternatively baseline dysfunction in the infiltrating MDM population may be contributing a larger proportion to the airway macrophages in COPD, leading to compromised immunity and recurrent infection.

We observed a selective defect in AM opsonic bacterial phagocytosis, which was not driven by an opsonin scarcity in the airways, and as established by previous studies, not driven by AM Fc receptor expression [38] [49]. Despite producing appropriate quantities of opsonin, impaired opsonic phagocytosis will likely influence the efficacy of pneumococcal vaccination in these patients in whom *S. pneumoniae* is the leading cause of community acquired pneumonia.

Impaired bacterial phagocytosis is one obvious cause for colonisation in the airways of COPD patients, which can be as high as 50%. Colonisation with pathogens such as *Haemophilus influenzae*, *Streptococcus pneumoniae* and

Pseudomonas aeruginosa is major risk factor for the exacerbations which are the lead cause of mortality in COPD patients [34]. In light of these high colonisation rates, we were surprised to observe no defect in the early bacterial killing of *Streptococcus* in COPD macrophages. It would thus appear that the initial inability to maintain homeostasis by quiescent clearing of pathogens, is due to a selective impairment of phagocytosis rather than a universal failure in macrophage function eg phagolysosomal acidification, though dedicated studies are required to verify this.

To establish the physiological significance of impaired macrophage phagocytosis and efferocytosis, we examined their relationship with clinical measures of disease severity. Spirometry (which measures FEV_1) is both the gold standard for diagnosing and for classifying disease severity in COPD. Airway narrowing and loss of elasticity due to inflammation leads to a reduction in FEV_1. Thus, we were interested to observe an inverse correlation between FEV_1 and bacterial phagocytosis, suggesting that ongoing inflammation due to impaired pathogen clearance affects airway functionality. It was particularly interesting to see that only AM efferocytosis correlated with FEV_1, not MDM, in contrast to the correlation in both populations with bacterial phagocytosis. The greatest discrepancy across both process was in AM efferocytosis, where rates in Healthy AM were >6 times that of COPD AM. It is unclear why this process, in this cell, would appear to be more sensitive to the deleterious environment of COPD but one possibility is direct impairment of efferocytosis by altered extracellular matrix proteins following cigarette smoke exposure [73]. Alternatively,

a correlation between AM efferocytosis only and FEV_1 ,may be due to tissue resident AM playing a greater role in efferocytosis in the lung, than infiltrating MDM.

The COPD assessment test (Appendix 7) is a well validated questionnaire exploring symptom severity such as mucus production and breathlessness. FEV_1 has previously been found to correlate poorly with patient symptomology[74]. It was therefore particularly significant to find a correlation between both bacterial phagocytosis and efferocytosis and high CAT scores . As mucus production, cough and wheeze are included in the CAT score, this suggests that the physiological processes leading to these symptoms may be driven by macrophage dysfunction.

Another key finding was the high correlation between donor phagocytosis and efferocytosis, providing convincing evidence for a shared underlying mechanism. Phagocytosis and efferocytosis involve the ligation and downstream signalling of some over lapping but many distinct cell surface receptors and so this correlation suggests a broader underlying defect is driving macrophage dysfunction in COPD. It is tempting to implicate points of convergence of both signalling pathways eg Rho activation and Phosphoinositide 3-kinase as the cause. However previous studies carried out by our group failed to improve both processes by manipulating these pathways[75].

The dramatically reduced transcriptional response to *S. pneumoniae* in COPD AM provides insights into the mechanisms driving impaired bacterial phagocytosis. As discussed, there is existing data showing a distinct transcriptional phenotype at baseline in COPD, but we were unsure how this would affect the induced response following infection. It was surprising to see that only complement receptors were induced in Healthy AM at 4 hours following co-incubation with *S. pneumoniae.* This may be because basal transcription of these receptors is lower than other pattern recognition receptors- which possess a broader functionality. A failure to upregulate these in COPD AM may account for the greater defect in opsonised phagocytosis compared to non opsonised (Figure 3.4). Upregulation of MARCO was an unexpected finding in COPD AM, as low levels of MARCO expression have previously been demonstrated in COPD macrophages[76] . Upregulation of MARCO expression has been proposed as the mechanism for reversal of impaired bacterial phagocytosis by sulforaphane, an antioxidant drug, which will be discussed later. Importantly, our data provides us with transcriptional information only as we did not interrogate MARCO cell surface receptor via flow cytometry in these cells.

As 4hrs of exposure to Streptococcus represents the early response to pathogens in macrophages, it was not too surprising to see minimal change in transcription of efferocytotic pathways in either Healthy or COPD AM.

However, in COPD AM, there was a striking failure to regulate modules required for actin polymerization, its localization to the phagocytic cup and closure of the cup following engulfment. It is important to note the

upregulation of RhoA in COPD AM following infection. Successful internalisation of particles requires care fine tuning of small-GTPases and actin arrangement modules with time critical upregulation and subsequent downregulation of core elements, required for success. Previous work by our group demonstrated an improvement in efferocytosis but not bacterial phagocytosis using a small molecule inhibitor of Rho kinase[75]. It is unclear why this did not work in bacterial phagocytosis considering our findings, but may relate to the timing of upregulation of RhoA.

Interestingly actin remodeling has been linked to MARCO cell surface expression[77]. A failure to upregulate actin remodeling programmes in COPD AM may account for our observed increase in MARCO transcripts, despite previous description of reduced MARCO cell surface expression in these cells.

The transcriptional response to infection in COPD AM was also altered in pathways relating to broader cellular function including metabolism and oxidative stress, which will be discussed in later chapters.

It is worth noting that the altered response across all pathways interrogated is does not merely represent a quiescent transcriptional response in COPD AM. In some instances, transcription of entirely different genes takes place in COPD AM compared to Healthy AM. This is all the more striking considering how few genes are comparatively induced or downregulated in COPD AM in response to infection. It is unclear if this suppression of transcription is driven by lack of

availability of required nucleotides, an inability to sense the microenvironment or an inability to react to it .

In summary, we observed impaired bacterial phagocytosis with preserved early bacterial killing in both alveolar macrophage and monocyte-derived macrophages from COPD patients. Efferocytosis of apoptotic neutrophils was likewise reduced in both COPD AM and MDM. Identifying the same phenotype in both AM and MDM highlighted the critical importance of interrogating cells within the inflammatory niche in conjunction with peripherally circulating cells, to provide mechanistic insight into macrophage dysfunction in COPD.

Impaired bacterial phagocytosis and efferocytosis correlate with both objective (FEV_1) and subjective (CAT scores) markers of disease severity, indicating impaired macrophage function has a significant physiological impact in this population. Macrophage efferocytosis and phagocytosis are highly correlated. This suggests that despite the ligation of different cell surface receptors and activation of different down-stream signalling pathways, these processes are linked on a fundamental level. The global transcriptional response to infection with *S. pneumoniae* is significantly suppressed in COPD AM. There was differential transcription of key pathways including phagocytic surface marker expression and actin remodeling. Transcriptional differences in oxidant responses and metabolism will be discussed in later chapters but taken together these differences provide crucial mechanistic clues for macrophage dysfunction in COPD.

4 COPD macrophages display an altered metabolic profile

4.1 *Introduction*

There is a growing body of evidence that metabolic reprogramming in macrophages is inextricably linked to function and activation states. As key effectors of the innate immune response, macrophages are required to rapidly switch from relatively quiescent cells to highly active immune effectors. Fuelling high energy requiring processes such as efferocytosis and phagocytosis, requires increased levels of ATP to be rapidly generated and maintained. To facilitate this, macrophages are equipped with the necessary machinery to generate ATP via multiple metabolic pathways, namely glycolysis, oxidative phosphorylation and fatty acid oxidation. Metabolic plasticity is a crucial feature of macrophage adaptability. How macrophages utilize metabolic pathways in order to generate adequate energy is critical not only for effector function but also facilitates key phenotypic shifts.

It is widely assumed that cells possess a “reserve metabolic capacity” which they can draw on to supply increased energy when required for maintenance of cellular function, instigation and resolution of the inflammatory response and detoxification of reactive species. Evidence for the necessity of this “bioenergetic reserve”, has been confirmed in a number of cell types, where loss of energy reserves result in death on exposure to oxidative stress [78,79].

While all metabolic pathways are linked in the cell via the relative flux of metabolic intermediaries, redistribution of these intermediaries can ensure that one metabolic pathway dominates. This can depend on the polarisation state of the cell, the speed ATP needs to be generated at or substrate availability, including oxygen. Glycolysis can be performed in anaerobic conditions and leads to the rapid generation of ATP. When oxygen is readily available, oxidative phosphorylation can occur. Pyruvate generated by glycolysis is shuttled through the tricarboxylic acid (TCA) cycle, generating reducing equivalents for the Electron Transport Chain, which utilizes them to generate ATP. Glycolysis produces a net ATP yield of 2 units, Oxidative Phosphorylation yields 30-36 units and Fatty Acid Oxidation -where β-oxidation of fatty acids generates Acetyl Co-A for the TCA cycle- yields 14 units of ATP (Figure 4.1). However, ATP generation via oxidative metabolism is far slower than glycolysis. It requires intact mitochondria for electron chain transport and for a high volume of ATP generation, a degree of mitochondrial biogenesis. Hence, despite the higher yields generated via oxidative metabolism, a rapid surge in energy requirements can drive immune cells to utilize aerobic glycolysis. This preferential use of glycolysis, even in the presence of sufficient oxygen, is termed the Warburg effect and was first observed in cancer cells - though it is now known to be a “normal phenomenon” in many immune cells. Preferential flux through certain metabolic pathways can have far reaching consequences, not only for energy production for also for driving macrophage phenotypes

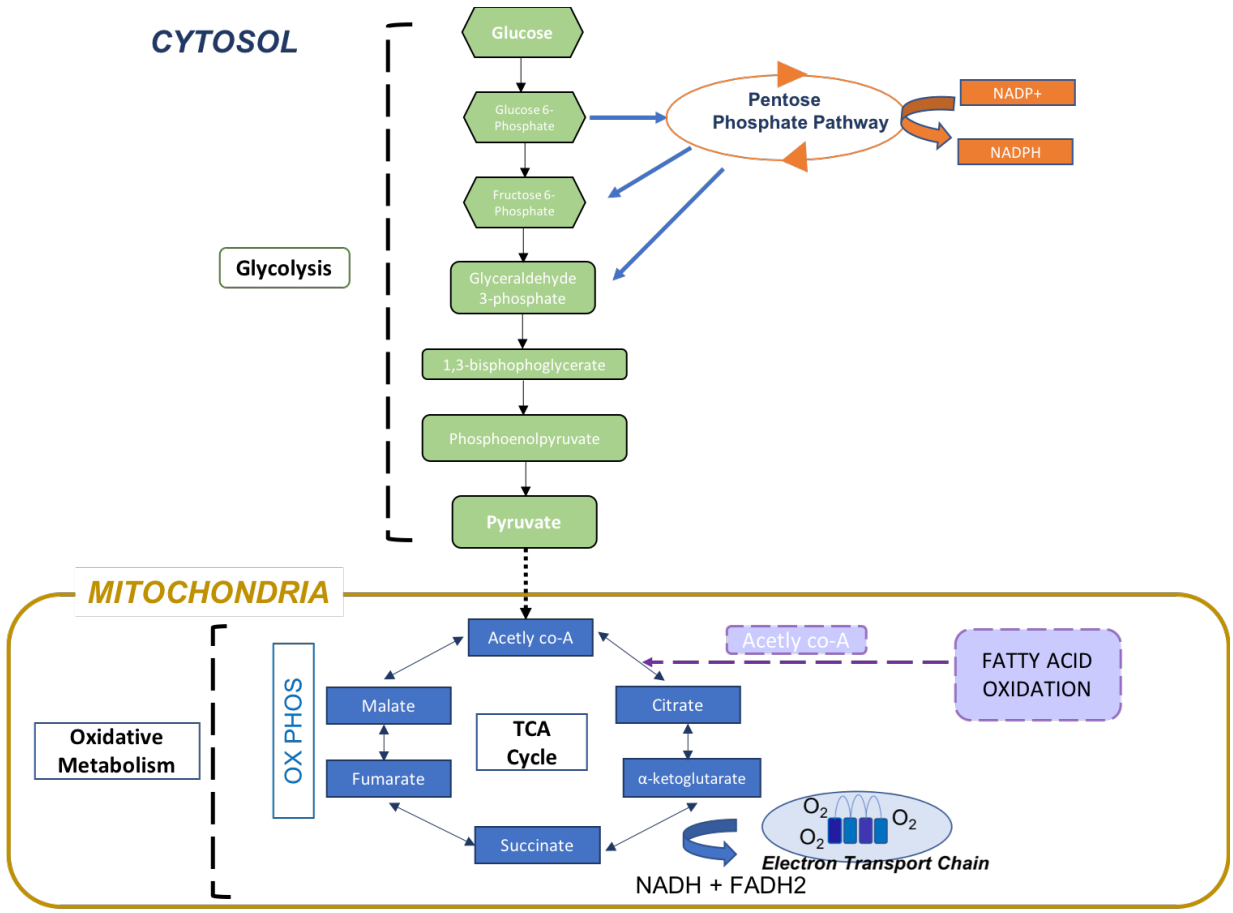

Figure 4.1: Macrophages can engage different metabolic pathways to drive energy production.
Green= Glycolysis, Blue= Oxidative phosphorylation, Purple= Fatty Acid oxidation.

In addition to their role in fuelling essential macrophage function, it has become increasingly clear that metabolic enzymes and intermediaries play key roles in modulating the macrophage immune response. Quiescent macrophages have a large capacity for mitochondrial metabolism and oxidative phosphorylation. However, activation of macrophages with pro-inflammatory/"M1" stimuli causes them to under-go a shift towards glycolysis as their main source of ATP, regardless of oxygen availability[18]. Treatment

with the proinflammatory stimulus, LPS, leads to increased glucose uptake, and similarly, over expression of GLUT-1 leads to a pro inflammatory macrophage phenotype[80]. Furthermore, two key breaks in the TCA cycle in pro-inflammatory/"M1"macrophages prime the cell for effective immune responses. A seminal study by Jha et al, identified an accumulation of Citrate and Succinate in LPS activated macrophages[19]. Excess Citrate was used to generate a key anti-microbial peptide, itaconate. More recently, it was discovered that itaconate induces the anti-inflammatory transcription factor Nrf2, following LPS stimulation[81]. Accumulation of Succinate leads to induction of pro-inflammatory IL-1β, via HIF1α stabilisation[82]. Increased flux through the Pentose Phosphate Pathway is also recognised as a feature of pro inflammatory macrophages, providing NADPH for use as a reducing equivalent and to generate Reactive Oxygen Species for microbial killing[83].

Critically, it is not just metabolic intermediaries which can exert immunomodulatory effects. Glycolytic enzymes induced by the switch to glycolysis serve a dual purpose by also acting as inflammatory signals. The glycolytic enzyme pyruvate kinase M2 (PKM2), which catalyses the final step in glycolysis, also induces IL-1β expression through HIF1α signalling. GADPH (Glyceraldehyde 3-phosphate dehydrogenase) another glycolytic pathway enzyme, can regulate expression of the inflammatory signal TNFα . If glycolysis is limited, GAPDH binds to TNFα mRNA, thereby supressing transcription.

The central role of metabolism in governing macrophage function is evident in the contrasting metabolic profile of anti-inflammatory/M2 macrophages. In vitro treatment of macrophages with cytokines such as IL-10, IL-4 and IL-13 can induce phenotypic changes in transcription, cellular function, cell surface markers and metabolism, which ultimately propel macrophages in to an "inflammation resolution" programme, or a so called M2 phenotype[12]. While M1 macrophages are heavily reliant on glycolysis to execute their inflammatory activity, M2 activation of macrophages leads to increased rates of oxidative phosphorylation and fatty acid oxidation (FAO). Disruption of these process leads to an impaired anti-inflammatory response. This has been particularly well characterised using IL-4 activation of macrophages. IL-4 activation leads to enhanced FAO and mitochondrial biogenesis with suppression of inflammatory cytokines, by inducing expression of STAT6 and PGC-1β respectively. Inhibition of oxidative metabolism or of PGC-1β (which governs mitochondrial biogenesis) abrogates this effect[84]. Similarly, over expression of CPT1 (a key mitochondrial transporter of Fatty Acids) attenuates inflammatory responses in adipose tissue[85]. Profiling of metabolic flux in M2 (IL-4 and IL-13 treated) macrophages revealed an unbroken TCA cycle, in contrast to M1 macrophages. There was increased dependence on glutamine metabolism for the TCA cycle and increased generation of amino-sugar and nucleotide sugar metabolites -characterized by high amounts of UDP-N-acetyl-alpha-D-glucosamine (UDP-GlcNAc). Disruption of these processes lead to reduced expression of classic M2 markers such as CD206[19].

Recent evidence has demonstrated that the dichotomy of glycolysis supporting acute inflammatory responses and oxidative metabolism fuelling sustained energy production, is as an over simplification of macrophage bioenergetics. Key studies have revealed that crosstalk between both metabolic pathways is indispensable for phenotype induction. LPS activation of macrophages induces glycolysis, but it also requires flux through the mitochondria. This is not to produce ATP but rather to increase mROS production, which in turn induces an inflammatory gene programme[86]. FAO , though recognised to drive macrophages towards an anti-inflammatory phenotype, was recently discovered to be dispensable for IL-4 mediated macrophage polarisation, however glycolysis was not[87]. Moreover, FAO was found to induce the inflammasome, conferring the pathway with both pro and anti-inflammatory roles[88]. A recent study examining metabolic reprogramming in human macrophages identified that mitochondrial health and activity was essential for metabolic plasticity[89]. While this area of interest is in its earlier stages of characterisation, it would appear that for effective metabolic and phenotypic reprogramming, the cross talk between metabolic pathways and the machinery required for this interplay, needs to be intact, particularly in human cells.

Substrate availability adds an additional layer of complexity to metabolic regulation. LPS activation increases glucose uptake to maintain high levels of glycolysis[90]. Similarly IL-4 mediated activation of macrophages increases expression of the scavenger receptor CD36 and consequent increased fatty

acid uptake[91]. As mentioned, M2 polarised macrophages facilitate TCA cycle anaplerosis by shuttling increased amounts of glutamine into the TCA cycle[19]. Evidently, polarisation states can influence substrate uptake to fuel their requisite metabolic pathways. It is then a natural conclusion that substrate availability can, in turn, regulate a cell's capacity to undergo polarisation. A study by Covarrubias et al was the first to provide a definite example of this by showing that Akt-mTORC1, a central axis for sensing intra and extracellular nutrient level, can couple nutrient availability with activation states. By limiting the supply of amino acids, they demonstrated impaired Akt-mTORC1 mediated induction of IL-4 macrophage activation genes[92]. Lastly , Hypoxia and activation of HIF (Hypoxia Inducible Factor) forces macrophages to shift to anaerobic metabolism and thus can exert a significant phenotypic effect. A seminal paper examining the role of hypoxia in macrophage function showed that HIF activation regulated macrophage glycolytic capacity and that knock down of HIF-1α resulted in profound impairment of myeloid function[59]. In keeping with this ,HIF-1α over expression in murine macrophages results in increased glycolysis and a hyper inflammatory state[58].

Our understanding of the relationship between macrophage function and immunometabolism is constantly expanding, with additional layers of complexity emerging all the time. What is abundantly clear however, is that macrophage phenotype is a composition of both external stimuli and internal signalling, the later strongly dictated by successful metabolic reprogramming.

No study to date has examined the specific metabolic profile of macrophages in COPD, however, there is evidence for altered metabolism in COPD. Gene expression profiling of whole lung tissue from COPD and Healthy donors revealed that oxidative phosphorylation and protein catabolism were the most differentially regulated pathways. Both modules were comparatively downregulated in COPD lung tissue[93]. Similarly, airway smooth muscle cells (ASM) isolated from COPD donors display impaired energy balance with increased accumulation of glycolytic products- lactate and alanine- compared to Healthy controls[94]. A study dating as far back as 1985, evaluated the metabolic profile of *Vastus lateralis* tissue biopsies in COPD patients compared to Healthy Controls. Here too, they identified reduced levels of ATP and increased abundance of glycolytic intermediaries in the COPD donors[95].

Perhaps the most investigated area relating to metabolism in COPD, is mitochondrial dysfunction. At low levels Mitochondrial ROS (mROS) are considered a physiological by product of cellular metabolism. Increased mROS levels, which have been described in COPD AM, can indicate mitochondrial damage and progressive leak through the electron transport chain [69]. Electron microscopy of bronchial epithelial cells from COPD donors revealed elongated and swollen mitochondria with increased fragmentation and cristae depletion. This was coupled with altered RNA regulation of key mitochondrial genes such as PINK1. These mitochondrial alterations mimicked some but not all of the features of cigarette smoke exposed (CSE)

BEAS2b cells[96]. Mitochondrial profiling of ASM from COPD patients showed a reduced mitochondrial membrane potential, reduced ATP levels and reduced mitochondrial reserve capacity, as measured by Seahorse technology. Once again, mROS levels were increased. It was suggested this was driven by oxidative stress, as some findings were replicated in Healthy cells exposed to hydrogen peroxide and in an ozone-exposed mouse model[97]. Correspondingly, cigarette smoke exposure, which induces high levels of oxidative stress, has been shown to reduce mitophagy with consequent mitochondrial dysfunction. This finding was also observed in smooth airway epithelial cells from COPD patients[98]. AM isolated from smokers with preserved spirometry i.e “Healthy Smokers”, were found to have reduced spare respiratory capacity, a measure of mitochondrial reserve, as measured by Seahorse technology[99].

Lastly, as discussed ,microenvironmental regulation via substrate availability can have a profound effect on cellular metabolism. Glucose concentrations in the lower respiratory tract are approximately 12.5 times lower than plasma concentrations, suggesting changes in glucose concentrations have the potential to exert a significant effect[100]. There have been conflicting findings relating to glucose content in bronchoalveolar (BAL) fluid of COPD patients. In one study, BAL glucose concentrations in COPD patients were found to be elevated, compared to Healthy controls and interestingly, this was in the context of comparable albumin and urea levels[101]. A similarly designed study found equal BAL glucose concentrations but increased sputum glucose

levels in COPD patients, which rose further during experimentally induced and naturally occurring exacerbations[102].

In summary ,metabolic plasticity is essential for effective macrophage function. Macrophage phenotypes are regulated by external influences such as cytokine stimulation and substrate availability, but also extensively by internal metabolic reprogramming. This requires intact metabolic machinery and finely tuned signalling between the metabolic pathways. Although there are no dedicated studies defining the metabolic profile of macrophages in COPD patients , studies of other tissues and cells in COPD suggest that they are highly glycolytic with downregulated oxidative metabolism and mitochondrial dysfunction - which is likely to have far reaching consequences for cellular bioenergetics. Moreover, failure to undergo appropriate metabolic reprogramming in response to various stimuli could lead to impaired macrophage function and may account for the altered polarisation state seen in COPD macrophages[51].

We hypothesised that COPD macrophages have an altered metabolic profile and that defective cellular energetics may be driving our observed phenotype of macrophage dysfunction. To investigate, this we sought to define the metabolic status of COPD macrophages on a transcriptional level, both at baseline and in response to stimuli. We aimed to couple this with dynamic profiling to further understand COPD macrophage energetics, particularly in the context of impaired phagocytosis and efferocytosis. Lastly, we sought to

establish if differential substrate availability may be influencing COPD macrophage behavior.

Results:

4.2 *AM from COPD and Healthy Donors differ in their baseline transcriptional profile*

Following identification of a differential transcriptional response to co-incubation with S. pneumoniae in COPD AM (Figure 3.8), we generated a new dataset to establish if alterations existed at baseline or only in evoked transcriptional responses. Healthy AM and COPD AM were isolated from donors via bronchoalveolar lavage and then cultured in RPMI for 16 hours prior to isolating and analysing total cellular RNA (n=3). Baseline Total RNA-Sequencing was then performed to compare Healthy AM with COPD AM.

Initial heat mapping revealed clear transcriptional differences between the two groups confirming that, at baseline, COPD AM are intrinsically different to Healthy AM. A total of 287 genes were significantly differentially expressed (DE) between resting state COPD and Healthy AM (significance was defined as P value ≤ 0.05,Fold Change > $\log_2 1.5$) (Figure 4.2.1). Of the 287 DE genes, 134 genes were more highly expressed in Healthy AM>COPD AM and 154 genes were more highly expressed in COPD AM>Heathy AM.

Gene Ontology grouping of the genes more highly expressed in Healthy AM , revealed that metabolic processing was the second most differentially regulated biological process ,at baseline (Figure 4.2.2). Interrogation of individual metabolism-related genes upregulated in Healthy AM revealed

changes in solute transporters and AMPK regulation (a central mechanism for sensing energy status). A key finding was that ME1(Malic Enzyme 1) was also comparatively upregulated in Healthy AM. ME1 encodes a cytosolic, NADP-dependent enzyme which generates NADPH and, via oxidative decarboxylation of malate to pyruvate, links the glycolytic and citric acid cycles [103,104].

A

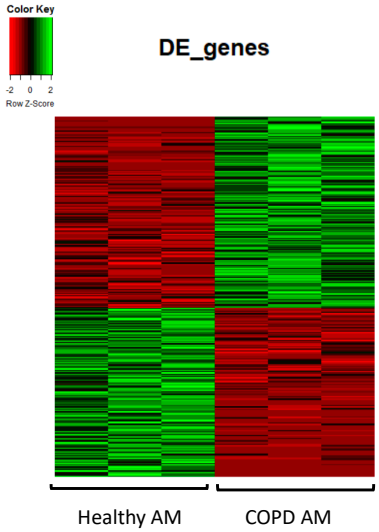

B

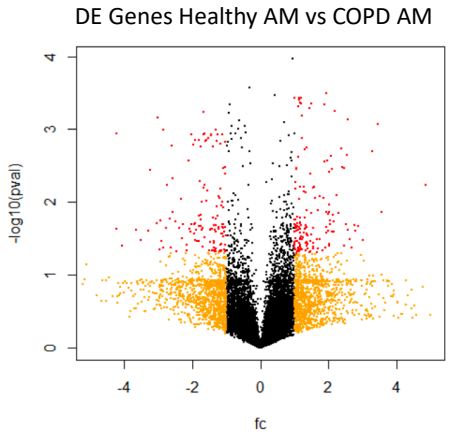

Figure 4.2.1: RNA-seq profiling reveals differences in baseline transcription between COPD and Healthy AM.
AM were isolated from COPD and Healthy donors via bronchoalveolar lavage and cultured for 16 hours prior to collecting RNA for Total RNA-seq. (A) Heatmap of column normalized Z-scores for each gene identified as significantly altered between COPD and Healthy AM. Green indicates high expression, red indicates low expression. (B) Volcano plots displaying the log2 fold change between COPD and Healthy Controls. Log10 P values are plotted on the y-axis. Red dots (n = 287) are genes that are both highly altered as well as contain a significant P value = FC > $\log_2 1.5$ and P value ≤ 0.05. Orange dots contain genes which are FC >$\log_2 1.5$ but P value > 0.05. N=3 both groups. fc= Fold Change, DE = Differentially Expressed.

A

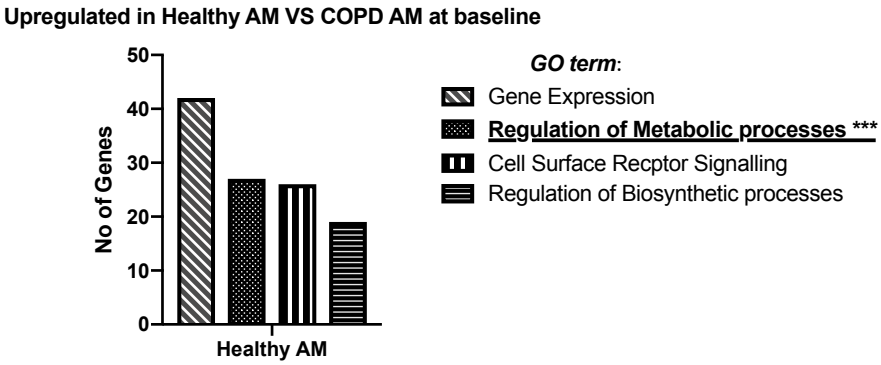

B

*** Regulation of Metabolic Processes. Gene ID:	Biological Role:	Healthy AM
SLC27A3	Solute Transporter: (Fatty Acid)	Upregulated
SLC36A3	Solute Transporter	Upregulated
SLC35C2	Solute Transporter	Upregulated
G6PC3 (Glucose -6-phosphatase)	Glycogen breakdown/ Gluconeogenesis	Upregulated
ME1 (Malic Enzyme 1)	TCA cycle shunt -generates NADPH via Malate to Pyruvate conversion	Upregulated
PRKAB (5'-AMP-activated protein kinase subunit beta-1)	Non Catalytic regulatory subunit of AMPkinase	Upregulated
CROT (Carnitine Octanoyltransferase)	Transfer of fatty acids from peroxisome to the cytosol and mitochondria	Upregulated

Figure 4.2.2: Transcriptional regulation of metabolism differs between COPD and Healthy AM at baseline.
(A) The top four Gene Ontology (GO) terms upregulated in Healthy AM , at baseline, compared to COPD AM. (B) Table illustrating key metabolic genes upregulated in Healthy AM compared to COPD AM, at baseline. N=3 for each group.

4.3 *AM from COPD have an altered metabolic response to Streptococcus pneumoniae.*

As transcriptional analysis revealed differences in metabolic regulation between COPD and Healthy AM at baseline, we investigated our existing transcriptomics data (outlined in figure 3.8) for a differential metabolic signature, in response to infection. COPD and Healthy AM were co-incubated with *Streptococcus pneumoniae* for four hours prior to generating RNA for transcriptional analysis. Once again, there was a clear difference in the metabolic transcriptional response between COPD and Healthy AM. After four hours co incubation with *S. pneumoniae*, Healthy AM had primarily upregulated genes related to oxidative phosphorylation, and to a lesser degree genes regulating glycolysis (no. of genes= 81 vs 16). This was in stark contrast to COPD AM, where only genes relating to glycolysis had been transcriptionally altered following infectious stimulus (n=40) (Figure 4.3 B). As discussed COPD AM have a globally reduced transcriptional response to infection, compared to Healthy AM (Figure 4.3A). Consequently, the upregulation of glycolytic genes represented over 6% of total transcriptional change following exposure to *S pneumoniae* in COPD AM.

A

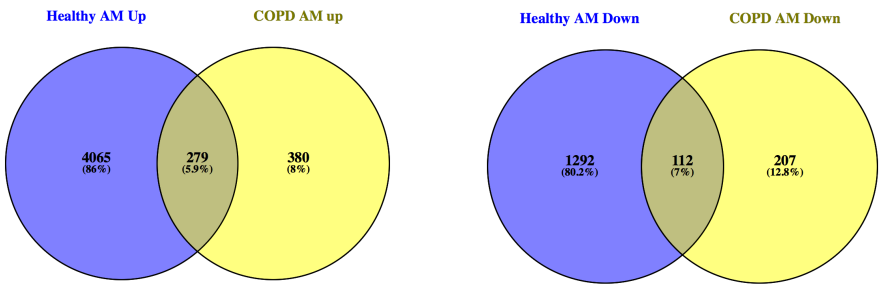

B

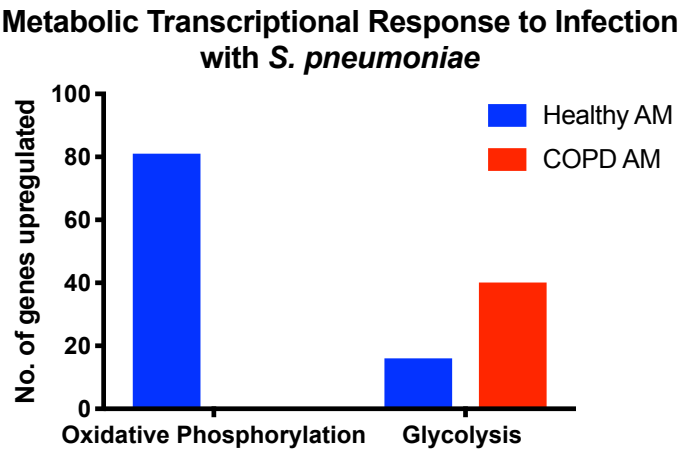

Figure 4.3: Affymetrix array reveals abnormal metabolic responses to infection in COPD AM.
COPD and Healthy Donor AM were co-incubated with opsonised D39 *Streptococcus pneumoniae,* MOI 10:1, for four hours prior to lysis and sequencing of total RNA via affymetrix array. (A) Venn diagram illustrating the number of genes upregulated or downregulated in Alveolar Macrophages in response to infection with *S. pneumoniae* D39. (B) COPD AM mount a distinctive metabolic response to infection, which differs from that of Healthy AM. Upregulation of glycolytic genes in COPD AM, represents 6% of the total genes upregulated in response to infection.

4.4 *Metabolically profiling COPD macrophages in real time*

Once we established that COPD AM possess an altered metabolic transcriptional programme, both at baseline and following infectious stimulus, we undertook dynamic profiling of COPD macrophages to establish if these transcriptional differences resulted in impaired cellular energetics

Seahorse technology provides a platform to metabolically profile cells in real time. The platform simultaneously measures changes in oxygen consumption (OCR -Oxygen Consumption Rate) to measure cellular respiration/oxidative metabolism and changes in pH (ECAR- Extracellular Acidification Rate), an indirect measure of glycolysis. These readings are taken at baseline and following injection of stressors compounds, enabling calculation of the reserve energy capacity of cells (Spare Respiratory Capacity and Glycolytic Reserve).

In the Mitochondrial Stress Test, cells are incubated in Seahorse media supplemented with Glucose and Glutamine for 45 minutes prior to commencing the test. Basal rates are recorded before sequential injection of mitochondrial metabolism stressors, enabling calculation of Spare Respiratory Capacity. The injected compounds are Oligomycin – which shuts down ATP-synthase; FCCP - a potent ionophore which uncouples oxidative phosphorylation in the mitochondria; and Antimycin A&Rotenone - which respectively shut down complex 3 & 1 in the electron transport chain.(Figure

4.4 A). For the Glycolytic Stress Test, cells are incubated in Seahorse media supplemented with Glutamine only for 45 minutes prior to beginning the test. Basal glycolytic rates are recorded following injection of Glucose. Subsequent injection of Oligomycin and 2DG (which shuts down glycolysis) enables calculation of Glycolytic reserve (Figure 4.4 B). Both protocols are outlined in detail in Chapter 2.14.

A

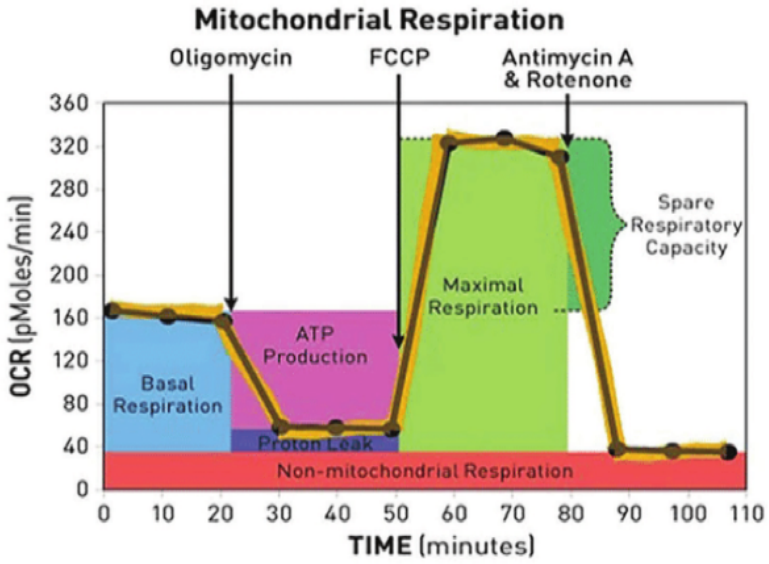

B

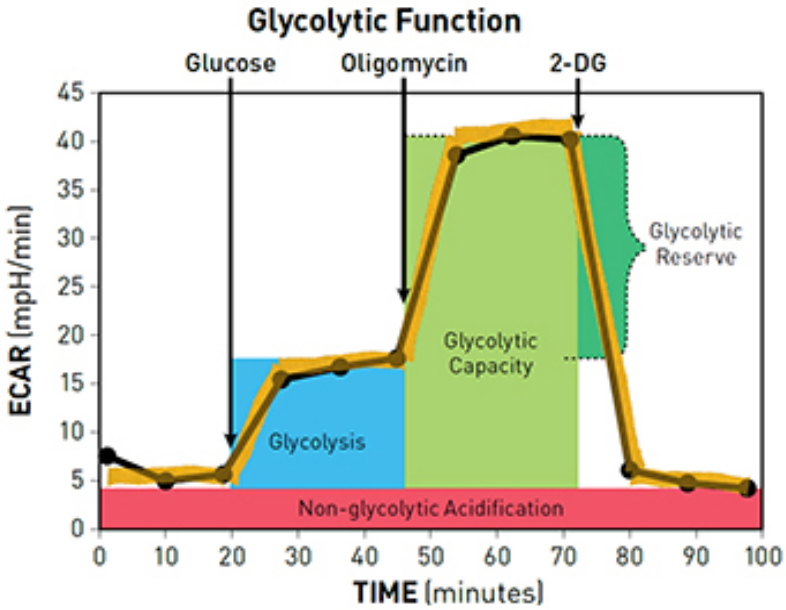

Figure 4.4: Seahorse profiling of cellular energetics.
(A)The Mitochondrial Stress test which determines the maximal oxidative metabolism of the cell, while also recording glycolytic metabolism (via changes in pH). (B) The Glycolysis Stress test which determines glycolytic parameters by measuring pH change.

* Figures from official Agilent Seahorse Xfe24 documentation

4.5 *COPD AM display impaired bioenergetics compared to Healthy Donors*

Metabolic profiling of COPD AM revealed highly significantly reduced energy reserves in both oxidative metabolism and glycolysis, compared to Healthy donor AM. Spare Respiratory Capacity was significantly reduced in COPD AM (8.5±0.4 vs 4.2± 0.4, a 51% reduction) (Figure 4.5.1 A). This was regardless of current smoking status (unpaired t-test, p value = 0.103). Similarly, Glycolytic Reserves were significantly reduced in COPD AM, irrelevant of smoking status (0.84±0.04 vs 0.17±0.04, an 80% reduction, smoking status p value= 0.15) (Figure 4.5.1 B). The metabolic potential of COPD AM - the ability to increase metabolic rates above basal rates in response to increased energy demand- was significantly reduced in COPD AM (254% vs 190% in Healthy AM).

Crucially, the loss of energetic reserves in both oxidative metabolism and glycolysis occurred in the context of reduced or equivalent basal metabolic rates. Basal OCR rates were, in fact, significantly lower in COPD AM with near equivalent basal rates in ECAR . While there was no significant difference between basal OCR rates in current and ex smoking COPD donors, a definite trend towards lower basal ECAR rates was observed in current smokers (Smoker vs Ex-smoker, OCR P value= 0.41, ECAR P value=0.06) (Figure 4.5.2 A - B).

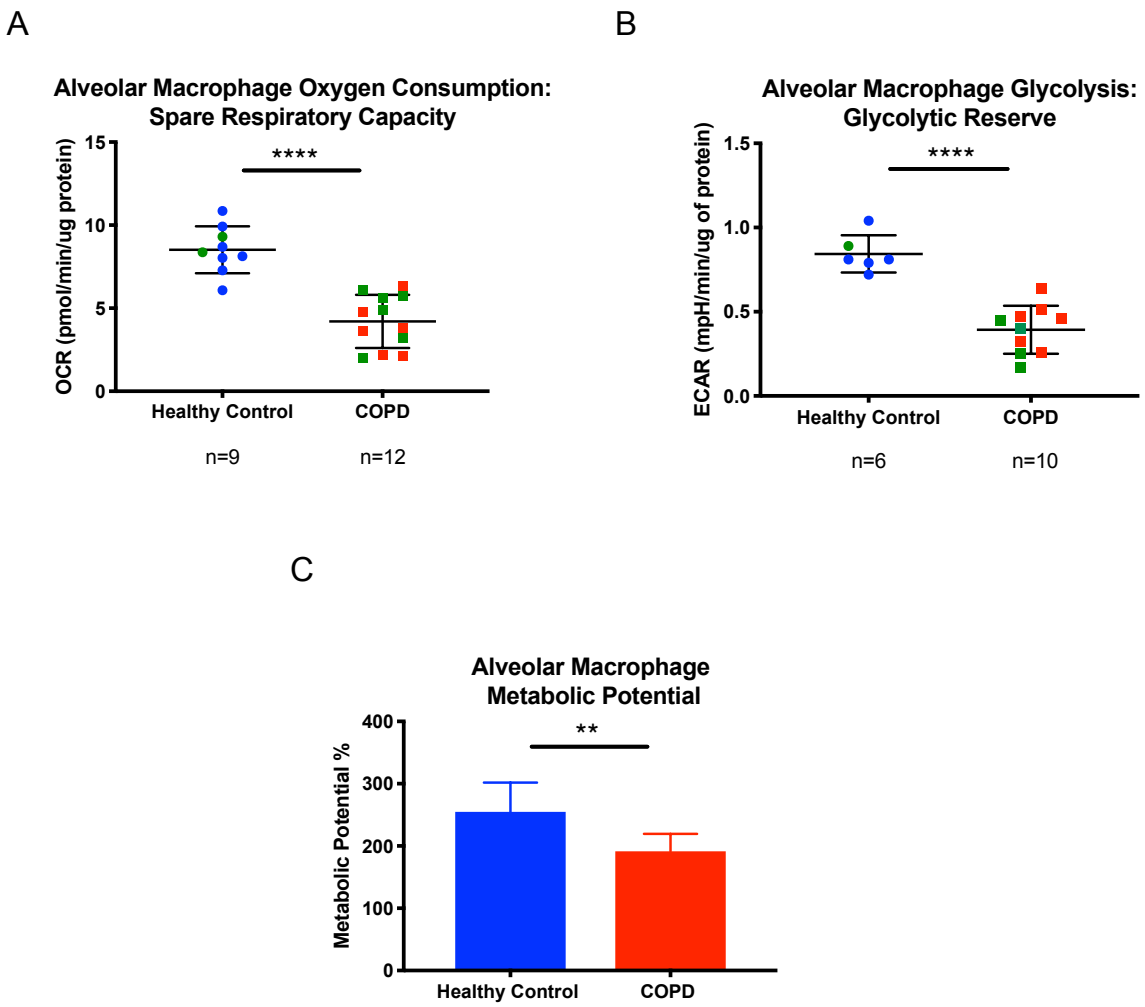

Figure 4.5.1: COPD Alveolar Macrophages display altered metabolic profiles with reduced energy reserves.
Mitochondrial Stress (A + C) and Glycolytic (B) stress testing was performed in COPD and Healthy Donor AM. Reserves in both Oxidative metabolism (A) and Glycolysis (B) were significantly reduced in COPD AM. (C) Metabolic potential was significantly reduced in COPD AM. Green circles/squares indicate current smokers. COPD Smoker vs Ex-smoker, Spare Respiratory Capacity P value= 0.103, Glycolytic Reserve P value=0.158. All P values calculated by unpaired t-test, ** P≤0.01, *** P≤0.001, **** P≤0.0001. Data represents individual values and mean ± SEM. ECAR= Extracellular Acidification Rate. OCR= Oxygen Consumption Rate.

A

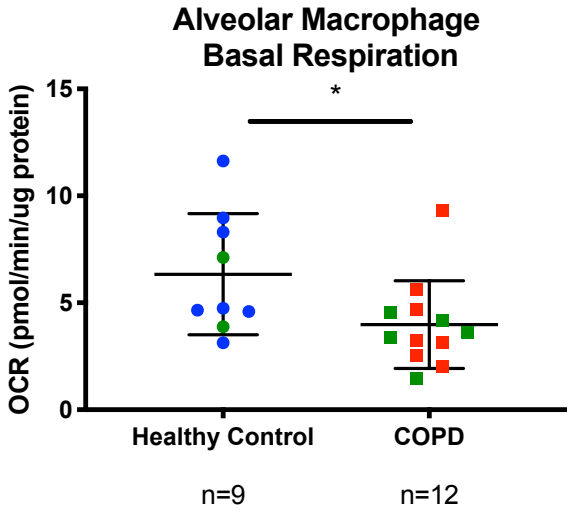

B

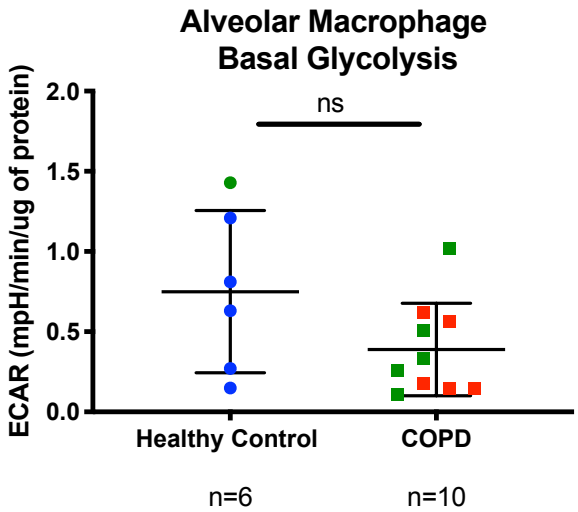

Figure 4.5.2: Basal OCR rates are reduced in COPD AM.
Mitochondrial Stress (A) and Glycolytic (B) stress testing was performed in COPD and Healthy Donor AM. (A) Basal OCR rates were significantly lower in COPD AM than in Healthy Donor AM. (B) Basal ECAR rates were comparable between the two donor groups. Green circles/squares indicate current smokers. COPD Smoker vs Ex-smoker, OCR P value= 0.41, ECAR P value=0.06. P values calculated by unpaired t-test, *P≤0.05, ns= not significant, p=0.08. Data represents individual values and mean ± SEM.

4.6 *COPD AM primarily upregulate glycolysis to meet increased energy demand*

In health, metabolic plasticity is a key feature of macrophage function. It enables a highly adaptable bioenergetic profile but also mediates key phenotypic switches. To evaluate the ability of COPD AM to engage different metabolic pathways we interrogated the energy response across both oxidative metabolism and glycolysis in COPD AM, using Seahorse.

Compared to Healthy AM, COPD AM had a significantly reduced OCR/ECAR ratio. This preponderance for glycolysis over oxidative phosphorylation was mirrored in the ATP-linked-OCR ratios. ATP-linked-OCR is calculated as the reduction in oxygen consummation following shut down of ATP synthase/Complex 5 with Oligomycin (Figure 4.4 A). In COPD AM, absolute ATP-linked-OCR was reduced at baseline. It represented a similar percentage of Basal OCR but, critically, a significantly higher percentage of the Maximal Respiratory Capacity in COPD AM (Figure 4.6.1 A–D). This suggests that COPD AM are operating closer to their maximal respiratory capacity at all times and are unable either to recruit additional mitochondria or to increase ATP production in existing mitochondria .

This apparent defect in mitochondrial function was particularly evident during energy phenotyping of COPD AM. To phenotype the energy response in the cell, absolute change in ECAR was plotted against absolute change in OCR

following injection of stressor compounds, to evaluate how the cell differentially employed either metabolic pathway to meet increased energy demand (Figure 4.6.2).

In response to injection of the stressor compounds ,Healthy AM increased both ECAR and OCR rates. In contrast, COPD AM increased ECAR rates , albeit not to the level of Healthy AM, but only displayed a modest increase in OCR compared to Healthy donors. (Figure 4.6.2 A) This was more apparent still when we co incubated the macrophages with an additional stimulus, mirroring our functional assays. AM were co incubated for 90 mins with 20 hr apoptotic neutrophils. Following co-incubation with neutrophils, there was a further exaggeration of the dominant glycolytic energy response in COPD AM compared to Healthy AM. Once more, Healthy AM employed both metabolic pathways , in contrast to COPD AM ,which displayed a persistent drive to meet increased energy demand primarily through glycolysis alone (Figure 4.6.2 B).

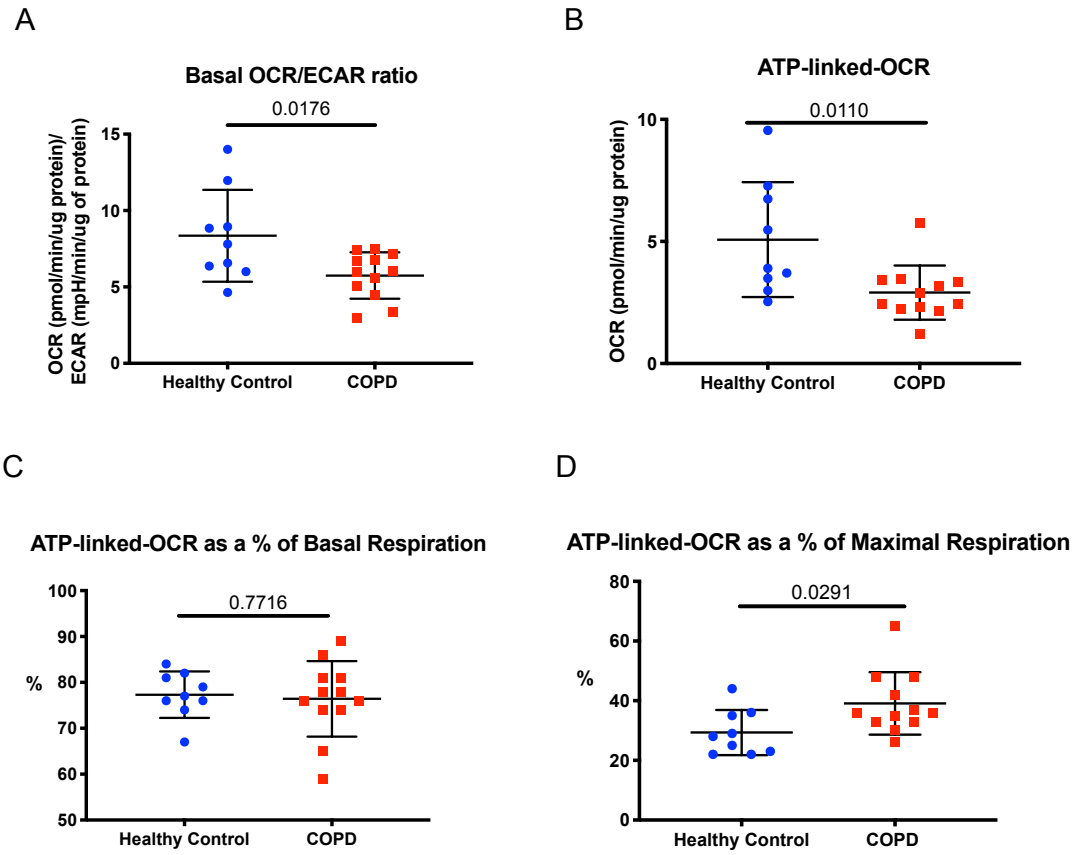

Figure 4.6.1: Mitochondrial stress testing suggests a redundancy in mitochondrial units in Healthy AM , which is not present in COPD AM. (A) Healthy AM display a significantly higher OCR/ECAR ratio than COPD AM. (B) OCR consumption linked to ATP generation, as calculated by the reduction in OCR following injection of Oligomycin, was significantly higher in Healthy AM. (C) ATP-linked-OCR was an equivalent percentage of Basal OCR consumption in Healthy and COPD AM. (D) However it presented a significantly higher percentage of Maximal OCR Consumption in COPD AM. All figures n=9/10 (Healthy/COPD). P values calculated by unpaired t-test, $P \leq 0.05$ used to determine significance. Data represents individual values and mean ± SEM.

A

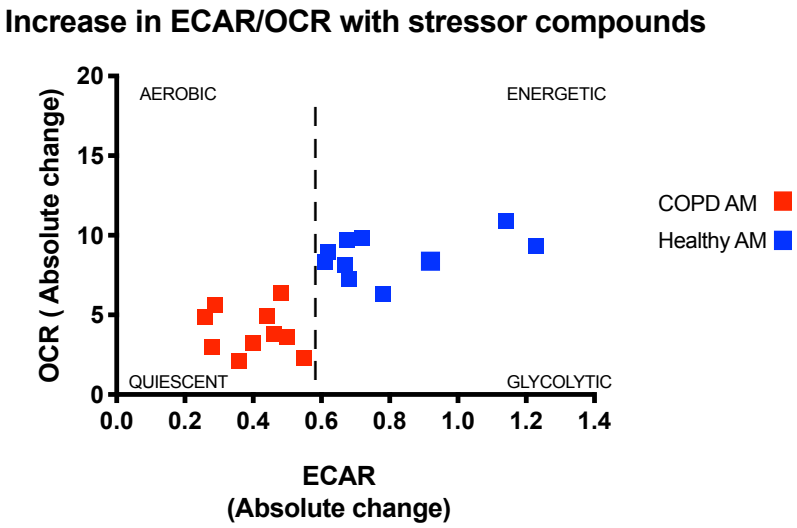

B

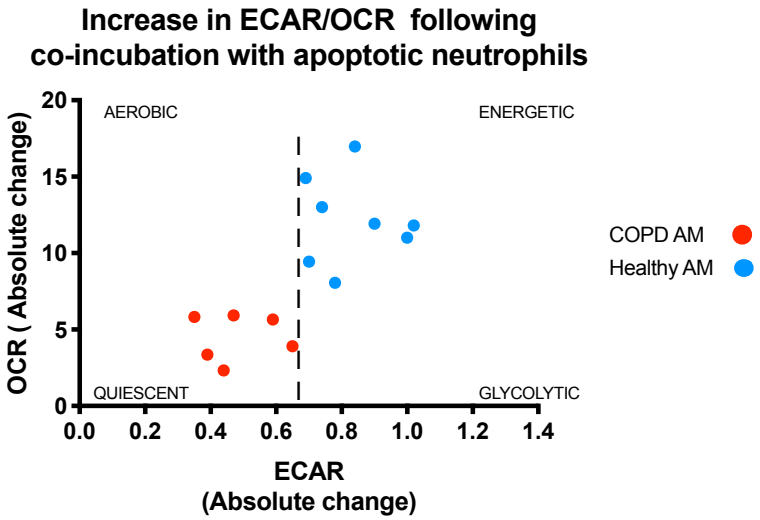

Figure 4.6.2: COPD AM have an over reliance on glycolysis to meet increased energy demand.

Mitochondrial stress testing was performed to phenotype the energy response in both COPD and Healthy donor AM after injection of the standard Seahorse stressor compounds. (A) Absolute change in ECAR was plotted against absolute change in OCR following injection of stressor compounds. (B) Cells were co-incubated with 20hr apoptotic neutrophils for 90 mins prior to conducting energy phenotyping. Again, absolute change in ECAR was plotted against absolute change in OCR following injection of stressor compounds. Apoptotic neutrophil MOI 10:2 Healthy AM; MOI 15:2 COPD AM.

4.7 *COPD MDM exhibit reduced energetic reserves when compared to Healthy donors*

To establish if the altered bioenergetics observed in COPD AM were driven by the lung microenvironment or reflected a systemic defect, we evaluated cellular energetics in COPD and Healthy donor peripherally derived MDM.

Seahorse metabolic profiling of COPD MDM revealed depleted reserves in both oxidative metabolism and glycolysis, compared to Healthy donors. COPD MDM had significantly reduced Spare Respiratory Capacity (5.16±0.9 vs 2.75±0.6, a 47% reduction), Glycolytic Reserve(0.19±0.03 vs 0.05±0.02, a 75% reduction) and a significantly reduced Metabolic Potential (22%vs159%) (Figure 4.7.1). Smoking status did not significantly alter Spare Respiratory Capacity in COPD MDM (unpaired t-test, p=0.17). The number of ex-smoker COPD donors assessed in the Glycolysis Stress Test was too small for statistical analysis.

Reduced energetic capacity in COPD MDM existed in the presence of basal metabolic rates equivalent to Healthy donor MDM (Figure 4.7.2).

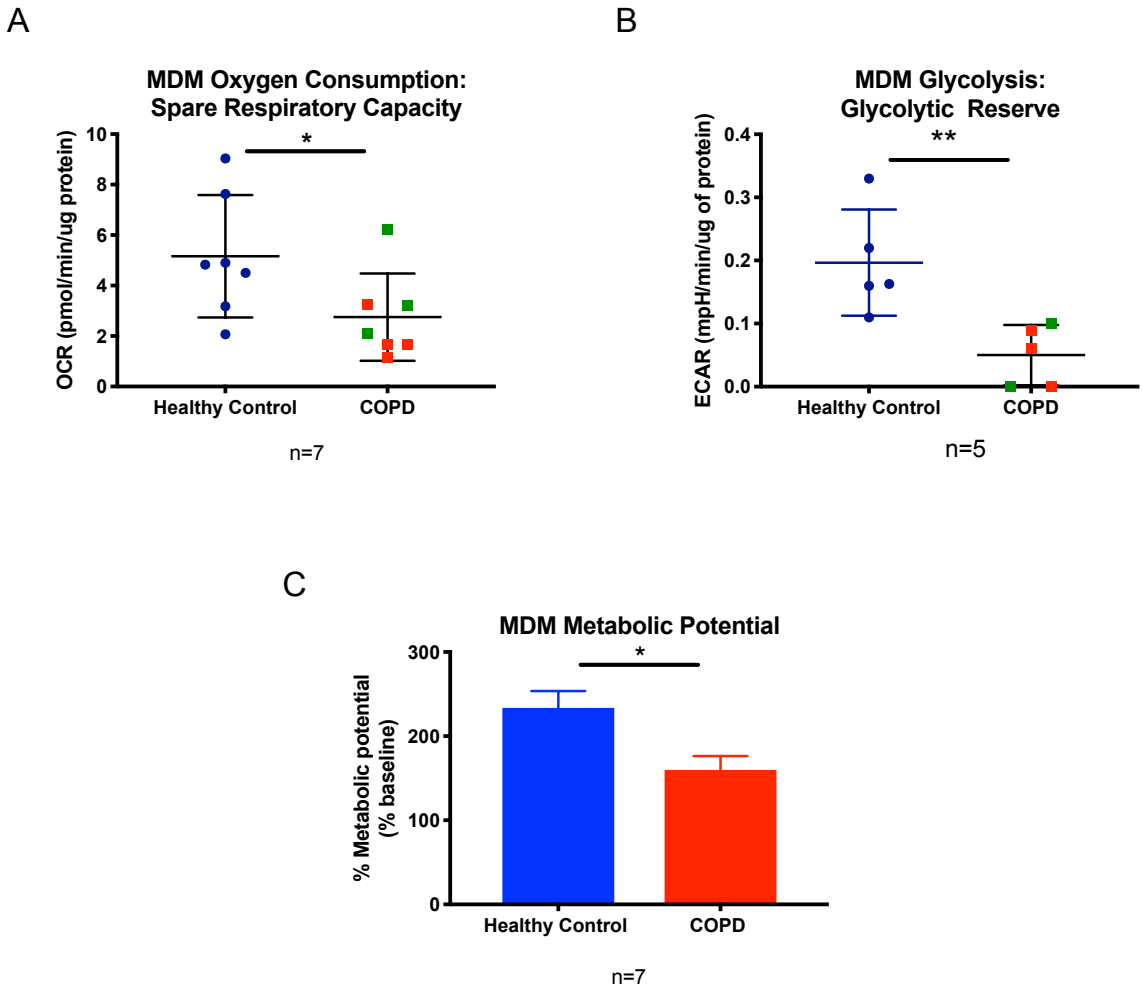

Figure 4.7.1: COPD Monocyte-Derived Macrophages display altered metabolic profiles with reduced energy reserves.
Mitochondrial Stress (A + C) and Glycolytic (B) stress testing was performed in COPD and Healthy Donor MDM. Reserves in both Oxidative metabolism (A) and Glycolysis (B) were significantly reduced in COPD MDM. (C) Metabolic potential was significantly reduced in COPD MDM. Green circles/squares indicate current smokers. P values calculated by unpaired t-test, * $P \leq 0.05$, ** $P \leq 0.01$. Data represents individual values and mean ± SEM.

A

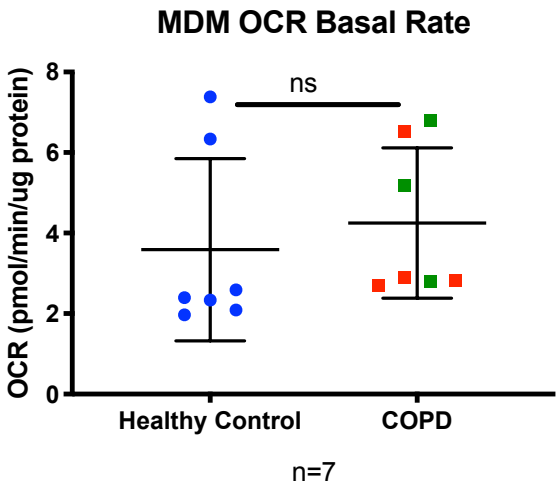

B

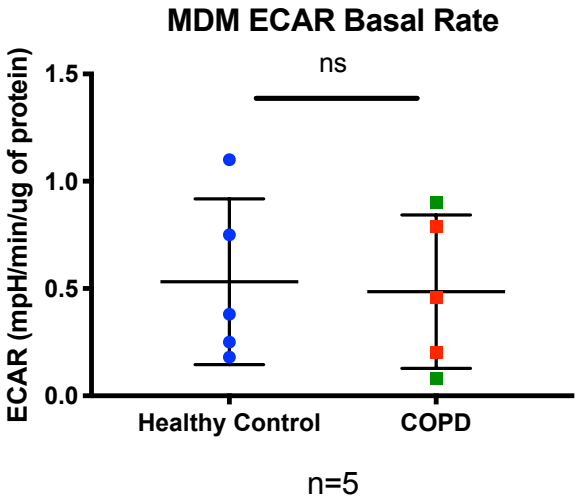

Figure 4.7.2: Basal metabolic rates are comparable in COPD and Healthy MDM.

Mitochondrial Stress (A) and Glycolytic (B) stress testing was performed in COPD and Healthy Donor MDM. There was no significant difference in Basal OCR (A) and ECAR (B) rates between COPD and Healthy MDM. Green circles/squares indicate current smokers P values calculated by unpaired t-test, $P \leq 0.05$ used to determine significance. (A) p= 0.56, (B) p= 0.84. Data represents individual values and mean ± SEM.

4.8 *Energy phenotyping reveals a divergent response in COPD MDM compared to COPD AM*

Whilst COPD AM and MDM both displayed reduced energy reserves, it was unclear if COPD MDM would share the marked reliance on glycolysis exhibited by COPD AM.

Unlike COPD AM, COPD MDM had equivalent OCR/ECAR ratios compared to Healthy Donors. They had a comparable ATP-linked-OCR profile compared to Healthy MDM, although, similar to COPD AM ,there was a trend towards ATP-linked-OCR representing a higher proportion of the Maximal Respiratory Capacity (38% vs 47%) (Figure 4.8.1 D).

Furthermore, phenotyping of the energy response in COPD MDM also revealed a divergent profile to that of COPD AM (Figure 4.8.2). COPD MDM had a reduced energetic response compared to Healthy MDM, but this did not predominately effect one metabolic pathway over the other, with similar reductions seen in both OCR and ECAR. Due to the more varied basal rates detected in MDM than AM, increases in OCR & ECAR in COPD MDM, were plotted as a percentage of the increase seen in Healthy donor MDM.

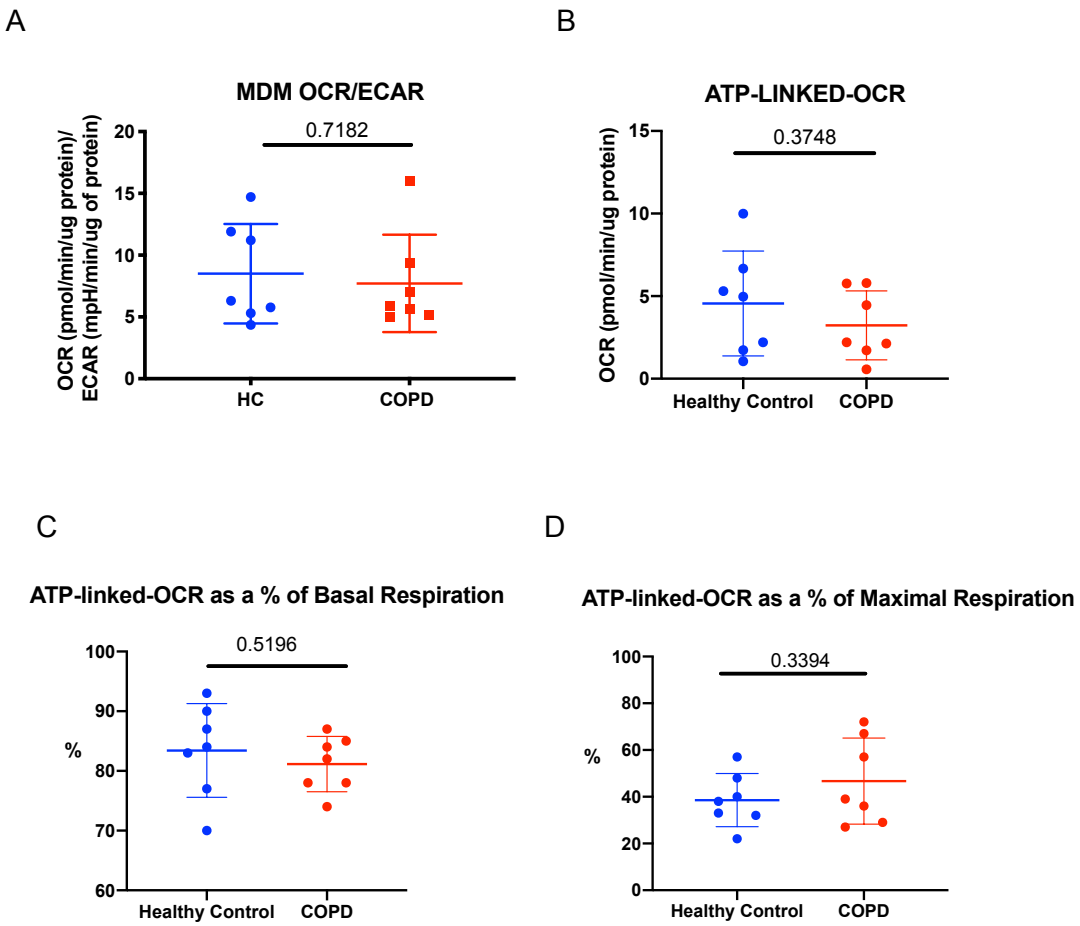

Figure 4.8.1: COPD MDM display similar rates of ATP linked OCR to Healthy MDM.

There was no significant difference in Basal OCR/ECAR ratios between COPD and Healthy donor MDM. OCR-linked-ATP was reduced but not significantly, in COPD MDM compared to Healthy MDM. ATP-Linked-OCR was a similar percentage of both Basal and Maximal respiration in Healthy and COPD MDM. P values calculated by unpaired t-test, $P \leq 0.05$ used to determine significance. Data represents individual values and mean ± SEM.

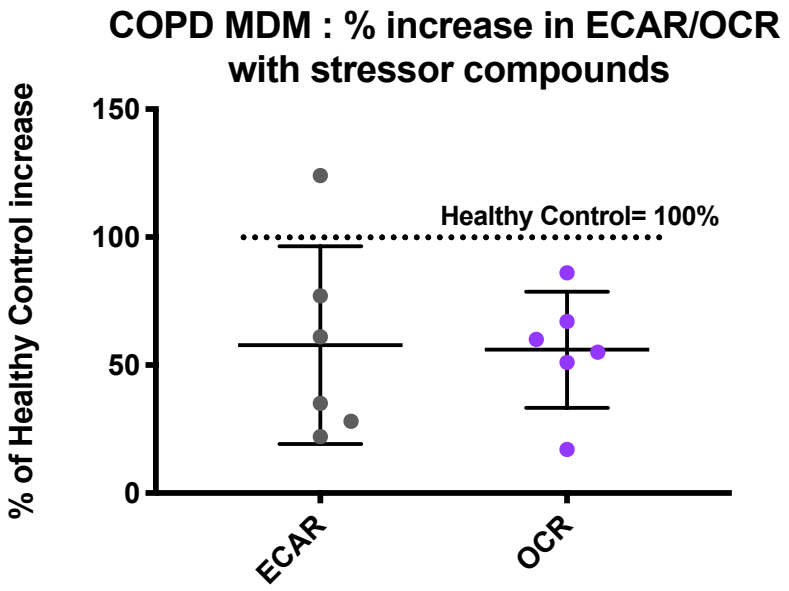

Figure 4.8.2: Energy Phenotyping of COPD MDM revealed a suppressed maximal energetic response, but comparable utilization of oxidative metabolism and glycolysis.
Mitochondrial stress testing was performed to phenotype the energy response to injection of standard seahorse stressor compounds in both COPD and Healthy donor MDM. In all but one donor , COPD MDM failed to reach the maximal energetic response of Healthy MDM- represented by the dotted line. Testing did not reveal a differential utilization of either pathway to meet increased energy demand in COPD MDM. N= 6.

4.9 *Resting state COPD Macrophages upregulate the glycolytic pathway, as detected by LC-MS*

Seahorse profiling provides dynamic information on the metabolic capacity and phenotype of macrophages. However, as it quantifies broad dynamic changes and is based on inferred measurements, we sought to measure individual metabolite abundance via High Performance Liquid Chromatography Mass Spectrometry (HPLC-MS).

HPLC-MS analysis of both COPD and Healthy donor macrophages revealed a significant and global increase in the abundance of glycolytic intermediaries, relative to Healthy Controls (Figure 4.9.1 A-B). Crucially, this happened throughout the glycolytic pathway suggesting this was not driven by a break in flux through glycolysis leading to accumulation of preceding metabolites (Figure 4.9.1 C). In contrast to glycolytic intermediaries, we did not detect a significant difference in TCA cycle metabolite abundance in COPD AM compared to Healthy donors (Figure 4.9.2 A). This indicates that in COPD AM there is a targeted increase in glycolysis, rather than global upregulation of metabolism. (Due to an issue with protein normalisation, TCA cycle MDM results were not of a usable standard).

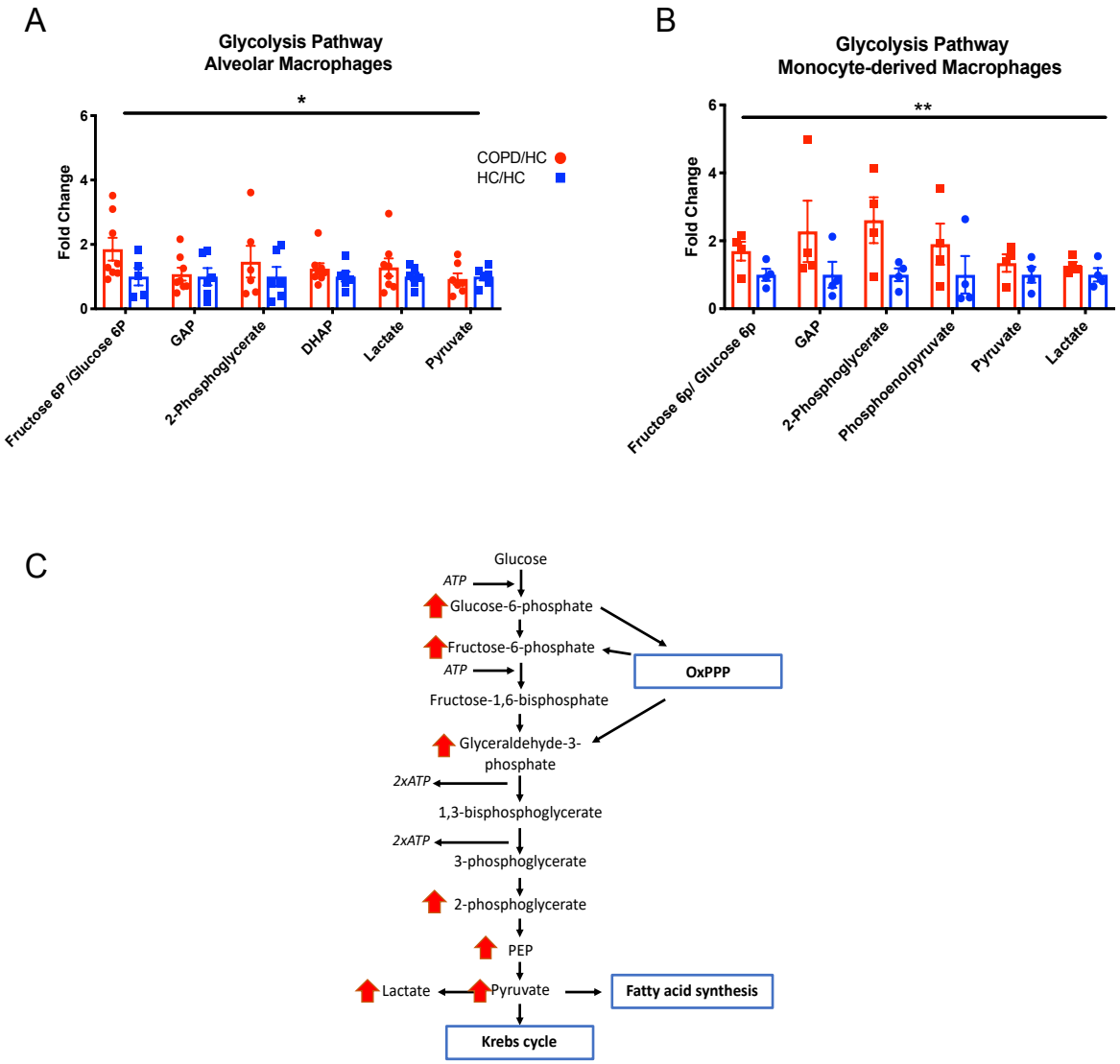

Figure 4.9.1: Resting state COPD AM and MDM exhibit a global increase in Glycolytic intermediaries.
Resting state AM (A) and MDM (B) from COPD and Healthy donors were lysed in methanol to determine metabolite abundance via Liquid-Chromatography-Mass-Spectrometry. Abundance is plotted as relative to Healthy Controls (Fold Change). Both COPD AM and MDM have an increase in glycolytic intermediaries throughout the Glycolytic pathway (C). (A) n=8/6 , (B) n= 4. P value calculated via 2-way ANOVA. P* ≤0.05, ** P≤0.01. Data represents individual values and mean ± SEM.

A

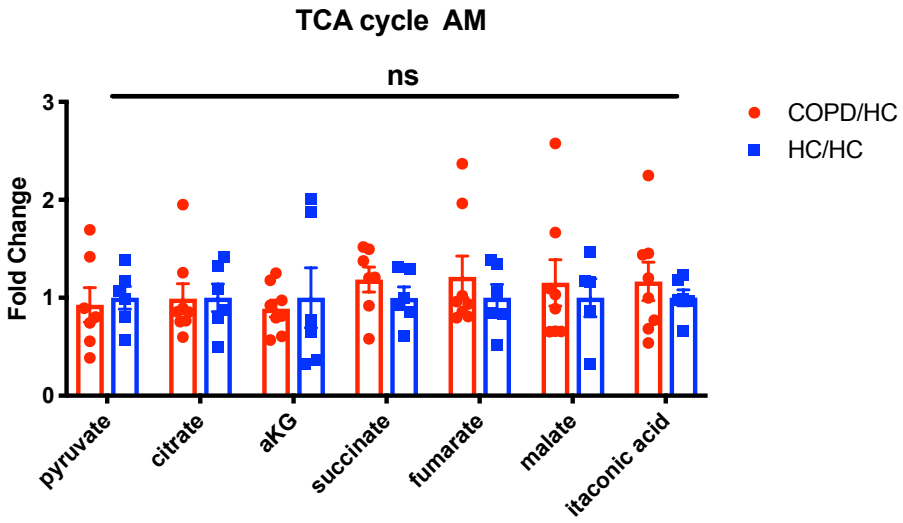

B

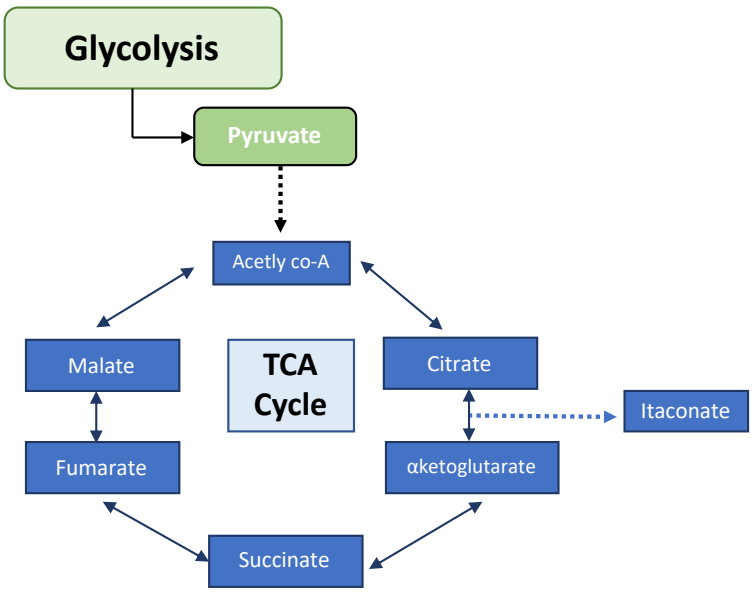

Figure 4.9.2. COPD and Healthy Donor AM display comparable levels of TCA cycle intermediaries.

Resting state AM from COPD and Healthy donors were lysed in methanol to determine relative metabolite abundance via Liquid-Chromatography-Mass-Spectrometry. There was no significant difference detected in TCA cycle metabolite abundance (A). COPD AM metabolite abundance is shown relative to Healthy donors (Fold change) N=8/6. P value calculated via 2-way ANOVA. P≤0.05 used to determine significance, (A) p= 0.336, Data represents individual values and mean ± SEM.

4.10 *Energy Charge is reduced in COPD AM compared to Healthy donors*

COPD AM displayed reduced reserves in both Glycolysis and Oxidative metabolism coupled with an over reliance on glycolysis, a less efficient metabolic pathway. We sought to determine the energetic consequences of this, particularly in the context of impaired phagocytosis and efferocytosis observed in COPD macrophages. Adenosine Triphosphate (ATP) is often referred to as the "molecular currency of intracellular energy transfer" and is used to power diverse cellular functions. Hydrolysis of the phosphate groups in ATP generates ADP and subsequently AMP, releasing a phosphate group and thus molecular energy with each reaction.

LC-MS analysis of COPD AM uncovered a significantly altered absolute abundance of ATP intermediaries, with reduced ATP levels in COPD AM (Figure 4.10 A). Energy charge as calculated by the equation [ATP + ½(ADP) / ATP + ADP + AMP], is a widely utilised index for measuring the energy status of a cell. COPD AM displayed significantly reduced Energy Charge compared to Healthy AM. Similarly the ATP:ADP ratio was significantly reduced in COPD AM. A reduction in both ratios coupled with alterations in absolute abundance, indicates that it is not just the absolute amount of ATP available, but also the energetic status of ATP molecules present, that is reduced in COPD.

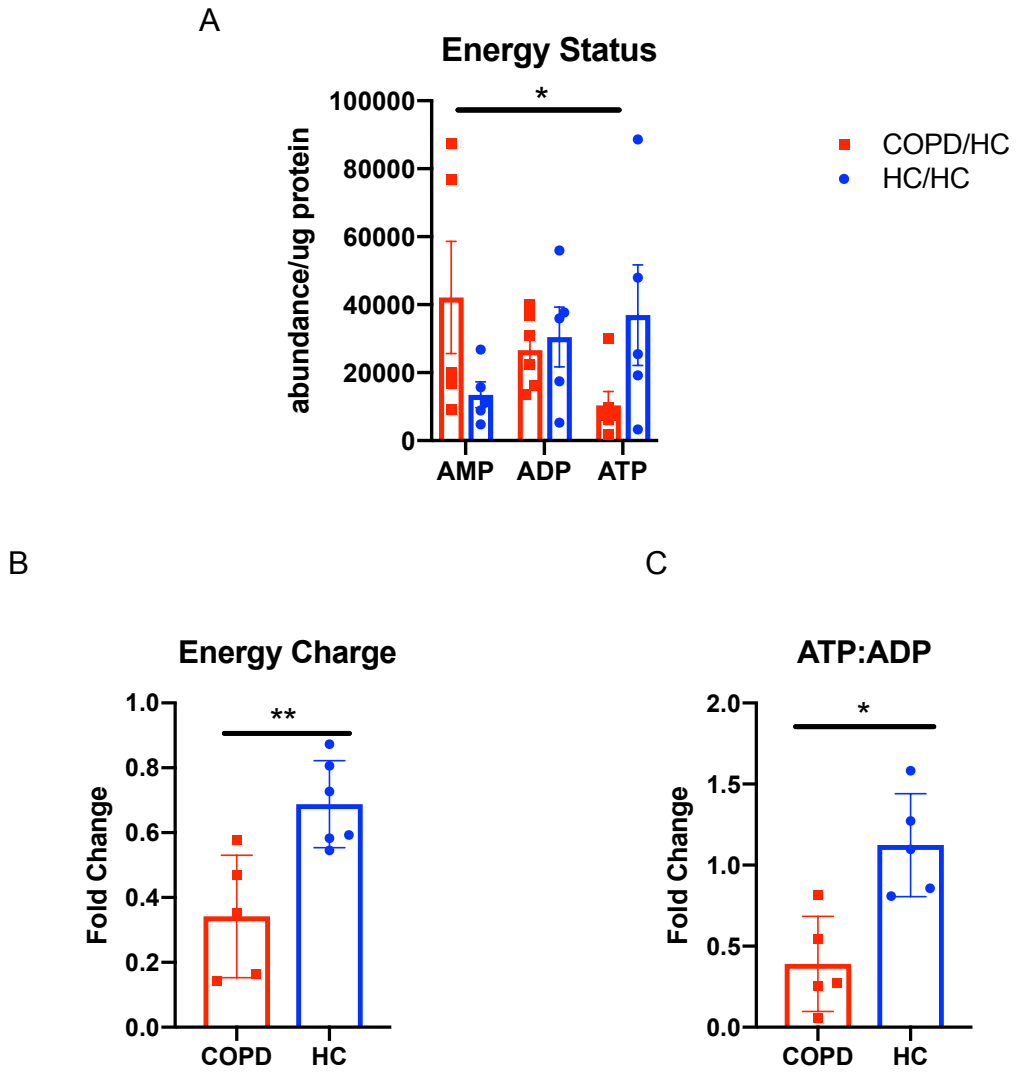

Figure 4.10: Resting state COPD AM have reduced Energy availability compared to Healthy Donor AM .
Resting state AM from COPD and Healthy and donors were lysed in methanol to determine relative metabolite abundance via Liquid-Chromatography-Mass-Spectrometry. ATP abundance was reduced in COPD AM (A) as was calculated energy charge(B) and ATP:ADP ratios (C), compared to Healthy AM. COPD AM metabolite abundance is shown relative to Healthy donors . P value calculated via 2-way ANOVA with Sidak's multiple comparisons (A), Unpaired T-test (B+ C) , * P≤0.05, ** P≤0.01. Data represents individual values and mean ± SEM.

4.11 *Differential substrate availability for glycolysis does not account for altered metabolism in COPD macrophages*

As substrate availability can exert a high degree of influence on macrophage metabolism, we measured glucose uptake in COPD and Healthy donor macrophages. Uptake of 2-NBDG, a commonly utilised fluorescently labelled glucose analogue, revealed comparable levels of glucose uptake in COPD and Healthy donor MDM (Figure 4.11 A). Due to marked auto fluorescence we were unable to conduct this assay in COPD AM.

Cells are glucose deprived for 45 mins prior to the Seahorse Glycolysis Stress test , consequently there is a large rise in ECAR following the initial glucose injection. We interrogated the increase in ECAR rates following glucose injection as an equivalent rise in ECAR in the 5 minutes following glucose injection would suggest a similar rate of glucose uptake between COPD and Healthy donor macrophages. We did not detect any difference in fold change increase in ECAR pre and post glucose injection in either AM or MDM (Figure 4.11 B-C) . As prolonged glucose deprivation can lead to upregulation of glucose transporters , we used pre-test 16 hour glucose deprivation as a positive control. Reassuringly this ratio did detect an inferred augmentation of glucose uptake in both AM and MDM (Figure 1.11 B-C).

Glycogen stores can be broken down to shuttle substrate into glycolysis, consequently we measured glycogen stores in macrophages from COPD and

Healthy donors. Although stores were low overall, there was no significant difference between COPD and Healthy control macrophages (Figure 4.12 D)

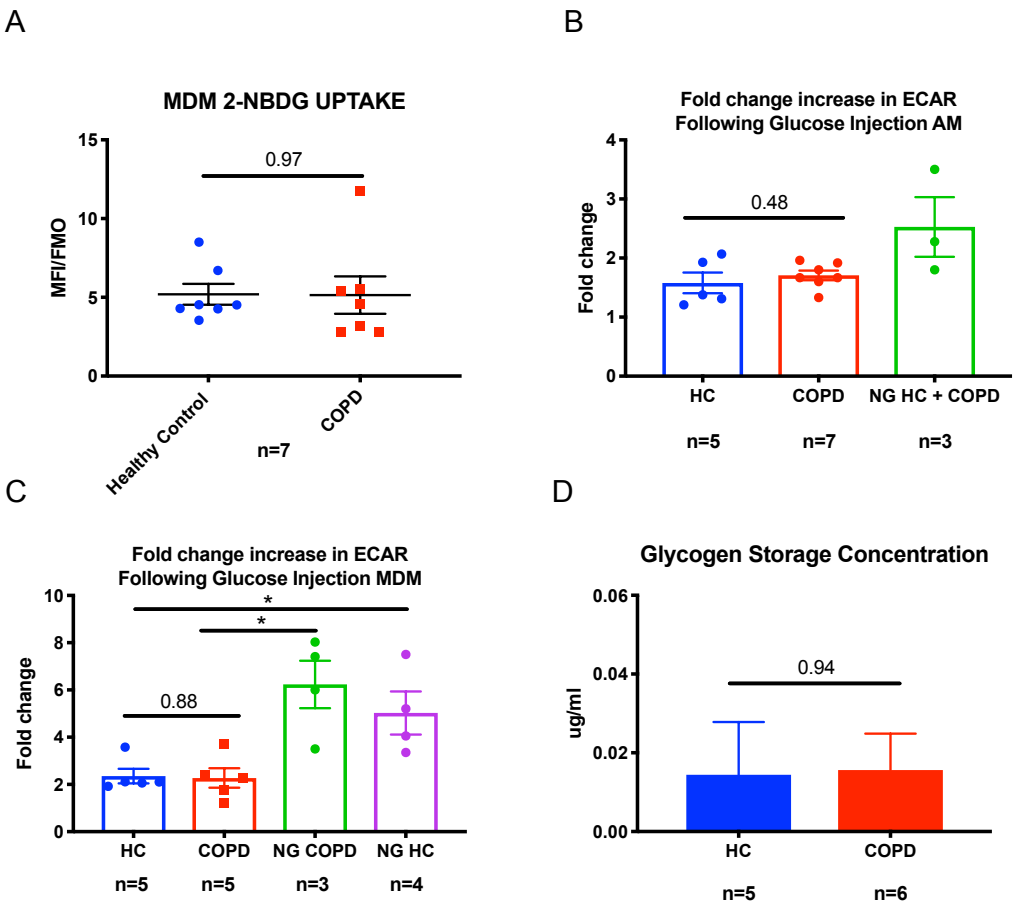

Figure 4.11: Differences in glycolytic rates are not determined by differential glucose uptake/glycogen breakdown in COPD Macrophages. **(**A) Glucose uptake was measured by culturing cells with 2-NBDG, a fluorescently-labelled deoxyglucose analogue for two hours prior to measuring uptake on flow cytometry. Uptake rates were normalised to median cell fluorescence of unstained cells. There was no significant difference detected between donor groups. (B)The increase in ECAR rates prior to and following injection of Glucose during Glycolysis Stress Tests was measured in AM (B) and MDM (C). Prior glucose deprivation x 16 hrs (NG) was used as a positive control.(D) Using a colorimetric assay, glycogen stores in MDM and AM were measured. $P \leq 0.05$ used to determine significance. Data represents individual values and mean ± SEM. MFI= Median Fluorescence Intensity, FMO =Fluorescence minus one, unstained cells.

4.12 *Profiling of Bronchoalveolar lavage fluid suggests that availability of substrate in the alveolar space does not differ between COPD and Healthy donors*

To determine if substrate availability in Bronchoalveolar lavage (BAL) fluid was influencing metabolic phenotypes in COPD, we quantified the two main substrates utilised by Alveolar macrophages- Glucose and Glutamine - in BAL from COPD and Healthy Donors. Both Glucose and Glutamine levels were comparable between the two groups (Figure 4.12 A+B). Interestingly lactate levels were elevated in COPD BAL (Figure 4.12 C). Coupled with increased lactate levels intracellularly in AM, as detected by LC-MS, this provides further evidence for increased glycolysis in COPD macrophages.

It is important to note that BAL return can vary with patients and so samples retrieved from one donor may be more dilute than another. It is challenging to normalise BAL in the context of our study group, as proteins such as Albumin or the cellularity of the BAL, will vary between disease state and Healthy lung. However, in profiling BAL fluid our aim was to identify if there were any large discrepancies present in substrate levels.

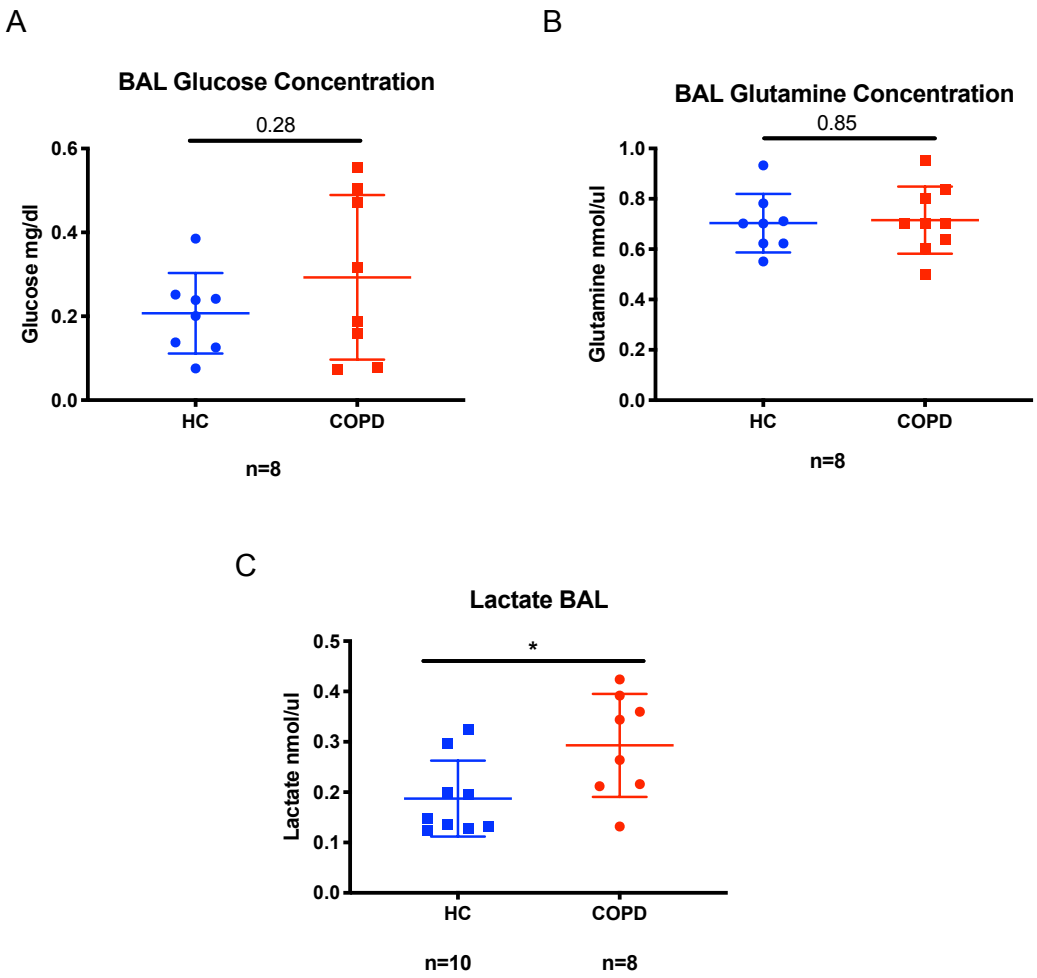

Figure 4.12: Profiling of Bronchoalveolar lavage fluid suggests substrate availability fluid does not account for metabolic differences in COPD macrophages.

Colorimetric assays were used to determine (A) Glucose, (B) Glutamine and (C) Lactate concentration in Bronchoalveolar Lavage (BAL) fluid from COPD and Healthy donors. P value calculated by unpaired t-test, * P≤0.05. Data represents individual values and mean ± SEM.

4.13 *COPD AM display a refractory metabolic profile.*

As discussed, metabolism is central to macrophage function and macrophage ability to undergo metabolic programming in response to varying stimuli is a critical feature of their plasticity. It is generally accepted that “M1” or pro-inflammatory stimulation leads to enhanced glycolysis in macrophages, where as “M2” or reparative type stimuli induce oxidative phosphorylation.

Apoptotic neutrophils represent an M2 stimulus but are also a source of substrate for metabolism following efferocytosis and subsequent breakdown[105]. To challenge metabolic plasticity and also to mirror our functional assays, we co incubated AM from COPD and Healthy donors with 20hr apoptotic neutrophils (AN). AN were co incubated with AM at an MOI 10:2 in Healthy Donors and 15:2 in COPD AM (to allow for reduced efferocytosis), for 90 minutes prior to their removal. A Mitochondrial stress test and Glycolytic stress test was subsequently performed.

Healthy AM displayed a significant increase in Spare Respiratory Capacity (SRC) following co-incubation with AN, with no change in Spare Respiratory Capacity evident in COPD AM (Figure 4.13 A). Strikingly there was no increase in Glycolytic Reserve in either Healthy or COPD AM following co-incubation with AN (Figure 4.13 B). Furthermore, treatment of Healthy AM with established M2 polarising stimuli, IL10 &IL4/13, failed to induce an

increase in SRC (Figure 4.13 C). Taken together these data suggest that the increase observed in SRC in Healthy AM following co-incubation with apoptotic neutrophils, is not due to a polarisation mediated increase in oxidative metabolism, instead, it is potentially driven by shuttling of scavenged substrate into this pathway. Despite an increased MOI to partially compensate for reduced efferocytosis rates, COPD AM did not show any change in metabolic parameters following presumed low level efferocytosis.

A

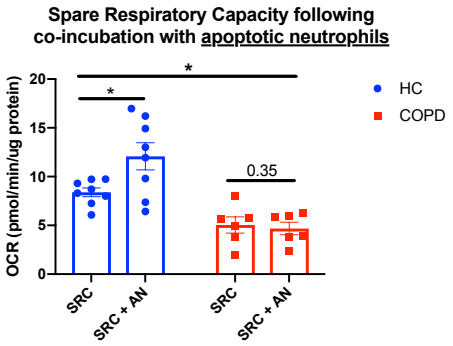

B

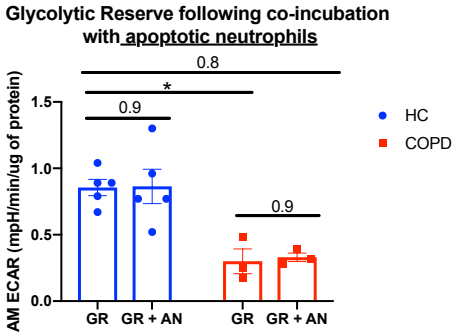

C

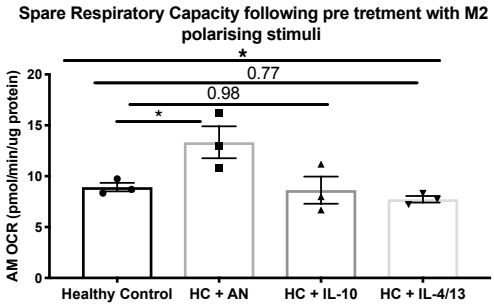

Figure 4.13: Healthy donor macrophages display efferocytosis mediated enhancement of oxidative metabolism.

Healthy and COPD donor macrophages were co incubated for 90mins with 20 hr apoptotic neutrophils (+AN) prior to performing Mitochondrial (A) and Glycolytic (B) stress testing. Spare Respiratory Capacity (SRC) and Glycolytic Reserve (GR) were calculated as before. (A) Healthy AM (n=8) have an increased SRC compared to COPD AM (n=5) .Healthy AM display a significant enhancement of their respiratory capacity following neutrophil efferocytosis.

(Figure 4.13 continued) (B) Healthy AM(n=5) have an increased GR compared to COPD AM (n=3), there was no change in GR induced by neutrophil efferocytosis in either group. (C) Healthy Donor AM (n=3) were co incubated with 20hr apoptotic neutrophils (+AN) or treated for 16 hours with 20ng/ml IL-10 or IL-4/13. M2 polarizing stimuli did not induce a change in respiratory capacity , in contrast with efferocytosis of apoptotic neutrophils. P values calculated via (A-B) Two-way ANOVA (C) One-way ANOVA , with Sidak's multiple comparisons. *P≤0.05, ****P≤0.0001. Data represents individual values and mean ± SEM. MOI 10:2 Healthy AM; MOI 15:2 COPD AM.

4.14 *Discussion*

These data highlight the markedly altered metabolic profile of COPD macrophages, both at baseline and in response to stimulation, with a likely profound effect on phenotype and cellular energetics.

It was interesting to note that the COPD AM transcriptome is intrinsically different to that of Healthy AM, even at baseline. In particular, the discovery that metabolic regulation was one of the most differentially expressed modules between the COPD and Healthy AM, provided evidence for our hypothesis that primary metabolism and cellular energetics are driving the phenotype of macrophage dysfunction in COPD. Perhaps the most striking finding however, was the divergence in transcriptional responses to co-incubation with *S. pneumoniae*. Bacterial pathogens are known to invoke an immediate glycolytic response but at 4 hours Healthy donor AM markedly upregulated genes for oxidative phosphorylation (oxphos). This likely represents a time dependent a switch in metabolism[106]. COPD AM, by comparison, failed to transcriptionally activate the oxphos module, instead there was a presumably persistent upregulation of glycolytic genes, at 4 hours. Though COPD AM have reduced bacterial phagocytosis, a reduction of ≈25% is unlikely to account for this discrepancy. Rather, this suggests an apparent failure to undergo appropriate metabolic reprogramming. This was evident also in the contrasting responses to co-incubation with apoptotic neutrophils. While Healthy donor AM increased oxidative metabolism

following efferocytosis, COPD AM metabolism remained unchanged. This occurred despite increasing the quantity of apoptotic neutrophils co-incubated with in COPD, to account for reduced efferocytosis. The findings raise the possibility that COPD macrophages have a refractory metabolic phenotype and may be unable to sense or respond appropriately to their environment.

Seahorse profiling of COPD macrophages revealed a profound depletion of critical energy reserves in COPD AM and MDM, in both glycolysis and mitochondrial respiration. A consequent reduction in ATP and energy charge was confirmed, using LC-MS. It is tempting to think that this metabolic exhaustion phenotype may be due to the hostile lung microenvironment encountered in COPD, characterised by poor substrate availability and chronic oxidant stress. Crucially, however, this phenotype was present in both AM and peripherally circulating monocytes (which we cultured into MDM) . Secondly, cells were cultured *ex vivo* in oxygen and glucose replete media prior to performing assays. This suggests that alterations in metabolic profile of COPD macrophages are “hard wired” and that cellular energetics in COPD remain altered despite culture conditions. The presence of a systemic defect in macrophage function raises important questions around epigenetic modification of cellular function in COPD, which merits further investigation.

Interestingly, while COPD AM and MDM both experienced depleted energy reserves, they exhibited a divergent dependence on glycolysis. Energy phenotyping revealed that COPD AM had reduced energy capacity

compared to Healthy AM, but COPD AM were comparatively overly reliant on glycolysis as the main source for ATP. This was even more pronounced when additional ATP was required (following co-incubation with Apoptotic neutrophils). It is possible that mitochondrial dysfunction , as previously described in COPD and suggested in our data by differences in OCR-Linked-ATP ratios between COPD and Healthy AM, may be driving this over reliance on glycolysis[96]. COPD MDM, in contrast, had an equally reduced energetic capacity across both glycolysis and oxidative metabolism, suggesting that COPD MDM may possess a higher degree of metabolic plasticity than AM. The monocytes, from which we cultured these MDM, circulate in a more substrate enriched environment and are less exposed to oxidative stress and subsequent mitochondrial damage than AM, which may account for this finding.

LC-MS quantification of individual metabolite abundance revealed that COPD AM and MDM had significantly higher levels of glycolytic intermediaries, compared to Healthy Controls. Coupled with the glycolytic dominance observed in energy phenotyping and the transcriptional responses of COPD macrophages to infection, this provides further compelling evidence for a refractory metabolism in COPD. As discussed, a persistently glycolytic metabolic programme will induce phenotypic changes in COPD macrophages via crosstalk between metabolic pathways and signalling via metabolic intermediaries and enzymes.

There are some discrepancies between Seahorse data and the LC-MS findings which require discussion - namely comparable basal ECAR readings between COPD and Healthy donors versus increased glycolysis in COPD as detected via LC-MS. This discrepancy may relate to methods of detection and or assay conditions. While seahorse provides excellent information about dynamic metabolic changes, it is an indirect measure of glycolysis. Thus, dynamic changes eg quantifying Glycolytic reserve, are likely more accurate than baseline Seahorse readings. Secondly, for the Glycolytic Stress Test, cells are deprived of glucose for 45 minutes prior to the test. This period of relative starvation may result in differential basal glycolysis rates between COPD and Healthy macrophages, giving rise to the observed discrepancy between LC-MS and Seahorse findings. Similarly, the utilisation of indirect measurements during Seahorse may account for the differences observed in basal OCR rates (reduced in COPD) against comparable TCA cycle intermediaries abundance in LC-MS.

Lastly, differences in substrate availability do not appear to be a driver for altered metabolism in COPD macrophages. Comparable levels of BAL Glucose and Glutamine coupled with equal intracellular glycogen storage, suggest that access to substrate is not directing the distinctive metabolic phenotype observed in COPD macrophages.

In summary, in keeping with previous findings of elevated glycolysis in COPD lung tissue and airway smooth muscle cells , COPD AM and MDM upregulated glycolysis, as detected by Affymetrix array, Seahorse energy

phenotyping and LC-MS measurement of metabolite abundance [93 94].

Crucially ,this increase in glycolysis was coupled with reduced energy reserves in both glycolysis and oxidative metabolism and a reduced energy charge. Taken together these data suggests that COPD macrophages lack the requisite metabolic arsenal to carry out high energy demanding processes such as efferocytosis and phagocytosis and that defective macrophage function in COPD may be a metabolic phenotype. In particular they display a rigid metabolic phenotype which suggests an inability to undergo appropriate metabolic reprogramming (Figure 4.12). Future directions should focus on the possibility that mitochondrial impairment-due to high level of oxidative stress- is responsible for the lack of metabolic plasticity observed in COPD. Similarly, examination of central metabolic sensing pathways such as mTOR may yield exciting insights into this phenotype. Additionally, certain noteworthy genes, identified as significantly altered at baseline in the transcriptomics data-set, merit particular attention. ME1 (Malic Enzyme 1) is the rate regulating enzyme for the cytosolic malate-pyruvate shut. In catalysing malate to pyruvate, it generates NADPH for redox power and fatty acid synthesis and the pyruvate generated can in turn be shuttled back into the TCA cycle. As high oxidative stress , mitochondrial dysfunction and supressed oxidative phosphorylation are features of COPD, changes in ME1 transcription may be of high importance in generating an altered metabolic phenotype in COPD AM.

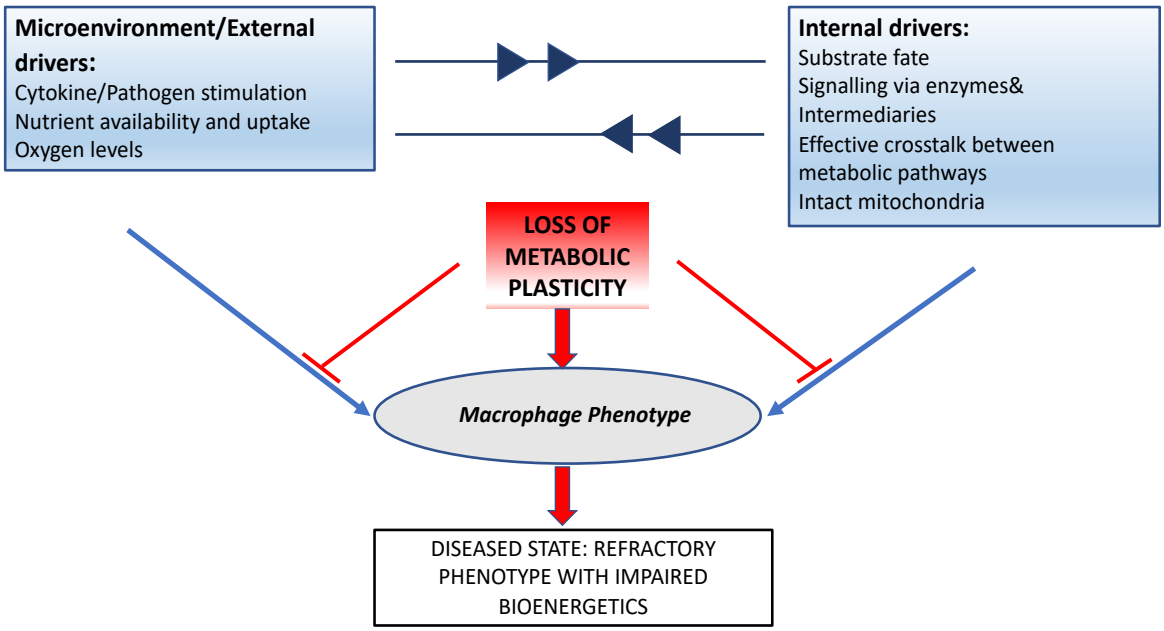

Figure 4.14: Proposed mechanism for altered metabolic status in COPD.

5 COPD macrophage dysfunction is rescued by activation of the Nrf2 module

5.1 *Introduction*

Endogenously produced reactive radical species are a normal by-product of cellular physiology. Cell derived oxidants or reactive oxygen species (ROS) such as superoxide anion (O_2-) and hydrogen peroxide (H_2O_2) are produced mostly by the mitochondria during respiration (mROS) but also by the NADPH oxidase unit in response to pathogens and via oxidoreductase and metal-binding reactions taking place in the cell. At physiological (low) levels ROS are considered critical for cell signalling and maintaining homeostasis. It is well documented that in macrophages, ROS abundance can influence a diverse array of cellular functions including induction of apoptosis, polarisation, migration and phagocytosis[107,108]. Similarly, ROS production via the NADPH oxidase unit, are crucial for bacterial killing[109]. In fact, deficiency of NADPH generated ROS gives rise to Chronic Granulomatous disease, characterised by recurrent severe infections.

As well as endogenously generated ROS, macrophages are also exposed to a variety of exogenous sources of ROS. Apoptotic cells can release ROS into the extracellular environment and ROS production can be induced by exposure to inflammatory cytokines. However, the largest contributor to exogenous ROS generation in the lung, is environmental exposure. A single

cigarette contains upwards of 10^{17} free radicals[110]. Tobacco smoke also contains high quantities of toxic compounds capable of inducing intracellular ROS production. More recently, increasing attention is being paid to the high volume of particulate matter caused by air pollution. This particulate matter is inhaled and retained in the lung where, similar to tobacco smoke, it has the capacity to generate reactive radical species[111].

As ROS production is a normal variant of cellular function, cells are well adapted to cope or "neutralise" ROS via enzymatic and non-enzymatic anti-oxidant responses, maintaining a healthy redox state within the cell. However if ROS levels become too high, either by aberrant intracellular production or via high level exposure to exogenously produced ROS, then these initial coping mechanisms can become overwhelmed, resulting in oxidative stress and consequent damage to DNA, proteins and lipid peroxidation. Organelles such as mitochondria – which due to limited repair mechanisms are exquisitely sensitive to oxidative stress- become damaged, leading to further mROS release and the generation of a self-perpetuating cycle of damage. Hence the cellular defence to oxidative stress, which is primarily regulated on a transcriptional level, is highly tuned.

The transcription of genes responsible for combatting oxidant stress is regulated by the ARE- the antioxidant response element. The transcription factor Nrf2 is considered the master regulator of the antioxidant response and acts on these AREs (*cis*-acting elements), thereby inducing the expression of key anti-oxidant and cytoprotective genes, minimising

oxidative-stress induced damage. The ARE was initially identified in the promoter regions of two key detoxifying genes – NQO1 (NAD(P)H:quinone oxidoreductase 1) and GSTA2 (glutathione S-transferaseα2)[112,113]. Since then it has been found to regulate upwards of 600 genes. Activation of the ARE leads to upregulation of phase 2 detoxifying genes, particularly those relating to the availability of Glutathione, the chief endogenous antioxidant. Antioxidants such as such as Heme Oxygenase 1 (HO1) and Superoxide dismutase (SOD1) are also upregulated via ARE activation. While these compounds and enzymes are able to bind to, and reduce reactive anions and metals, they rely on nicotinamide pairs $NADP^+$/NADPH (Nicotinamide adenine dinucleotide phosphate) and NAD^+/NADH (Nicotinamide adenine dinucleotide) to enable these reactions. These co factors donate a hydrogen ion to reducing equivalents such as Glutathione and Thioredoxin, restoring them from their oxidised to reduced form. Here again Nrf2 mediated activation of the ARE dictates redox power by increasing NAPDH generation. Expression of G6PD (Glucose-6-phosphate dehydrogenase) and PGD (Phosphogluconate dehydrogenase) -which increase NADPH generation through the Pentose Phosphate Pathway- and ME1 (Malic Enzyme 1) and IDH1 (Isocitrate dehydrogenase 1) -via NADPH generating shunts in the Kreb's Cycle- are regulated by Nrf2. Interestingly, Nrf2 mediated ARE activation regulates certain antioxidant gene expression under basal conditions also, suggesting the enhancer plays a critical role in maintaining redox balance , not only during stressed conditions but also in neutralising ROS generated under physiological conditions[114].In addition, recent evidence

suggests that Nrf2 anti-inflammatory effects are not just limited to the elimination of ROS. Nrf2 was found to interrupt lipopolysaccharide-induced transcriptional upregulation of proinflammatory cytokines, including IL-6 and IL-1β, cementing it as the cardinal regulator of cellular defence to oxidant stress[115].

Emerging experimental evidence suggests that Nrf2 regulated networks are not limited to antioxidant responses, but also modulate primary metabolism and bioenergetics (Figure 5.1). Studies have shown the Nrf2 activation increases glucose uptake and as mentioned, increases flux through the Pentose Phosphate Pathway (PPP) . Moreover, interference with glucose supply or flux through the PPP leads to a reduction in Nrf2 mediated Antioxidant responses, emphasising the crosstalk between metabolism and detoxification [116,117]. In keeping with impaired mitochondrial oxidation, a seminal study establishing the role of Nrf2 in cellular energetics demonstrated impaired mitochondrial respiration, reduced mitochondrial membrane potential and a reduced ATP level, in $Nrf2^{-/-}$ mice [118] . Conversely, Nrf2 deficiency lead to an increase in glycolytic intermediaries and an increase in Glycolysis-derived ATP [118,119] . While it was not definitely established in either of these studies, it was suggested that Nrf2 mediated improvement in oxidative stress protected the mitochondria from damage, enabling it to process substrate successfully. It has also been hypothesised that increased flux through the non oxidative branch of the PPP generates the requisite nucleotides for mitochondrial biogenesis[120]. Thus it would

appear that Nrf2 activation can induce metabolic reprogramming which supports the anti-oxidant response and vice versa.

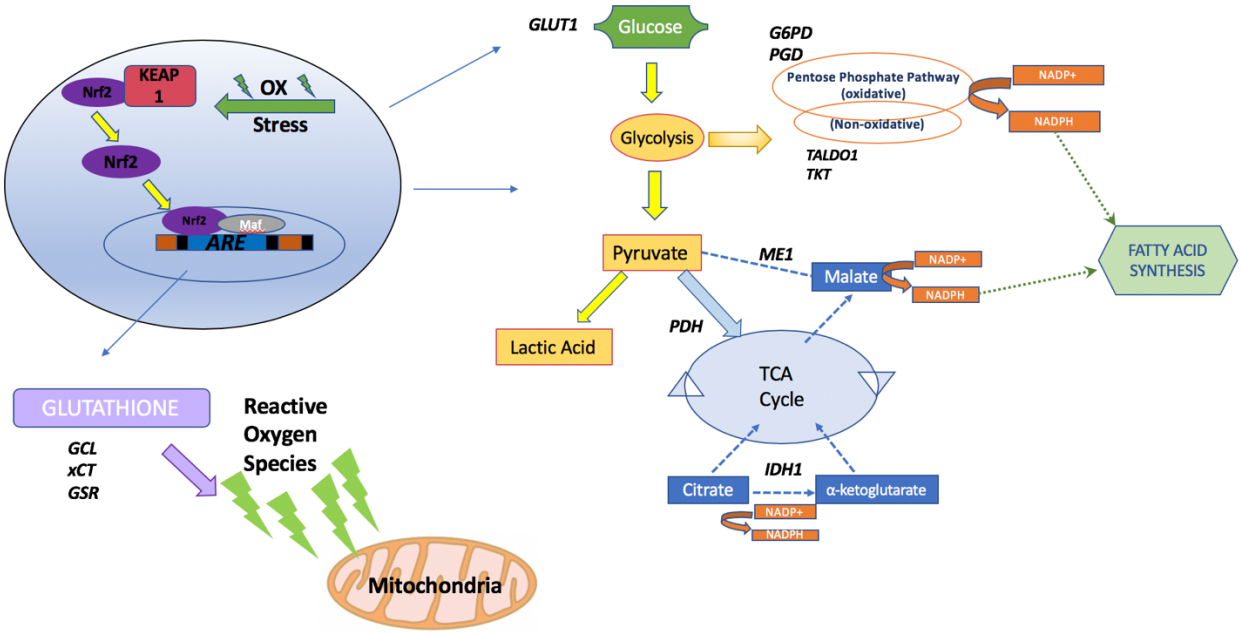

Figure 5.1: Nrf2 mediated modulation of cellular metabolism and anti-oxidant responses. Known Nrf2 targets are listed in *black italics*. ARE= Anti-oxidant Response Element. GCL= Glutathione Cysteine Ligase, xCT=Cystine transporter, GSR= Glutathione Synthase Reductase, GLUT1=Glucose Transporter 1, G6PD= Glucose-6-phosphate dehydrogenase, PGD=Phosphogluconate dehydrogenase, TALDO1= Transaldolase 1, TKT=Transketolase, $NADP^+$/NADPH=Nicotinamide adenine dinucleotide phosphate, ME1=Malic Enzyme 1, PDH=Pyruvate Dehydrogenase. IDH1=Isocitrate dehydrogenase 1.

Nrf2 tissue expression is most pronounced in the lung, intestine and kidney-sites where key detoxification occurs. In the lungs, it is predominantly expressed by alveolar macrophages and epithelial cells. Under normal conditions Nrf2 is predominantly cytoplasmic where its expression is

regulated by Kelch ECH Associating Protein 1 (KEAP-1). A recurrent theme in oxidant signalling and antioxidant regulation is reactive cysteine thiol–based redox signalling, which is the premise for Nrf2 regulation by KEAP1. When basal levels of oxidative stress are low, KEAP-1 binds to the N2 Ne-h terminal of NRF2, leading to its cytoplasmic sequestration, ubiquitination and subsequent proteasomal degradation. However in the presence of oxidative electrophiles, key modifications of the cysteine thiol residues on KEAP-1, lead to its dissociation from Nrf2. Nrf2 is then free to migrate to the nucleus where it heterodimerizes with another basic leucine zipper protein, such as small Maf or Jun and then binds to the antioxidant response element (ARE) in target gene promoters[121]. At present our understanding is that Nrf2 self regulates by reducing oxidative stress and so increasing its sequestration by KEAP1. In addition to this, one study has found that Nrf2 can induce KEAP1 expression, establishing a feedback loop [122].Another transcription factor Bach1, is known to competitively bind to the ARE, supressing gene expression[146]. Hence the status of the Nrf2/KEAP1/Bach1 axis ultimately dictates the anti-oxidant response.

High levels of oxidant stress have been implicated in a large number of pathological conditions such as Alzheimer's, Multiple Sclerosis , Diabetes and COPD. In 2004 a seminal study identified that Nrf2 deficient mice were extremely sensitive to oxidant stress and developed early-onset emphysema when exposed to cigarette smoke extract[123]. Following on from this, research examining the role of Nrf2 in COPD patients, established that both Nrf2

mRNA and protein were reduced in Alveolar Macrophages from COPD subjects, compared with age matched controls and regardless of smoking status[124]. A similar study found that Nrf2 protein levels were reduced in whole tissue homogenates from COPD patients. Importantly, in this study, they quantified nuclear and cytosolic Nrf2, Bach1 and Keap1 in AM and confirmed decreased nuclear and cytosolic Nrf2, increased nuclear Bach1 and increased cytosolic Keap1, in the emphysema group compared to controls. Reduced Nrf2 levels in the AM of emphysema patients correlated with reduced expression of key ARE genes such as HO-1 and NQO1 and importantly, expression of antioxidant genes inversely corelated with airway obstruction[125] .

This body of research raises a crucial question – if Nrf2 is induced by oxidative stress, then why are both cytosolic and nuclear Nrf2 levels reduced in COPD , a condition defined by high levels of oxidative stress. While it is tempting to consider that persistent Nrf2 signalling may lead to eventual desensitisation, constitutive Nrf2 expression continues to confer survival benefit in certain cancer cell lines[126]. Instead, the association of COPD with genetic polymorphisms in KEAP1 and GSR (Glutathione synthase reduction), coupled with increased nuclear Bach1 levels, may offer an explanation for altered Nrf2 signalling in COPD [127].

Having established that Nrf2 activity plays a role in COPD, research is currently focused on the potential augmentation of this pathway as a therapeutic strategy. Sulforaphane is a bioactive phytochemical derived from

cruciferous vegetables. It was first identified in 1992 as a major inducer of the antioxidant response element [128]. It is now known that Sulforaphane is able to react with the thiol groups of Keap1, covalently binding to KEAP1 and forming thionacyl adducts, promoting its dissociation from Nrf2 and subsequent activation of ARE. The ability of SFN to activate Nrf2-driven detoxifying genes is well documented both in vitro and in vivo, in murine and human models [129,130]. Based on the above evidence for impaired Nrf2 activity in COPD, a cardinal study by Harvey et al showed that Sulforaphane enhanced bacterial phagocytosis in COPD Alveolar Macrophages via upregulation of the scavenger receptor MARCO[49]. However its role in COPD monocyte derived macrophages and efferocytosis has yet to be established. As sulforaphane is not a specific activator of Nrf2, there are also some obvious concerns regarding co-activation of alternative pathways and off target effects[131].

We hypothesised that, in response to infection with *S. pneumoniae ,*COPD AM would have a defective antioxidant response. We sought to examine the therapeutic role of highly specific Nrf2 activation in restoring function to COPD AM and MDM . Using a transcriptomics approach, we aimed to identify the mechanism of action of Nrf2 activators on COPD macrophages. Lastly we wished to clarify if a potential Nrf2 mediated augmentation of macrophage function would be limited to cells with baseline abnormalities, or if, in fact macrophages from Healthy donors could also be enhanced.

Results:

5.2 *COPD Alveolar Macrophages fail to appropriately upregulate the Nrf2 module following infection with serotype D39 Streptococcus Pneumoniae*

To further dissect the COPD macrophage dysfunction we examined the transcriptional response of Alveolar Macrophages to infection with *Streptococcus pneumoniae.* Both COPD and Healthy Donor Alveolar Macrophages were exposed for 4 hours to serotype D39 *S. pneumoniae* prior to lysis and subsequent analysis via affymetrix array. As previously discussed in Chapter 3, there was a markedly reduced transcriptional response to infection seen in COPD AM compared to Healthy AM (Figure 3.18). Interestingly, this was particularly pronounced when examining the transcriptional response to oxidant stress (Figure 5.2 A). Detailed interrogation of the stress response revealed a failure by COPD AM to appropriately upregulate antioxidant modules, many of which are established Nrf2 targets, following co-incubation with *S. pneumoniae* (Figure 5.2 B). These included several detoxifying pathways for combatting cellular levels of reactive oxygen species (ROS). The transcriptional levels of vital ROS scavengers such as SOD1, which reduces superoxide and NQO1 which fully oxidizes quinones to prevent formation of semiquinones and subsequent ROS generation, were all upregulated in Healthy Donor macrophages but

remained unchanged in COPD. More strikingly still, several key regulatory steps of Glutathione, which are subject to Nrf2 activation, were upregulated in Healthy AMs in response to infection, with no transcriptional change induced in COPD AM (Figure 5.2 C).

A

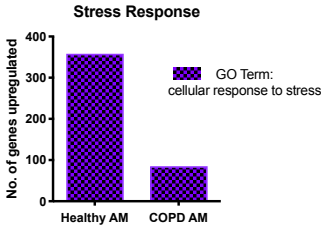

B

Gene :	Ensemble ID:	COPD AM:	Healthy AM:	Fold Increase: (log2)
GCLC	ENSG00000001084	⟺	⬆	1.287
GSS	ENSG00000100983	⟺	⬆	0.848
GPx7	ENSG00000116157	⟺	⬆	2.397
xCT	ENSG00000151012	⟺	⬆	4.408
SOD1	ENSG00000142168	⟺	⬆	1.13
NQO1	ENSG00000181019	⟺	⬆	0.771
TXN2	ENSG00000100348	⟺	⬆	0.87
GSTZ1	ENSG00000100577	⟺	⬆	1.52

C

Examples of Nrf2 mediated Antioxidant pathways which are upregualted in Healthy AM only, after infection with S. pneumoniae.

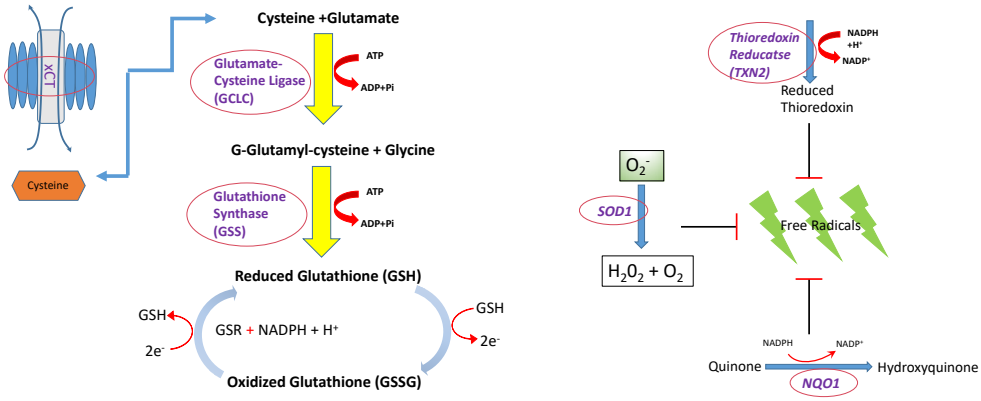

Figure 5.2: Affymetrix array reveals aberrant stress response to infection in COPD donors.

AM from COPD and Healthy donors were co-incubated with D39 *S. pneumoniae* prior to lysis for affymetrix array.(A) The stress response to infection is reduced in AM from COPD donors compared to Healthy donor AM. (B) A number of established Nrf2 targets, a key transcription factor in the response to increased cellular stress, were upregulated in Healthy donors but remained transcriptionally unchanged in COPD donor AM. (C) Schematic representation of Nrf2 mediated antioxidant pathways listed in (B). Nrf2 targets are circled in red.

5.3 *Treatment with the Nrf2 activator, Sulforaphane, upregulates the Anti-Oxidant Response element in Alveolar and Monocyte-derived macrophages*

Following identification that COPD AM failed to appropriately upregulate antioxidant responses, we sought to establish if Nrf2 mediated activation of the ARE could reverse COPD macrophage dysfunction .

Sulforaphane is a naturally occurring electrophilic compound which is a potent inducer of the antioxidant response. As discussed, sulforaphane mimics oxidant stress in the cytosol by modifying key cysteine residues on KEAP[132]. This leads to KEAP1 dissociation from the transcription factor Nrf2, when then migrates to the nucleus and activates the Anti-oxidant response element (ARE), leading to upregulation of 100s of key detoxifying genes.

Heme oxygenase 1 (HO-1) catalyses the degradation of heme to biliverdin/bilirubin, ferrous iron, and carbon monoxide. Increased HO-1 protein and mRNA expression is widely accepted as a marker for ARE activation. Healthy AM (Figure 5.3 C) and MDM (Figure 5.3 D) treated with Sulforaphane 10μm for 16 hours have increased expression of HO-1 as measured by Western Blot. This Western blot was generated by Dr Martin Bewley, a post-doctoral researcher in the lab of our collaborator on this project, Professor David Dockrell and has been published [38].

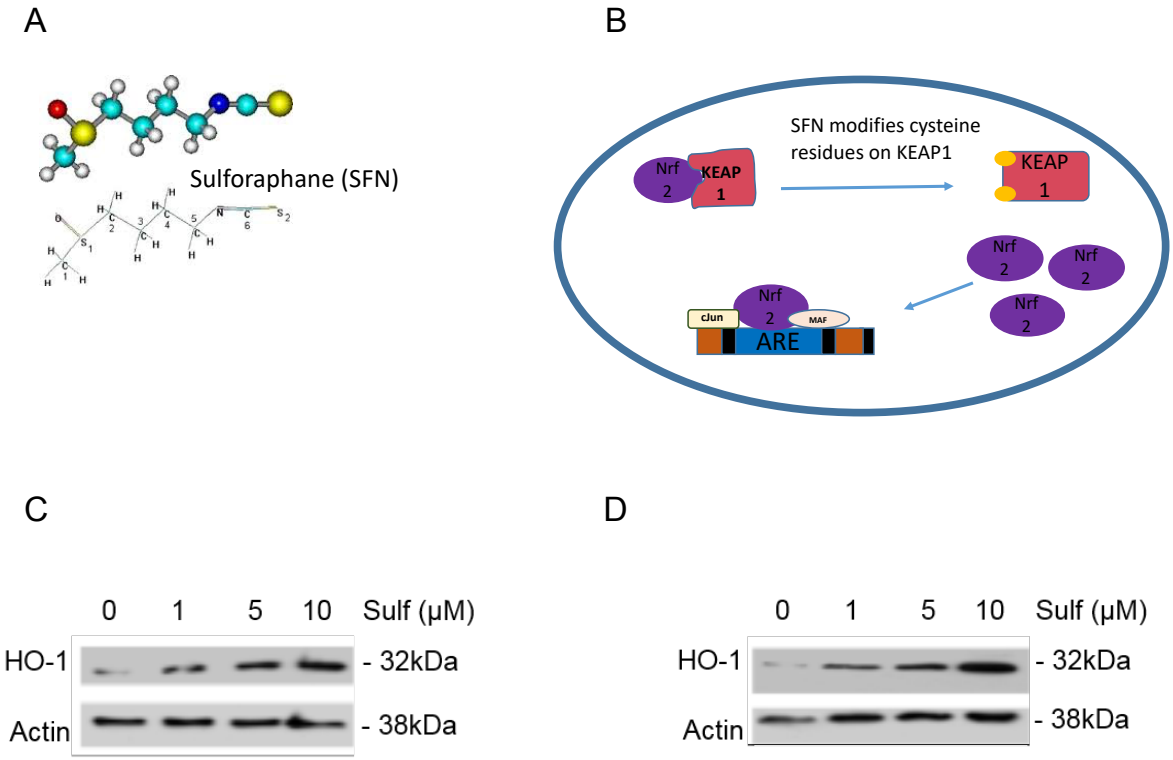

Figure 5.3: Sulforaphane disrupts the KEAP1/NrF2 complex to activate the Anti-oxidant Response Element (ARE).
(A) The chemical structure of Sulforaphane. (B) Sulforaphane modifies key cysteine residues on KEAP1, leading to its dissociation from Nrf2 and activation of the ARE. (C) AM and (D) MDM were pretreated for 16hrs with increasing doses of sulforaphane, then lysed and blotted for expression of Heme-oxygenase 1 (HO-1). B-actin was used as a loading control.

♦Figures C+D were generated by Dr Martin Bewley

5.4 *Activation of Nrf2 by Sulforaphane partially recues impaired bacterial macrophage phagocytosis in COPD , with preserved anti-microbial killing*

In COPD donors there was a significant increase in bacterial phagocytosis of opsonised S14 *S. pneumoniae* following 16 hour pretreatment with Sulforaphane 10μm. COPD AM bacterial phagocytosis was increased by a mean of 383 cfu/ml(12%) and MDM by 341cfu/ml (11%) with Sulforaphane treatment (Figure 5.4 A) There was no significant increase in macrophage bacterial phagocytosis in either MDM or AM from Healthy donors (Figure 5.4 A + B)

Although Sulforaphane treatment did improve bacterial phagocytosis in COPD macrophages, it did not elevate it to the same level as that of healthy donors. (mean Healthy AM = $\log_{10}$ 2.93±0.18cfu/ml vs Mean COPD AM + Sulforaphane $\log_{10}$ 2.87±0.08cfu/ml. Mean Healthy MDM $\log_{10}$ 3.32±0.1cfu/ml vs Mean COPD MDM + Sulforaphane $\log_{10}$ 2.89±0.1cfu/ml)

Reactive oxygen species (ROS) are key components of the antimicrobial repertoire of macrophages. As activation of the ARE improves redox balance and neutralizes ROS, we questioned if Sulforaphane treatment could impair bacterial killing capacity in treated cells. As evidenced in Figure 5.4 C, pre-treatment with Sulforaphane increased internalisation rates while preserving bacterial killing in COPD macrophages.

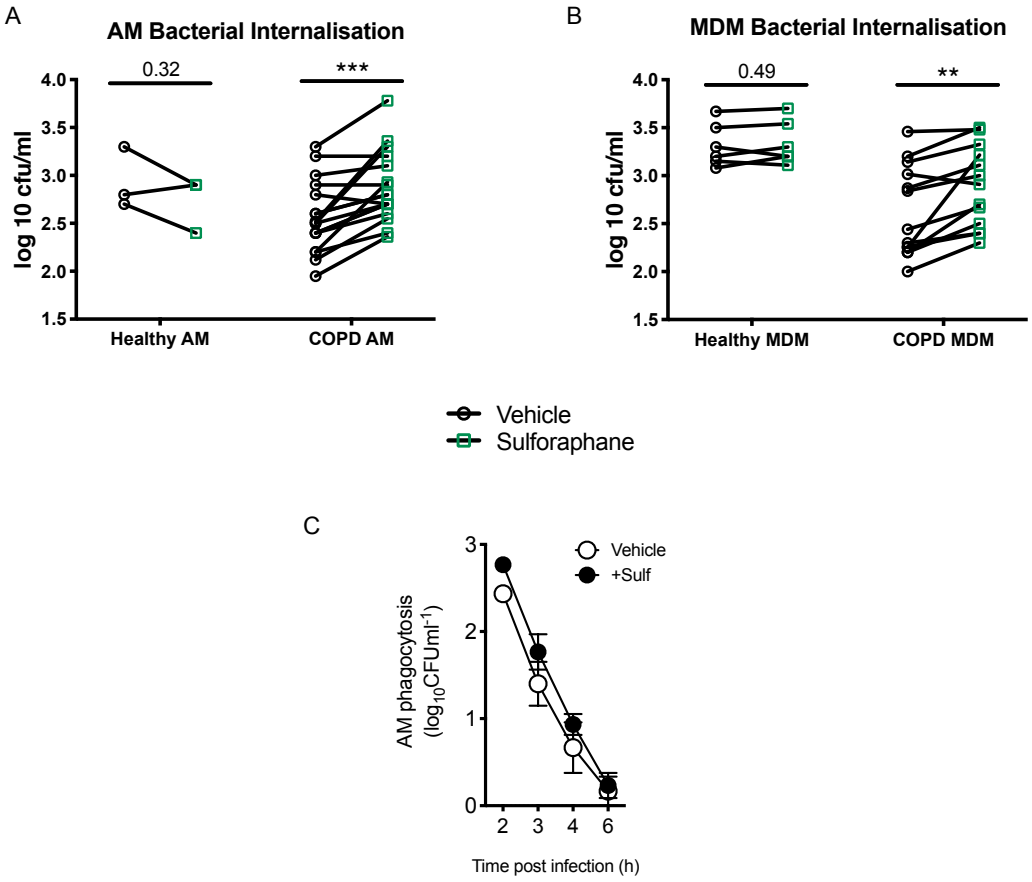

Figure 5.4: Treatment with Sulforaphane increases phagocytosis of serotype 14 *S. pneumoniae* in COPD without compromising intracellular bacterial killing.

(A) COPD AM and (B) MDM were pretreated with Sulforaphane 10μM for 16 hours prior to challenge with opsonised serotype 14 *S.pneumoniae* and numbers of viable intracellular bacteria were assessed 4 hours post challenge or (C) COPD AM at the designated time post antibiotics. (A) n= 3/ 17; (B) n= 6/13;(C) n= 3. P values calculated by paired t-test, *P ≤0.05, ** P≤0.01 , *** P≤0.001.

5.5 *Treatment with Sulforaphane rescues defective efferocytosis in both Alveolar and Monocyte-Derived Macrophages in COPD patients*

AM and MDM from COPD and Healthy Donors were co-incubated with apoptotic neutrophils labelled with the membrane dye PKH26 for 90 mins before efferocytosis rates were measured on flow cytometry. Pre-Treatment with 10μm Sulforaphane for 16 hours significantly enhanced efferocytosis rates in macrophages form COPD but not Healthy donors (Figure 5.5 A + B). Mean efferocytosis was increased in COPD AM from 14.3±1.9% to 29.6±4.5%, a 106% increase and MDM from 16.9±1.5% to 26.3±2.4%, a 54% increase following treatment with Sulforaphane in COPD donors. Following Sulforaphane treatment mean efferocytosis rates remained lower in treated COPD macrophages than Healthy donors cells (AM = 41.1±2.3% vs 29.6±4.5%; MDM = 31.4±4.2 % vs 26.3±2.4%).

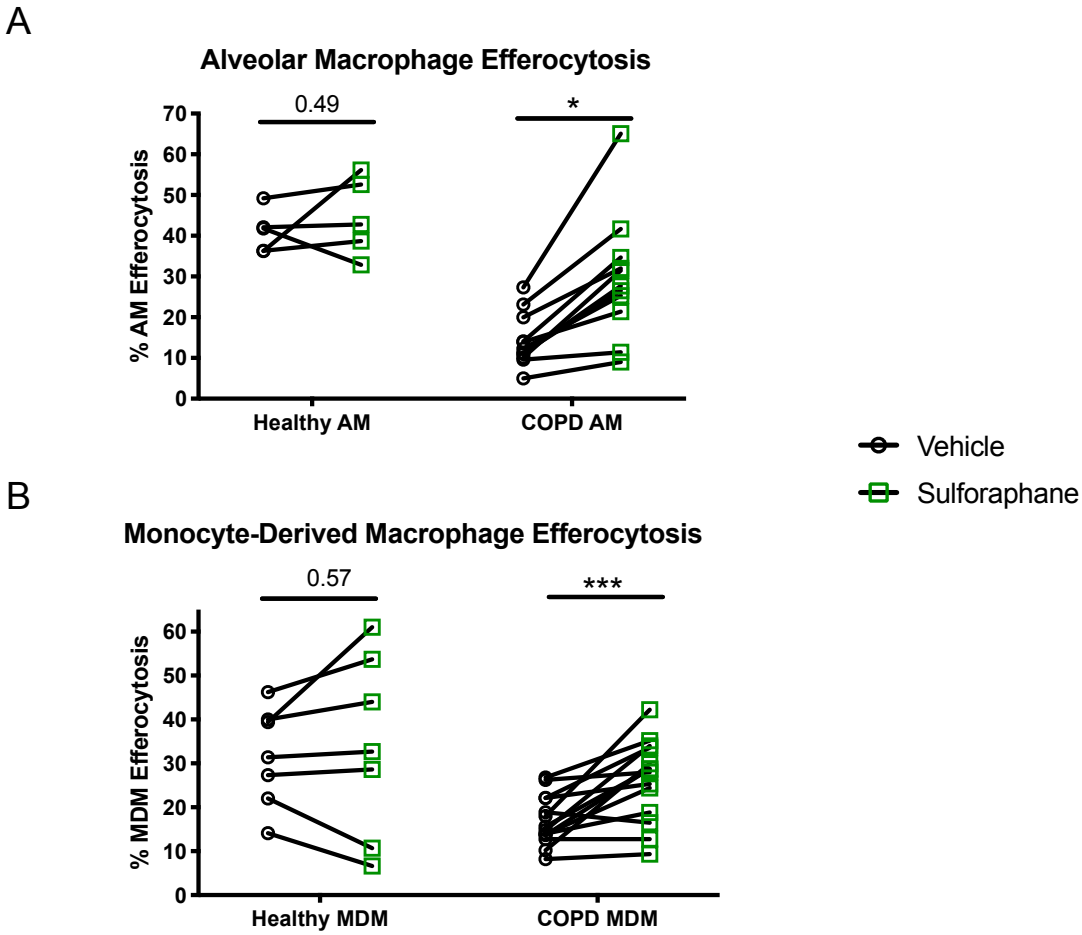

Figure 5.5: Treatment with Sulforaphane partially recues efferocytosis in COPD macrophages.

(A) COPD AM and (B) MDM were pre-treated with Sulforaphane 10μM for 16 hours prior to co-incubation with PKH26 labelled 20hr apoptotic neutrophils. Efferocytosis was measured via flow cytometry. (A) n= 5/11; (B) n = 7/14. P values calculated by paired t-test, * P ≤0.05, *** P≤0.001.

5.6 *Treatment with a novel, highly specific Nrf2 activator also upregulates HO-1 in COPD macrophages*

While Sulforaphane has been found to activate the ARE in a wide range of cells and tissues, there are concerns regarding its specificity and thus its suitability as a therapeutic agent[133]. Sulforaphane mimics oxidant stress by altering cysteine modules on KEAP1 but this process is not specific to KEAP1 and it may alter cysteine modules on other complexes. It is known to have a number of off target effects such as cell cycle arrest, DNA hypomethylation, and to cause alterations in *long terminal repeat* transcriptional activity, potentially conferring genome instability [134,135]. It is also recognised to induce non Nrf2 mediated suppression of IL-1β[136]. In addition, Sulforaphane possesses an undesirable pharmacokinetic profile. In its naturally occurring state it is an oil and so has poor aqueous and thermal stability. It has a low potency and bioavailability is influenced by gut microbiota, with consequent issues arising around predictable dosing scheduling [137,138] .

Due to its lack of specificity, it was not clear if improved macrophage function in COPD macrophages following treatment with Sulforaphane, was specifically due to upregulation of the Nrf2 mediated antioxidant response. Fortunately, we were able to test this hypothesis by obtaining a panel of highly specific Nrf2 activators, Compounds A, B and C, through a collaboration with GSK via COPDMAP. These compounds are currently

unpublished and although their specific structure is unknown to us, they work by disrupting protein-protein interactions between Nrf2 and KEAP1, with nanomolar efficacy.

Treatment with Compounds A, B and C activated the ARE in both COPD and Healthy donor MDM, as measured by HO-1 activity (Figure 5.6 A+B). There was a greater uplift in HO-1 expression following treatment with Compound A than there was with the non-specific activator Sulforaphane, though interestingly HO-1 expression in COPD MDM following treatment did not appear to equate to levels seen in Healthy MDM.

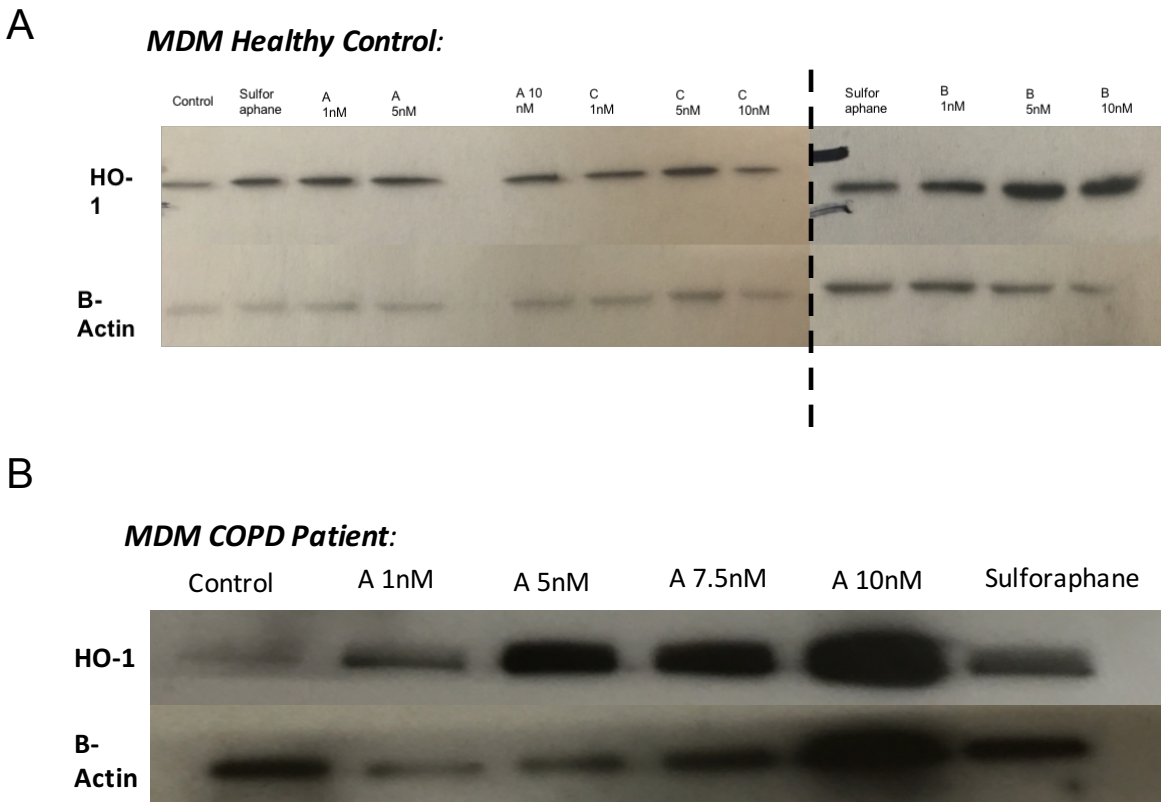

Figure 5.6: Highly specific activation of Nrf2 upregulates HO-1 in Healthy and COPD Donor MDM.

(A) Healthy donor and (B) COPD donor MDM were pretreated with novel highly specific Compounds A , B and C at increasing doses and Sulforaphane 10μM for 16 hours then lysed and blotted for expression of Heme-oxygenase 1 (HO-1). B-actin was used as a loading control. The dashed line in (A) indicates a separate gel.

5.7 *Treatment with the specific Nrf2 activator, Compound A significantly enhances both bacterial phagocytosis and efferocytosis in AM and MDM from COPD donors, but not Healthy donors*

Following a review of both our data and pharmacokinetic data generated by our GSK collaborators, it was decided by their novel drug review panel that all further testing in COPD donors would focus only on Compound A from the originally provided panel.

Using Compound A ,we were able to replicate the uplift in bacterial internalisation and efferocytosis rates in COPD macrophages seen with Sulforaphane treatment , confirming that this was a specific Nrf2 activation phenomenon (Figure 5.7 A-D). Again, there was no significant change in bacterial internalisation rates following treatment with Compound A in macrophages from Healthy Volunteers.

Treated COPD AM and MDM showed significantly increased levels of phagocytosis (Figure 5.7 A+C). In COPD AM, mean cfu/ml of 633±1.3 in vehicle treated cells increased to 1174±1.5cfu/ml in Compound A treated cells, an 85% increase. Similarly, in COPD MDM, mean cfu/ml of 909 in vehicle treated cells rose to a mean of 2032±1.8cfu/ml following Compound A treatment, a 123% increase. Healthy AM failed to show significantly enhanced phagocytosis following treatment with Compound A.

Treatment with Compound A also enhanced efferocytosis in COPD AM and MDMs but as with phagocytosis rates, rates of change in Healthy Volunteer AMs failed to reach statistical significance (Figure 5.7 B+D). Mean efferocytosis rates increased from 6.3±1,4% to 8.7±1.6% (a 35% increase) in COPD AM and from 18.6±3.17% to 22.1±2.6%(a 19% increase) in COPD MDM.

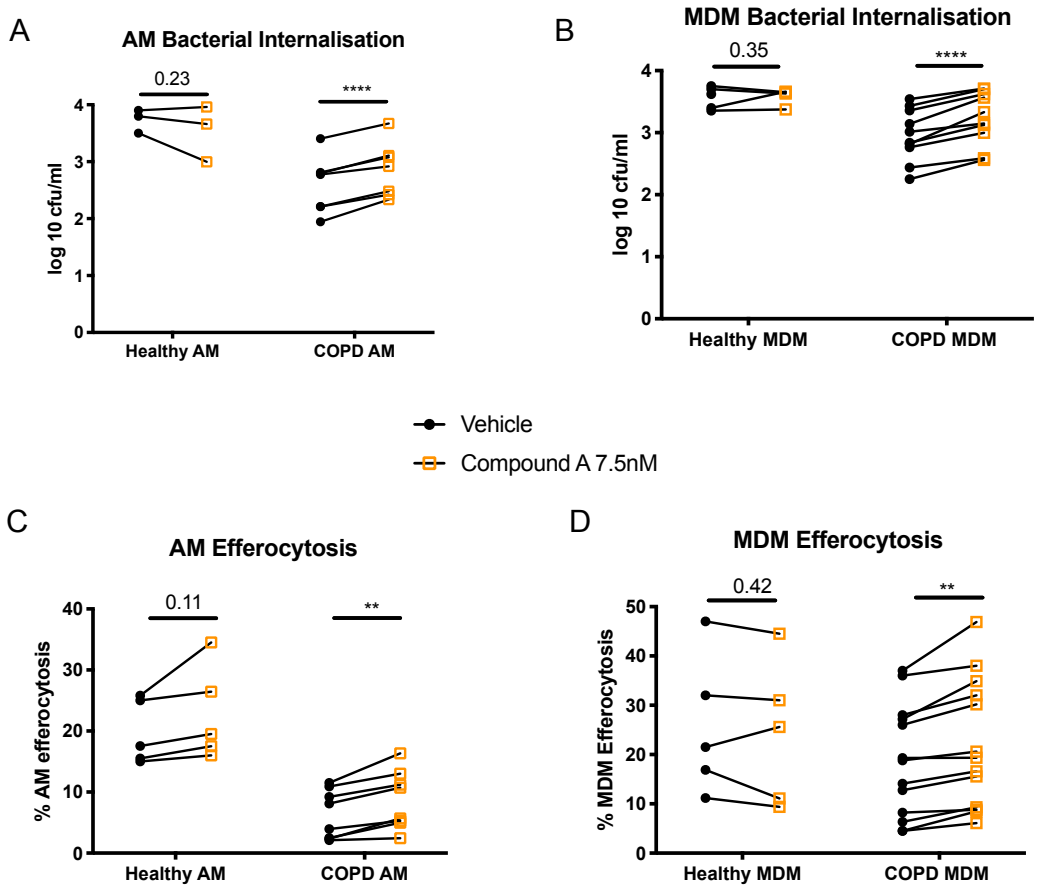

Figure 5.7: The Nrf2 activator, Compound A ,enhances efferocytosis and bacterial phagocytosis in COPD AM and MDM.

COPD and Healthy AM (A, C) and MDM (B ,D) were pretreated for 16 hours with the Nrf2 agonist, Compound A at 7.5nM. (A, B) Cells were then co-incubated with opsonised S14 *S. pneumoniae*, 4hrs post challenge the number of viable bacteria was measured. (C, D) Cells were pre-treated prior to co-incubation with PKH26 labelled 20hr apoptotic neutrophils, efferocytosis rates were measured by flow cytometry. (A) n= 3/7;(B) n= 5/10; (C) n=5/8;(D) n=5/13 . P values calculated by paired t-test, **P≤0.01, **** P≤0.0001.

Compound A enhances COPD macrophage bacterial internalisation and efferocytosis in a dose dependent manner without impairing bacterial killing

To establish the potency and efficacy of Compound A in macrophages, in tangent with our standard functional assays, we performed dose response curves of phagocytosis of opsonised S14 S pneumoniae and efferocytosis of 20 hr apoptotic neutrophils. Doses were calculated using the IC_{50} previously generated by GSK in Beas-2B cells.

There was no obvious functional benefit seen above a dose of 7.5nM in either efferocytosis or bacterial internalisation(Figure 5.8 A, B and C) . Unfortunately, as there is only a n=2 for this data, we were unable to determine significance. To ensure cfu/ml counts in Figures 5.8 B+C, represented changes in internalisation rather than changes in bacterial killing rates, a killing assay was performed in COPD AM. Compound A did not appear to impair early phase killing of *S. pneumoniae* in COPD macrophages, as assessed by an adjusted gentamicin protection assay (Figure 5.8 D). However, this graph represents an n=1 only. Based on these results and those generated by GSK this drug is now progressing to phase Ib testing with GSK.

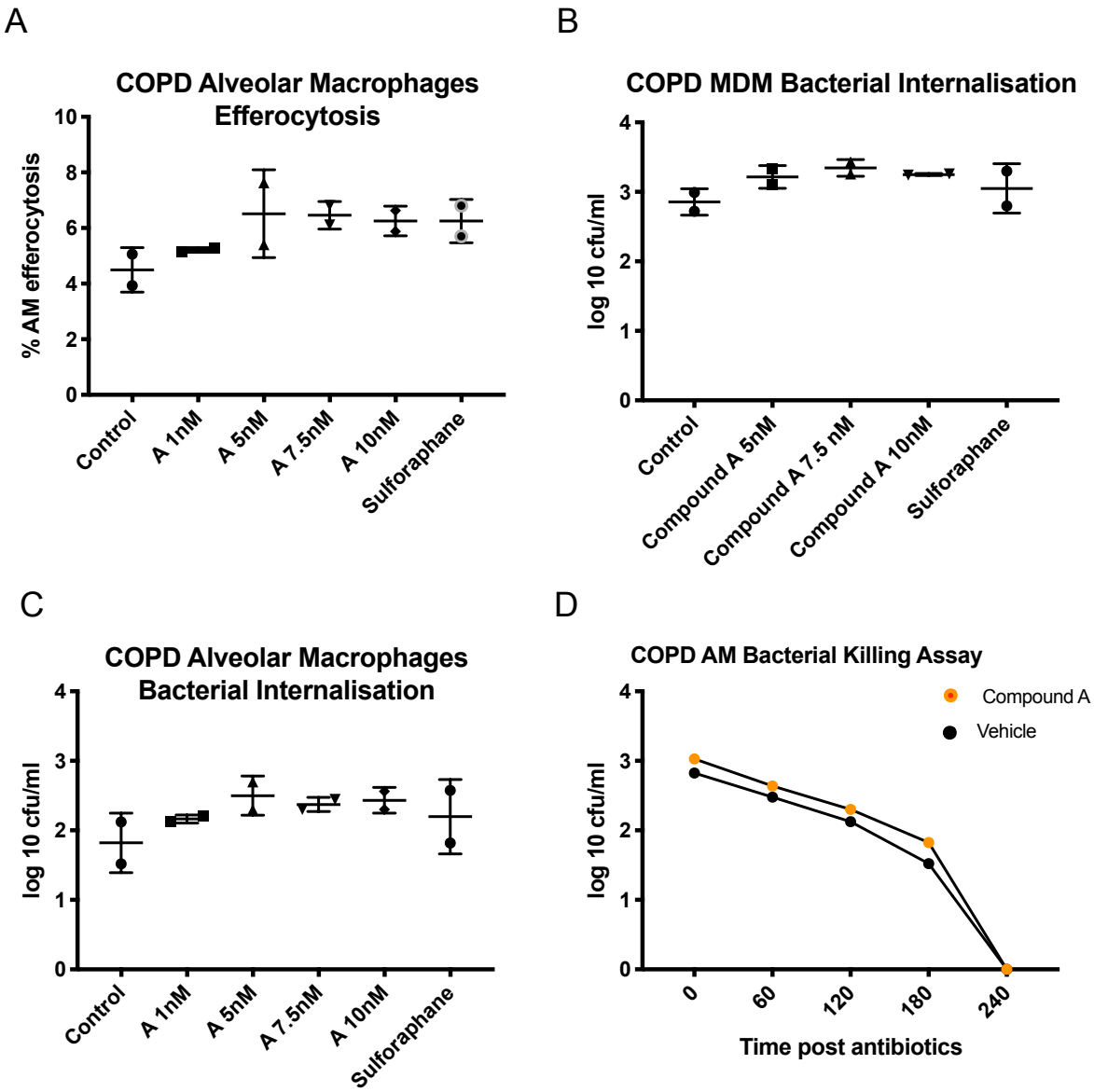

Figure 5.8: Dose response of Compound A in COPD MDM and AM , with no change detected in early bacterial killing following treatment.
(A,C,D) COPD AM and MDM (B) were pretreated with Compound A and Sulforaphane 10μM for 16 hours prior to challenge with (A) PKH26 labelled 20hr apoptotic neutrophils and (B+C) opsonised serotype 14 *S.pneumoniae* ,with numbers of viable intracellular bacteria assessed 4 hours post challenge or (D) at the designated time post antibiotics. (A), n=2;(B+ C) ,n=2; (D) n=1.

5.8 *Utilizing a published specific Nrf2 activator, Compound 7 , to target macrophage dysfunction in COPD*

As the panel of compounds supplied to us by GSK is currently unpublished, we had significant concerns about the feasibility of publishing this work within the desired time frame. Consequently we sought to re produce the uplift seen with Compound A, in a similar but already published GSK Nrf2 activator. Compound 7 ,analogous to Compound A, is a non-electrophile small molecule which works by disrupting protein-protein interactions on KEAP1, as opposed to modifying cysteine residues like Sulforaphane. Compound 7 occupies the binding site for Nrf2 on KEAP1 and so is a highly specific activator of Nrf2 (Figure 5.9 A+B). It is also one of the few types of PPI inhibitor to be thoroughly tested for off targets and is highly selective for disruption of the NRF2- KEAP1 interface[139]. Compound 7 works by occupying the C-terminal Kelch repeat domain, which is a protein-recognition module for NRF2 on KEAP1 (Figure 5.9 B). As seen with Sulforaphane and Compound A, Compound 7 also leads to upregulation of the ARE – as measured by HO-1 , NQO1 and GCLC- in COPD MDM and AM (Figure 5.9 A+C) identifying it as a suitable compound to utilize in our functional assays.

I generated these samples and the western blot was run by Ms Jennifer Marshall, a research technician in the lab of Prof David Dockrell and has since been published [38].

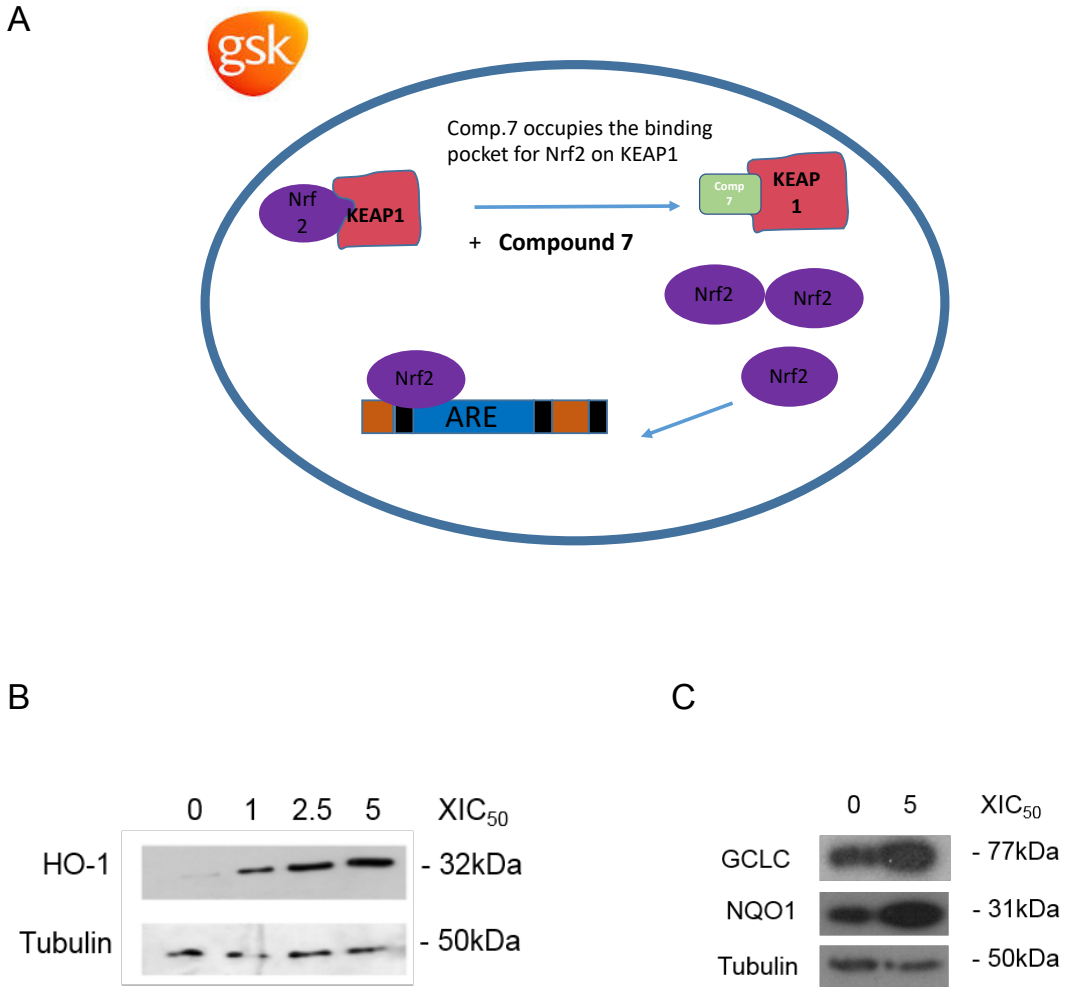

Figure 5.9: Compound 7 prevents Nrf2/KEAP1 binding , leading to activation of the Anti-oxidant Response Element (ARE).
(A) Compound 7 occupies the binding site for Nrf2 on KEAP-1 leading to migration of Nrf2 into the nucleus where it binds to and activates the ARE. (B) COPD MDM and AM (C) were pretreated with Compound 7 0.065uM for 16 hours then lysed and blotted for expression of Heme-oxygenase 1 (HO-1) and GCLC, NQO1. B-actin was used as a loading control.

♦ The blots in Figure B + C were run by Ms Jennifer Marshall

5.9 *The Nrf2 agonist Compound 7, significantly enhances efferocytosis and bacterial phagocytosis in COPD MDM and AM, but not in Healthy donor macrophages*

Pre-treatment with Compound 7, 0.065μM for 16 hrs, improved macrophage function in COPD AM and MDM. Bacterial phagocytosis of opsonised S14 *S. pneumoniae* in both COPD AM and MDM was significantly increased following treatment (Figure 5.10 A+B). There was a mean increase in AM bacterial phagocytosis of 594cfu/ml (a 92% increase) and in MDM of 1481cfu/ml (an 80% increase). In COPD donors mean efferocytosis in AM increased from 8.27±2.1% to 11.77±2.8% (a 42% increase) and in MDM from 22.4±1.5% to 27.4±2.1% (an increase of 19%) following treatment with Compound 7 (Figure 5.10 C+D). As seen with Compound A and Sulforaphane, there was no significant increase in either bacterial phagocytosis or MDM efferocytosis in Healthy donor macrophages following treatment with Compound 7. Due to limitation with donor numbers we could only perform Healthy AM efferocytosis with Compound 7 in 2 donors and so were unable to carry out statistical analysis on this group.

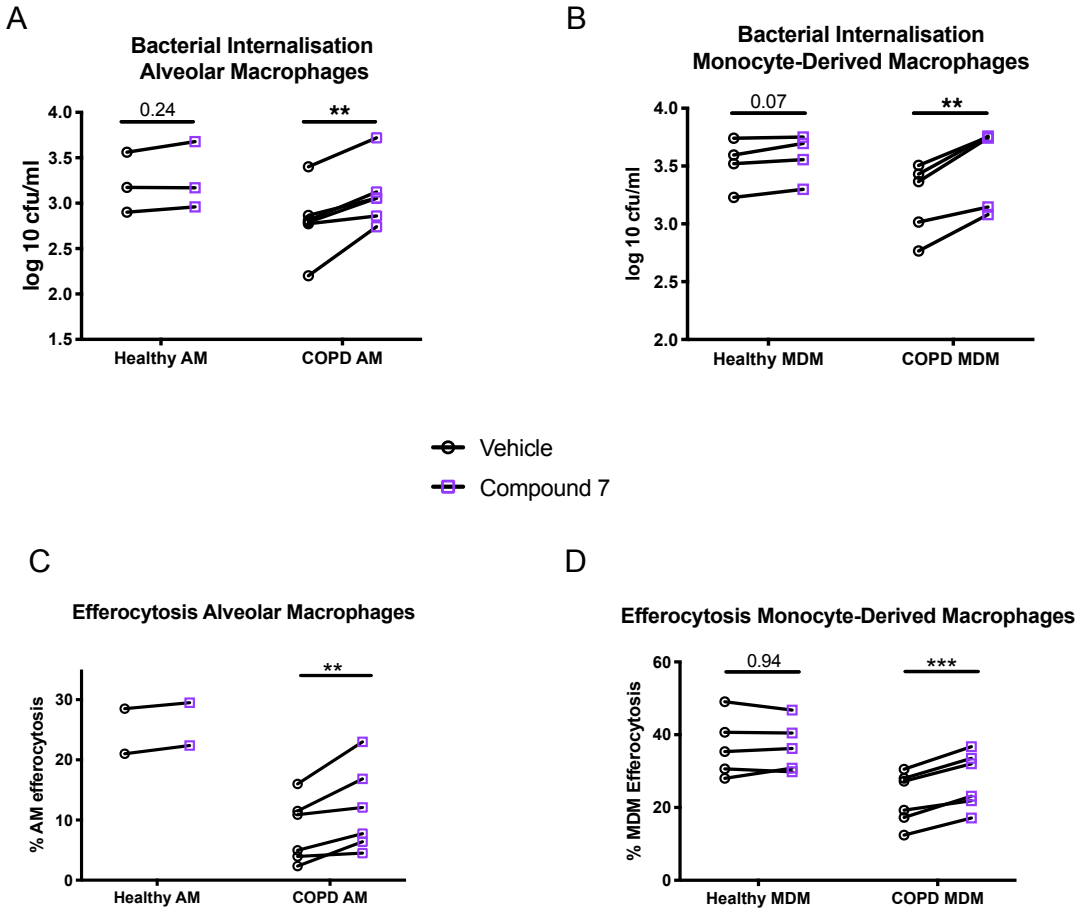

Figure 5.10: The Nrf2 agonist Compound 7, enhances efferocytosis and bacterial phagocytosis in COPD MDM and AM.
COPD AM (A, C) and MDM (B, D) were pretreated for 16 hours with the Nrf2 agonist Compound 7 at 0.065μM. (A, B) Cells were then co-incubated with opsonised S14 *S. pneumoniae*, 4hrs post challenge the number of viable bacteria was measured. (C, D) Cells were pre-treated prior to co-incubation with PKH26 labelled 20hr apoptotic neutrophils, efferocytosis rates were measured by flow cytometry. (A) n= 3/6;(B) n= 4/5; (C) n=2/6;(D) n=5/6. P values calculated by paired t-test, **P≤0.01, ***P≤0.001.

5.10 *Treatment with Compound 7 induces transcriptional change in COPD and Healthy Alveolar Macrophages*

As activation of Nrf2 had improved COPD macrophage efferocytosis and bacterial phagocytosis, we sought to identify the mechanism of action using an unbiased transcriptomics approach.

When generating the data set discussed in 4.2, we also compared the transcriptional response to Nrf2 activation between Healthy and COPD AM. We chose to use GSK's Compound 7 for this assay as its exact mechanism of action and structure is known to us and it has been published in the public domain[139]. As before, COPD and Healthy donor AM (n=3 for both groups) were cultured for 16 hours +/- Compound 7 prior to collecting RNA for total RNA-seq.

Treatment with Compound 7 induced a significant transcriptional change in both COPD and Healthy donor AM (Figure 5.11 A-D). A total number of 134 genes in COPD AM and 105 genes in Healthy donor AM met the criteria for significance = $>\log_2 1.5$ change in transcription and p value <0.05.

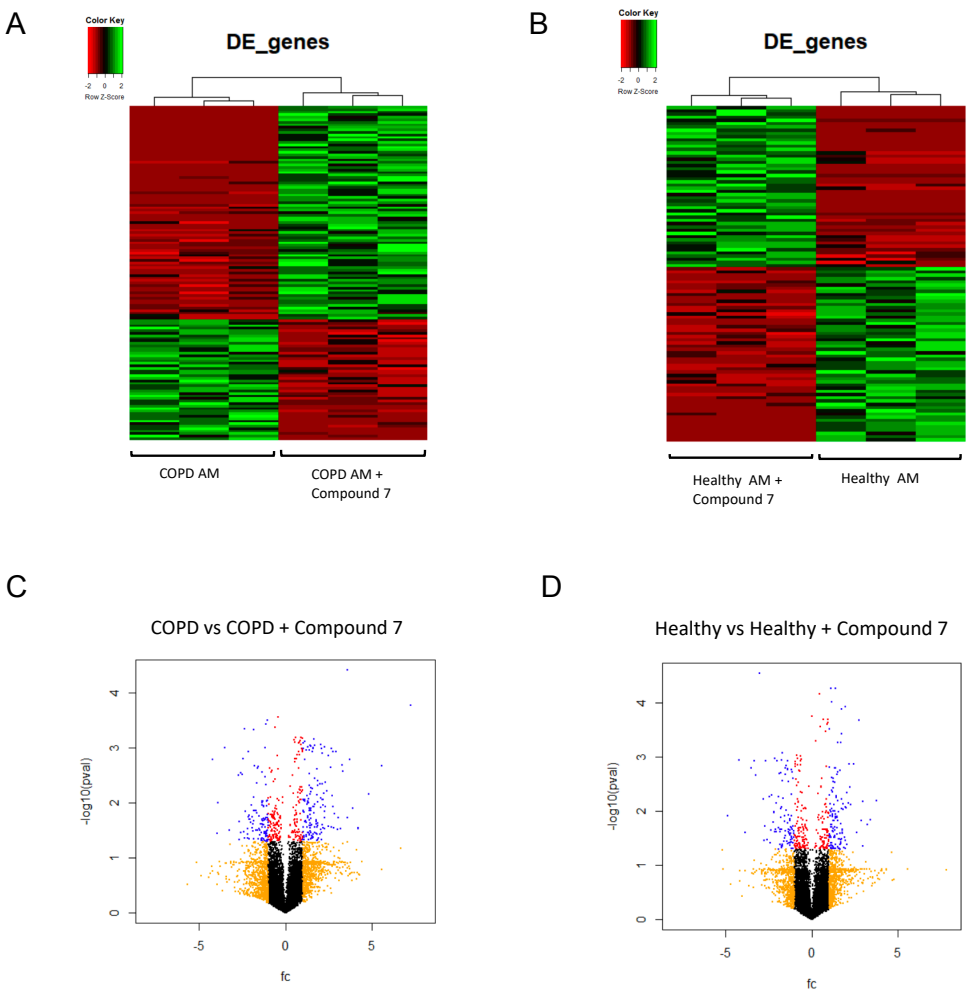

Figure 5.11: Nrf2 activation induces a significant transcriptional response in COPD and Healthy Donor AM.
AM were isolated from COPD (A+C) and Healthy (B+D) donors via bronchoalveolar lavage and treated with the Nrf2 activator, Compound 7 for 16 hrs prior to collecting RNA for Total RNA-seq.(A) Heatmap of normalized Z-scores for each gene identified as significantly altered between COPD (A) and Healthy AM (B) + Compound 7. Green indicates a relative high expression state, red indicates a relative low expression state. (B) Volcano plots displaying the $\log_2$ fold change between COPD (C) and Healthy (D) AM + Compound 7. Log_{10} P values are plotted on the y-axis. Blue dots are genes that are both highly altered as well as contain a significant P value = FC > $\log_2 1.5$ and P value ≤ 0.05 . No of blue dots in (C) n= 134 (D) , n= 105 . Orange dots contain genes which are FC >$\log_2 1.5$ but P value > 0.05, Red dots contain genes which are FC <$\log_2 1.5$ but p value ≤ 0.05. n=3 both groups. fc= Fold Change, DE = Differentially Expressed.

5.11 *COPD AM transcriptional profile more closely resembles Healthy AM , after treatment with Compound 7*

Treatment of COPD AM with Compound 7 induces bidirectional change in gene expression which “resets” the COPD AM transcriptome to more closely resemble Healthy AM (Figure 5.12.1 A+B).

Correlation analysis across the 27,000 gene set confirmed that COPD AM were more highly correlated with Healthy AM following treatment with Compound 7 (R^2= 0.8881 to R^2= 0.9027) (Figure 5.12.2 A). Furthermore genes which were significantly differentially expressed between COPD and Healthy AM at baseline (red dots) can be seen to correlate more closely after treatment of COPD AM with Compound 7 (Figure 5.12.2 B). There are a number of outliers, however, indicating that the shift in previously DE genes between COPD and Healthy AM at baseline, account for some , but not all of the changes responsible for the more closely aligned transcriptome following treatment.

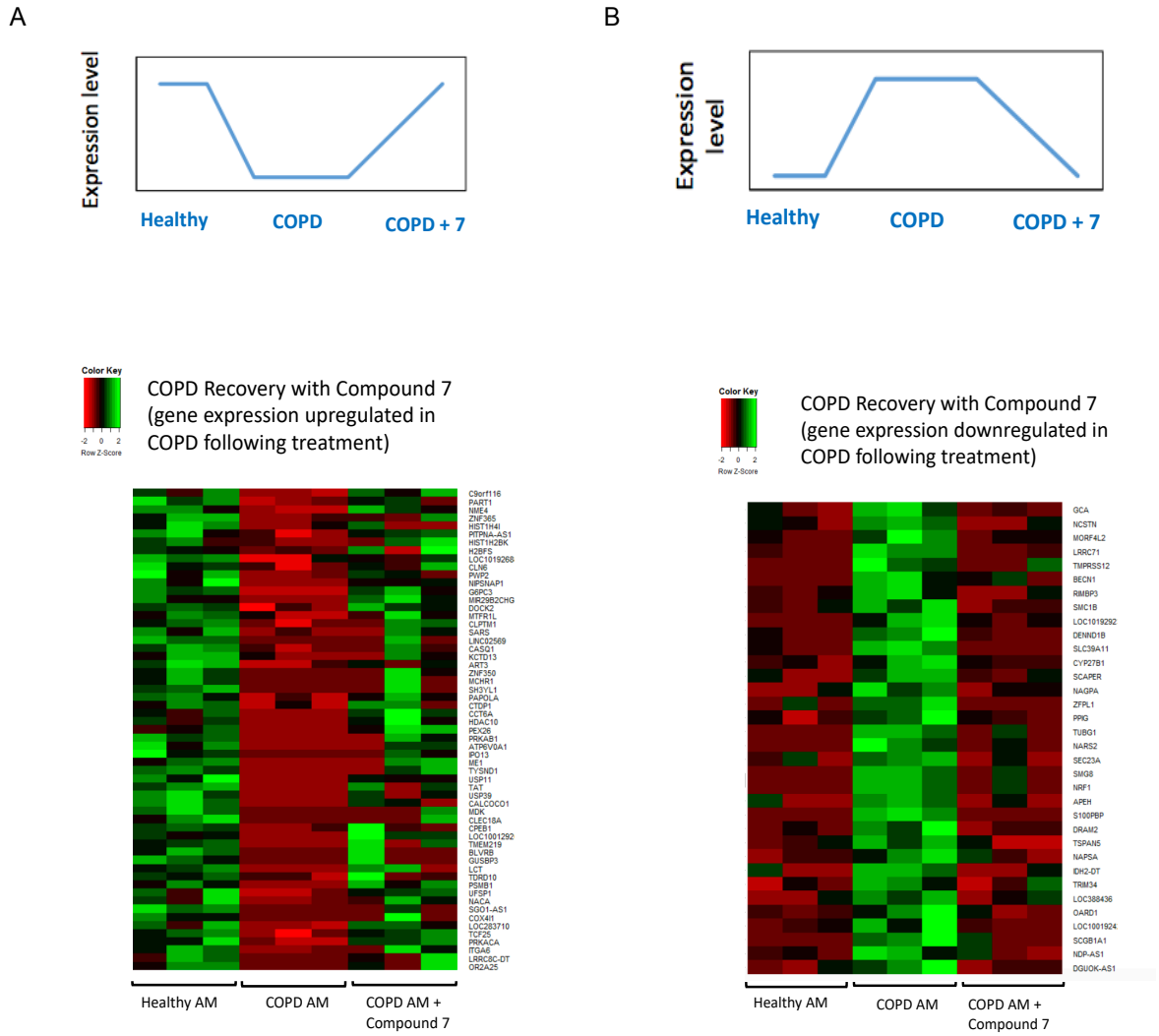

Figure 5.12.1: Nrf2 activation induces a transcriptional shift in COPD AM towards Healthy AM.

All cells were cultured for 16 hours (COPD AM +/- Compound 7) prior to collection of RNA for Total RNA-seq.(A-B) Heatmap of normalized Z-scores for each gene identified as significantly reduced (A) or induced (B) between COPD AM vs Healthy AM which are then restored in COPD AM + Compound 7. Green indicates high expression, red indicates low expression.

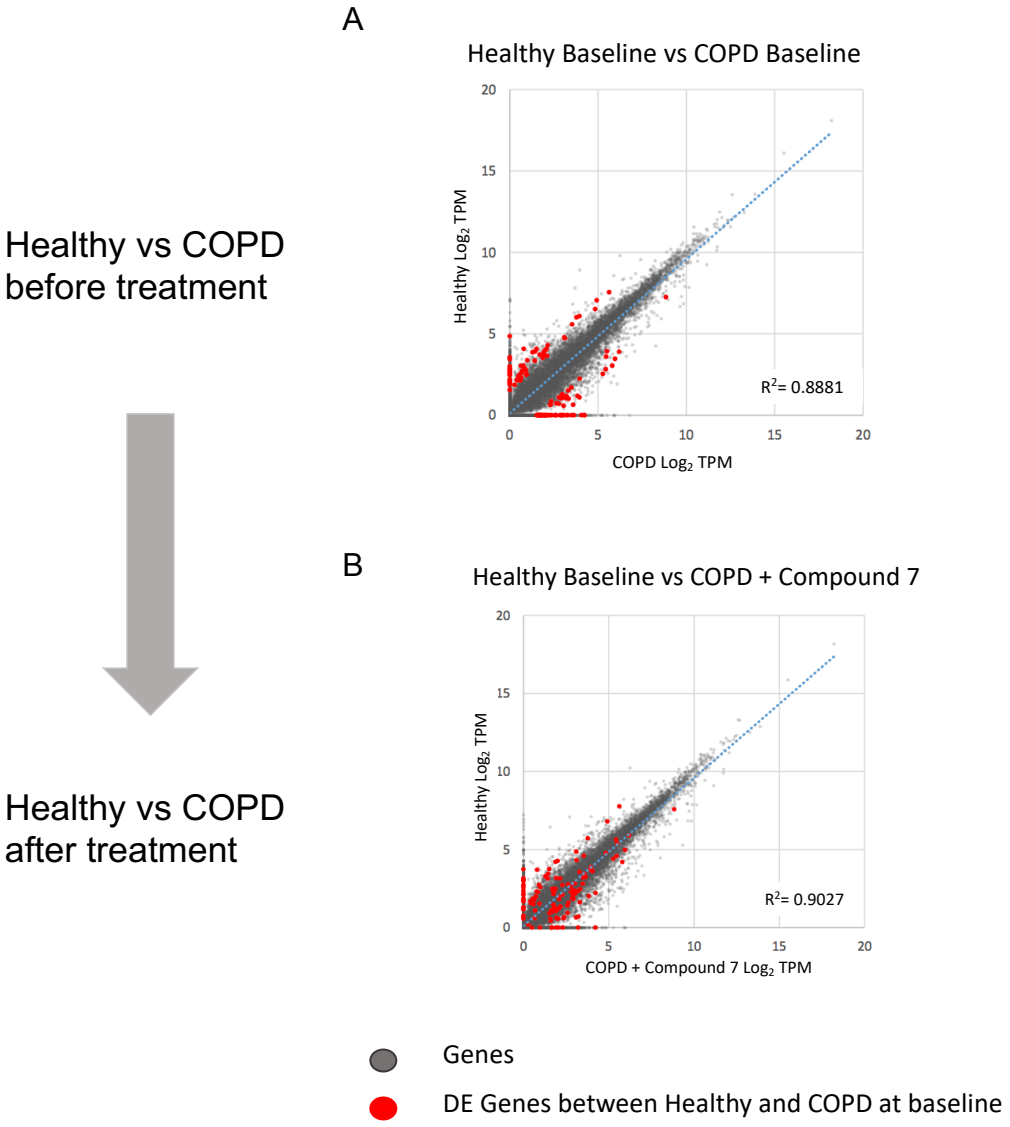

Figure 5.12.2: COPD AM correlate more closely with Healthy AM after treatment with Compound 7.

Scatter plots were generated by plotting the average Log_2 Tags Per Million (TPM) scores for a given sample cohort (i.e. Healthy AM) vs the average Log2 TPM scores for a second sample cohort (i.e. COPD AM + Compound 7). R^2 squared values are calculated from the slope of the correlation trendline. Correlation analysis confirms a higher correlation between Healthy AM and COPD AM following treatment with Compound 7 (A - B). n particular, significantly differentially expressed (DE) genes between COPD and Healthy AM at baseline, which are highlighted in (A), are seen to move towards the trendline in (B), indicating a “resetting” of abnormal expression in COPD AM following Nrf2 activation.

5.12 *Transcriptional changes induced by Compound 7-mediated Nrf2 activation, are disease specific*

To better understand the disease specific changes induced by Nrf2 activation, we compared the transcriptional profile of COPD + Compound 7 to Healthy AM + Compound 7. Interestingly, there were no overlapping genes either up or downregulated between COPD and Healthy Donor AM following treatment, suggesting that activation of Nrf2 via Compound 7 exerts a disease specific effect (Figure 5.13 A + D). Moreover, the lead Gene Ontology (GO) terms transcriptionally altered in COPD AM versus Healthy AM encompassed different biological processes. Of particular note was that "*Regulation of Metabolic processes*" was the most differentially upregulated biological process in COPD AM following Nrf2 activation (Figure 5.13 B).Importantly, included within this grouping, were two genes with central roles in regulating metabolism - RPTOR, which in conjunction with mTORC1 signalling and MAPK14 ,controls a regulatory, non-catalytic subunit of AMP kinase. Also included was TKL1 (Transketolase 1) which catalyses the conversion of ribose-5-phosphate to glyceraldehyde-3-phosphate phosphate in the pentose phosphate pathway. The NADPH oxidase, NOX1 was downregulated in COPD AM following treatment with Compound 7. NOX1 deletion dramatically reduces ROS levels in macrophages (Figure 5.13.E).

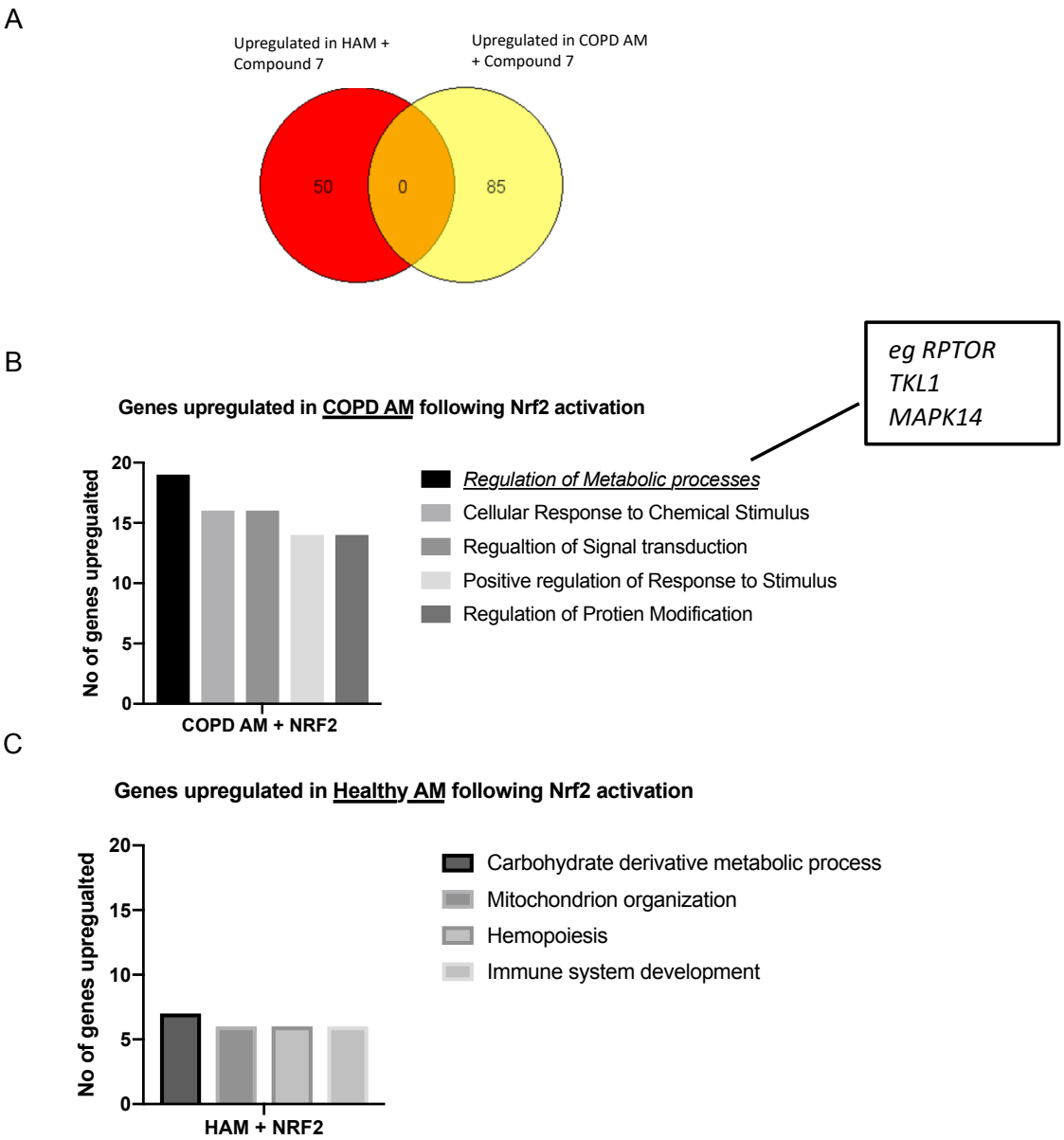

Figure 5.13: Nrf2 activation induces a divergent transcriptional responses in COPD vs Healthy donor AM.

AM were treated with the Nrf2 activator, Compound 7, for 16 hours prior to collection of RNA for Total RNA-seq. (A-F). Venn diagram showing the number of shared genes upregulated in COPD and Healthy donor AM in response to Nrf2 activation n= 0. (B-C) The top Gene Ontology (GO) terms upregulated in COPD (B) and Healthy (C) AM following treatment with Compound 7. N=3 for each group

D

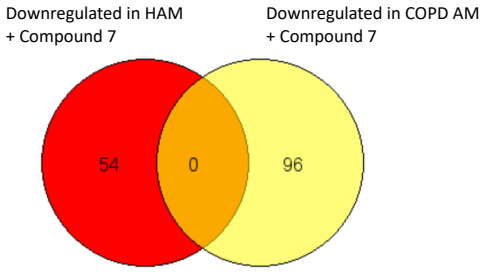

E

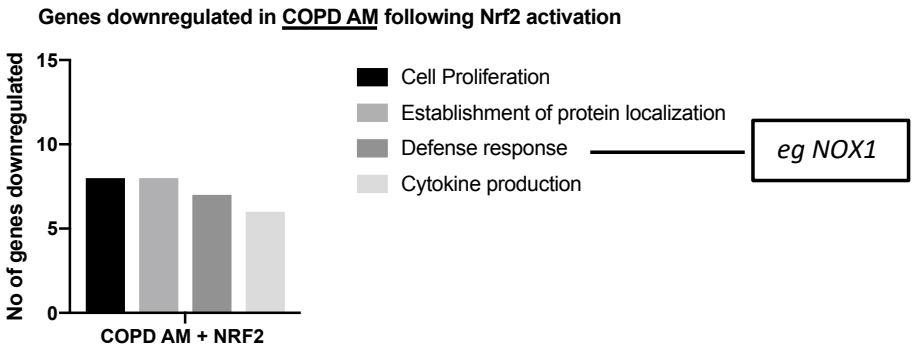

F

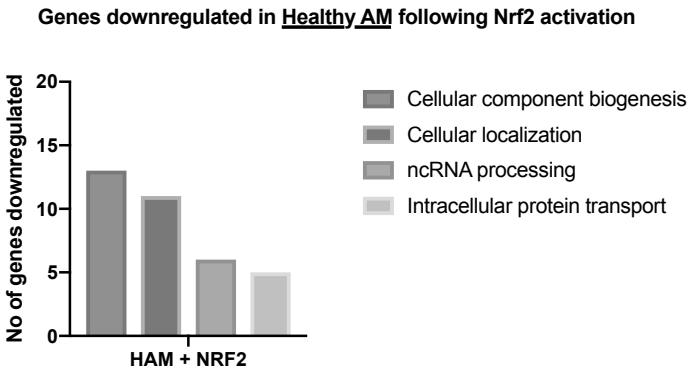

Figure 5.13 continued : (D) Venn diagram showing the number of shared genes downregulated in COPD and Healthy donor AM in response to Nrf2 activation n= 0. (E-F) The top Gene Ontology (GO) terms downregulated in COPD (E) and Healthy (F) AM following treatment with Compound 7. N=3 for each group. HAM= Healthy AM.

5.13 *Nrf2 activation via Compound 7 reprogrammes COPD AM metabolism leading to improved cellular energetics*

As GO analysis had identified that "*Regulation of Metabolic processes* " was the biological process most significantly altered by treatment with Compound 7 in COPD AM, we focused our attention on identifying the specific metabolic reprogramming induced by Nrf2 activation.

As discussed Nrf2 can modulate glucose uptake and flux through the pentose phosphate pathway [116]. It also enhances glucose oxidation by promoting flux through Pyruvate Dehydrogenase, increasing substrate entry into the TCA cycle[140]. Consequently, using LC-MS, we sought to define changes in baseline metabolism induced by Nrf2 activation, by measuring relative changes in intermediary abundance. NADPH is both rapidly degraded in the cell and also very poorly detected by LC-MS , as are Pentose Phosphate Pathway intermediaries.Therefore, our analysis was limited to Glycolysis and the TCA cycle.

Compound 7 mediated Nrf2 activation did not significantly alter Glycolytic metabolite abundance. However, it did significantly increase TCA cycle intermediaries , relative to baseline abundance in untreated COPD AM. Importantly, abundance of all TCA cycle intermediaries was increased, suggesting this was not a result of an interruption of flux through the cycle leading to accumulation of preceding metabolites (Figure 5.14.1).

Crucially Nrf2 activation, perhaps via modulation of the TCA cycle, enhanced cellular energetics. Energy Charge is calculated by the equation [ATP + ½(ADP) / ATP + ADP + AMP], and is a widely utilised index for measuring the energy status of a cell. Compound 7-mediated Nrf2 activation significantly improved both Energy Charge and ATP:ADP ratios. (Figure 5.14.2) .

A

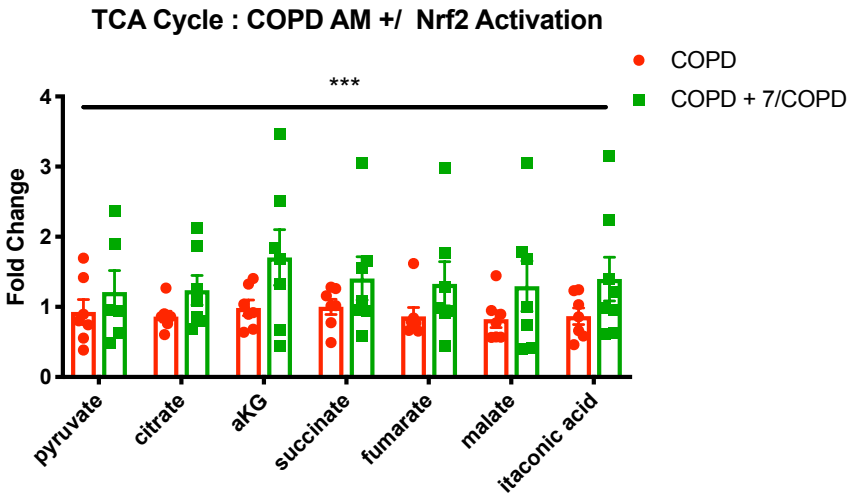

B

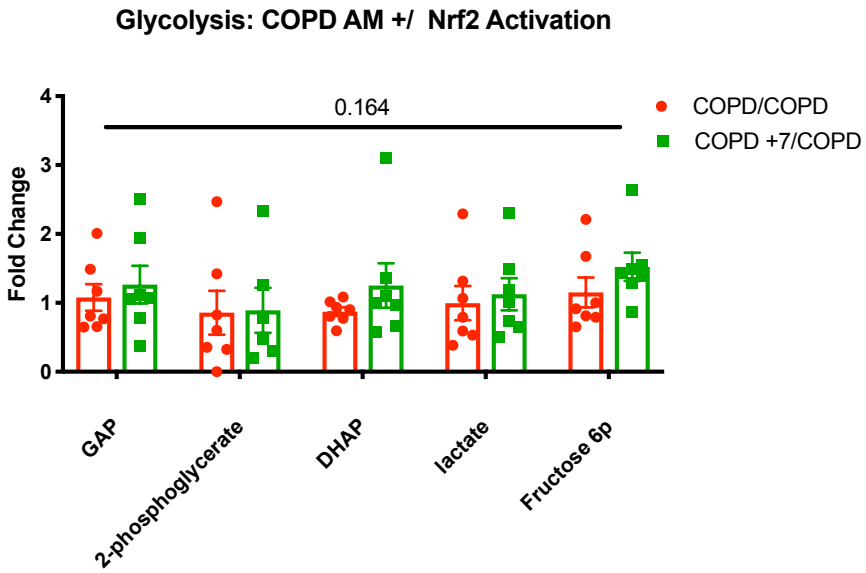

Figure 5.14.1: Nrf2 activation leads to a significant increase in TCA cycle metabolite abundance.

COPD AM were treated with the Nrf2 activator, Compound 7, for 16 hours prior to lysing cells in methanol to determine metabolite abundance via Liquid-Chromatography-Mass-Spectrometry. Abundance is plotted as relative to untreated COPD AM (Fold change). (A) Treatment with Compound 7 significantly increased relative metabolite abundance throughout the TCA cycle in comparison to Glycolysis (B) which was not significantly altered. N =7/6 throughout. P value calculated via 2-way ANOVA, $P \leq 0.05$ was used to determine significance, ***$P \leq 0.001$. Data represents individual values and mean ± SEM.

A

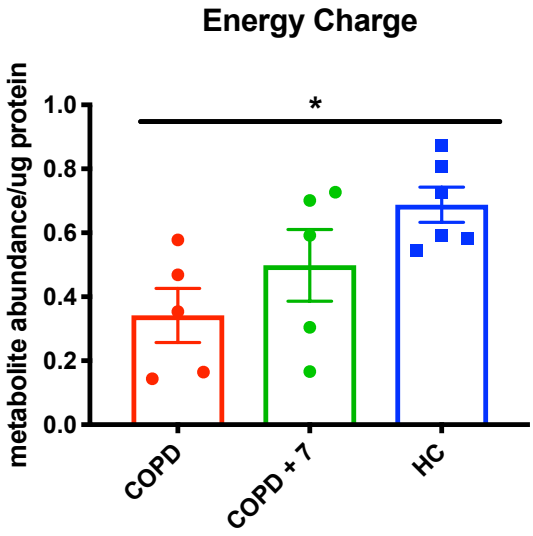

B

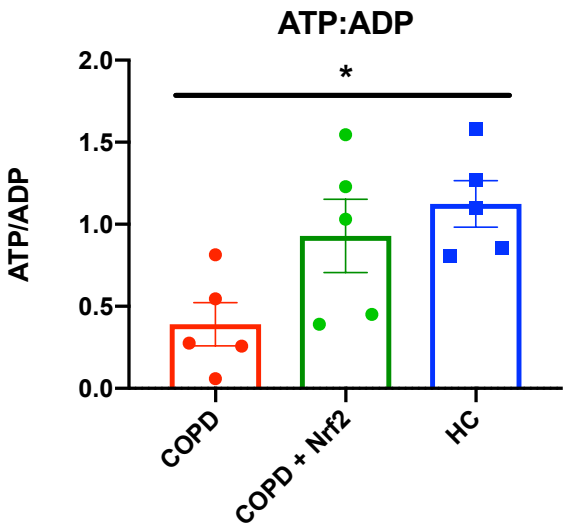

Figure 5.14.2 Nrf2 activation improves cellular energetics.
COPD and Healthy AM were treated with the Nrf2 activator , Compound 7, for 16 hours prior to lysing cells in methanol to determine metabolite abundance via Liquid-Chromatography-Mass-Spectrometry. (A) Energy charge and (B) ATP:ADP ratios were significantly improved following treatment with Compound 7. N=5 throughout. P value calculated via 1-way ANOVA, * P≤0.05. Data represents individual values and mean ± SEM. HC=Healthy Control

5.14 *Nrf2 improves cellular redox balance in COPD AM.*

As we had observed a failure in COPD AM to appropriately upregulate antioxidant responses following infection with *S. pneumoniae* (Figure 5.2), we sought to establish if Compound 7-mediated Nrf2 activation had indeed restored redox balance in COPD AM. The ratio of reduced to oxidised Glutathione (GSH:GSSG), is considered a marker of cellular health and favourable redox balance. Key genes regulating glutathione synthesis and reduction were upregulated in Healthy AM but not in COPD AM on exposure to *S. pneumoniae* (Figure 5.2). As Glutathione Reductase (GSR) uses NADPH to reduce oxidised Glutathione, the GSH:GSSG ratio also acts as a measure of NADPH production.

Activation of the Nrf2 module via Compound 7 increased absolute glutathione abundance in COPD AM, in keeping with it known role in activating Glutamine Cystine ligase, the rate limiting enzyme of glutathione synthesis[141]. Nrf2 activation also increased the ratio of GSH:GSSG, establishing an improved redox state following treatment with Compound 7 (Figure 5.15). Furthermore, as NADPH is required to maintain GSH, this suggests increased availability of NADPH in COPD AM, following treatment with Compound 7.

A

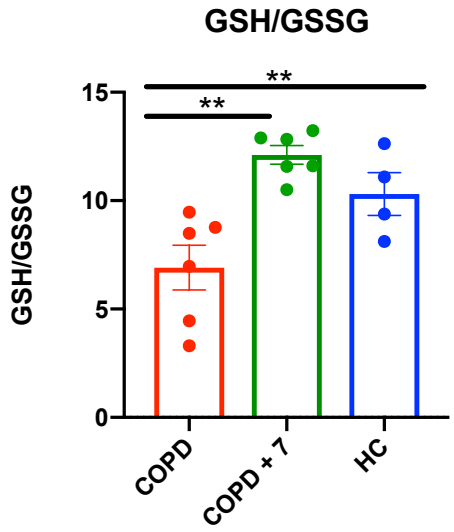

B

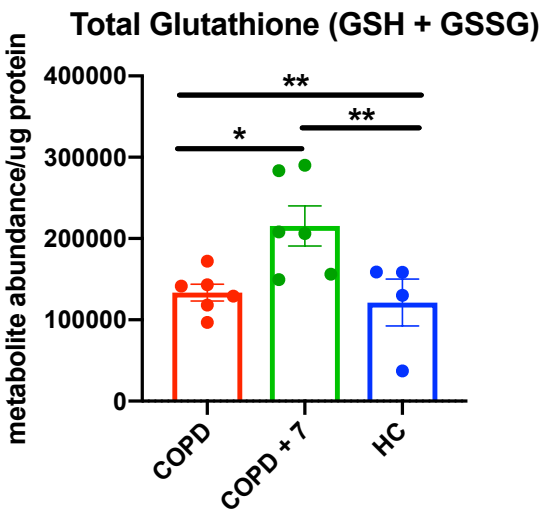

Figure 5.15: Nrf2 activation improves cellular redox state.
COPD and Healthy AM were treated with the Nrf2 activator, Compound 7, for 16 hours prior to lysing cells in methanol to determine metabolite abundance via Liquid-Chromatography-Mass-Spectrometry. (A) The ratio of reduced to oxidised glutathione was significantly improved by treatment with Compound 7. (B) The overall abundance of Glutathione was increased following treatment with Compound 7. P value calculated via 1-way ANOVA and Sidak's multiple comparisons.* $P \leq 0.05$, ** $P \leq 0.01$. Data represents individual values and mean ± SEM, COPD AM n=6, Healthy AM n=4.

5.15 *Activation of the Nrf2 Module does not increase macrophage phagocytosis or efferocytosis in Healthy Volunteers, including under hostile culture conditions:*

As Nrf2 activation induced a divergent transcriptional programme in resting state Healthy and COPD AM , we questioned if Nrf2 enhancement of macrophage activity i.e. phagocytosis and efferocytosis, may be limited to a diseased state. We had previously observed that blood monocyte-derived macrophages from Healthy volunteers, pre-treated with Compound A-C or Sulforaphane did not show significantly altered phagocytosis of serotype 14 *Streptococcus pneumoniae* or PKH26 labelled neutrophils (Figure 5.16 A-B). Consequently we sought to mimic elements of the COPD microenvironment while culturing Healthy Control MDM, to establish if this would unmask an effect of Nrf2 agonists in healthy volunteer cells.

The COPD lung is characterized by chronic inflammation, oxidant stress and inflammation induced hypoxia, which AM and MDM must be able to readily adapt to[142,143]. These cells are also highly regulated by nutrient availability[19]. As increasing numbers of cells are recruited, there is a progressive scarcity of crucial substrates such as oxygen and glucose. Thus, to mimic the hostile environment of COPD , healthy MDM were cultured in hypoxia (defined as 1% O_2) for ten days or in glucose deplete media with dialysed Fetal Calf Serum (FCS) for 16 hours prior to use. All MDM were pre-treated with either

vehicle or Compounds A, B, C or Sulforaphane prior to performing assays (Figure 5.16.2)

Interestingly exposure to hostile environments prior to, and during these assays, did not unmask an Nrf2 activation effect in Healthy donor macrophages, though it is important to note these are small numbers. This does still suggest, however, that the uplift in macrophage function seen with Nrf2 activators in COPD is a disease specific phenomenon (Figure 5.16.2).

A

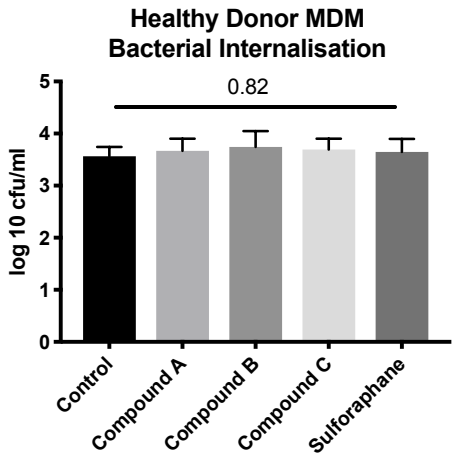

B

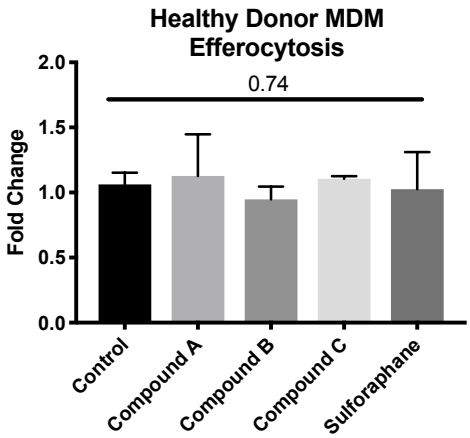

Figure 5.16.1: Nrf2 activation does not enhance MDM phagocytosis or efferocytosis in Healthy Volunteers.

MDM isolated from Healthy Controls were pre-treated with Nrf2 agonists - Compounds A, B and C 10nM and Sulforaphane 10μM -for 16 hours prior to challenge with (A) opsonised *S. pneumoniae* S14 , 4hrs post challenge the number of viable bacteria was measured (n=5) .(B) Following pretreatment cells were co-incubated with PKH26 labelled 20hr apoptotic neutrophils, efferocytosis rates were measured by flow cytometry (n=5) P value calculated by One-way ANOVA with Sidak's multiple comparisons.

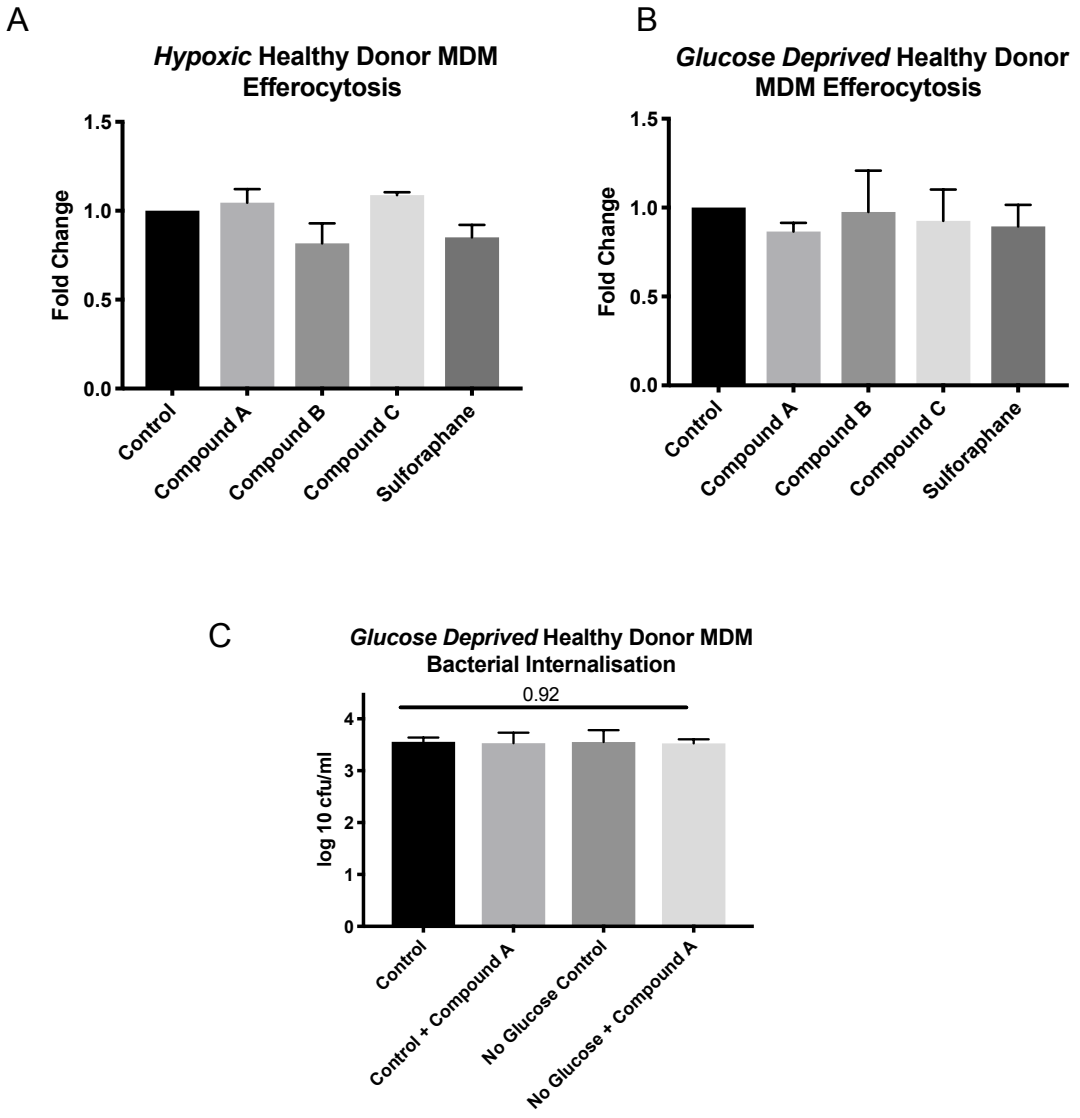

Figure 5.16.2: Nrf2 activation augments neither efferocytosis nor phagocytosis in cells cultured in hypoxic and glucose deprived environments.

MDMs were cultured in (A) hypoxia (1% O2) x 10 days or (B) glucose deprived media with dialysed FCS x 16hrs prior to co-incubation with PKH26 labelled apoptotic neutrophils, efferocytosis rates were measured by flow cytometry. (C) MDM's cultured in glucose deprived media with dialysed FCS x 16hrs prior to co-incubation with *S. pneumoniae* S14, 4hrs post challenge the number of viable bacteria was measured. All MDM were pretreated for 16 hours with Nrf2 agonists - Compounds A, B and C 10nM and Sulforaphane 10μM prior to performing assays. Fold change was calculated as the ratio of treated to untreated cells, n=2 (A+B) and n=3 (C).

5.16 *ME1 expression is reduced in COPD AM at baseline and augmented following treatment with Nrf2 .*

Lastly, we had identified ME1 (Malic Enzyme 1) as a significantly differentially expressed gene between COPD and Healthy AM at baseline. ME1 increases NADPH production by converting cytosolic Citrate to Pyruvate .The Pyruvate thus generated, can be shuttled back into the TCA cycle or converted to Acetyl Co-A for Fatty Acid Synthesis (Figure 5.17 C). The newly generated NADPH can be used to maintain redox balance or again, for reductive biosynthesis. In fact, ME1 has been shown to generate approximately 60% of the cytosolic NADPH pool ,in normoxic conditions[147]. ME1 activity has also been shown to influence both metabolism and antioxidant responses. ME1 knock down in the human colon cancer cell line, HCT116 , resulted in increased lactate production and disruption of redox balance, as measured by induction of HO-1[104].

Total RNA-seq data confirmed that ME1 expression is significantly reduced at baseline in COPD AM , compared to Healthy AM (Figure 5.17 A). ME1 expression was highly upregulated in two of the donors in the transcriptomics dataset but did not reach significance, as a limited change only was detected in the third donor. Therefore , PCR quantification of ME1 expression was undertaken in both the original “transcriptomics data set donors” and a further 3 COPD donors. This revealed a significant increase in ME1 expression following treatment with Compound 7 (Figure 5.17 B). Based on this

preliminary data and published studies, we are now exploring if reduced ME1 levels may play a significant role in altered metabolism in COPD . Furthermore we will investigate if augmentation of ME1 expression is central to the observed Nrf2-mediated rescue macrophage dysfunction in COPD.

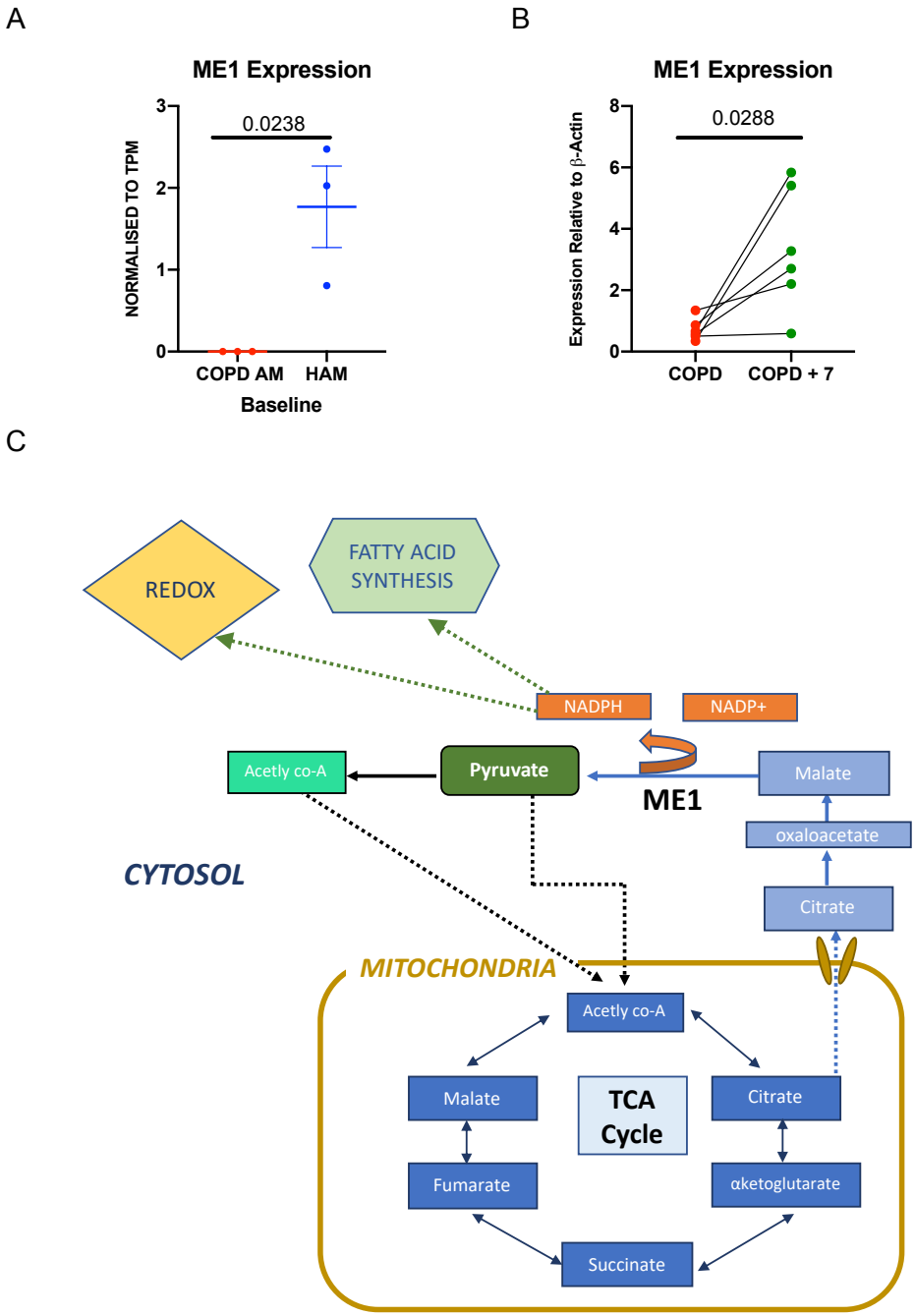

Figure 5.17: Nrf2 activation restores ME1 expression in COPD AM. (C) Malic Enzyme 1 (ME1) increases NADPH and pyruvate production via the malate-pyruvate shunt. (A) Transcriptomic analysis revealed a significant reduction in COPD AM compared to Healthy AM at baseline.(B) PCR quantification of ME1 expression revealed a significant increase in COPD AM following treatment with Compound 7. (A) n= 3, (B) n= 6. P values calculated by unpaired (A) and paired (B) t-test.

5.17 *Discussion*

The data in this chapter provides compelling evidence for the role of Nrf2 activation in reversing macrophage dysfunction in COPD .

In COPD AM, the failure to upregulate several Nrf2-controlled antioxidant modules in response to *S. pneumoniae,* provides vital mechanistic insight into macrophage dysfunction in COPD. The antioxidant response induced in Healthy AM, included key detoxifying pathways for combatting cellular levels of ROS, a major cause of cell and tissue damage in COPD[144] .The transcriptional levels of vital ROS scavengers such as SOD1, which reduces superoxide and NQO1, which fully oxidizes quinones to prevent formation of semiquinones and subsequent ROS generation, were all upregulated in Healthy Donor macrophages but remained unchanged in COPD. More strikingly still, several key regulatory steps of Glutathione, which are subject to Nrf2 activation, were upregulated in Healthy AM, in response to infection, with no transcriptional change induced in COPD AM. As one of the chief endogenous antioxidants, the ratio of reduced (GSH) to oxidised glutathione (GSSG) is often used as readout of the redox potential of a cell. Failure to upregulate glutathione synthesis in response to infection in COPD AM represents a severely impaired transcriptional response to a noxious stimulus. It renders the cell incapable of maintaining adequate redox balance in the context of infection, with ensuing high levels of oxidant stress, aberrant cell signalling and damage to sensitive organelles such as mitochondria [145].

In keeping with a failure of COPD AM to upregulate antioxidant responses, activation of Nrf2 via a panel of specific and non-specific compounds, partially rescued both phagocytosis and efferocytosis in COPD AM and MDM. Noticeably, there was a differential impact on macrophage dysfunction between Sulforaphane and the novel Nrf2 compounds. The greatest uplift in bacterial phagocytosis was seen with the novel GSK Nrf2 activators whereas, a greater enhancement was seen in efferocytosis with Sulforaphane. It is possible that, as of yet unidentified, off-target effects of Sulforaphane are improving efferocytotic function. A study by Campanella et al provides a possible alternative explanation. They used a novel Nrf2 activator which was a non-covalently binding KEAP1 protein-protein interaction inhibitor (PPI), similar to our Compounds- A and 7. They discovered a differential effect on mitochondrial function, particularly mitophagy, between their PPI compound and Sulforaphane [146]. It is possible that an increase in mitophagy, with resulting improved mitochondrial health, is of an additional benefit in bacterial phagocytosis. COPD AM displayed impaired mitochondrial responses to *S. pneumoniae*, which was presumed to be due to impaired mitochondrial health [69]. Improved mitophagy may reverse this phenomenon and explain why PPI compounds such as Compound A + 7 induce a relatively greater improvement in bacterial phagocytosis rather than efferocytosis. Regardless of the degrees of improvement between processes, the ability to enhance both efferocytosis and phagocytosis using highly specific Nrf2 activators, is further evidence still for a shared underlying mechanism driving macrophage dysfunction in COPD macrophages.

We had previously hypothesised that incomplete rescue of COPD macrophage phagocytosis and efferocytosis by Nrf2 agonists, was due to a limited induction of the ARE via Nrf2, as measured by HO-1 expression. While acknowledging that our Healthy and COPD MDM lysates were run on separate blots, the expression of HO-1 relative to β-actin was increased in COPD MDM with Sulforaphane and Compound A , but still appeared lower than in Healthy MDM. We postulated that increased levels of Bach1, which competitively binds to the ARE and have previously found in COPD AM, could potentially account for this phenomenon [125]. It was therefore of great interest to observe that while treatment with Compound 7 appeared to "normalise " the COPD transcriptome towards that of Healthy AM, a degree of divergence in transcriptomes persisted between the two donor groups. Therefore, alternatively, failure to fully reverse impaired macrophage function in COPD ,may occur because certain abnormally expressed genes in COPD AM are refractory to Nrf2 modulation. If this proved to be the case, the potential for epigenetic modification of COPD macrophages in preventing transcription of particular genes, may prove highly significant. Either the differential induction of the ARE following treatment, or the inability of Nrf2 to modulate all relevant gene sets in COPD macrophages, may explain why Sulforaphane and our panel of specific Nrf2 agonists, can greatly improve macrophage function in COPD, but are unable to fully reverse the phenotype.

The identification of "Metabolic processing" as a lead biological process altered by Nrf2 activation in COPD AM, was particularly noteworthy in the

context of our observed metabolic phenotype, outlined in Chapter 3. As discussed, we observed exhausted energy reserves and comparatively upregulated glycolysis with downregulated oxidative metabolism in COPD macrophages. In keeping with enhancement of macrophage phagocytosis and efferocytosis with Nrf2 activation, treatment of COPD AM with Compound 7 significantly increased flux through the TCA cycle and improved Energy Charge. This may well reflect an improvement in mitochondrial health and consequently bioenergetics, due to enhanced redox balance - treatment with Compound 7 also significantly improved the GSH:GSSG ratio. Previous exploration of the effect of Nrf2 deletion in murine embryonic fibroblasts, confirmed impaired mitochondrial health with subsequent reduction in mitochondrial generated ATP [118] . Another possibility is that Nrf2 activation reprogrammes metabolism in COPD macrophages. For example, RPTOR (Regulatory-associated protein of mTOR) was found to be significantly upregulated in COPD AM following treatment with Compound 7. RPTOR plays a major role in sensing and orchestrating the response to nutrient and energy state in macrophages (via its role in the mTORC1/ AMPK axis) [147]. Lastly, the role of ME1 induction via Nrf2 is of particular interest to us, especially as it is a significant differentially expressed gene between COPD and Healthy AM at baseline. ME1 (Malic Enzyme 1) is a NADP-dependent cytosolic enzyme which generates NADPH during the conversion of Malate to Pyruvate. Therefore increasing ME1 expression could improve redox balance in the cell by generating more NADPH, and also increase flux through the TCA cycle by producing Pyruvate. Thus ME1 upregulation,

warrants further characterisation in the context of Nrf2 mediated enhancement of COPD macrophage function.

Interestingly, in contrast to COPD MDM, Nrf2 stabilisation failed to induce an increase in efferocytosis or bacterial phagocytosis rates in Healthy Volunteer AM and MDM and occurred even when MDM were deprived of vital substrates- oxygen and glucose. This was despite an increase in HO-1 protein expression in Healthy MDM following treatment with Compound A and Sulforaphane, indicating that augmentation of antioxidant responses with subsequent improvement in macrophage function, is disease specific. It is possible that when the Nrf2/KEAP1/Bach1 axis is working correctly , as in Healthy macrophages, further augmentation of the ARE will not result in an increased functional output. Alternatively that fact that Nrf2 induces an entirely different transcriptional programme in in Healthy AM than it does in COPD AM, suggests that many of the transcriptional effects of Nrf2 are dependent on baseline gene expression. These experiments also contradict the concept that a substrate limited environment is largely driving the macrophage phenotype in COPD, particularly when coupled with the persistence of our observed COPD phenotype in an oxygen and glucose replete tissue culture environment.

In summary, we have established that COPD AM fail to appropriately upregulate anti-oxidant pathways in response to infection. We have also shown partial recuse of COPD macrophage function via pharmacological manipulation of these anti-oxidant pathways. A previous study by Harvey et

al had shown an increase in bacterial phagocytosis following treatment with Sulforaphane[49]. Our data, however, is the first to establish a role for Sulforaphane in enhancing both bacterial phagocytosis and efferocytosis in AM and MDM from COPD patients. Moreover, using a highly specific Nrf2 activator, we have confirmed that this uplift in macrophage function is exclusively mediated via upregulation of the Nrf2 module. By conducting these experiments in Healthy donors, including Healthy donor macrophages which have been substrate deprived, we had confirmed that Nrf2 mediated enhancement of macrophage function is also disease specific. Transcriptomics data, coupled with measurement of metabolite abundance via LC-MS, has outlined a major role for Nrf2 in reprogramming aberrant metabolism in COPD macrophages, with consequent improvement in energy status . Crucially, this provides a mechansim for Nrf2 mediated restoration of macrophage function in COPD. Future directions will focus on how Nrf2 activation can influence mitochondrial health and energetics in COPD macrophages, with particular attention to the role of ME1 upregulation .

6 Discussion and Future Directions

6.1 *Discussion*

COPD is characterised by persistent inflammation of the airways , destruction of lung tissue and mucus hypersecretion resulting in airflow limitation and impaired gas exchange. Pathogen colonisation and recurrent infective exacerbations are the largest contributor to morbidity and mortality within the disease[34]. Failure of COPD macrophages to adequately phagocytose bacteria and to instigate inflammation resolution via efferocytosis, places macrophage dysfunction at the centre of both disease pathology and progression in COPD.

The aim of the project was to employ a multimodality approach to characterise macrophage dysfunction in COPD. We combined transcriptional profiling of COPD macrophages, both at rest and in response to a pathogen, with functional assays and metabolic phenotyping- again both at rest and following stimulation. Critically, we have conducted many of these experiments in both AM and MDM to explore if the defects encountered in AM are limited to macrophages exposed to the pulmonary niche.

<u>COPD AM AND MDM have impaired function:</u>

We have confirmed that COPD macrophages have impaired bacterial phagocytosis of *S. pneumoniae*-one of the most commonly encountered

pathogens in COPD-and efferocytosis of apoptotic neutrophils. Crucially, we have identified that macrophage dysfunction in COPD is a systemic defect. Both Alveolar Macrophages, existing in the inflammatory pulmonary niche, and circulating Monocyte-derived macrophages, demonstrate impaired phagocytosis and efferocytosis. This firmly establishes that the phenotype of impaired macrophage function in COPD is not driven solely by hostile microenvironmental signalling within the lung. As all cells were cultured in a glucose and oxygen replete environment prior to performing assays, the determinants of COPD macrophage dysfunction are evidently hard wired.

Our transcriptomics data sets confirmed that COPD AM are intrinsically different to Healthy AM at baseline. Importantly, COPD AM also mounted a divergent and markedly supressed transcriptional response to *Streptococcus pneumoniae* compared to Healthy Donor AM. Interrogation of transcriptional differences between COPD and Healthy AM, highlighted two major areas of interest for us to explore - metabolism and the antioxidant response.

Altered metabolism in COPD:

Transcriptomic analysis, both at baseline and in response to co-incubation with *S. pneumoniae*, revealed significantly altered metabolic profiles between COPD and Healthy AM. At baseline, “metabolic processing” was one of the most differentially regulated modules between COPD and Healthy AM, with alterations in key genes such as Malic Enzyme 1. Furthermore, comparison of the metabolic transcriptional response to *S. pneumoniae* revealed a

dominant glycolytic response in COPD AM, compared to Healthy AM. This apparent over reliance on glycolysis in COPD AM, was replicated during phenotyping of the energy response using Seahorse technology and again when measuring metabolic intermediaries using LC-MS. Seahorse profiling revealed a predominantly ECAR driven response to increased energy demand in COPD AM. Similarly, a relative increase in the abundance of glycolytic intermediaries was detected in COPD macrophages compared to Healthy AM, using LC-MS. Crucially, this glycolytic phenotype in COPD macrophages, co-existed with impaired bioenergetics, as detected by Seahorse. Both AM and MDM from COPD donors displayed exhausted energy reserves in oxidative metabolism and glycolysis. The discovery of significantly diminished energy reserves, coupled with a reduced energy charge as detected by LC-MS, in COPD macrophages is perhaps finding most relevant to our observed phenotype of impaired macrophage function in COPD. Moreover, reduced energy reserves were detected in both AM and MDM , providing further evidence still of a widespread systemic defect in macrophage function in COPD.

It was imperative to determine if the metabolic phenotype discovered in COPD macrophages, was driven by substrate availability. We did not detect a difference in either glucose uptake, glycogen storage levels or substrate availability in the bronchoalveolar lavage fluid . Critically COPD AM also failed to reprogramme oxidative metabolism following ingestion of apoptotic neutrophils, compared to Healthy AM. Together these data suggest that

altered metabolism in COPD, is a product of impaired metabolic plasticity coupled with bioenergetic exhaustion rather than environmental regulation through substrate availability.

The role of antioxidant responses in restoring function in COPD macrophages:

Another significant finding in our transcriptomics data set, was a markedly reduced antioxidant response in COPD AM, following exposure to *S. pneumoniae*. This was of particular interest as Nrf2 , the master regulator of the antioxidant response, has previously been shown to be reduced in COPD AM and Nrf2 $^{-/-}$ mice exhibit early onset emphysema following cigarette smoke exposure[123,148]. We established that treatment with Sulforaphane and crucially, highly specific Nrf2 activators, partially restores bacterial phagocytosis and efferocytosis in COPD macrophages. The ability to restore both processes via pharmalogical manipulation is further evidence still for a shared underlying mechanistic defect.

As Nrf2 is well established to regulate a number of metabolic processes and we had already identified a metabolic defect in COPD macrophages, we profiled the COPD AM transcriptome following treatment with Nrf2 activators, with a focus on metabolism. This revealed that pharmacological activation of Nrf2 “reprogrammed” COPD macrophages to more closely resemble Healthy AM. Fascinatingly, this involved major changes in the regulation of metabolism. Altered expression of cardinal metabolic regulators such as

RPTOR, Transketolase 1 and Malic Enzyme 1 in COPD AM following treatment, provided evidence that Nrf2 activation can “recalibrate” elements of COPD macrophage metabolism. Moreover, treatment with Nrf2 activators increased TCA cycle metabolite abundance and improved energy charge and redox balance in COPD AM. These data suggest that Nrf2 treatment, potentially by improving redox state, can modify aberrant metabolism in COPD macrophages with consequent rescue of Phagocytosis and Efferocytosis.

6.2 *Future directions*

The work presented here highlights a number of areas which are worthy of further investigation.

There is ample evidence of impaired mitochondrial health and function in COPD macrophages [65, 92, 93, 94, 95]. While impaired OCR responses coupled with altered OCR/ECAR ratios in COPD macrophages strongly suggest mitochondrial damage, we did not have the opportunity, due to cell number limitations, to interrogate mitochondrial health specifically in our cohort. This is of particular significance when considering the rescue phenotype demonstrated by Nrf2 activation. Mitochondria are extremely sensitive to oxidative stress, due to their limited repair mechanisms and our data confirmed that Nrf2 activation improved redox balance in COPD macrophages. Furthermore, there was also an increase in both TCA cycle metabolite abundance and Energy Charge, suggesting a favourable energetic outcome from Nrf2 activation in these cells. As intact metabolic

machinery is indispensable for metabolic plasticity , improvements in mitochondrial health due to improved redox balance, may play a role in restoring metabolism plasticity to COPD macrophages, reducing reliance on glycolysis for ATP generation and improving energy reserves. Measurement of mitochondrial DNA to nuclear DNA ratios (mtDNA/nDNA) has previously been used to asses for reduced mitochondrial bodies [149]. However as this is a ratio, and we have already demonstrated that COPD macrophages have a quiescent nDNA mediated transcriptional response, this ratio may be globally reduced and mask a reduction in mitochondrial number in COPD macrophages. Measuring mitochondrial membrane potential, a marker of mitochondrial health and a crucial element for energy generation and storage in mitochondria, both pre and post treatment with Nrf2 activators is likely to yield a more relevant response [149,150] . Moreover, isolation of individual mitochondrial complexes could reveal exciting information of the drivers of mitochondrial dysfunction in COPD macrophages and provide further more specific therapeutic targets. Our future plan is to assess COPD macrophage mitochondrial health and function and importantly to assess if pharmacological activation of Nrf2 generates changes in these parameters translate into alterations in OCR readings and mitochondrial reserves.

Another area of particular future interest, is the potential role of Malic Enzyme 1 activity in driving the observed phenotype in COPD macrophages. Malic Enzyme 1, as discussed ,increases the cytosolic pool of NADPH -enhancing redox potential - while also generating Pyruvate for the TCA cycle. The pool

of generated NADPH can also be used for Fatty Acid Synthesis and Oxidation, which has been shown to play a significant role in driving a “pro resolution” phenotype in macrophages. Importantly, ME1 levels were significantly transcriptionally reduced in COPD AM at baseline and were significantly increased following Nrf2 activation. ME1 expression, particularly in a low glucose environment – such as that experienced in the airways - has been shown to regulate glucose metabolism, flux through the pentose phosphate pathway and the TCA cycle and to regulate cell motility [104,151]. Moreover, ME1 knock out mice display reduced body weights, reduced body and retroperitoneal fat due to impaired lipogenesis [152,153]. This phenotype certainly echoes the highly catabolic clinical state of many emphysema patients, who struggle to maintain a BMI within healthy range, and is considered a marker for increased mortality in this cohort [154]([155]. We are currently generating, with our collaborators, a CRISPR-Cas9 ME1 knock out in a THP-1 cell line, which we are aiming to metabolically and functionally profile using Seahorse technology and efferocytosis assays respectively. Once we have characterised the baseline phenotype of these cells , using compound 7 we will activate the Nrf2 pathway with the hypothesis that Nrf2 activation cannot augment efferocytosis in these cells.

While $Nrf2^{-/-}$ mice have been studied extensively in the context of COPD, to date the role of Nrf2 overexpression in protecting against emphysema, has not been examined. Long term exposure of Nrf2 OE mice to cigarette smoke

could provide valuable insights in to the mechanism of functional rescue seen with Nrf2 activation.

Lastly, this data as a whole, raises fascinating questions regarding the systemic nature of macrophage dysfunction in COPD. While elements of defective alveolar macrophage function can be attributed to the high levels of oxidative stress experienced in the pulmonary niche, the existence of the phenotype in circulating bone marrow derived cells merits careful consideration. It is possible that signalling from the damaged pulmonary niche to the bone marrow is inducing defects, potentially via epigenetic modification, in newly released monocytes. However, recurrent infections and colonisation in COPD patients is largely limited to the lung . A possible explanation for this is impaired tissue imprinting in the lungs of COPD patients, due to chronic inflammation. This would give rise to a “dual hit” where by baseline defective cells would migrate from the bone marrow to the damaged COPD lung. An inability to reprogramme the infiltrating cells correctly within the inflammatory niche could result in further loss of function. To dissect this theory, it would be essential to recruit and follow an early cohort of smokers firstly, to delineate if detected alterations in circulating and airway cells, were due directly to cigarette smoke exposure or to disease mechanisms and secondly to determine causality between AM and MDM dysfunction. Recruitment for this cohort of patients has already begun in Edinburgh University.

As discussed, it has long been recognised that COPD displays a high level of inheritability [156],[157]. Despite this, GWAS studies failed to reveal a meaningful genetic footprint for the disease [27]. Thus the role of epigenetic modification in COPD or familial imprinting leading to marked susceptibly to the disease, is an area of great interest and unmet clinical need. Already, epigenetic analysis of established COPD patients have revealed a number of differentially methylated sites (DMSs) associated with lung function which may play a role in disease development [158]. It is particularly interesting to reflect on the role of mitochondrial dysfunction in COPD, with respect to genetic susceptibility. Mitochondria DNA is inherited only from the maternal lineage, however familial trends are not determined by sex of parent [157] – it is possible that inherited epigenetic modifications could leading to impaired function and or repair mechanisms. Epigenetic analysis of AM and MDM from established COPD patients, in parallel with early smokers with preserved lung function from our early smoker cohort, and if possible screening of first degree relatives, may finally provide critical insights into disease susceptibility. The development of drugs targeting epigenetic modification makes this an ever more urgent area for exploration [159].

6.3 *Conclusions*

This body of work outlines significant systemic functional impairment of COPD macrophages. It provides evidence that altered metabolism in COPD macrophages, may be driving the observed functional impairment. We have shown that COPD macrophages have diminished antioxidant responses and that pharmalogical induction of the antioxidant response, via Nrf2 activation, partially rescues functional defects . Moreover our data suggests that manipulation of antioxidant responses in COPD macrophages, transcriptionally reprogrammes cells, with a particular emphasis on cellular metabolism, resulting in restoration of function.

Future work will focus on mitochondrial health and potential gain of function following Nrf2 activation in COPD macrophages, with a view to trialling Nrf2 activation as a therapy in established disease. The role of ME1 in driving aberrant metabolism in COPD macrophages requires specific characterisation . Ultimately, the drivers of the systemic defect in the COPD macrophage population require investigation using an early cohort of smokers with a view to preventing disease progression in these patients.

7 References:

1. Watts ER, Ryan E, Walmsley SR, Whyte MKB. *Microenvironmental Regulation of Innate Immune Cell Function*. Vol 41. Weinheim, Germany: John Wiley & Sons, Ltd; 2017:947-970. doi:10.1002/9783527692156.ch36.

2. van Furth R, Cohn ZA, Hirsch JG, Humphrey JH, Spector WG, Langevoort HL. The mononuclear phagocyte system: a new classification of macrophages, monocytes, and their precursor cells. *Bull World Health Organ*. 1972;46(6):845-852.

3. Ginhoux F, Guilliams M. Tissue-Resident Macrophage Ontogeny and Homeostasis. *Immunity*. 2016;44(3):439-449. doi:10.1016/j.immuni.2016.02.024.

4. Gomez Perdiguero E, Klapproth K, Schulz C, et al. Tissue-resident macrophages originate from yolk-sac-derived erythro-myeloid progenitors. *Nature*. 2015;518(7540):547-551. doi:10.1038/nature13989.

5. Guilliams M, De Kleer I, Henri S, et al. Alveolar macrophages develop from fetal monocytes that differentiate into long-lived cells in the first week of life via GM-CSF. *J Exp Med*. 2013;210(10):1977-1992. doi:10.1084/jem.20131199.

6. Hashimoto D, Chow A, Noizat C, et al. Tissue-resident macrophages self-maintain locally throughout adult life with minimal contribution from circulating monocytes. *Immunity*. 2013;38(4):792-804. doi:10.1016/j.immuni.2013.04.004.

7. Janssen WJ, Barthel L, Muldrow A, et al. Fas determines differential fates of resident and recruited macrophages during resolution of acute lung injury. *Am J Respir Crit Care Med*. 2011;184(5):547-560. doi:10.1164/rccm.201011-1891OC.

8. Gibbings SL, Goyal R, Desch AN, et al. Transcriptome analysis highlights the conserved difference between embryonic and postnatal-derived alveolar macrophages. *Blood*. 2015;126(11):1357-1366. doi:10.1182/blood-2015-01-624809.

9. Lavin Y, Winter D, Blecher-Gonen R, et al. Tissue-resident macrophage enhancer landscapes are shaped by the local microenvironment. *Cell*. 2014;159(6):1312-1326. doi:10.1016/j.cell.2014.11.018.

10. Desch AN, Gibbings SL, Goyal R, et al. Flow Cytometric Analysis of Mononuclear Phagocytes in Nondiseased Human Lung and Lung-Draining Lymph Nodes. *Am J Respir Crit Care Med*. 2016;193(6):614-626. doi:10.1164/rccm.201507-1376OC.

11. Papp AC, Azad AK, Pietrzak M, et al. AmpliSeq transcriptome analysis of human alveolar and monocyte-derived macrophages over time in response to Mycobacterium tuberculosis infection. Neyrolles O, ed. *PLoS ONE*. 2018;13(5):e0198221. doi:10.1371/journal.pone.0198221.

12. Martinez FO, Gordon S. The M1 and M2 paradigm of macrophage activation: time for reassessment. *F1000Prime Rep*. 2014;6(13):13. doi:10.12703/P6-13.

13. Lambrecht BN. Alveolar macrophage in the driver's seat. *Immunity*. 2006;24(4):366-368. doi:10.1016/j.immuni.2006.03.008.

14. Lawrence T, Gilroy DW. Chronic inflammation: a failure of resolution? *Int J Exp Pathol*. 2007;88(2):85-94. doi:10.1111/j.1365-2613.2006.00507.x.

15. Xu W, Roos A, Schlagwein N, Woltman AM, Daha MR, van Kooten C. IL-10-producing macrophages preferentially clear early apoptotic cells. *Blood*. 2006;107(12):4930-4937. doi:10.1182/blood-2005-10-4144.

16. Fadok VA, Bratton DL, Konowal A, Freed PW, Westcott JY, Henson PM. Macrophages that have ingested apoptotic cells in vitro inhibit proinflammatory cytokine production through autocrine/paracrine mechanisms involving TGF-beta, PGE2, and PAF. *J Clin Invest*. 1998;101(4):890-898. doi:10.1172/JCI1112.

17. Ward C, Murray J, Clugston A, Dransfield I, Haslett C, Rossi AG. Interleukin-10 inhibits lipopolysaccharide-induced survival and extracellular signal-regulated kinase activation in human neutrophils. *Eur J Immunol*. 2005;35(9):2728-2737. doi:10.1002/eji.200425561.

18. Rodriguez-Prados J-C, Traves PG, Cuenca J, et al. Substrate fate in activated macrophages: a comparison between innate, classic, and alternative activation. *J Immunol*. 2010;185(1):605-614. doi:10.4049/jimmunol.0901698.

19. Jha AK, Huang SC-C, Sergushichev A, et al. Network integration of parallel metabolic and transcriptional data reveals metabolic modules that regulate macrophage polarization. *Immunity*. 2015;42(3):419-430. doi:10.1016/j.immuni.2015.02.005.

20. Mathers CD, Loncar D. Projections of Global Mortality and Burden of Disease from 2002 to 2030. Samet J, ed. *PLOS Med*. 2006;3(11):e442. doi:10.1371/journal.pmed.0030442.

21. Eisner MD, Anthonisen N, Coultas D, Kuenzli N. *Health Assembly. an Official American Thoracic Society Public Policy Statement: Novel Risk Factors and the Global Burden of Chronic Obstructive Pulmonary.* Am J Respir Crit Care Med; 2010.

22. Silverman EK. Applying Functional Genomics to Chronic Obstructive Pulmonary Disease. *Annals ATS*. 2018;15:S239-S242. doi:10.1513/AnnalsATS.201808-530MG.

23. Willemse B, Hacken Ten N. Effect of 1-year smoking cessation on airway inflammation in COPD and asymptomatic smokers. European Respiratory Journal 2005 26: 835-845; DOI: 10.1183/09031936.05.00108904.

24. Restrepo MI, Mortensen EM, Pugh JA, Anzueto A. COPD is associated with increased mortality in patients with community-acquired pneumonia. *European Respiratory Journal*. 2006;28(2):346-351. doi:10.1183/09031936.06.00131905.

25. Niewoehner DE, Kleinerman J, Rice DB. Pathologic changes in the peripheral airways of young cigarette smokers. *The New England journal of medicine*. 1974;291(15):755-758. doi:10.1056/NEJM197410102911503.

26. AUERBACH O, FORMAN JB, GERE JB, et al. Changes in the bronchial epithelium in relation to smoking and cancer of the lung; a report of progress. *The New England journal of medicine*. 1957;256(3):97-104. doi:10.1056/NEJM195701172560301.

27. Deckers J, De Bosscher K, Lambrecht BN, Hammad H. Interplay between barrier epithelial cells and dendritic cells in allergic sensitization through the lung and the skin. *Immunol Rev*. 2017;278(1):131-144. doi:10.1111/imr.12542.

28. Robbins CS, Dawe DE, Goncharova SI, et al. Cigarette smoke decreases pulmonary dendritic cells and impacts antiviral immune responsiveness. *Am J Respir Cell Mol Biol*. 2004;30(2):202-211. doi:10.1165/rcmb.2003-0259OC.

29. Rogers AV, Adelroth E, Hattotuwa K, Dewar A, Jeffery PK. Bronchial mucosal dendritic cells in smokers and ex-smokers with COPD: an electron microscopic study. *Thorax*. 2008;63(2):108-114. doi:10.1136/thx.2007.078253.

30. Butler A, Walton GM, Sapey E. Neutrophilic Inflammation in the Pathogenesis of Chronic Obstructive Pulmonary Disease. *COPD*. 2018;15(4):392-404. doi:10.1080/15412555.2018.1476475.

31. Sapey E, Stockley JA, Greenwood H, et al. Behavioral and structural differences in migrating peripheral neutrophils from patients with chronic obstructive pulmonary disease. *Am J Respir Crit Care Med*. 2011;183(9):1176-1186. doi:10.1164/rccm.201008-1285OC.

32. Hogg JC, Chu F, Utokaparch S, et al. The Nature of Small-Airway Obstruction in Chronic Obstructive Pulmonary Disease. *The New England journal of medicine*. 2004;350(26):2645-2653. doi:10.1056/NEJMoa032158.

33. Lim D, Kim W, Lee C, Bae H, Kim J. Macrophage Depletion Protects against Cigarette Smoke-Induced Inflammatory Response in the Mouse Colon and Lung. *Front Physiol*. 2018;9:47. doi:10.3389/fphys.2018.00047.

34. Patel IS, Seemungal TAR, Wilks M, Lloyd-Owen SJ, Donaldson GC, Wedzicha JA. Relationship between bacterial colonisation and the frequency, character, and severity of COPD exacerbations. *Thorax*. 2002;57(9):759-764. doi:10.1136/thorax.57.9.759.

35. Oltmanns U, Sukkar MB, Xie S, John M, Chung KF. Induction of human airway smooth muscle apoptosis by neutrophils and neutrophil elastase. *Am J Respir Cell Mol Biol*. 2005;32(4):334-341. doi:10.1165/rcmb.2004-0321OC.

36. Taylor AE, Finney-Hayward TK, Quint JK, et al. Defective macrophage phagocytosis of bacteria in COPD. *European Respiratory Journal*. 2010;35(5):1039-1047. doi:10.1183/09031936.00036709.

37. Berenson CS, Garlipp MA, Grove LJ, Maloney J, Sethi S. Impaired phagocytosis of nontypeable Haemophilus influenzae by human alveolar macrophages in chronic obstructive pulmonary disease. *J Infect Dis*. 2006;194(10):1375-1384. doi:10.1086/508428.

38. Bewley MA, Budd RC, ryan E, et al. Opsonic Phagocytosis in Chronic Obstructive Pulmonary Disease Is Enhanced by Nrf2 Agonists. *Am J Respir Crit Care Med*. 2018;198(6):739-750. doi:10.1164/rccm.201705-0903OC.

39. Hodge S, Hodge G, Ahern J, Jersmann H, Holmes M, Reynolds PN. Smoking Alters Alveolar Macrophage Recognition and Phagocytic Ability. *Am J Respir Cell Mol Biol*. 2007;37(6):748-755. doi:10.1165/rcmb.2007-0025OC.

40. Hodge S, Hodge G, Scicchitano R, Reynolds PN, Holmes M. Alveolar macrophages from subjects with chronic obstructive pulmonary disease are deficient in their ability to phagocytose apoptotic airway epithelial cells. *Immunol Cell Biol*. 2003;81(4):289-296. doi:10.1046/j.1440-1711.2003.t01-1-01170.x.

41. Russell REK, Culpitt SV, DeMatos C, et al. Release and activity of matrix metalloproteinase-9 and tissue inhibitor of metalloproteinase-1 by alveolar macrophages from patients with chronic obstructive pulmonary disease. *Am J Respir Cell Mol Biol*. 2002;26(5):602-609. doi:10.1165/ajrcmb.26.5.4685.

42. Molet S, Belleguic C, Lena H, et al. Increase in macrophage elastase (MMP-12) in lungs from patients with chronic obstructive pulmonary disease. *Inflamm Res*. 2005;54(1):31-36. doi:10.1007/s00011-004-1319-4.

43. Hiemstra PS. Altered macrophage function in chronic obstructive pulmonary disease. *Annals ATS*. 2013;10 Suppl(Supplement):S180-S185. doi:10.1513/AnnalsATS.201305-123AW.

44. Hodge S, Reynolds PN. Low-dose azithromycin improves phagocytosis of bacteria by both alveolar and monocyte-derived macrophages in chronic obstructive pulmonary disease subjects. *Respirology*. 2012;17(5):802-807. doi:10.1111/j.1440-1843.2012.02135.x.

45. Stolberg VR, McCubbrey AL, Freeman CM, et al. Glucocorticoid-Augmented Efferocytosis Inhibits Pulmonary Pneumococcal Clearance in Mice by Reducing Alveolar Macrophage Bactericidal Function. *J Immunol*. 2015;195(1):174-184. doi:10.4049/jimmunol.1402217.

46. Morimoto K, Janssen WJ, Fessler MB, et al. Lovastatin enhances clearance of apoptotic cells (efferocytosis) with implications for chronic obstructive pulmonary disease. *The Journal of Immunology*. 2006;176(12):7657-7665.

47. Xiao H, Qin X, Ping D, Zuo K. Inhibition of Rho and Rac geranylgeranylation by atorvastatin is critical for preservation of endothelial junction integrity. Lafrenie R, ed. *PLoS ONE*. 2013;8(3):e59233. doi:10.1371/journal.pone.0059233.

48. Croasdell A, Thatcher TH, Kottmann RM, et al. Resolvins attenuate inflammation and promote resolution in cigarette smoke-exposed human macrophages. *American Journal of Physiology - Lung Cellular and Molecular Physiology*. 2015;309(8):L888-L901. doi:10.1152/ajplung.00125.2015.

49. Harvey CJ, Thimmulappa RK, Sethi S, et al. Targeting Nrf2 Signaling Improves Bacterial Clearance by Alveolar Macrophages in Patients with COPD and in a Mouse Model. *Science Translational Medicine*. 2011;3(78):78ra32-78ra32. doi:10.1126/scitranslmed.3002042.

50. Shaykhiev R, Krause A, Salit J, et al. Smoking-dependent reprogramming of alveolar macrophage polarization: implication for pathogenesis of chronic obstructive pulmonary disease. *J Immunol*. 2009;183(4):2867-2883. doi:10.4049/jimmunol.0900473.

51. Chung EY, Liu J, Homma Y, et al. Interleukin-10 expression in macrophages during phagocytosis of apoptotic cells is mediated by homeodomain proteins Pbx1 and Prep-1. *Immunity*. 2007;27(6):952-964. doi:10.1016/j.immuni.2007.11.014.

52. Li C, Wang Y, Li Y, et al. HIF1α-dependent glycolysis promotes macrophage functional activities in protecting against bacterial and fungal infection. *Sci Rep*. 2018;8(1):3603. doi:10.1038/s41598-018-22039-9.

53. Morioka S, Perry JSA, Raymond MH, et al. Efferocytosis induces a novel SLC program to promote glucose uptake and lactate release. *Nature*. 2018;563(7733):714-718. doi:10.1038/s41586-018-0735-5.

54. Wang T, Liu H, Lian G, Zhang S-Y, Wang X, Jiang C. HIF1α-Induced Glycolysis Metabolism Is Essential to the Activation of Inflammatory

Macrophages. *Mediators Inflamm*. 2017;2017(11):9029327–10. doi:10.1155/2017/9029327.

55. Cramer T, Yamanishi Y, Clausen BE, et al. HIF-1alpha is essential for myeloid cell-mediated inflammation. *Cell*. 2003;112(5):645-657.

56. Diskin C, Pålsson-McDermott EM. Metabolic Modulation in Macrophage Effector Function. *Front Immunol*. 2018;9:270. doi:10.3389/fimmu.2018.00270.

57. Finkelstein R, Ma HD, Ghezzo H, Whittaker K, Fraser RS, Cosio MG. Morphometry of small airways in smokers and its relationship to emphysema type and hyperresponsiveness. *Am J Respir Crit Care Med*. 1995;152(1):267-276. doi:10.1164/ajrccm.152.1.7599834.

58. Ravi AK, Plumb J, Gaskell R, et al. COPD monocytes demonstrate impaired migratory ability. *Respir Res*. 2017;18(1):90. doi:10.1186/s12931-017-0569-y.

59. Yang S-R, Chida AS, Bauter MR, et al. Cigarette smoke induces proinflammatory cytokine release by activation of NF-kappaB and post translational modifications of histone deacetylase in macrophages. *American Journal of Physiology - Lung Cellular and Molecular Physiology*. 2006;291(1):L46-L57. doi:10.1152/ajplung.00241.2005.

60. Hodge S, Matthews G, Mukaro V, et al. Cigarette smoke-induced changes to alveolar macrophage phenotype and function are improved by treatment with procysteine. *Am J Respir Cell Mol Biol*. 2011;44(5):673-681. doi:10.1165/rcmb.2009-0459OC.

61. Pons AR, Noguera A, Blanquer D, Sauleda J, Pons J, Agustí AGN. Phenotypic characterisation of alveolar macrophages and peripheral blood monocytes in COPD. *European Respiratory Journal*. 2005;25(4):647-652. doi:10.1183/09031936.05.00062304.

62. Kunz LIZ, Lapperre TS, Snoeck-Stroband JB, et al. Smoking status and anti-inflammatory macrophages in bronchoalveolar lavage and induced sputum in COPD. *Respir Res*. 2011;12(1):34. doi:10.1186/1465-9921-12-34.

63. Bazzan E, Turato G, Tinè M, et al. Dual polarization of human alveolar macrophages progressively increases with smoking and COPD severity. *Respir Res*. 2017;18(1):40. doi:10.1186/s12931-017-0522-0.

64. Xue J, Schmidt SV, Sander J, et al. Transcriptome-based network analysis reveals a spectrum model of human macrophage activation. *Immunity*. 2014;40(2):274-288. doi:10.1016/j.immuni.2014.01.006.

65. Bewley MA, Preston JA, Mohasin M, et al. Impaired Mitochondrial Microbicidal Responses in Chronic Obstructive Pulmonary Disease

Macrophages. *Am J Respir Crit Care Med*. 2017;196(7):845-855. doi:10.1164/rccm.201608-1714OC.

66. Waterborg CEJ, Beermann S, Broeren MGA, et al. Protective Role of the MER Tyrosine Kinase via Efferocytosis in Rheumatoid Arthritis Models. *Front Immunol*. 2018;9:577. doi:10.3389/fimmu.2018.00742.

67. Pollitt AY, Insall RH. WASP and SCAR/WAVE proteins: the drivers of actin assembly. *J Cell Sci*. 2009;122(Pt 15):2575-2578. doi:10.1242/jcs.023879.

68. Schlam D, Bagshaw RD, Freeman SA, et al. Phosphoinositide 3-kinase enables phagocytosis of large particles by terminating actin assembly through Rac/Cdc42 GTPase-activating proteins. *Nat Commun*. 2015;6(1):8623. doi:10.1038/ncomms9623.

69. Kirkham PA, Spooner G, Rahman I, Rossi AG. Macrophage phagocytosis of apoptotic neutrophils is compromised by matrix proteins modified by cigarette smoke and lipid peroxidation products. *Biochem Biophys Res Commun*. 2004;318(1):32-37. doi:10.1016/j.bbrc.2004.04.003.

70. Agusti A, Calverley PMA, Celli B, et al. Characterisation of COPD heterogeneity in the ECLIPSE cohort. *Respir Res*. 2010;11(1):122. doi:10.1186/1465-9921-11-122.

71. Bewley MA, Belchamber KBR, Chana KK, et al. Differential Effects of p38, MAPK, PI3K or Rho Kinase Inhibitors on Bacterial Phagocytosis and Efferocytosis by Macrophages in COPD. Maus UA, ed. *PLoS ONE*. 2016;11(9):e0163139. doi:10.1371/journal.pone.0163139.

72. Dewhurst JA, Lea S, Hardaker E, Dungwa JV, Ravi AK, Singh D. Characterisation of lung macrophage subpopulations in COPD patients and controls. *Sci Rep*. 2017;7(1):7143. doi:10.1038/s41598-017-07101-2.

73. Li Z, Jiao Y, Fan EK, et al. Aging-Impaired Filamentous Actin Polymerization Signaling Reduces Alveolar Macrophage Phagocytosis of Bacteria. *J Immunol*. 2017;199(9):3176-3186. doi:10.4049/jimmunol.1700140.

74. Dranka BP, Hill BG, Darley-Usmar VM. Mitochondrial reserve capacity in endothelial cells: The impact of nitric oxide and reactive oxygen species. *Free Radic Biol Med*. 2010;48(7):905-914. doi:10.1016/j.freeradbiomed.2010.01.015.

75. Hill BG, Dranka BP, Zou L, Chatham JC, Darley-Usmar VM. Importance of the bioenergetic reserve capacity in response to cardiomyocyte stress induced by 4-hydroxynonenal. *Biochem J*. 2009;424(1):99-107. doi:10.1042/BJ20090934.

76. Freemerman AJ, Johnson AR, Sacks GN, et al. Metabolic reprogramming of macrophages: glucose transporter 1 (GLUT1)-mediated glucose

metabolism drives a proinflammatory phenotype. *J Biol Chem*. 2014;289(11):7884-7896. doi:10.1074/jbc.M113.522037.

77. Mills EL, Ryan DG, Prag HA, et al. Itaconate is an anti-inflammatory metabolite that activates Nrf2 via alkylation of KEAP1. *Nature*. 2018;556(7699):113-117. doi:10.1038/nature25986.

78. Tannahill GM, Curtis AM, Adamik J, et al. Succinate is an inflammatory signal that induces IL-1β through HIF-1α. *Nature*. 2013;496(7444):238-242. doi:10.1038/nature11986.

79. Nagy C, Haschemi A. Time and Demand are Two Critical Dimensions of Immunometabolism: The Process of Macrophage Activation and the Pentose Phosphate Pathway. *Front Immunol*. 2015;6. doi:10.3389/fimmu.2015.00164.

80. Vats D, Mukundan L, Odegaard JI, et al. Oxidative metabolism and PGC-1β attenuate macrophage-mediated inflammation. *Cell Metabolism*. 2006;4(1):13-24. doi:10.1016/j.cmet.2006.05.011.

81. Feingold KR, Shigenaga JK, Kazemi MR, et al. Mechanisms of triglyceride accumulation in activated macrophages. *J Leukoc Biol*. 2012;92(4):829-839. doi:10.1189/jlb.1111537.

82. Mills EL, Kelly B, Logan A, et al. Repurposing mitochondria from ATP production to ROS generation drives a pro-inflammatory phenotype in macrophages that depends on succinate oxidation by complex II. *Cell*. 2016;167(2):457–470.e13. doi:10.1016/j.cell.2016.08.064.

83. Namgaladze D, Brüne B. Fatty acid oxidation is dispensable for human macrophage IL-4-induced polarization. *Biochimica et Biophysica Acta (BBA) - Molecular and Cell Biology of Lipids*. 2014;1841(9):1329-1335. doi:10.1016/j.bbalip.2014.06.007.

84. Moon J-S, Nakahira K, Chung K-P, et al. NOX4-dependent fatty acid oxidation promotes NLRP3 inflammasome activation in macrophages. *Nature Medicine 2016 22:9*. 2016;22(9):1002-1012. doi:10.1038/nm.4153.

85. Van den Bossche J, Baardman J, Otto NA, et al. Mitochondrial Dysfunction Prevents Repolarization of Inflammatory Macrophages. *Cell reports*. 2016;17(3):684-696. doi:10.1016/j.celrep.2016.09.008.

86. Fukuzumi M, Shinomiya H, Shimizu Y, Ohishi K, Utsumi S. Endotoxin-induced enhancement of glucose influx into murine peritoneal macrophages via GLUT1. *Infect Immun*. 1996;64(1):108-112.

87. Feng J, Han J, Pearce SF, et al. Induction of CD36 expression by oxidized LDL and IL-4 by a common signaling pathway dependent on protein kinase C and PPAR-gamma. *J Lipid Res*. 2000;41(5):688-696.

88. Covarrubias AJ, Aksoylar HI, Yu. Akt-mTORC1 signaling regulates Acly to integrate metabolic input to control of macrophage activation. Elife. 2016 Feb 19;5. pii: e11612. doi: 10.7554/eLife.11612.

89. Kim WJ, Lim JH, Lee JS, Lee S-D, Kim JH, Oh Y-M. Comprehensive Analysis of Transcriptome Sequencing Data in the Lung Tissues of COPD Subjects. *Int J Genomics*. 2015;2015:206937-206939. doi:10.1155/2015/206937.

90. Michaeloudes C, Kuo C-H, Haji G, et al. Metabolic re-patterning in COPD airway smooth muscle cells. *Eur Respir J*. 2017;50(5):1700202. doi:10.1183/13993003.00202-2017.

91. Green HJ, Burnett ME, D'Arsigny CL, O'Donnell DE, Ouyang J, Webb KA. Altered metabolic and transporter characteristics of vastus lateralis in chronic obstructive pulmonary disease. *J Appl Physiol*. 2008;105(3):879-886. doi:10.1152/japplphysiol.90458.2008.

92. Hoffmann RF, Zarrintan S, Brandenburg SM, et al. Prolonged cigarette smoke exposure alters mitochondrial structure and function in airway epithelial cells. *Respir Res*. 2013;14(1):97. doi:10.1186/1465-9921-14-97.

93. Wiegman CH, Michaeloudes C, Haji G, et al. Oxidative stress-induced mitochondrial dysfunction drives inflammation and airway smooth muscle remodeling in patients with chronic obstructive pulmonary disease. *J Allergy Clin Immunol*. 2015;136(3):769-780. doi:10.1016/j.jaci.2015.01.046.

94. Ahmad T, Sundar IK, Lerner CA, et al. Impaired mitophagy leads to cigarette smoke stress-induced cellular senescence: implications for chronic obstructive pulmonary disease. *FASEB J*. 2015;29(7):2912-2929. doi:10.1096/fj.14-268276.

95. Gleeson LE, O'Leary SM, Ryan D, McLaughlin AM, Sheedy FJ, Keane J. Cigarette Smoking Impairs the Bioenergetic Immune Response to Mycobacterium tuberculosis Infection. *Am J Respir Cell Mol Biol*. 2018;59(5):572-579. doi:10.1165/rcmb.2018-0162OC.

96. Baker EH, Clark N, Brennan AL, et al. Hyperglycemia and cystic fibrosis alter respiratory fluid glucose concentrations estimated by breath condensate analysis. *Journal of Applied Physiology*. 2007;102(5):1969-1975. doi:10.1152/japplphysiol.01425.2006.

97. Chronic obstructive pulmonary disease: measuring disease progression. *Thorax*. 2008;63(Suppl 7):A39.

98. Mallia P, Webber J, Gill SK, et al. Role of airway glucose in bacterial infections in patients with chronic obstructive pulmonary disease. *Journal of Allergy and Clinical Immunology*. 2018;142(3):815-823.e816. doi:10.1016/j.jaci.2017.10.017.

99. Garcia D, Shaw RJ. AMPK: Mechanisms of Cellular Energy Sensing and Restoration of Metabolic Balance. *Mol Cell*. 2017;66(6):789-800. doi:10.1016/j.molcel.2017.05.032.

100. Murai S, Ando A, Ebara S, Hirayama M, Satomi Y, Hara T. Inhibition of malic enzyme 1 disrupts cellular metabolism and leads to vulnerability in cancer cells in glucose-restricted conditions. *Oncogenesis 2017 6:5*. 2017;6(5):e329-e329. doi:10.1038/oncsis.2017.34.

101. Voll RE, Herrmann M, Roth EA, Stach C, Kalden JR, Girkontaite I. Immunosuppressive effects of apoptotic cells. *Nature*. 1997;390(6658):350-351. doi:10.1038/37022.

102. Kelly B, O'Neill LAJ. Metabolic reprogramming in macrophages and dendritic cells in innate immunity. *Cell Res*. 2015;25(7):771-784. doi:10.1038/cr.2015.68.

103. Redza-Dutordoir M, Averill-Bates DA. Activation of apoptosis signalling pathways by reactive oxygen species. *Biochimica et Biophysica Acta (BBA) - Molecular Cell Research*. 2016;1863(12):2977-2992. doi:10.1016/j.bbamcr.2016.09.012.

104. Zhang Y, Choksi S, Chen K, Pobezinskaya Y, Linnoila I, Liu Z-G. ROS play a critical role in the differentiation of alternatively activated macrophages and the occurrence of tumor-associated macrophages. *Cell Res*. 2013;23(7):898-914. doi:10.1038/cr.2013.75.

105. Kraus D, Peschel A. Staphylococcus aureus evasion of innate antimicrobial defense. *http://dxdoiorg/102217/1746091334437*. 2008;3(4):437-451. doi:10.2217/17460913.3.4.437.

106. Judit Bartalis, W Geoffrey Chan A, Jan B Wooten. A New Look at Radicals in Cigarette Smoke. *Anal. Chem.*2007, 79,13, 5103-5106. doi:10.1021/ac070561.

107. Valavanidis A, Vlachogianni T, Fiotakis K, Loridas S. Pulmonary Oxidative Stress, Inflammation and Cancer: Respirable Particulate Matter, Fibrous Dusts and Ozone as Major Causes of Lung Carcinogenesis through Reactive Oxygen Species Mechanisms. *International Journal of Environmental Research and Public Health 2009, Vol 6, Pages 445-462*. 2013;10(9):3886-3907. doi:10.3390/ijerph10093886.

108. Rushmore TH, Pickett CB. Transcriptional regulation of the rat glutathione S-transferase Ya subunit gene. Characterization of a xenobiotic-responsive element controlling inducible expression by phenolic antioxidants. *J Biol Chem*. 1990;265(24):14648-14653.

109. Rushmore TH, Morton MR, Pickett CB. The antioxidant responsive element. Activation by oxidative stress and identification of the DNA consensus sequence required for functional activity. *J Biol Chem*. 1991;266(18):11632-11639.

110. McMahon M, Itoh K, Yamamoto M, et al. The Cap “n” Collar Basic Leucine Zipper Transcription Factor Nrf2 (NF-E2 p45-related Factor 2) Controls Both Constitutive and Inducible Expression of Intestinal Detoxification and Glutathione Biosynthetic Enzymes. *Cancer Res*. 2001;61(8):3299-3307. doi:10.1080/01635589209514201.

111. Kobayashi EH, Suzuki T, Funayama R, et al. Nrf2 suppresses macrophage inflammatory response by blocking proinflammatory cytokine transcription. *Nat Commun*. 2016;7(1):11624. doi:10.1038/ncomms11624.

112. Heiss EH, Schachner D, Zimmermann K, Dirsch VM. Glucose availability is a decisive factor for Nrf2-mediated gene expression. *Redox Biol*. 2013;1(1):359-365. doi:10.1016/j.redox.2013.06.001.

113. Baardman J, Verberk SGS, Prange KHM, et al. A Defective Pentose Phosphate Pathway Reduces Inflammatory Macrophage Responses during Hypercholesterolemia. *Cell reports*. 2018;25(8):2044-2052.e2045. doi:10.1016/j.celrep.2018.10.092.

114. Holmström KM, Baird L, Zhang Y, et al. Nrf2 impacts cellular bioenergetics by controlling substrate availability for mitochondrial respiration. *Biol Open*. 2013;2(8):761-770. doi:10.1242/bio.20134853.

115. Mitsuishi Y, Taguchi K, Kawatani Y, et al. Nrf2 redirects glucose and glutamine into anabolic pathways in metabolic reprogramming. *Cancer Cell*. 2012;22(1):66-79. doi:10.1016/j.ccr.2012.05.016.

116. Dinkova-Kostova AT, Abramov AY. The emerging role of Nrf2 in mitochondrial function. *Free Radic Biol Med*. 2015;88(Pt B):179-188. doi:10.1016/j.freeradbiomed.2015.04.036.

117. Motohashi H, Yamamoto M. Nrf2–Keap1 defines a physiologically important stress response mechanism. *Trends in Molecular Medicine*. 2004;10(11):549-557. doi:10.1016/j.molmed.2004.09.003.

118. Lee O-H, Jain AK, Papusha V, Jaiswal AK. An auto-regulatory loop between stress sensors INrf2 and Nrf2 controls their cellular abundance. *J Biol Chem*. 2007;282(50):36412-36420. doi:10.1074/jbc.M706517200.

119. Rangasamy T, Cho CY, Thimmulappa RK, et al. Genetic ablation of Nrf2 enhances susceptibility to cigarette smoke-induced emphysema in mice. *J Clin Invest*. 2004;114(9):1248-1259. doi:10.1172/JCI21146.

120. Suzuki M, Betsuyaku T, Ito Y, et al. Down-Regulated NF-E2–Related Factor 2 in Pulmonary Macrophages of Aged Smokers and Patients with Chronic Obstructive Pulmonary Disease. *Am J Respir Cell Mol Biol*. 2008;39(6):673-682. doi:10.1165/rcmb.2007-0424OC.

121. Goven D, Boutten A, Leçon-Malas V, et al. Altered Nrf2/Keap1-Bach1 equilibrium in pulmonary emphysema. *Thorax*. 2008;63(10):916-924. doi:10.1136/thx.2007.091181.

122. Kansanen E, Kuosmanen SM, Leinonen H, Levonen A-L. The Keap1-Nrf2 pathway: Mechanisms of activation and dysregulation in cancer. *Redox Biol*. 2013;1(1):45-49. doi:10.1016/j.redox.2012.10.001.

123. Korytina GF, Akhmadishina LZ, Aznabaeva YG, et al. Associations of the NRF2/KEAP1 pathway and antioxidant defense gene polymorphisms with chronic obstructive pulmonary disease. *Gene*. 2019;692:102-112. doi:10.1016/j.gene.2018.12.061.

124. Zhang Y, Talalay P, Cho CG, Posner GH. A major inducer of anticarcinogenic protective enzymes from broccoli: isolation and elucidation of structure. *PNAS*. 1992;89(6):2399-2403. doi:10.1073/pnas.89.6.2399.

125. Hu R, Xu C, Shen G, et al. Gene expression profiles induced by cancer chemopreventive isothiocyanate sulforaphane in the liver of C57BL/6J mice and C57BL/6J/Nrf2 (−/−) mice. *Cancer Letters*. 2006;243(2):170-192. doi:10.1016/j.canlet.2005.11.050.

126. Jeong W-S, Keum Y-S, Chen C, et al. Differential Expression and Stability of Endogenous Nuclear Factor E2-related Factor 2 (Nrf2) by Natural Chemopreventive Compounds in HepG2 Human Hepatoma Cells. *BMB Reports*. 2005;38(2):167-176. doi:10.5483/BMBRep.2005.38.2.167.

127. Pham N-A, Jacobberger JW, Schimmer AD, Cao P, Gronda M, Hedley DW. The dietary isothiocyanate sulforaphane targets pathways of apoptosis, cell cycle arrest, and oxidative stress in human pancreatic cancer cells and inhibits tumor growth in severe combined immunodeficient mice. *Mol Cancer Ther*. 2004;3(10):1239-1248.

128. Zhang DD, Hannink M. Distinct cysteine residues in Keap1 are required for Keap1-dependent ubiquitination of Nrf2 and for stabilization of Nrf2 by chemopreventive agents and oxidative stress. *Mol Cell Biol*. 2003;23(22):8137-8151. doi:10.1128/mcb.23.22.8137-8151.2003.

129. Dinkova-Kostova AT, Fahey JW, Kostov RV, Kensler TW. KEAP1 and Done? Targeting the NRF2 Pathway with Sulforaphane. *Trends Food Sci Technol*. 2017;69(Pt B):257-269. doi:10.1016/j.tifs.2017.02.002.

130. Lewinska A, Adamczyk-Grochala J, Deregowska A, Wnuk M. Sulforaphane-Induced Cell Cycle Arrest and Senescence are accompanied by DNA Hypomethylation and Changes in microRNA Profile in Breast Cancer Cells. *Theranostics*. 2017;7(14):3461-3477. doi:10.7150/thno.20657.

131. Baier SR, Zbasnik R, Schlegel V, Zempleni J. Off-target effects of sulforaphane include the derepression of long terminal repeats through histone acetylation events. *J Nutr Biochem*. 2014;25(6):665-668. doi:10.1016/j.jnutbio.2014.02.007.

132. Durham A, Jazrawi E, Rhodes JA, et al. The anti-inflammatory effects of sulforaphane are not mediated by the Nrf2 pathway. *European Respiratory Journal*. 2014;44(Suppl 58):P3332.

133. Boehm J, Davis R, Murar CE, et al. Discovery of a crystalline sulforaphane analog with good solid-state stability and engagement of the Nrf2 pathway in vitro and in vivo. *Bioorg Med Chem*. 2019;27(4):579-588. doi:10.1016/j.bmc.2018.12.026.

134. Fahey JW, Holtzclaw WD, Wehage SL, Wade KL, Stephenson KK, Talalay P. Sulforaphane Bioavailability from Glucoraphanin-Rich Broccoli: Control by Active Endogenous Myrosinase. Mukhopadhyay P, ed. *PLoS ONE*. 2015;10(11):e0140963. doi:10.1371/journal.pone.0140963.

135. Davies TG, Wixted WE, Coyle JE, et al. Monoacidic Inhibitors of the Kelch-like ECH-Associated Protein 1: Nuclear Factor Erythroid 2-Related Factor 2 (KEAP1:NRF2) Protein-Protein Interaction with High Cell Potency Identified by Fragment-Based Discovery. *J Med Chem*. 2016;59(8):3991-4006. doi:10.1021/acs.jmedchem.6b00228.

136. Singh A, Happel C, Manna SK, et al. Transcription factor NRF2 regulates miR-1 and miR-206 to drive tumorigenesis. *J Clin Invest*. 2013;123(7):2921-2934. doi:10.1172/JCI66353.

137. Moinova HR, Mulcahy RT. Up-regulation of the human gamma-glutamylcysteine synthetase regulatory subunit gene involves binding of Nrf-2 to an electrophile responsive element. *Biochem Biophys Res Commun*. 1999;261(3):661-668. doi:10.1006/bbrc.1999.1109.

138. Tuder RM, Petrache I. Pathogenesis of chronic obstructive pulmonary disease. *J Clin Invest*. 2012;122(8):2749-2755. doi:10.1172/JCI60324.

139. Karhausen J, Haase VH, Colgan SP. Inflammatory hypoxia: role of hypoxia-inducible factor. *Cell Cycle*. 2005;4(2):256-258.

140. Rahman I, Adcock IM. Oxidative stress and redox regulation of lung inflammation in COPD. *European Respiratory Journal*. 2006;28(1):219-242. doi:10.1183/09031936.06.00053805.

141. Ribas V, García-Ruiz C, Fernández-Checa JC. Glutathione and mitochondria. *Front Pharmacol*. 2014;5(223ra20):151. doi:10.3389/fphar.2014.00151.

142. Georgakopoulos ND, Frison M, Alvarez MS, Bertrand H, Wells G, Campanella M. Reversible Keap1 inhibitors are preferential pharmacological tools to modulate cellular mitophagy. *Sci Rep*. 2017;7(1):10303. doi:10.1038/s41598-017-07679-7.

143. Linke M, Fritsch SD, Sukhbaatar N, Hengstschläger M, Weichhart T. mTORC1 and mTORC2 as regulators of cell metabolism in immunity. Ellmeier W, Nagy L, eds. *FEBS Lett*. 2017;591(19):3089-3103. doi:10.1002/1873-3468.12711.

144. Suzuki M, Betsuyaku T, Ito Y, Nagai K, Nasuhara Y. Downregulated NF-E2-related Factor 2 in Pulmonary Macrophages of Aged Smokers and COPD

Patients. Am J Respir Cell Mol Biol. 2008 Dec;39(6):673-82. doi: 10.1165/rcmb.2007-0424OC.

145. Zheng F-J, Ye H-B, Wu M-S, Lian Y-F, Qian C-N, Zeng Y-X. Repressing malic enzyme 1 redirects glucose metabolism, unbalances the redox state, and attenuates migratory and invasive abilities in nasopharyngeal carcinoma cell lines. *Chin J Cancer*. 2012;31(11):519-531. doi:10.5732/cjc.012.10088.

146. Dhakshinamoorthy S[1], Jain AK, Bloom DA, Jaiswal AK. Bach1 competes with Nrf2 leading to negative regulation of the antioxidant response element (ARE)-mediated NAD(P)H:quinone oxidoreductase 1 gene expression and induction in response to antioxidants. J Biol Chem. 2005 Apr29;280(17):16891-900. doi: 10.1074/jbc.M500166200

147. Ling Liu,Supriya Shah, Jing Fan, Junyoung O Park,Kathryn E Wellen,Joshua D Rabinowitz Malic enzyme tracers reveal hypoxia-induced switch in adipocyte NADPH pathway usage. Nat Chem Biol. 2016 May; 12(5): 345–352. doi: 10.1038/nchembio.2047

8 Appendices:

8.1 *Appendix 1: Percoll Preparations*

Human peripheral blood leucocyte preparation:

Percoll concentration	For 10 mls (ie 3 gradients)	
	90% Percoll	1 x PBS
73%	8.1ml	1.9ml
61%	6.8ml	3.2ml
49%	5.5ml	4.5ml

8.2 *Appendix 2: Western Blot*

SDS-PAGE gels: To generate 1.5mm gel plates

Stacking gel	1 gel
Water	3ml
40% Acrylamide	620µl
0.5M Tris pH6.8	1260µl
20% SDS	25µl
20% APS	50µl
TEMED	5µl

Resolving Gel:	15%
Water	5.4ml
40% Acrylamide	5.6ml

0.5M Tris pH6.8	3.8ml
20% SDS	75µl
20% APS	150µl
TEMED	6µl

Buffers for Immunoblot:

10X Running Buffer	
Glycine	190g
Tris Base	30.3g
20% SDS	50ml
dH2O	to 1 litre

1x Running buffer was made by adding 100ml of 10x running buffer and 900ml of dH_2O

10X Transfer Buffer	
Glycine	145g
Tris Base	29g
dH2O	to 800ml

1X Transfer Buffer made by adding 100ml of 10X transfer buffer, 200ml methanol and 700ml dH_2O

10X TBS-Tween	
Tris-HCl 1M pH 8.0 M	100ml
NaCl	97.3g
Water	to 1000ml
Tween-20	5ml

1X TBS-Tween (0.05%) made with 100ml 10X TBS-Tween and 900ml dH_2O

8.3 *Appendix 3 Seahorse Compounds*

For the Glycolysis stress test:

Use Glycolysis Stress Test Seahorse Media (prepared as per 2.14)

Vial 1= Glucose, 3000µl of media was added to the vial and vortexed well.

Vial 2= Oligomycin, 720µl of media was added to the vial.

Vial 3- 2DG, 3000µl of media was added to the vial and vortexed well.

Compounds were added to ports A,B and C of the Seahorse Cartridge as detailed below:

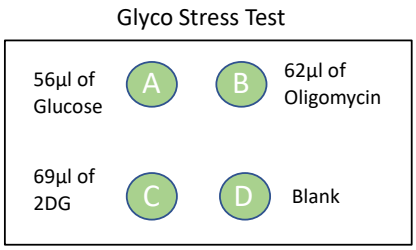

For the Mitochondrial Stress Test:

Use Mitochondrial Stress Test Seahorse Media (prepared as per 2.14)

Vial 1= Oligomycin,630µl of media was added to the vial. Then, 225µl of this stock was added to 1.275mls of Mitochondrial Stress Test Media.

Vial 2= FCCP, 720µl of media was added to the vial. Then 300µl of this stock was added to 1.2mls of Mitochondrial Stress Test Media.

Vial 3= Rotenone& Antimycin A, 540µl of media was added to the vial. Then 300µl of this stock was added to 1.2mls of Mitochondrial Stress Test Media.

Final concertation of Compounds were added to ports A,B and C of the Seahorse Cartridge as detailed below:

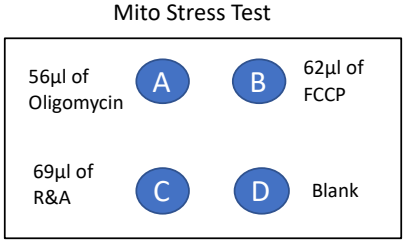

8.4 *Appendix 4: Report from Edinburgh Clinical Research Facility*

Genetics Core for Total RNA sequencing data E161715 RNA-Seq :

Summary of Sequencing Protocol

1)Quality Control: Total RNA samples were assessed on the Agilent Bioanalyser (Agilent Technologies, #G2939AA) with the RNA 6000 Nano Kit (#5067-1512) for quality and integrity of total RNA, and then quantified using the Qubit 2.0 Fluorometer (Thermo Fisher Scientific Inc, #Q32866) and the Qubit RNA HS assay kit (#Q32855).

2)Library Preparation: Libraries were prepared from total-RNA samples using the NEBNext Ultra 2 Directional RNA library prep kit for Illumina (#E7760S) with the NEBNext rRNA Depletion kit (#E6310) according to the provided protocol.

150ng of total-RNA was added to the ribosomal RNA (rRNA) depletion reaction using the NEBNext rRNA depletion kit (Human/mouse/rat) (#E6310). This step used specific probes that bind to the rRNA in order to cleave it. rRNA-depleted RNA was then DNase treated and purified using Agencourt RNAClean XP beads (Beckman Coulter Inc, #66514). RNA was then fragmented using random primers before undergoing first strand and second strand synthesis to create cDNA.

cDNA was end-repaired before ligation of sequencing adapters, and adapter-ligated libraries were enriched by 12 cycles of PCR using the NEBNext Multiplex oligos for Illumina (#E7500). Final libraries (including inserts and sequencing adapters/indexes) had an average peak size of 400bp.

3)Library QC: Libraries were quantified by fluorometry using the Qubit dsDNA HS assay and assessed for quality and fragment size using the Agilent Bioanalyser with the DNA HS Kit (#5067-4626).

4)Sequencing: Sequencing was performed using the NextSeq 500/550 High-Output v2 (150 cycle) Kit (# FC- 404-2002) on the NextSeq 550 platform (Illumina Inc, #SY-415-1002). Libraries were combined in two equimolar pools based on the library quantification results and run across 2 High-Output Flow Cell v2.5.

5) Summary of Analysis Pipeline: Basecall data produced by the NextSeq 550 is automatically uploaded to BaseSpace, a cloud- based data management and analysis service provided by Illumina. Here it is converted into FASTQ files in order

to allow analysis using a number of apps accessible directly through BaseSpace, or to download so that alternative analysis pipelines can be used.

6) Summary: A 2x75bp sequencing run on the Nextseq 550 using a high output flow cell is expected to generate up to 400M paired-end (PE) reads (50-60Gb) with a data quality of >80% higher than Q30, based on a cluster density of 170-230K/mm2. When multiplexing 6 samples on a flow cell we would therefore expect to see up to 66M PE reads per sample. Run performance is shown in table 1 below.

Table 1: Sequencing metrics by flow cell.

Run ID	Cluster Density (K/mm^2)	Clusters PF (%)	Estimated Yield (Gb)	≥Q30 (%)
190319_NB551016_0391_AH3F2CBGXB	281	83.0	94.0	89.8
190320_NB551016_0393_AH3FKCBGCB	231	89.0	82.7	91.7

Coverage of all libraries was variable in part due to the difference in output between the two flow cells. However, all libraries bar one (C264) produced >66M PE reads (Min: 58.5M, Max 118.6M, Mean: 93.1M). The number of clusters PF per library is shown in Table 2 below.

Table 2: Number of Clusters PF

Sample ID	Run ID	Number of Clusters PF
C4096	190319_NB551016_0391_AH3F2CBGXB	79,153,661
C4096 + Comp 7	190319_NB551016_0391_AH3F2CBGXB	118,614,227
C136	190319_NB551016_0391_AH3F2CBGXB	113,272,491
C136 + Comp 7	190319_NB551016_0391_AH3F2CBGXB	104,469,628
C2096	190319_NB551016_0391_AH3F2CBGXB	91,329,344
C2096 + Comp 7	190319_NB551016_0391_AH3F2CBGXB	88,610,520

C255	190320_NB551016_0393_AH3FKCBGCB	69,781,633
C255 + Comp 7	190320_NB551016_0393_AH3FKCBGCB	95,990,755
22894	190320_NB551016_0393_AH3FKCBGCB	73,108,227
22894 +7	190320_NB551016_0393_AH3FKCBGCB	106,176,077
C264	190320_NB551016_0393_AH3FKCBGCB	58,515,396
C264+7	190320_NB551016_0393_AH3FKCBGCB	118,385,584

8.5 *Appendix 5: cDNA generation and TaqMan analysis*

Reverse transcription PCR master mix (Promega UK)

Reagent	Volume per sample:
5 x AMV buffer	8µl
10nM dNTPs	16µl
RNasin	1.2µl
Random primers	1.2µl
AMV-RT	1.2µl
Final Volume =	27.6 µl

Primer Probes:

Malic Enzyme 1	IDT	Hs.PT.58.38957126
B-Actin	IDT	Hs.PT.39a.22214847

8.6 *Appendix 6: GOLD Criteria for COPD severity*

Classification of airflow limitation severity in COPD (based on post bronchodilator FEV_1) in patients with a FEV_1:FVC ration <0.70)		
GOLD 1	Mild	FEV1≥ 80% predicted
GOLD 2	Moderate	50% ≤ FEV1 < 80% predicted
GOLD 3	Severe	30% ≤ FEV1 < 50% predicted
GOLD 4	Very Severe	FEV1 <30% predicted

8.7 *Appendix 7: COPD Assessment Test*

Your name:

Today's date:

CAT
COPD Assessment Test

How is your COPD? Take the COPD Assessment Test™ (CAT)

This questionnaire will help you and your healthcare professional measure the impact COPD (Chronic Obstructive Pulmonary Disease) is having on your wellbeing and daily life. Your answers, and test score, can be used by you and your healthcare professional to help improve the management of your COPD and get the greatest benefit from treatment.

For each item below, place a mark (X) in the box that best describes you currently. Be sure to only select one response for each question.

Example: I am very happy 0 X 2 3 4 5 I am very sad

			SCORE
I never cough	0 1 2 3 4 5	**I cough all the time**	
I have no phlegm (mucus) in my chest at all	0 1 2 3 4 5	**My chest is completely full of phlegm (mucus)**	
My chest does not feel tight at all	0 1 2 3 4 5	**My chest feels very tight**	
When I walk up a hill or one flight of stairs I am not breathless	0 1 2 3 4 5	**When I walk up a hill or one flight of stairs I am very breathless**	
I am not limited doing any activities at home	0 1 2 3 4 5	**I am very limited doing activities at home**	
I am confident leaving my home despite my lung condition	0 1 2 3 4 5	**I am not at all confident leaving my home because of my lung condition**	
I sleep soundly	0 1 2 3 4 5	**I don't sleep soundly because of my lung condition**	
I have lots of energy	0 1 2 3 4 5	**I have no energy at all**	
		TOTAL SCORE	

1. Watts ER, ryan E, Walmsley SR, Whyte MKB. *Microenvironmental Regulation of Innate Immune Cell Function*. Vol 41. Weinheim, Germany: John Wiley & Sons, Ltd; 2017:947-970. doi:10.1002/9783527692156.ch36.

2. van Furth R, Cohn ZA, Hirsch JG, Humphrey JH, Spector WG, Langevoort HL. The mononuclear phagocyte system: a new classification of macrophages, monocytes, and their precursor cells. *Bull World Health Organ*. 1972;46(6):845-852.

3. Ginhoux F, Guilliams M. Tissue-Resident Macrophage Ontogeny and Homeostasis. *Immunity*. 2016;44(3):439-449. doi:10.1016/j.immuni.2016.02.024.

4. Gomez Perdiguero E, Klapproth K, Schulz C, et al. Tissue-resident macrophages originate from yolk-sac-derived erythro-myeloid progenitors. *Nature*. 2015;518(7540):547-551. doi:10.1038/nature13989.

5. Guilliams M, De Kleer I, Henri S, et al. Alveolar macrophages develop from fetal monocytes that differentiate into long-lived cells in the first week of life via GM-CSF. *J Exp Med*. 2013;210(10):1977-1992. doi:10.1084/jem.20131199.

6. Hashimoto D, Chow A, Noizat C, et al. Tissue-resident macrophages self-maintain locally throughout adult life with minimal contribution from circulating monocytes. *Immunity*. 2013;38(4):792-804. doi:10.1016/j.immuni.2013.04.004.

7. Janssen WJ, Barthel L, Muldrow A, et al. Fas determines differential fates of resident and recruited macrophages during resolution of acute lung injury. *Am J Respir Crit Care Med*. 2011;184(5):547-560. doi:10.1164/rccm.201011-1891OC.

8. Gibbings SL, Goyal R, Desch AN, et al. Transcriptome analysis highlights the conserved difference between embryonic and postnatal-derived alveolar macrophages. *Blood*. 2015;126(11):1357-1366. doi:10.1182/blood-2015-01-624809.

9. Lavin Y, Winter D, Blecher-Gonen R, et al. Tissue-resident macrophage enhancer landscapes are shaped by the local microenvironment. *Cell*. 2014;159(6):1312-1326. doi:10.1016/j.cell.2014.11.018.

10. Desch AN, Gibbings SL, Goyal R, et al. Flow Cytometric Analysis of Mononuclear Phagocytes in Nondiseased Human Lung and Lung-Draining Lymph Nodes. *Am J Respir Crit Care Med*. 2016;193(6):614-626. doi:10.1164/rccm.201507-1376OC.

11. Papp AC, Azad AK, Pietrzak M, et al. AmpliSeq transcriptome analysis of human alveolar and monocyte-derived macrophages over time in response to Mycobacterium tuberculosis infection. Neyrolles O, ed. *PLoS ONE*. 2018;13(5):e0198221. doi:10.1371/journal.pone.0198221.

12. Martinez FO, Gordon S. The M1 and M2 paradigm of macrophage activation: time for reassessment. *F1000Prime Rep*. 2014;6(13):13. doi:10.12703/P6-13.

13. Lambrecht BN. Alveolar macrophage in the driver's seat. *Immunity*. 2006;24(4):366-368. doi:10.1016/j.immuni.2006.03.008.

14. Lawrence T, Gilroy DW. Chronic inflammation: a failure of resolution? *Int J Exp Pathol*. 2007;88(2):85-94. doi:10.1111/j.1365-2613.2006.00507.x.

15. Xu W, Roos A, Schlagwein N, Woltman AM, Daha MR, van Kooten C. IL-10-producing macrophages preferentially clear early apoptotic cells. *Blood*. 2006;107(12):4930-4937. doi:10.1182/blood-2005-10-4144.

16. Fadok VA, Bratton DL, Konowal A, Freed PW, Westcott JY, Henson PM. Macrophages that have ingested apoptotic cells in vitro inhibit proinflammatory cytokine production through autocrine/paracrine mechanisms involving TGF-beta, PGE2, and PAF. *J Clin Invest*. 1998;101(4):890-898. doi:10.1172/JCI1112.

17. Ward C, Murray J, Clugston A, Dransfield I, Haslett C, Rossi AG. Interleukin-10 inhibits lipopolysaccharide-induced survival and extracellular signal-regulated kinase activation in human neutrophils. *Eur J Immunol*. 2005;35(9):2728-2737. doi:10.1002/eji.200425561.

18. Rodriguez-Prados J-C, Traves PG, Cuenca J, et al. Substrate fate in activated macrophages: a comparison between innate, classic, and alternative activation. *J Immunol*. 2010;185(1):605-614. doi:10.4049/jimmunol.0901698.

19. Jha AK, Huang SC-C, Sergushichev A, et al. Network integration of parallel metabolic and transcriptional data reveals metabolic modules that regulate macrophage polarization. *Immunity*. 2015;42(3):419-430. doi:10.1016/j.immuni.2015.02.005.

20. Mathers CD, Loncar D. Projections of Global Mortality and Burden of Disease from 2002 to 2030. Samet J, ed. *PLOS Med*. 2006;3(11):e442. doi:10.1371/journal.pmed.0030442.

21. Eisner MD, Anthonisen N, Coultas D, Kuenzli N. *… Health Assembly. an Official American Thoracic Society Public Policy Statement: Novel Risk Factors and the Global Burden of Chronic Obstructive Pulmonary …*. Am J Respir Crit Care Med; 2010.

22. Silverman EK. Applying Functional Genomics to Chronic Obstructive Pulmonary Disease. *Annals ATS*. 2018;15(Supplement_4):S239-S242. doi:10.1513/AnnalsATS.201808-530MG.

23. Willemse B, Hacken Ten N. Effect of 1-year smoking cessation on airway inflammation in COPD and asymptomatic smokers. *European …*. 2005.

24. Restrepo MI, Mortensen EM, Pugh JA, Anzueto A. COPD is associated with increased mortality in patients with community-acquired pneumonia. *European Respiratory Journal*. 2006;28(2):346-351. doi:10.1183/09031936.06.00131905.

25. Niewoehner DE, Kleinerman J, Rice DB. Pathologic changes in the peripheral airways of young cigarette smokers. *The New England journal of medicine*. 1974;291(15):755-758. doi:10.1056/NEJM197410102911503.

26. AUERBACH O, FORMAN JB, GERE JB, et al. Changes in the bronchial epithelium in relation to smoking and cancer of the lung; a report of progress. *The New England journal of medicine*. 1957;256(3):97-104. doi:10.1056/NEJM195701172560301.

27. Deckers J, De Bosscher K, Lambrecht BN, Hammad H. Interplay between barrier epithelial cells and dendritic cells in allergic sensitization through the lung and the skin. *Immunol Rev*. 2017;278(1):131-144. doi:10.1111/imr.12542.

28. Robbins CS, Dawe DE, Goncharova SI, et al. Cigarette smoke decreases pulmonary dendritic cells and impacts antiviral immune responsiveness. *Am J Respir Cell Mol Biol*. 2004;30(2):202-211. doi:10.1165/rcmb.2003-0259OC.

29. Rogers AV, Adelroth E, Hattotuwa K, Dewar A, Jeffery PK. Bronchial mucosal dendritic cells in smokers and ex-smokers with COPD: an electron microscopic study. *Thorax*. 2008;63(2):108-114. doi:10.1136/thx.2007.078253.

30. Butler A, Walton GM, Sapey E. Neutrophilic Inflammation in the Pathogenesis of Chronic Obstructive Pulmonary Disease. *COPD*. 2018;15(4):392-404. doi:10.1080/15412555.2018.1476475.

31. Sapey E, Stockley JA, Greenwood H, et al. Behavioral and structural differences in migrating peripheral neutrophils from patients with chronic obstructive pulmonary disease. *Am J Respir Crit Care Med*. 2011;183(9):1176-1186. doi:10.1164/rccm.201008-1285OC.

32. Hogg JC, Chu F, Utokaparch S, et al. The Nature of Small-Airway Obstruction in Chronic Obstructive Pulmonary Disease. *The New England journal of medicine*. 2004;350(26):2645-2653. doi:10.1056/NEJMoa032158.

33. Lim D, Kim W, Lee C, Bae H, Kim J. Macrophage Depletion Protects against Cigarette Smoke-Induced Inflammatory Response in the Mouse Colon and Lung. *Front Physiol*. 2018;9:47. doi:10.3389/fphys.2018.00047.

34. Patel IS, Seemungal TAR, Wilks M, Lloyd-Owen SJ, Donaldson GC, Wedzicha JA. Relationship between bacterial colonisation and the frequency, character, and severity of COPD exacerbations. *Thorax*. 2002;57(9):759-764. doi:10.1136/thorax.57.9.759.

35. Oltmanns U, Sukkar MB, Xie S, John M, Chung KF. Induction of human airway smooth muscle apoptosis by neutrophils and neutrophil elastase. *Am J Respir Cell Mol Biol*. 2005;32(4):334-341. doi:10.1165/rcmb.2004-0321OC.

36. Taylor AE, Finney-Hayward TK, Quint JK, et al. Defective macrophage phagocytosis of bacteria in COPD. *European Respiratory Journal*. 2010;35(5):1039-1047. doi:10.1183/09031936.00036709.

37. Berenson CS, Garlipp MA, Grove LJ, Maloney J, Sethi S. Impaired phagocytosis of nontypeable Haemophilus influenzae by human alveolar macrophages in chronic obstructive pulmonary disease. *J Infect Dis*. 2006;194(10):1375-1384. doi:10.1086/508428.

38. Bewley MA, Budd RC, ryan E, et al. Opsonic Phagocytosis in Chronic Obstructive Pulmonary Disease Is Enhanced by Nrf2 Agonists. *Am J Respir Crit Care Med*. 2018;198(6):739-750. doi:10.1164/rccm.201705-0903OC.

39. Hodge S, Hodge G, Ahern J, Jersmann H, Holmes M, Reynolds PN. Smoking Alters Alveolar Macrophage Recognition and Phagocytic Ability. *Am J Respir Cell Mol Biol*. 2007;37(6):748-755. doi:10.1165/rcmb.2007-0025OC.

40. Hodge S, Hodge G, Scicchitano R, Reynolds PN, Holmes M. Alveolar macrophages from subjects with chronic obstructive pulmonary disease are deficient in their ability to phagocytose apoptotic airway epithelial cells. *Immunol Cell Biol*. 2003;81(4):289-296. doi:10.1046/j.1440-1711.2003.t01-1-01170.x.

41. Russell REK, Culpitt SV, DeMatos C, et al. Release and activity of matrix metalloproteinase-9 and tissue inhibitor of metalloproteinase-1 by alveolar macrophages from patients with chronic obstructive pulmonary disease. *Am J Respir Cell Mol Biol*. 2002;26(5):602-609. doi:10.1165/ajrcmb.26.5.4685.

42. Molet S, Belleguic C, Lena H, et al. Increase in macrophage elastase (MMP-12) in lungs from patients with chronic obstructive pulmonary disease. *Inflamm Res*. 2005;54(1):31-36. doi:10.1007/s00011-004-1319-4.

43. Hiemstra PS. Altered macrophage function in chronic obstructive pulmonary disease. *Annals ATS*. 2013;10 Suppl(Supplement):S180-S185. doi:10.1513/AnnalsATS.201305-123AW.

44. Hodge S, Reynolds PN. Low-dose azithromycin improves phagocytosis of bacteria by both alveolar and monocyte-derived macrophagesin chronic obstructive pulmonary disease subjects. *Respirology*. 2012;17(5):802-807. doi:10.1111/j.1440-1843.2012.02135.x.

45. Stolberg VR, McCubbrey AL, Freeman CM, et al. Glucocorticoid-Augmented Efferocytosis Inhibits Pulmonary Pneumococcal Clearance in Mice by Reducing Alveolar Macrophage Bactericidal Function. *J Immunol*. 2015;195(1):174-184. doi:10.4049/jimmunol.1402217.

46. Morimoto K, Janssen WJ, Fessler MB, et al. Lovastatin enhances clearance of apoptotic cells (efferocytosis) with implications for chronic obstructive pulmonary disease. *The Journal of Immunology*. 2006;176(12):7657-7665.

47. Xiao H, Qin X, Ping D, Zuo K. Inhibition of Rho and Rac geranylgeranylation by atorvastatin is critical for preservation of endothelial junction integrity. Lafrenie R, ed. *PLoS ONE*. 2013;8(3):e59233. doi:10.1371/journal.pone.0059233.

48. Croasdell A, Thatcher TH, Kottmann RM, et al. Resolvins attenuate inflammation and promote resolution in cigarette smoke-exposed human macrophages. *American Journal of Physiology - Lung Cellular and Molecular Physiology*. 2015;309(8):L888-L901. doi:10.1152/ajplung.00125.2015.

49. Harvey CJ, Thimmulappa RK, Sethi S, et al. Targeting Nrf2 Signaling Improves Bacterial Clearance by Alveolar Macrophages in Patients with COPD and in a Mouse Model. *Science Translational Medicine*. 2011;3(78):78ra32-78ra32. doi:10.1126/scitranslmed.3002042.

50. Chandak PG, Radovic B, Aflaki E, et al. Efficient phagocytosis requires triacylglycerol hydrolysis by adipose triglyceride lipase. *J Biol Chem*. 2010;285(26):20192-20201. doi:10.1074/jbc.M110.107854.

51. Shaykhiev R, Krause A, Salit J, et al. Smoking-dependent reprogramming of alveolar macrophage polarization: implication for pathogenesis of chronic obstructive pulmonary disease. *J Immunol*. 2009;183(4):2867-2883. doi:10.4049/jimmunol.0900473.

52. Gordon SB, Irving GR, Lawson RA, Lee ME, Read RC. Intracellular trafficking and killing of Streptococcus pneumoniae by human alveolar macrophages are influenced by opsonins. *Infect Immun*. 2000;68(4):2286-2293.

53. Divakaruni AS, Paradyse A, Ferrick DA, Murphy AN, Jastroch M. Analysis and interpretation of microplate-based oxygen consumption and pH data. *Meth Enzymol*. 2014;547:309-354. doi:10.1016/B978-0-12-801415-8.00016-3.

54. Sadiku P, Willson JA, Dickinson RS, et al. Prolyl hydroxylase 2 inactivation enhances glycogen storage and promotes excessive neutrophilic responses. *J Clin Invest*. 2017;127(9):3407-3420. doi:10.1172/JCI90848.

55. Chung EY, Liu J, Homma Y, et al. Interleukin-10 expression in macrophages during phagocytosis of apoptotic cells is mediated by homeodomain proteins Pbx1 and Prep-1. *Immunity*. 2007;27(6):952-964. doi:10.1016/j.immuni.2007.11.014.

56. Li C, Wang Y, Li Y, et al. HIF1α-dependent glycolysis promotes macrophage functional activities in protecting against bacterial and fungal infection. *Sci Rep*. 2018;8(1):3603. doi:10.1038/s41598-018-22039-9.

57. Morioka S, Perry JSA, Raymond MH, et al. Efferocytosis induces a novel SLC program to promote glucose uptake and lactate release. *Nature*. 2018;563(7733):714-718. doi:10.1038/s41586-018-0735-5.

58. Wang T, Liu H, Lian G, Zhang S-Y, Wang X, Jiang C. HIF1α-Induced Glycolysis Metabolism Is Essential to the Activation of Inflammatory Macrophages. *Mediators Inflamm*. 2017;2017(11):9029327–10. doi:10.1155/2017/9029327.

59. Cramer T, Yamanishi Y, Clausen BE, et al. HIF-1alpha is essential for myeloid cell-mediated inflammation. *Cell*. 2003;112(5):645-657.

60. Diskin C, Pålsson-McDermott EM. Metabolic Modulation in Macrophage Effector Function. *Front Immunol*. 2018;9:270. doi:10.3389/fimmu.2018.00270.

61. Finkelstein R, Ma HD, Ghezzo H, Whittaker K, Fraser RS, Cosio MG. Morphometry of small airways in smokers and its relationship to emphysema type and hyperresponsiveness. *Am J Respir Crit Care Med*. 1995;152(1):267-276. doi:10.1164/ajrccm.152.1.7599834.

62. Ravi AK, Plumb J, Gaskell R, et al. COPD monocytes demonstrate impaired migratory ability. *Respir Res*. 2017;18(1):90. doi:10.1186/s12931-017-0569-y.

63. Yang S-R, Chida AS, Bauter MR, et al. Cigarette smoke induces proinflammatory cytokine release by activation of NF-kappaB and posttranslational modifications of histone deacetylase in macrophages. *American Journal of Physiology - Lung Cellular and Molecular Physiology*. 2006;291(1):L46-L57. doi:10.1152/ajplung.00241.2005.

64. Pons AR, Noguera A, Blanquer D, Sauleda J, Pons J, Agustí AGN. Phenotypic characterisation of alveolar macrophages and peripheral blood monocytes in COPD. *European Respiratory Journal*. 2005;25(4):647-652. doi:10.1183/09031936.05.00062304.

65. Kunz LIZ, Lapperre TS, Snoeck-Stroband JB, et al. Smoking status and anti-inflammatory macrophages in bronchoalveolar lavage and induced sputum in COPD. *Respir Res*. 2011;12(1):34. doi:10.1186/1465-9921-12-34.

66. Bazzan E, Turato G, Tinè M, et al. Dual polarization of human alveolar macrophages progressively increases with smoking and COPD severity. *Respir Res*. 2017;18(1):40. doi:10.1186/s12931-017-0522-0.

67. Xue J, Schmidt SV, Sander J, et al. Transcriptome-based network analysis reveals a spectrum model of human macrophage activation. *Immunity*. 2014;40(2):274-288. doi:10.1016/j.immuni.2014.01.006.

68. Hodge S, Matthews G, Mukaro V, et al. Cigarette smoke-induced changes to alveolar macrophage phenotype and function are improved by treatment

with procysteine. *Am J Respir Cell Mol Biol*. 2011;44(5):673-681. doi:10.1165/rcmb.2009-0459OC.

69. Bewley MA, Preston JA, Mohasin M, et al. Impaired Mitochondrial Microbicidal Responses in Chronic Obstructive Pulmonary Disease Macrophages. *Am J Respir Crit Care Med*. 2017;196(7):845-855. doi:10.1164/rccm.201608-1714OC.

70. Waterborg CEJ, Beermann S, Broeren MGA, et al. Protective Role of the MER Tyrosine Kinase via Efferocytosis in Rheumatoid Arthritis Models. *Front Immunol*. 2018;9:577. doi:10.3389/fimmu.2018.00742.

71. Pollitt AY, Insall RH. WASP and SCAR/WAVE proteins: the drivers of actin assembly. *J Cell Sci*. 2009;122(Pt 15):2575-2578. doi:10.1242/jcs.023879.

72. Schlam D, Bagshaw RD, Freeman SA, et al. Phosphoinositide 3-kinase enables phagocytosis of large particles by terminating actin assembly through Rac/Cdc42 GTPase-activating proteins. *Nat Commun*. 2015;6(1):8623. doi:10.1038/ncomms9623.

73. Kirkham PA, Spooner G, Rahman I, Rossi AG. Macrophage phagocytosis of apoptotic neutrophils is compromised by matrix proteins modified by cigarette smoke and lipid peroxidation products. *Biochem Biophys Res Commun*. 2004;318(1):32-37. doi:10.1016/j.bbrc.2004.04.003.

74. Agusti A, Calverley PMA, Celli B, et al. Characterisation of COPD heterogeneity in the ECLIPSE cohort. *Respir Res*. 2010;11(1):122. doi:10.1186/1465-9921-11-122.

75. Bewley MA, Belchamber KBR, Chana KK, et al. Differential Effects of p38, MAPK, PI3K or Rho Kinase Inhibitors on Bacterial Phagocytosis and Efferocytosis by Macrophages in COPD. Maus UA, ed. *PLoS ONE*. 2016;11(9):e0163139. doi:10.1371/journal.pone.0163139.

76. Dewhurst JA, Lea S, Hardaker E, Dungwa JV, Ravi AK, Singh D. Characterisation of lung macrophage subpopulations in COPD patients and controls. *Sci Rep*. 2017;7(1):7143. doi:10.1038/s41598-017-07101-2.

77. Li Z, Jiao Y, Fan EK, et al. Aging-Impaired Filamentous Actin Polymerization Signaling Reduces Alveolar Macrophage Phagocytosis of Bacteria. *J Immunol*. 2017;199(9):3176-3186. doi:10.4049/jimmunol.1700140.

78. Dranka BP, Hill BG, Darley-Usmar VM. Mitochondrial reserve capacity in endothelial cells: The impact of nitric oxide and reactive oxygen species. *Free Radic Biol Med*. 2010;48(7):905-914. doi:10.1016/j.freeradbiomed.2010.01.015.

79. Hill BG, Dranka BP, Zou L, Chatham JC, Darley-Usmar VM. Importance of the bioenergetic reserve capacity in response to cardiomyocyte stress

induced by 4-hydroxynonenal. *Biochem J*. 2009;424(1):99-107. doi:10.1042/BJ20090934.

80. Freemerman AJ, Johnson AR, Sacks GN, et al. Metabolic reprogramming of macrophages: glucose transporter 1 (GLUT1)-mediated glucose metabolism drives a proinflammatory phenotype. *J Biol Chem*. 2014;289(11):7884-7896. doi:10.1074/jbc.M113.522037.

81. Mills EL, Ryan DG, Prag HA, et al. Itaconate is an anti-inflammatory metabolite that activates Nrf2 via alkylation of KEAP1. *Nature*. 2018;556(7699):113-117. doi:10.1038/nature25986.

82. Tannahill GM, Curtis AM, Adamik J, et al. Succinate is an inflammatory signal that induces IL-1β through HIF-1α. *Nature*. 2013;496(7444):238-242. doi:10.1038/nature11986.

83. Nagy C, Haschemi A. Time and Demand are Two Critical Dimensions of Immunometabolism: The Process of Macrophage Activation and the Pentose Phosphate Pathway. *Front Immunol*. 2015;6. doi:10.3389/fimmu.2015.00164.

84. Vats D, Mukundan L, Odegaard JI, et al. Oxidative metabolism and PGC-1β attenuate macrophage-mediated inflammation. *Cell Metabolism*. 2006;4(1):13-24. doi:10.1016/j.cmet.2006.05.011.

85. Feingold KR, Shigenaga JK, Kazemi MR, et al. Mechanisms of triglyceride accumulation in activated macrophages. *J Leukoc Biol*. 2012;92(4):829-839. doi:10.1189/jlb.1111537.

86. Mills EL, Kelly B, Logan A, et al. Repurposing mitochondria from ATP production to ROS generation drives a pro-inflammatory phenotype in macrophages that depends on succinate oxidation by complex II. *Cell*. 2016;167(2):457–470.e13. doi:10.1016/j.cell.2016.08.064.

87. Namgaladze D, Brüne B. Fatty acid oxidation is dispensable for human macrophage IL-4-induced polarization. *Biochimica et Biophysica Acta (BBA) - Molecular and Cell Biology of Lipids*. 2014;1841(9):1329-1335. doi:10.1016/j.bbalip.2014.06.007.

88. Moon J-S, Nakahira K, Chung K-P, et al. NOX4-dependent fatty acid oxidation promotes NLRP3 inflammasome activation in macrophages. *Nature Medicine 2016 22:9*. 2016;22(9):1002-1012. doi:10.1038/nm.4153.

89. Van den Bossche J, Baardman J, Otto NA, et al. Mitochondrial Dysfunction Prevents Repolarization of Inflammatory Macrophages. *Cell reports*. 2016;17(3):684-696. doi:10.1016/j.celrep.2016.09.008.

90. Fukuzumi M, Shinomiya H, Shimizu Y, Ohishi K, Utsumi S. Endotoxin-induced enhancement of glucose influx into murine peritoneal macrophages via GLUT1. *Infect Immun*. 1996;64(1):108-112.

91. Feng J, Han J, Pearce SF, et al. Induction of CD36 expression by oxidized LDL and IL-4 by a common signaling pathway dependent on protein kinase C and PPAR-gamma. *J Lipid Res*. 2000;41(5):688-696.

92. Covarrubias AJ, Aksoylar HI, Yu J, elife NS, 2016. Akt-mTORC1 signaling regulates Acly to integrate metabolic input to control of macrophage activation. *cdnelifesciencesorg*

.

93. Kim WJ, Lim JH, Lee JS, Lee S-D, Kim JH, Oh Y-M. Comprehensive Analysis of Transcriptome Sequencing Data in the Lung Tissues of COPD Subjects. *Int J Genomics*. 2015;2015:206937-206939. doi:10.1155/2015/206937.

94. Michaeloudes C, Kuo C-H, Haji G, et al. Metabolic re-patterning in COPD airway smooth muscle cells. *Eur Respir J*. 2017;50(5):1700202. doi:10.1183/13993003.00202-2017.

95. Green HJ, Burnett ME, D'Arsigny CL, O'Donnell DE, Ouyang J, Webb KA. Altered metabolic and transporter characteristics of vastus lateralis in chronic obstructive pulmonary disease. *J Appl Physiol*. 2008;105(3):879-886. doi:10.1152/japplphysiol.90458.2008.

96. Hoffmann RF, Zarrintan S, Brandenburg SM, et al. Prolonged cigarette smoke exposure alters mitochondrial structure and function in airway epithelial cells. *Respir Res*. 2013;14(1):97. doi:10.1186/1465-9921-14-97.

97. Wiegman CH, Michaeloudes C, Haji G, et al. Oxidative stress-induced mitochondrial dysfunction drives inflammation and airway smooth muscle remodeling in patients with chronic obstructive pulmonary disease. *J Allergy Clin Immunol*. 2015;136(3):769-780. doi:10.1016/j.jaci.2015.01.046.

98. Ahmad T, Sundar IK, Lerner CA, et al. Impaired mitophagy leads to cigarette smoke stress-induced cellular senescence: implications for chronic obstructive pulmonary disease. *FASEB J*. 2015;29(7):2912-2929. doi:10.1096/fj.14-268276.

99. Gleeson LE, O'Leary SM, Ryan D, McLaughlin AM, Sheedy FJ, Keane J. Cigarette Smoking Impairs the Bioenergetic Immune Response to Mycobacterium tuberculosis Infection. *Am J Respir Cell Mol Biol*. 2018;59(5):572-579. doi:10.1165/rcmb.2018-0162OC.

100. Baker EH, Clark N, Brennan AL, et al. Hyperglycemia and cystic fibrosis alter respiratory fluid glucose concentrations estimated by breath condensate analysis. *Journal of Applied Physiology*. 2007;102(5):1969-1975. doi:10.1152/japplphysiol.01425.2006.

101. Chronic obstructive pulmonary disease: measuring disease progression. *Thorax*. 2008;63(Suppl 7):A39.

102. Mallia P, Webber J, Gill SK, et al. Role of airway glucose in bacterial infections in patients with chronic obstructive pulmonary disease. *Journal of Allergy and Clinical Immunology*. 2018;142(3):815-823.e816. doi:10.1016/j.jaci.2017.10.017.

103. Garcia D, Shaw RJ. AMPK: Mechanisms of Cellular Energy Sensing and Restoration of Metabolic Balance. *Mol Cell*. 2017;66(6):789-800. doi:10.1016/j.molcel.2017.05.032.

104. Murai S, Ando A, Ebara S, Hirayama M, Satomi Y, Hara T. Inhibition of malic enzyme 1 disrupts cellular metabolism and leads to vulnerability in cancer cells in glucose-restricted conditions. *Oncogenesis 2017 6:5*. 2017;6(5):e329-e329. doi:10.1038/oncsis.2017.34.

105. Voll RE, Herrmann M, Roth EA, Stach C, Kalden JR, Girkontaite I. Immunosuppressive effects of apoptotic cells. *Nature*. 1997;390(6658):350-351. doi:10.1038/37022.

106. Kelly B, O'Neill LAJ. Metabolic reprogramming in macrophages and dendritic cells in innate immunity. *Cell Res*. 2015;25(7):771-784. doi:10.1038/cr.2015.68.

107. Redza-Dutordoir M, Averill-Bates DA. Activation of apoptosis signalling pathways by reactive oxygen species. *Biochimica et Biophysica Acta (BBA) - Molecular Cell Research*. 2016;1863(12):2977-2992. doi:10.1016/j.bbamcr.2016.09.012.

108. Zhang Y, Choksi S, Chen K, Pobezinskaya Y, Linnoila I, Liu Z-G. ROS play a critical role in the differentiation of alternatively activated macrophages and the occurrence of tumor-associated macrophages. *Cell Res*. 2013;23(7):898-914. doi:10.1038/cr.2013.75.

109. Kraus D, Peschel A. Staphylococcus aureus evasion of innate antimicrobial defense. *http://dxdoiorg/102217/1746091334437*. 2008;3(4):437-451. doi:10.2217/17460913.3.4.437.

110. Judit Bartalis, W Geoffrey Chan A, Jan B Wooten. A New Look at Radicals in Cigarette Smoke. May 2007. doi:10.1021/ac070561.

111. Valavanidis A, Vlachogianni T, Fiotakis K, Loridas S. Pulmonary Oxidative Stress, Inflammation and Cancer: Respirable Particulate Matter, Fibrous Dusts and Ozone as Major Causes of Lung Carcinogenesis through Reactive Oxygen Species Mechanisms. *International Journal of Environmental Research and Public Health 2009, Vol 6, Pages 445-462*. 2013;10(9):3886-3907. doi:10.3390/ijerph10093886.

112. Rushmore TH, Pickett CB. Transcriptional regulation of the rat glutathione S-transferase Ya subunit gene. Characterization of a xenobiotic-responsive element controlling inducible expression by phenolic antioxidants. *J Biol Chem*. 1990;265(24):14648-14653.

113. Rushmore TH, Morton MR, Pickett CB. The antioxidant responsive element. Activation by oxidative stress and identification of the DNA consensus sequence required for functional activity. *J Biol Chem*. 1991;266(18):11632-11639.

114. McMahon M, Itoh K, Yamamoto M, et al. The Cap “n” Collar Basic Leucine Zipper Transcription Factor Nrf2 (NF-E2 p45-related Factor 2) Controls Both Constitutive and Inducible Expression of Intestinal Detoxification and Glutathione Biosynthetic Enzymes. *Cancer Res*. 2001;61(8):3299-3307. doi:10.1080/01635589209514201.

115. Kobayashi EH, Suzuki T, Funayama R, et al. Nrf2 suppresses macrophage inflammatory response by blocking proinflammatory cytokine transcription. *Nat Commun*. 2016;7(1):11624. doi:10.1038/ncomms11624.

116. Heiss EH, Schachner D, Zimmermann K, Dirsch VM. Glucose availability is a decisive factor for Nrf2-mediated gene expression. *Redox Biol*. 2013;1(1):359-365. doi:10.1016/j.redox.2013.06.001.

117. Baardman J, Verberk SGS, Prange KHM, et al. A Defective Pentose Phosphate Pathway Reduces Inflammatory Macrophage Responses during Hypercholesterolemia. *Cell reports*. 2018;25(8):2044-2052.e2045. doi:10.1016/j.celrep.2018.10.092.

118. Holmström KM, Baird L, Zhang Y, et al. Nrf2 impacts cellular bioenergetics by controlling substrate availability for mitochondrial respiration. *Biol Open*. 2013;2(8):761-770. doi:10.1242/bio.20134853.

119. Mitsuishi Y, Taguchi K, Kawatani Y, et al. Nrf2 redirects glucose and glutamine into anabolic pathways in metabolic reprogramming. *Cancer Cell*. 2012;22(1):66-79. doi:10.1016/j.ccr.2012.05.016.

120. Dinkova-Kostova AT, Abramov AY. The emerging role of Nrf2 in mitochondrial function. *Free Radic Biol Med*. 2015;88(Pt B):179-188. doi:10.1016/j.freeradbiomed.2015.04.036.

121. Motohashi H, Yamamoto M. Nrf2–Keap1 defines a physiologically important stress response mechanism. *Trends in Molecular Medicine*. 2004;10(11):549-557. doi:10.1016/j.molmed.2004.09.003.

122. Lee O-H, Jain AK, Papusha V, Jaiswal AK. An auto-regulatory loop between stress sensors INrf2 and Nrf2 controls their cellular abundance. *J Biol Chem*. 2007;282(50):36412-36420. doi:10.1074/jbc.M706517200.

123. Rangasamy T, Cho CY, Thimmulappa RK, et al. Genetic ablation of Nrf2 enhances susceptibility to cigarette smoke-induced emphysema in mice. *J Clin Invest*. 2004;114(9):1248-1259. doi:10.1172/JCI21146.

124. Suzuki M, Betsuyaku T, Ito Y, et al. Down-Regulated NF-E2–Related Factor 2 in Pulmonary Macrophages of Aged Smokers and Patients with Chronic

Obstructive Pulmonary Disease. *Am J Respir Cell Mol Biol*. 2008;39(6):673-682. doi:10.1165/rcmb.2007-0424OC.

125. Goven D, Boutten A, Leçon-Malas V, et al. Altered Nrf2/Keap1-Bach1 equilibrium in pulmonary emphysema. *Thorax*. 2008;63(10):916-924. doi:10.1136/thx.2007.091181.

126. Kansanen E, Kuosmanen SM, Leinonen H, Levonen A-L. The Keap1-Nrf2 pathway: Mechanisms of activation and dysregulation in cancer. *Redox Biol*. 2013;1(1):45-49. doi:10.1016/j.redox.2012.10.001.

127. Korytina GF, Akhmadishina LZ, Aznabaeva YG, et al. Associations of the NRF2/KEAP1 pathway and antioxidant defense gene polymorphisms with chronic obstructive pulmonary disease. *Gene*. 2019;692:102-112. doi:10.1016/j.gene.2018.12.061.

128. Zhang Y, Talalay P, Cho CG, Posner GH. A major inducer of anticarcinogenic protective enzymes from broccoli: isolation and elucidation of structure. *PNAS*. 1992;89(6):2399-2403. doi:10.1073/pnas.89.6.2399.

129. Hu R, Xu C, Shen G, et al. Gene expression profiles induced by cancer chemopreventive isothiocyanate sulforaphane in the liver of C57BL/6J mice and C57BL/6J/Nrf2 (−/−) mice. *Cancer Letters*. 2006;243(2):170-192. doi:10.1016/j.canlet.2005.11.050.

130. Jeong W-S, Keum Y-S, Chen C, et al. Differential Expression and Stability of Endogenous Nuclear Factor E2-related Factor 2 (Nrf2) by Natural Chemopreventive Compounds in HepG2 Human Hepatoma Cells. *BMB Reports*. 2005;38(2):167-176. doi:10.5483/BMBRep.2005.38.2.167.

131. Pham N-A, Jacobberger JW, Schimmer AD, Cao P, Gronda M, Hedley DW. The dietary isothiocyanate sulforaphane targets pathways of apoptosis, cell cycle arrest, and oxidative stress in human pancreatic cancer cells and inhibits tumor growth in severe combined immunodeficient mice. *Mol Cancer Ther*. 2004;3(10):1239-1248.

132. Zhang DD, Hannink M. Distinct cysteine residues in Keap1 are required for Keap1-dependent ubiquitination of Nrf2 and for stabilization of Nrf2 by chemopreventive agents and oxidative stress. *Mol Cell Biol*. 2003;23(22):8137-8151. doi:10.1128/mcb.23.22.8137-8151.2003.

133. Dinkova-Kostova AT, Fahey JW, Kostov RV, Kensler TW. KEAP1 and Done? Targeting the NRF2 Pathway with Sulforaphane. *Trends Food Sci Technol*. 2017;69(Pt B):257-269. doi:10.1016/j.tifs.2017.02.002.

134. Lewinska A, Adamczyk-Grochala J, Deregowska A, Wnuk M. Sulforaphane-Induced Cell Cycle Arrest and Senescence are accompanied by DNA Hypomethylation and Changes in microRNA Profile in Breast Cancer Cells. *Theranostics*. 2017;7(14):3461-3477. doi:10.7150/thno.20657.

135. Baier SR, Zbasnik R, Schlegel V, Zempleni J. Off-target effects of sulforaphane include the derepression of long terminal repeats through histone acetylation events. *J Nutr Biochem*. 2014;25(6):665-668. doi:10.1016/j.jnutbio.2014.02.007.

136. Durham A, Jazrawi E, Rhodes JA, et al. The anti-inflammatory effects of sulforaphane are not mediated by the Nrf2 pathway. *European Respiratory Journal*. 2014;44(Suppl 58):P3332.

137. Boehm J, Davis R, Murar CE, et al. Discovery of a crystalline sulforaphane analog with good solid-state stability and engagement of the Nrf2 pathway in vitro and in vivo. *Bioorg Med Chem*. 2019;27(4):579-588. doi:10.1016/j.bmc.2018.12.026.

138. Fahey JW, Holtzclaw WD, Wehage SL, Wade KL, Stephenson KK, Talalay P. Sulforaphane Bioavailability from Glucoraphanin-Rich Broccoli: Control by Active Endogenous Myrosinase. Mukhopadhyay P, ed. *PLoS ONE*. 2015;10(11):e0140963. doi:10.1371/journal.pone.0140963.

139. Davies TG, Wixted WE, Coyle JE, et al. Monoacidic Inhibitors of the Kelch-like ECH-Associated Protein 1: Nuclear Factor Erythroid 2-Related Factor 2 (KEAP1:NRF2) Protein-Protein Interaction with High Cell Potency Identified by Fragment-Based Discovery. *J Med Chem*. 2016;59(8):3991-4006. doi:10.1021/acs.jmedchem.6b00228.

140. Singh A, Happel C, Manna SK, et al. Transcription factor NRF2 regulates miR-1 and miR-206 to drive tumorigenesis. *J Clin Invest*. 2013;123(7):2921-2934. doi:10.1172/JCI66353.

141. Moinova HR, Mulcahy RT. Up-regulation of the human gamma-glutamylcysteine synthetase regulatory subunit gene involves binding of Nrf-2 to an electrophile responsive element. *Biochem Biophys Res Commun*. 1999;261(3):661-668. doi:10.1006/bbrc.1999.1109.

142. Tuder RM, Petrache I. Pathogenesis of chronic obstructive pulmonary disease. *J Clin Invest*. 2012;122(8):2749-2755. doi:10.1172/JCI60324.

143. Karhausen J, Haase VH, Colgan SP. Inflammatory hypoxia: role of hypoxia-inducible factor. *Cell Cycle*. 2005;4(2):256-258.

144. Rahman I, Adcock IM. Oxidative stress and redox regulation of lung inflammation in COPD. *European Respiratory Journal*. 2006;28(1):219-242. doi:10.1183/09031936.06.00053805.

145. Ribas V, García-Ruiz C, Fernández-Checa JC. Glutathione and mitochondria. *Front Pharmacol*. 2014;5(223ra20):151. doi:10.3389/fphar.2014.00151.

146. Georgakopoulos ND, Frison M, Alvarez MS, Bertrand H, Wells G, Campanella M. Reversible Keap1 inhibitors are preferential

pharmacological tools to modulate cellular mitophagy. *Sci Rep*. 2017;7(1):10303. doi:10.1038/s41598-017-07679-7.

147. Linke M, Fritsch SD, Sukhbaatar N, Hengstschläger M, Weichhart T. mTORC1 and mTORC2 as regulators of cell metabolism in immunity. Ellmeier W, Nagy L, eds. *FEBS Lett*. 2017;591(19):3089-3103. doi:10.1002/1873-3468.12711.

148. Suzuki M, Betsuyaku T, Ito Y, Nagai K, Nasuhara Y. Downregulated NF-E2-related Factor 2 in Pulmonary Macrophages of Aged Smokers and COPD Patients. 2008.

149. Plataki M, Cho SJ, Harris RM, et al. Mitochondrial Dysfunction in Aged Macrophages and Lung during Primary Streptococcus pneumoniae Infection is Improved with Pirfenidone. *Sci Rep*. 2019;9(1):971–16. doi:10.1038/s41598-018-37438-1.

150. Zorova LD, Popkov VA, Plotnikov EY, et al. Mitochondrial membrane potential. *Anal Biochem*. 2018;552:50-59. doi:10.1016/j.ab.2017.07.009.

151. Zheng F-J, Ye H-B, Wu M-S, Lian Y-F, Qian C-N, Zeng Y-X. Repressing malic enzyme 1 redirects glucose metabolism, unbalances the redox state, and attenuates migratory and invasive abilities in nasopharyngeal carcinoma cell lines. *Chin J Cancer*. 2012;31(11):519-531. doi:10.5732/cjc.012.10088.

152. Yang X, Deignan JL, Qi H, et al. Validation of candidate causal genes for obesity that affect shared metabolic pathways and networks. *Nat Genet*. 2009;41(4):415-423. doi:10.1038/ng.325.

153. Al-Dwairi A, Pabona JMP, Simmen RCM, Simmen FA. Cytosolic malic enzyme 1 (ME1) mediates high fat diet-induced adiposity, endocrine profile, and gastrointestinal tract proliferation-associated biomarkers in male mice. Singh SR, ed. *PLoS ONE*. 2012;7(10):e46716. doi:10.1371/journal.pone.0046716.

154. Vestbo J, Prescott E, Almdal T, et al. Body mass, fat-free body mass, and prognosis in patients with chronic obstructive pulmonary disease from a random population sample: findings from the Copenhagen City Heart Study. *Am J Respir Crit Care Med*. 2006;173(1):79-83. doi:10.1164/rccm.200506-969OC.

155. Schols AM, Slangen J, Volovics L, Wouters EF. Weight loss is a reversible factor in the prognosis of chronic obstructive pulmonary disease. *Am J Respir Crit Care Med*. 1998;157(6 Pt 1):1791-1797. doi:10.1164/ajrccm.157.6.9705017.

156. Silverman EK. Progress in chronic obstructive pulmonary disease genetics. *Proc Am Thorac Soc*. 2006;3(5):405-408. doi:10.1513/pats.200603-092AW.

157. Tager I, Tishler PV, Rosner B, Speizer FE, Litt M. Studies of the familial aggregation of chronic bronchitis and obstructive airways disease. *Int J Epidemiol*. 1978;7(1):55-62. doi:10.1093/ije/7.1.55.

158. Bermingham ML, Walker RM, Marioni RE, et al. Identification of novel differentially methylated sites with potential as clinical predictors of impaired respiratory function and COPD. *EBioMedicine*. 2019;43:576-586. doi:10.1016/j.ebiom.2019.03.072.

159. Mohammad HP, Barbash O, Creasy CL. Targeting epigenetic modifications in cancer therapy: erasing the roadmap to cancer. *Nature Medicine 2016 22:9*. 2019;25(3):403-418. doi:10.1038/s41591-019-0376-8.